DESIGN, PERFORMANCE AND OPTIMIZATION OF REFLECTION - TYPE PIN DIODE PHASE SHIFTERS

A Thesis Submitted
in Partial Fulfilment of the Requirements
for the Degree of
DOCTOR OF PHILOSOPHY

By
DEVESH KUMAR TRIVEDI

to the
DEPARTMENT OF ELECTRICAL ENGINEERING
INDIAN INSTITUTE OF TECHNOLOGY, KANPUR
JANUARY, 1981

L. I. Knapp
Acc No. 98587

EE-1981-D-TRI-DES

..... TO NEELAM,

SHASHANK AND RAVI

CERTIFICATE

This is to certify that the work reported in this thesis entitled 'DESIGN, PERFORMANCE AND OPTIMIZATION OF REFLECTION-TYPE PIN DIODE PHASE SHIFTERS' by Mr. Devesh Kumar Trivedi has been carried out under my supervision and has not been submitted elsewhere for a degree.

10.1.1981

(K.C. GUPTA)
Professor
Department of Electrical Engineering
Indian Institute of Technology
Kanpur 208016
INDIA

... has been approved
... the award of the Degree of
Doctor of Philosophy (Ph.D.)
in accordance with the
regulations of the Indian
Institute of Technology Kanpur
Dated: 29/4/1982

ACKNOWLEDGEMENTS

I wish to acknowledge with great pleasure and deep sense of gratitude the guidance and continuous encouragement of Prof. K.C. Gupta throughout the duration of this work. The ideas which I obtained during those numerous sessions of discussions were of immense value to this work.

I extend my sincere thanks to the administration of the Advanced Centre for Electronic Systems for providing support to me during the course of this work.

Thanks are also due to all my friends and the staff of the ACES for extending their help and cooperation during various stages of this work.

I also thank Mr. J.S. Rawat and Mr. C.M. Abraham for excellent typing of this manuscript. The tracings have been drawn neatly by Mr. Bajpai and Mr. Verma.

Finally, I would like to thank my wife, Neelam for her understanding and help throughout the various stages of this work.

- DEVESH KUMAR TRIVEDI

TABLE OF CONTENTS

LIST OF TABLES vii

LIST OF FIGURES viii

SYNOPSIS xvi

CHAPTER 1 : INTRODUCTION 1

1.1 Phase Shifters 1

1.2 Reflection-Type Phase Shifters 6

1.3 Outline of the Thesis 10

CHAPTER 2 : ROLE OF HYBRIDS IN REFLECTION-TYPE PHASE SHIFTERS 14

2.1 Hybrid Coupled Phase Shifter Circuits 15

2.2 Effect of Hybrid Parameters on Performance of Phase Shifters 25

CHAPTER 3 : PERFORMANCE OF PHASE SHIFTERS USING IDEAL SWITCHES 40

3.1 General Considerations 42

3.2 Bandwidth of Hybrids 44

3.3 Phase Shifters Using Branch Line Hybrids 44

3.4 Phase Shifters Using Rat-Race Hybrid 67

3.5 Bandwidth of Phase Shifters Using Ideal Switches 75

3.6 Phase Shifters Using Parallel Coupled Line Hybrids 85

CHAPTER 4 : DESIGN OF REFLECTION-TYPE PHASE SHIFTERS 96

4.1 Review of Available Design Procedures 99

4.2 General Considerations for the Design of Transforming Networks 104

4.3 Design of Three Types of Transforming Networks 108

CHAPTER 5 : PERFORMANCE OF REFLECTION-TYPE PHASE SHIFTERS 122

5.1 Bandwidth of Phase Shifter Circuits 123

5.2 Insertion Loss of Phase Shifter Circuits 148

5.3 Comparison of Phase Shifter Circuits for Bandwidth, Insertion Loss and Size. 159

CHAPTER 6 : EFFECT OF DIODE PARAMETERS ON PHASE SHIFTER PERFORMANCE 169

6.1 Effect of Diode Reactances 171

6.2 Effect of Diode Resistances 182

6.3 Effect of Mismatched Diodes 194

6.4 Discussions 201

CHAPTER 7 : DISCONTINUITY REACTANCES AND OPTIMIZATION OF PHASE SHIFTER CIRCUITS 205

7.1 Effect of Discontinuity Reactances on Phase Shifter Performance 206

7.2 Optimization of Hybrids 219

7.3 Optimization of Phase Shifter Circuits 231

7.4 Experiments using Optimized Design 237

CHAPTER 8 : CONCLUSION 250

8.1 Summary of Results 251

8.2 Suggestions for Further Work 255

APPENDIX A : HOOK AND JEEVES ALGORITHM 257

REFERENCES 260

LIST OF TABLES

Table No.	Caption	Page
3.1	Comparison of hybrid bandwidths	45
3.2	Maximum phase deviation for ±10 percent frequency deviation for three-branch hybrid.	82
5.1(a)	Bandwidth of phase shifters using 'low L-C' diodes (X_F=2 ohm and X_R = -400 ohm).	164
5.1(b)	Bandwidth of phase shifters using 'low L-C' diodes (X_F= 20 ohm and X_R = 62.5 ohm).	165
5.2(a)	Insertion loss of phase shifters using 'low L-C' diodes (X_F = 20 ohm and X_R = -400 ohm).	166
5.2(b)	Insertion loss of phase shifters using 'high L-C' diodes (X_F=20 ohm and X_R = 62.5 ohm).	167
7.1	Parameter values in the optimization of two-branch hybrid.	224
7.2	VSWR and isolation for two-branch hybrids.	227
7.3	VSWR and isolation for two-branch impedance transforming hybrids (50 Ω to 82.2 Ω)	230
7.4	Parameter values in the optimization of two-branch impedance transforming hybrid (50 Ω to 82.2 Ω)	231
7.5	Parameter values in the optimization of 180° phase bit.	234
7.6	Performance of 180° bits with only hybrid, optimized and with complete phase bit optimized.	236
7.7	Parameter value for 90° phase bit	237
7.8	Performance of 90° bits with only hybrid optimized and with complete phase bit optimized.	239

LIST OF FIGURES

Figure No.		Page No.
1.1	A Classification of Phase Shifters	3
1.2	Reflection Phase Shifters Using (a) Shorted Line Length Behind Shunt Mounted Diode or Open Ended Line Length Behind Series Mounted Diode, and (b) PIN Diodes Connected at the End of the Transmission Line.	8
2.1	Phase Shifter Circuits Using (a) 90° Hybrids, and (b) 180° Hybrids	16
2.2	(a) Block Representation of a 90° Hybrid (b) A Phase Bit Using 90° Hybrid.	18
2.3	(a) A Rat-Race Hybrid (b) A Phase Bit Using Rat-Race Hybrid	22
2.4	VSWR of Phase shifter as a Function of Isolation of the Hybrid.	31
2.5	Variation of Insertion Loss of the Phase Shifter with Isolation of the Hybrid	32
2.6	Variation of Phase Error of the Phase Shifter with Isolation of the Hybrid.	33
2.7	Variation of Phase Shifter Characteristics with Ratio of Powers in Coupled Ports.	36
2.8	Variation of VSWR of Phase Shifter with Phase Error in Coupled Signals ($\pm \Delta\theta$).	38
3.1	Electrical Equivalent Circuit for (a) Two-Branch Hybrid, and (b) Two-Branch Hybrid Phase Bit Using Ideal Switches.	47
3.2	Even Mode and Odd Mode Representations for the Circuit of Fig. 3.1(b).	48
3.3	Calculated VSWR Plot for 90° Phase Bit Using Two-Branch Hybrid.	53
3.4	Calculated Insertion Loss Plot for 90° Phase Bit Using Two-Branch Hybrid.	54

Figure No.		Page
3.5	Calculated Differential Phase Shift ($\Delta\phi$) Plot for 90^{o} Phase Bit Using Two-Branch Hybrid.	55
3.6	Electrical Equivalent Circuit for (a) Three-Branch Hybrid, and (b) Three-Branch Hybrid Phase Bit Using Ideal Switches.	57
3.7	Even Mode and Odd Mode Representations for the Circuit of Fig. 3.6(b).	58
3.8	Calculated VSWR Plot for 180^{o} Phase Bit Using Three-Branch Hybrid.	61
3.9	Calculated Insertion Loss Plot for 180^{o} Phase Bit Using Three-Branch Hybrid.	62
3.10	Calculated Differential Phase Shift ($\Delta\phi$)Plot for 180^{o} Phase Bit Using Three-Branch Hybrid.	63
3.11	Calculated VSWR Plot for 90^{o} Phase Bit Using Three-Branch Hybrid.	64
3.12	Calculated Insertion Loss Plot for 90^{o} Phase Bit Using Three-Branch Hybrid.	65
3.13	Calculated Differential Phase Shift ($\Delta\phi$)Plot for 90^{o} Phase Bit Using Three-Branch Hybrid.	66
3.14	Electrical Equivalent Circuit for (a) Rat-Race Hybrid and (b) Rat-Race Hybrid Phase Bit Using Ideal Switches.	68
3.15	Even Mode and Odd Mode Representation for the Circuit of Fig. 3.14(a).	70
3.16	Calculated VSWR Plot for 90^{o} Phase Bit Using Rat-Race Hybrid.	72
3.17	Calculated Insertion Loss Plot for 90^{o} Phase Bit Using Rat-Race Hybrid.	73
3.18	Calculated Differential Phase Shift ($\Delta\phi$)Plot for 90^{o} Phase Bit Using Rat-Race Hybrid.	74
3.19	Variation of Phase Shifter Bandwidth with Line Length L for 180^{o} Phase Bit Using Two-Branch Hybrid and Ideal Switches.	76

Figure No.		Page
3.20	Variation of Phase Shifter Bandwidth with Line Length L for 90° Phase Bit Using Two-Branch Hybrid and Ideal Switches.	77
3.21	Variation of Phase Shifter Bandwidth with Line Length L for 180° Bit Using Three-Branch Hybrid and Ideal Switches.	79
3.22	Variation of Phase Shifter Bandwidth with Line Length L for 90° Bit Using Three-Branch Hybrid and Ideal Switches.	80
3.23	Variation of Phase Shifter Bandwidth with Line Length L for 180° Bit Using Rat-Race Hybrid and Ideal Switches.	83
3.24	Variation of Phase Shifter Bandwidth with Line Length L for 90° Bit Using Rat-Race Hybrid and Ideal Switches.	84
3.25	Electrical Equivalent Circuit for (a) Parallel Coupled Hybrid (b) Parallel Coupled Hybrid Phase Bit.	86
3.26	Calculated Performance of 180° Phase Bit Using Parallel Coupled Hybrid.	89
3.27	Electrical Equivalent Circuit for (a) Tandem Connection of Two Single Section Parallel Coupled Hybrids (b) Tandem Hybrid Phase Bit.	91
3.28	Calculated Performance of 180° Phase Bit Using Tandem Connection of Two Single Section Parallel Coupled Hybrids.	92
4.1	A Reflection Phase Bit (a) Using Ideal Switches (b) Using Nonideal Switches	98
4.2	Various Transforming Networks	100
4.3	Variation of Z_m/Z_o with X_R for 180° Bit	106

Figure No.		Page
4.4	Variation of Z_m/Z_o with X_R for 90° Bit	107
4.5	Variation of θ_m with X_R for 180° and 90° Bits Using Network for Use with Impedance Transforming Hybrid.	111
4.6	Variation of Z_T/Z_o with X_R for 180° and 90° Bits Using Quarter Wave Transforming Network.	112
4.7	Variation of θ_T with X_R for 180° and 90° Bits Using Quarter Wave Transforming Network.	113
4.8	Variation of Line Lengths θ_1, θ_s and θ_2 with X_R for 180° Bit Using Single Stub Transforming Network.	117
4.9	Variation of Line Lengths θ_1, θ_s and θ_2 with X_R for 90° Bit Using Single Stub Transforming Network.	120
5.1	Variation of Bandwidth with X_R for 180° Phase Bit Using Two-Branch Hybrid and Quarter Wave Transforming Network.	126
5.2	Variation of Bandwidth with X_R for 90° Phase Bit Using Two-Branch Hybrid and Quarter Wave Transforming Network.	127
5.3	Variation of Bandwidth with X_R for 180° Phase Bit Using Two-Branch Hybrid and Single Stub Transforming Network.	129
5.4	Variation of Bandwidth with X_R for 90° Phase Bit Using Two-Branch Hybrid and Single Stub Transforming Network.	131
5.5	Variation of Bandwidth with X_R for 180° Phase Bit Using Two-Branch Impedance Transforming Hybrid.	133
5.6	Variation of Bandwidth with X_R for 90° Phase Bit Using Two-Branch Impedance Transforming Hybrid.	135

Figure No. Page

5.7 Variation of Bandwidth with X_R for 180° Phase Bit Using Three-Branch Hybrid and Quarter Wave Transforming Network. 137

5.8 Variation of Bandwidth with X_R for 90° Phase Bit Using Three-Branch Hybrid and Quarter Wave Transforming Network. 138

5.9 Variation of Bandwidth with X_R for 180° Phase Bit Using Three-Branch Hybrid and Single Stub Transforming Network. 140

5.10 Variation of Bandwidth with X_R for 90° Phase Bit Using Three-Branch Hybrid and Single Stub Transforming Network. 141

5.11 Variation of Bandwidth with X_R for 180° Phase Bit Using Rat-Race Hybrid and Quarter Wave Transforming Network. 143

5.12 Variation of Bandwidth with X_R for 90° Phase Bit Using Rat-Race Hybrid and Quarter Wave Transforming Network. 144

5.13 Variation of Bandwidth with X_R for 180° Phase Bit Using Rat-Race Hybrid and Single Stub Transforming Network. 146

5.14 Variation of Bandwidth with X_R for 90° Phase Bit Using Rat-Race Hybrid and Single Stub Transforming Network. 147

5.15 Variation of Insertion Loss with X_R for 180° and 90° Phase Bits Using Quarter Wave Transforming Network. 149

5.16 Variation of Insertion Loss with X_R for 180° and 90° Phase Bits Using Two-Branch Hybrid and Quarter Wave Transforming Network. 151

5.17 Variation of Insertion Loss with X_R for 180° and 90° Phase Bits Using Three-Branch Hybrid and Quarter Wave Transforming Network. 152

5.18 Variation of Insertion Loss with X_R for 180° and 90° Phase Bits Using Rat-Race Hybrid and Quarter Wave Transforming Network. 153

Figure No. Page

5.19 Variation of Insertion Loss with X_R for 180° and 90° Phase Bits Using Single Stub Transforming Network. 155

5.20 Variation of Insertion Loss with X_R for 180° and 90° Phase Bits Using Two-Branch Hybrid and Single Stub Transforming Network. 156

5.21 Variation of Insertion Loss with X_R for 180° and 90° Phase Bits Using Three-Branch Hybrid and Single Stub Transforming Network. 158

5.22 Variation of Insertion Loss with X_R for 180° and 90° Phase Bits Using Rat-Race Hybrid and Single Stub Transforming Network. 157

5.23 Variation of Insertion Loss with X_R for 180° and 90° Phase Bits Using Two-Branch Impedance Transforming Hybrid. 160

6.1 Variation of $S^{\Delta\phi}_{X_F}$ and $S^{\Delta\phi}_{X_R}$ with X_R/X_F for 180° and 90° Phase Bits Using i) Network for Use with Impedance Transforming Hybrid ii) Quarter wave Transforming Network. 174

6.2 (a) Variation of $S^{\Delta\phi}_{X_F}$ with X_R/X_F for 180° and 90° Phase Bits Using Single Stub Transforming Network 180

(b) Variation of $S^{\Delta\phi}_{X_R}$ with X_R/Z_o for 180° and 90° Phase Bits Using Single Stub Transforming Network.

6.3 (a) Variation of ϕ_{DF} with R_F/X_F 185

(b) Variation of R.B. Loss with R_R/X_R

6.4 (a) Variation of ϕ_{DF} with R_F/X_F 188

(b) Variation of ϕ_{DR} with R_R/X_R

6.5 (a) Variation of ϕ_{DF} with R_F/X_F 190

(b) Variation of F.B. Loss with R_F/X_F

Figure No.		Page
6.6	(a) Variation of ϕ_{DR} with R_R/X_R	193
	(b) Variation of R.B. Loss with R_R/X_R	
6.7	(a) Variation of ϕ_{DF} with R_F/X_F	195
	(b) Variation of F.B. Loss with R_F/X_F.	
6.8	(a) Variation of ϕ_{DR} with R_R/X_R	196
	(b) Variation of R.B. Loss with R_R/X_R.	
6.9	(a) Plot of Phase Shifter Characteristics due to Phase Difference in Γ's	202
	(b) Plot of Phase Shifter Characteristics due to Amplitude Difference in Γ's.	
	(c) Plot of Insertion Loss of Phase Shifter with $2-(\lvert\Gamma_2\rvert + \lvert\Gamma_3\rvert)$.	203
7.1	Microstrip Open End and Its Equivalent Circuit.	208
7.2	Microstrip T-Junction and its Equivalent Circuit.	210
7.3	(a) Configuration of 180° Phase Bit Using Two-Branch Hybrid and Stub Type Transforming Network	212
	(b) Equivalent Circuit of Fig. 7.3(a) including Discontinuity Reactances.	
7.4	Equivalent Circuit of PIN Diode in Forward and Reverse Bias with Measured Parameters.	214
7.5	Performance of 180° Phase Bit with and without Discontinuities.	215
7.6	(a) Configuration of 90° Phase Bit Using Two-Branch Impedance Transforming Hybrid	216
	(b) Equivalent Circuit of 7.6(a) Including Discontinuity Reactances	
7.7	Performance of 90° Phase Bit with and without Discontinuities.	218

Figure No. Page

7.8 Flow Chart for Optimization Procedure 221

7.9 Variation of VSWR with Frequency for Two-Branch Hybrid with and without Discontinuities and of the Optimized Circuit. 225

7.10 Performance of Two-Branch Hybrid with and without Discontinuities and of the Optimized Circuit. 226

7.11 Variation of VSWR with Frequency for Two-Branch Impedance Transforming Hybrid with and without Discontinuities and of the Optimized Circuit. 228

7.12 Performance of Two-Branch Impedance Transforming Hybrid with and without Discontinuities and of the Optimized Circuit. 229

7.13 Performance of 180° Phase Bit with optimized Hybrid alone and with Complete Phase Shifter Optimized. 235

7.14 Performance of 90° Phase Bit with Optimized Hybrid alone and with Complete Phase Shifter Optimized. 238

7.15 Layout for 180° Optimized Phase Bit along with Various Dimensions. 241

7.16 Plot of Experimental and Theoretical Performance for Optimized 180° Phase Bit. 242

7.17 Plot of Experimental and Theoretical Performance for Optimized 180° Phase Bit. 243

7.18 Photograph of Optimized 180° Phase Bit 244

7.19 Layout for 90° Optimized Phase Bit along with Various Dimensions. 245

7.20 Plot of Experimental and Theoretical Performance for Optimized 90° Phase Bit. 246

7.21 Plot of Experimental and Theoretical Performance for Optimized 90° Phase Bit. 247

7.22 Photograph of Optimized 90° Phase Bit 248

SYNOPSIS

DESIGN, PERFORMANCE AND OPTIMIZATION OF REFLECTION-TYPE PIN DIODE PHASE SHIFTERS

A Thesis submitted
In Partial Fulfilment of the Requirements
for the Degree of
DOCTOR OF PHILOSOPHY
by

Devesh Kumar Trivedi
Department of Electrical Engineering
Indian Institute of Technology, Kanpur
January 1981

Reflection-type hybrid coupled PIN diode digital phase shifters find several applications in microwave systems. Investigations reported in this thesis are aimed at (i) evolving design procedures for various 180° and 90° phase shifter circuits of this kind for a given set of diode parameters, (ii) comparison of these circuits, and (iii) their optimization to attain best performance taking into account, various discontinuity reactances contributed by microstrip circuitry.

The study reported here begins with exploring as to which parameters of the hybrid play critical role in phase shifter behaviour. The most important hybrid parameter for phase shifter performance is the directivity. It is found that a directivity of 20 dB in a 90° hybrid can cause, in the worst case, an input VSWR of the phase shifter to be 1.56, an insertion loss of 0.215 d and a phase error as high as $\pm$ 22.8°. An inequality of 1.0 dB in amplitudes of the two signals at the coupled ports of the hybrid can increase the input VSWR of the phase shifter to 1.26, but does not contribute to any phase error (ϕ_e).

Performance of phase shifters using ideal 180° and 90° switches allows one to study phase shifter circuits independent of PIN diode characteristics and thus enables one to investigate the limitations in performance imposed by the characteristics of the hybrids. Five types of hybrids have been considered. Results of this study point out the need of designing the transforming networks such that the two impedances, seen by the hybrid in the two bias states of the diode, are placed symmetrically on two sides of the X=0 axis on the Smith chart. For 180° phase bits using two-branch and rat-race hybrids, this is achieved by inserting an interconnecting line length of $\lambda/8$ between the switches and the hybrid ports. This results in maximum bandwidth of the phase shifter. Corresponding line length for the 90° phase bit is $\lambda/16$. Phase bits using three-branch hybrids are found to give maximum bandwidth for zero line length.

The design of phase shifters using nonideal diodes is essentially the design of the transforming network to achieve the desired phase shift at the centre frequency and minimum phase error over the band of frequencies. Closed form design equations are derived for the design of three types of transforming networks, namely: (i) single line length (to be used with impedance transforming hybrid), (ii) quarter wave transformer and (iii) a single stub.

Performances of phase shifters using three types of transforming networks with two-branch, three-branch and rat-race hybrids are evaluated. Bandwidths for various designs have been computed for two specifications of bandwidth and for wide range of diode reactances. Insertion losses for the above designs have also been calculated. It is observed that in most of the cases wide bandwidth is obtained when the forward bias reactance of the diode X_F is large and the reverse bias reactance X_R is small. Circuits using two-branch impedance transforming hybrid give lowest loss and have smallest size when compared to the other circuits considered.

Another aspect analyzed is the effect of variations in diode parameters on phase shifter performance. This study is useful in specifying the tolerances in diode parameters for given performance characteristics of the phase shifter. Sensitivities of differential phase shift ($\Delta \phi$) with respect to diode reactances for 180° and 90° phase bits have been evaluated for the three types of transforming networks. It is found that tighter tolerances in diode capacitances are needed for 90° bits than for 180° bits. It is observed that the effect of diode resistances R_F and R_R on the phase shift is small as compared to that of the reactances. Hence, the design equations, derived by ignoring diode losses, may also be used for lossy

diodes. Phase shifter performance using mismatched diodes is more sensitive to the inequality of the phases of the two reflection coefficients of the phase shift networks, than that in their magnitudes.

There is a significant effect of microstrip discontinuity reactances on the phase shifter performance. A 180° phase bit using two-branch hybrid and single stub type of transforming network (ε_r = 2.53 and substrate height = 0.0625 inch) gives a differential phase shift of 190° instead of 180°. Compensation of these discontinuities (mainly contributed by T-junctions) is carried out by an optimization process. The optimized phase shifter gives slightly wider bandwidth than an ideal circuit without discontinuities. Both 180° and 90° optimized phase bits have been fabricated. Diodes used were characterized experimentally. The theoretical and experimental results are found to agree within the specified tolerance of the dielectric constant of the substrate.

CHAPTER 1

INTRODUCTION

1.1 PHASE SHIFTERS 1

1.2 REFLECTION-TYPE PHASE SHIFTERS 6

1.3 OUTLINE OF THE THESIS 10

CHAPTER 1

INTRODUCTION

1.1 PHASE SHIFTERS

An ideal phase shifter is a two-port circuit element whose insertion in the network changes the phase of the transmitted signal by the specified amount and does not introduce any loss.

In general, the phase shifters have been discussed by several authors [1-4] . Tree shown in Fig. 1.1 represents a classification of phase shifters. A phase shifter can be either digital which provides discrete phase shift values or analog (which provides a continuously variable phase shift). The digital phase shifters have found wider application because of their compatibility with the digital driving circuitry and the computer control. These phase shifters can be designed using ferrites or semiconductor devices such as PIN diodes. Phase shifters using semiconductor devices can be divided in two general groups: the transmission-type and the reflection-type. The phase shift in a transmission-type phase shifter is obtained due to the difference in phase angles associated with the transmission coefficients of a two-port network obtained in two states of the diodes therein. In reflection-type phase shifters the phase shift is due to the difference in phase anglesassociated with the reflection coefficients in the two states. The transmission type circuits currently used are:

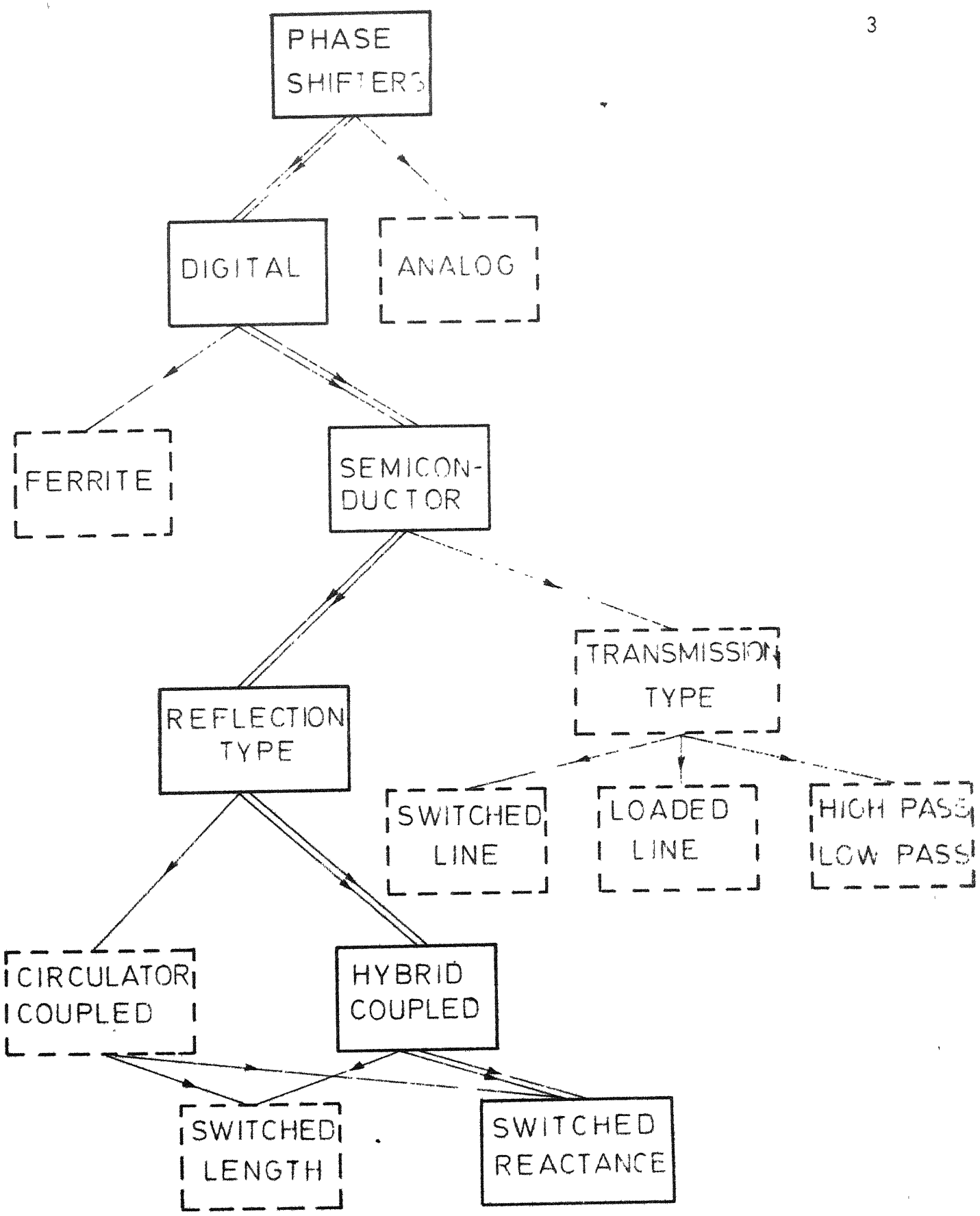


FIG. 1.1 A CLASSIFICATION OF PHASE SHIFTERS

switched line, loaded line and high pass-low pass type. The reflection type phase shifter circuits may use a circulator or a hybrid. The most commonly used reflection-type phase shifters employ 3 dB hybrids. Reflection phase shifter using circulator or 3 dB hybrid can be either a switched length type or a switched reactance type. Switched length type uses a short circuited or a open circuited line behind the diode depending on whether the diode is shunt mounted or series mounted. Switched reactance type use no transmission line length behind the diode. In this case, a suitable transforming network is used before the diode to obtain the desired phase shift.

One of the most important application of phase shifters is in phased array antennas. Conventional radar antennas have high inertia and it is difficult to change back and forth between rotating search-scan and relatively less mobile track-scan operations. An electronically controlled beam steering can provide inertialess scanning. One of the methods for steering the beam electronically in a Phased Array Radar (PAR) is by changing the phase of the RF power fed to each radiating element in a phased array antenna. This phase relationship determines the direction of the radiated beam. A single PAR may require thousands of small sized, highly reliable and low cost phase shifters.

The phased array antennas in PAR are used both for transmitting and receiving the signal. Therefore, the phase

shifters have to be reciprocal. Since the array is switched with the help of an electronic computer, phase shifters with very low switching times (< 1 μsec) are required. Digital phase shifters are more suited to this application than analog ones, since an electronic computer can drive digital phase shifters directly while D/A converters are required to drive analog phase shifters. It is difficult to get a linear relationship between the control voltage and the phase shift in analog phase shifters. Also, the variable capacitance of the diode used causes harmonic generation resulting in intermodulation products.

In ferrite phase shifters, a change in magnetic permeability due to application of biasing magnetic field is responsible for the phase shift. In phase shifters using semiconductor diodes, the phase shift is obtained due to change in phase values associated with reactances in two bias states of the diodes. Thus, these two classes of phase shifters are based on entirely different principles. Development of one class does not require any knowledge of the other. In this thesis, only a particular type of the diode phase shifters have been investigated.

Work on semiconductor diode phase shifters for phased array antennas started in late 1950's [5]. PIN diodes were used as the control elements. Switched line phase shifters were reported in 1957 [6] . The reflection phase shifters [7] appeared in 1959. The concept of loaded line phase shifters

emerged in 1959 [8]. The high pass - low pass phase shifters [9] were reported only in 1970. During early days of their development, cost of these phase shifters was high due to expensive diodes and costly circuit fabrication using machined parts. Over the years the diode performance has been improved and with the introduction of batch processing techniques the costs have also gone down significantly. At the same time, circuit designers have adopted planar transmission lines such as microstrips, striplines, etc. Circuits using these lines, apart from having low cost, have other advantages too, such as high reliability, miniaturization and compatibility with large scale production.

1.2 REFLECTION TYPE PHASE SHIFTERS

In reflection type phase shifters, phase shift results from the change in reflection coefficient at the termination of a line. A transmission line terminated by a PIN diode (switching between the forward and the reverse bias states) acts as a one port reflection phase bit. To make it a useful phase shifter circuit, the incident and reflected signals must be separated. This separation of signals can be done by using a circulator or a hybrid. Phase shifters using hybrids are more popular because of the absence of ferrite material and magnet needed for circulator coupled phase shifters. The investigations reported in this thesis are restricted to this class.

There are two approaches available for the design of reflection-type phase shifters. One of the approaches uses a shorted length of the line behind a shunt mounted diode [10] or an open-ended length of the line behind a series mounted diode as shown in Fig. 1.2(a). The other approach uses PIN diodes connected at the end of the transmission line [11-13] as shown in Fig. 1.2(b). Phase shifters based on the second approach yield wider constant-phase bandwidth. This thesis considers hybrid coupled reflection phase shifters using the second design approach.

If ideal PIN diodes are connected to the coupled ports of a hybrid, the two impedances in forward and reverse bias states differ in phase by 180° and a differential phase shift of 180° is obtained from the phase bit. In order to get 180° phase shift from imperfect diodes as well as to get lower phase bits, a suitable network between the hybrid port and the diode is needed. These networks are termed as transforming networks, since they transform the diode impedance to the desired value at the hybrid ports.

Hybrid coupled reflection type digital phase shifters using PIN diodes connected to the coupled ports of the hybrid without length of line behind the diode have been studied by various researchers [11-16] . Circuits with five different types of transforming networks have been reported in literature. Two out of these networks use lumped elements only. Garver [2,10,11] has described a circuit using lumped elements L and C

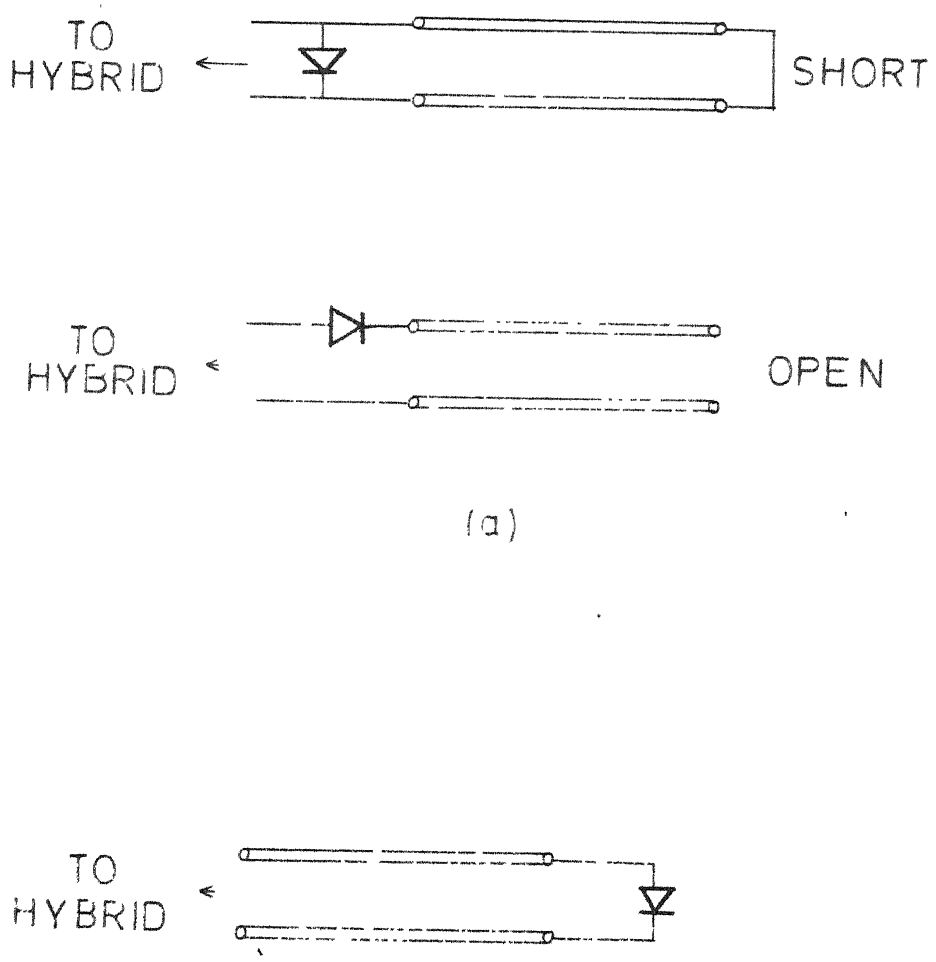


FIG. 1.2 REFLECTION PHASE SHIFTERS USING

(a) SHORTED LINE LENGTH BEHIND SHUNT MOUNTED DIODE OR OPEN ENDED LINE LENGTH BEHIND SERIES MOUNTED DIODE, AND

(b) PIN DIODES CONNECTED AT THE END OF THE TRANSMISSION LINE.

along with the diode. Basic design parameters and constants are optimized to get the desired phase error for the given phase bit. The other design given by Burns and Stark [4,12] is known as series and parallel resonant type phase shift network. It involves addition of tuning elements to obtain alternately series and parallel resonance in the two bias states. The third type, named as transformed LC is described by White[3]. This uses both lumped and distributed circuit elements. Fourth type of network [19] uses single length of transmission line. The fifth type of transforming networks [20,16] uses stubs (single stub or double stub). Design for 180° bit using a single stub network has been discussed in [20] .

Networks using transmission lines alone have become more popular for modest bandwidth phase shifters (less than 20 percent). Closed form expressions for the design of these networks (various line lengths and impedances) for a given set of diode parameters are not available in the literature. Design of loaded line phase shifters for obtaining minimum insertion loss, maximum bandwidth and minimum size are available [17] . Similar information on hybrid coupled reflection phase shifters is not available.

It is desirable to know effects of diode parameters on phase shifter performance. This helps in selection of diodes and evaluation of the tolerances required on their parameter values. Effect of diode parameters on reflection type-phase

shifters using first design approach (i.e. shorted or open transmission line length behind the diode) are included in [18]. Similar effects on the reflection phase shifters using the second design approach have not been studied.

Because of the discontinuity reactances contributed by the microstrip circuitry, one never obtains the desired phase shifter performance even at the centre frequency. Optimum design of phase shifters is not possible unless these discontinuity reactances are compensated either by an analytical approach or by computer optimization. The effect of junction reactances on reflection phase shifters and their compensation has not been discussed in the available literature.

1.3 OUTLINE OF THE THESIS

The material in the rest of the thesis is divided into seven chapters.

Chapter 2 discusses the importance of hybrid parameters in the design of phase shifters. Scattering parameters of the phase shifters using 90° and 180° hybrids are evaluated in terms of the scattering parameters of the hybrid and the reflection coefficients of the phase shift network (transforming network and diode). These expressions are used to find the effect of hybrid parameters (for 90° hybrids) on the phase shifter performance. Hybrid parameters are found to affect the performance of reflection phase shifters significantly. The most important hybrid parameter in this connection is the

directivity (and hence the input VSWR). Results of this study are useful in specifying the performance of hybrids for use in reflection type phase shifters.

In Chapter 3, the performance of phase shifters using ideal switches with various types of hybrids (2-branch, 3-branch, rat-race parallel coupled and tandem connection of parallel coupled hybrids) is evaluated. Modest bandwidth phase shifters using 2-branch, 3-branch and rat-race hybrids are studied in detail for their bandwidth. It is observed that a suitable line length between the hybrid port and the diode maximizes the bandwidth of the phase shifter. This happens when the two impedance points in the two states of the ideal switch are located symmetrically about X=0 axis on the Smith chart. For each phase bit (other than the 180° bit) two sets of such points are available which give maximum and nearly equal bandwidths. For the 180° bit, there is only a single design.

Chapter 4 deals with the design of reflection phase shifters using non-ideal diodes. Closed form design equations are derived for three types of transforming networks namely, (i) single line length (to be used with impedance transforming hybrids), (ii) quarter wave transformer, and (iii) a single stub. These design equations also include the design of suitable line length between the hybrid port and the diode which maximizes the bandwidth. Design curves giving transmission line lengths and impedances of the transforming network for the given diode reactances are also included.

Performance of reflection phase shifters using three types of transforming networks (discussed in Chapter 4) with two-branch, three-branch and rat-race hybrid is discussed in Chapter 5. Bandwidths for various designs are computed for two specifications of the bandwidth and for wide range of diode reactances. Insertion losses of phase shifters for the three types of transforming networks are also evaluated. Optimum design of these circuits for obtaining minimum circuit size, minimum insertion loss and maximum bandwidth are discussed. Based on these considerations a comparison between various types of circuits is presented for typical diode characteristics.

Chapter 6 describes the effect of variations in diode reactances and diode resistance on the performance of reflection phase shifters of the type discussed in this thesis. Designs with three types of transforming networks are considered. Also, the effect of mismatched diodes on phase shifter characteristics is evaluated. The study of this chapter is useful in predicting the maximum deviations in diode parameters which can be tolerated for the given specifications of a phase bit. This study also brings out the critical diode parameters affecting the phase shifter performance.

Chapter 7 discusses the effect of discontinuity reactances and the optimization of phase shifter circuits. Performances of typical 180° and 90° bits are evaluated. Junction reactances are considered by making use of the

available characterization for the microstrip line discontinuities encountered. It is noted that the discontinuities affect the performance significantly. Compensation of these discontinuities is carried out by optimization. First the hybrid is optimized separately. It is observed that the hybrid performance achieved after optimization is found to be better than that of the standard hybrid without junction reactances. For optimizing complete phase shifter typical 180° and 90° bits are considered. While optimizing the complete phase shifter, it is observed that better optimum results are obtained if both hybrid and transforming network parameters are made variable, instead of optimizing transforming network alone. Both 180° and 90° phase bits (using optimized design) have been fabricated using microstrip transmission lines on Rexolite substrate ($\epsilon_r = 2.53$). Diodes used have been characterized by measuring their impedances in the two bias states. The theoretical and experimental results are found to agree within the specified tolerance of the dielectric constant of the substrate.

The last chapter summarises the major conclusions of this investigation. Suggestions for further work are also listed in this chapter.

CHAPTER 2

ROLE OF HYBRIDS IN REFLECTION-TYPE PHASE SHIFTERS

2.1 HYBRID COUPLED PHASE SHIFTER CIRCUITS 15

2.1.1 Phase Shifters Using 90° Hybrids. 17

2.1.2 Phase Shifters Using 180° Hybrids. 21

2.2 EFFECT OF HYBRID PARAMETERS ON PERFORMANCE OF PHASE SHIFTERS 25

2.2.1 Effect of Finite Isolation and VSWR on Phase Shifter Characteristics. 26

2.2.2 Effect of Imperfect Coupling. 34

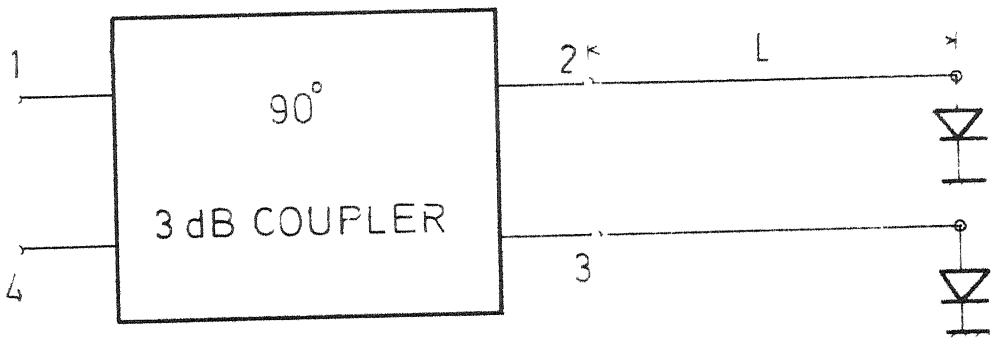
CHAPTER 2

ROLE OF HYBRIDS IN REFLECTION-TYPE PHASE SHIFTERS

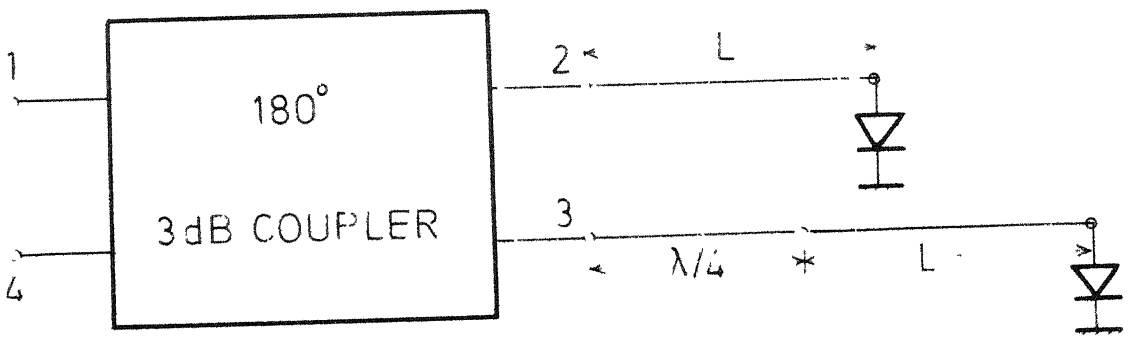
As mentioned in Chapter 1, there are two design approaches shown in Fig. 1.2 for reflection-type phase shifters. Hybrid coupled reflection-type phase shifters with PIN diodes connected at the end of the transmission lines are considered in the present study. Expressions for the scattering parameters of the phase shifters using general 90° and 180° hybrids are derived in terms of the scattering parameters of the hybrid and the reflection coefficients of the phase shift networks. These expressions are used to evaluate the effect of hybrid parameters on reflection phase shifters.

2.1 HYBRID COUPLED PHASE SHIFTER CIRCUITS

A hybrid (3 dB coupler) coupled reflection-type phase bit consists of a 3 dB coupler with identical terminations using PIN diodes at two coupled ports as shown in Fig. 2.1. One may use either a 90° or a 180° hybrid. When two PIN diodes are connected to the coupled output ports of a 90°, 3 dB coupler, power coupled to these ports is reflected from the diodes and comes out at the normally isolated port of the coupler. If 180°, 3 dB coupler is used,



(a)



(b)

FIG. 2.1 PHASE SHIFTER CIRCUITS USING
(a) 90° HYBRIDS, AND
(b) 180° HYBRIDS.

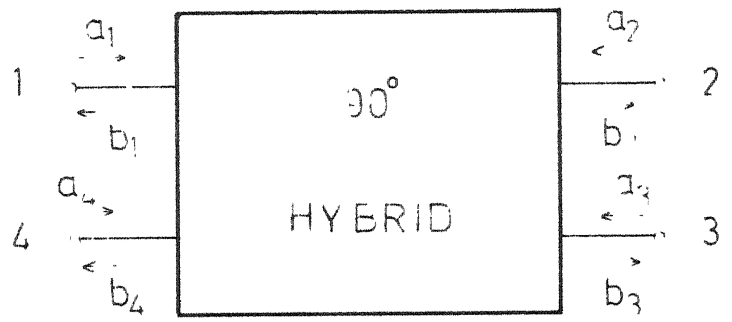
an extra $\lambda/4$ transmission line length is added to one of the coupled ports as shown in Fig. 2.1(b). Due to an extra line length of $\lambda/4$ the terminating impedances as seen at the port locations become Z and 1/Z. The reflection coefficients at these ports have opposite signs and the reflected signals reaching the isolated port of the coupler are in phase and hence they combine.

2.1.1 Phase Shifters Using 90° Hybrids

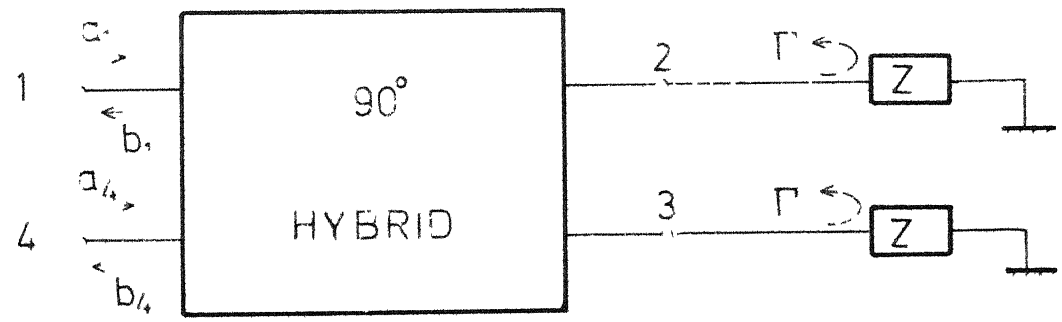
90° hybrids are widely used for reflection phase shifters. Most common forms of these hybrids in waveguide configuration are short slot or narrow wall coupler, top slot or broad wall coupler and branch guide couplers. In stripline or microstrip configuration the most common forms are branch line and parallel coupled couplers. Due to size and weight advantage, microstrip or stripline configurations are preferred over waveguide couplers for phase shifter applications.

Figure 2.2(a) shows a block representation of a 90° hybrid coupler. Using symmetry considerations, the scattering matrix of the coupler may be written as

$$\begin{bmatrix} b_1 \\ b_2 \\ b_3 \\ b_4 \end{bmatrix} = \begin{bmatrix} S_{11} & S_{21} & S_{31} & S_{41} \\ S_{21} & S_{11} & S_{41} & S_{31} \\ S_{31} & S_{41} & S_{11} & S_{21} \\ S_{41} & S_{31} & S_{21} & S_{11} \end{bmatrix} \begin{bmatrix} a_1 \\ a_2 \\ a_3 \\ a_4 \end{bmatrix} \qquad (2.1)$$



(a)



(b)

FIG. 2.2 (a) BLOCK REPRESENTATION OF A 90° HYBRID
(b) A PHASE BIT USING 90° HYBRID.

A reflection phase bit can be designed by terminating coupled ports into identical reflection coefficients Γ. Fig. 2.2(b) shows the arrangement of this phase shifter bit. Then the Eqn. (2.1) may be written as

$$\begin{bmatrix} b_1 \\ b_2 \\ b_3 \\ b_4 \end{bmatrix} = \begin{bmatrix} S_{11} & S_{21} & S_{31} & S_{41} \\ S_{21} & S_{11} & S_{41} & S_{31} \\ S_{31} & S_{41} & S_{11} & S_{21} \\ S_{41} & S_{31} & S_{21} & S_{11} \end{bmatrix} \begin{bmatrix} a_1 \\ \Gamma b_2 \\ \Gamma b_3 \\ a_4 \end{bmatrix} \qquad (2.2)$$

The scattering matrix for the phase shifter would be a 2x2 matrix, which can be obtained by eliminating the wave variables b_2 and b_3 in Eqn. (2.2) and can be written as

$$\begin{bmatrix} b_1 \\ b_4 \end{bmatrix} = \begin{bmatrix} S_{11p} & S_{14p} \\ S_{41p} & S_{44p} \end{bmatrix} \begin{bmatrix} a_1 \\ a_4 \end{bmatrix} \qquad (2.3)$$

where,

$$S_{11p}=S_{44p}=S_{11}+\frac{(S_{21}^2+S_{31}^2)(1-S_{11}\Gamma)\Gamma+2S_{21}S_{31}S_{41}\Gamma^2}{(1-S_{11}\Gamma)^2-S_{41}^2\Gamma^2} \qquad (2.4)$$

$$S_{41p}=S_{14p}=S_{41}+\frac{(S_{21}^2+S_{31}^2)S_{41}\Gamma^2+2S_{21}S_{31}\Gamma(1-S_{11}\Gamma)}{(1-S_{11}\Gamma)^2-S_{41}^2\Gamma^2} \qquad (2.5)$$

By knowing the scattering parameters of the hybrid and the reflection coefficients of the terminations, S parameters for

the phase shifters (S_{ijp}'s) can be evaluated. If the hybrid is assumed to be perfectly matched and has infinite isolation* then

$$S_{11} = S_{41} = 0 \tag{2.6}$$

Equation (2.3) then reduces to

$$\begin{bmatrix} b_1 \\ \\ b_4 \end{bmatrix} = \begin{bmatrix} (S_{21}^2+S_{31}^2)\,\Gamma & 2S_{21}S_{31}\Gamma \\ \\ 2S_{21}S_{31}\,\Gamma & (S_{21}^2+S_{31}^2)\Gamma \end{bmatrix} \begin{bmatrix} a_1 \\ \\ a_4 \end{bmatrix} \tag{2.7}$$

For an ideal 90° hybrid

$$\begin{aligned} S_{21} &= \frac{1}{\sqrt{2}} \angle \phi_2 \\ S_{31} &= \frac{1}{\sqrt{2}} \angle \phi_2 - 90^\circ \end{aligned} \tag{2.8}$$

For a single section branch line coupler $\phi_2 = -90^\circ$ and the phase shifter is characterized by

$$\begin{aligned} &S_{11p} = S_{44p} = 0 \\ \text{and} \qquad & \\ &S_{41p} = S_{14p} = j\Gamma \end{aligned} \tag{2.9}$$

---

*It has been shown [22] that a perfectly matched hybrid will have infinite isolation.

Equation (2.7) suggests that if the hybrid is ideal, the transmission coefficient of the phase shifter is equal to magnitude of the reflection coefficient Γ of the termination.

2.1.2 Phase Shifters Using 180° Hybrids

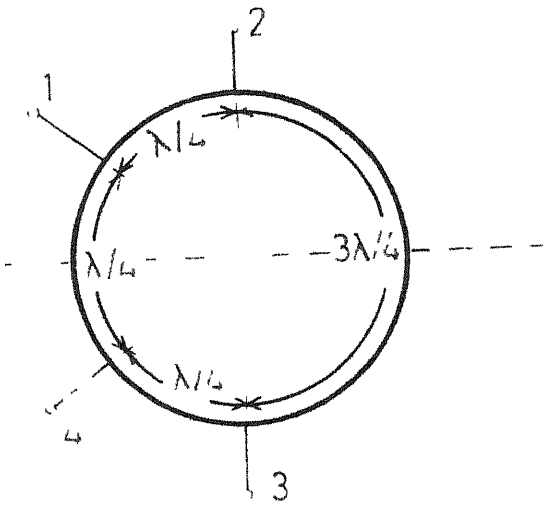
The most common forms of 180° hybrids in waveguide configuration are the magic-T, and the hybrid ring (also called rat-race hybrid). In stripline or microstrip configuration rat-race type hybrid is commonly used.

The scattering matrix for the 180° rat-race hybrid (Fig. 2.3(a)), using symmetry considerations ($S_{21}=S_{34}$ etc.) can be written [21,22] as

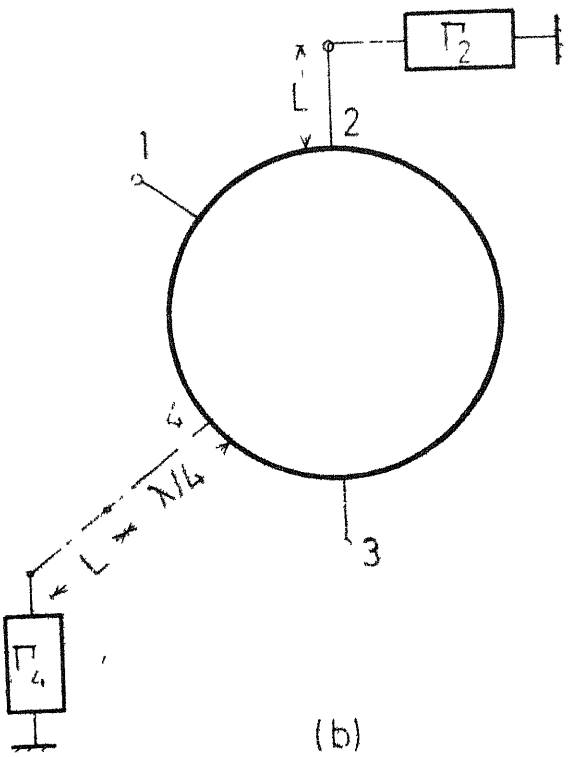
$$\begin{bmatrix} b_1 \\ b_2 \\ b_3 \\ b_4 \end{bmatrix} = \begin{bmatrix} S_{11} & S_{21} & S_{31} & S_{41} \\ S_{21} & S_{22} & S_{32} & S_{31} \\ S_{31} & S_{32} & S_{22} & S_{21} \\ S_{41} & S_{31} & S_{21} & S_{11} \end{bmatrix} \begin{bmatrix} a_1 \\ a_2 \\ a_3 \\ a_4 \end{bmatrix} \qquad (2.10)$$

It may be noted that this matrix contains 6 different parameters where as Eqn.(2.1) for 90° hybrid has only four different parameters.

A reflection phase bit using 180° hybrid is designed by connecting an extra 90° line length to one of the coupled ports before terminating it in the reflection coefficient Γ



(a)



(b)

FIG. 2.3 (a) A RAT-RACE HYBRID
(b) A PHASE BIT USING RAT-RACE HYBRID.

as shown in Fig. 2.3(b). The reflection coefficients at the coupled ports will be different in this case due to extra line length. The Eqn. (2.10) may now be written as

$$\begin{bmatrix} b_1 \\ b_2 \\ b_3 \\ b_4 \end{bmatrix} = \begin{bmatrix} S_{11} & S_{21} & S_{31} & S_{41} \\ S_{21} & S_{22} & S_{32} & S_{31} \\ S_{31} & S_{32} & S_{22} & S_{21} \\ S_{41} & S_{31} & S_{21} & S_{11} \end{bmatrix} \begin{bmatrix} a_1 \\ \Gamma_2 b_2 \\ a_3 \\ \Gamma_4 b_4 \end{bmatrix} \qquad (2.11)$$

By eliminating b_2 and b_4 in Eqn. (2.11), we get a 2x2 S-matrix for the phase shifter as follows:

$$\begin{bmatrix} b_1 \\ b_3 \end{bmatrix} = \begin{bmatrix} S_{11}+X_1S_{21}+X_3S_{41} & S_{31}+X_2S_{21}+X_4S_{41} \\ S_{31}+X_1S_{32}+X_3S_{21} & S_{22}+X_2S_{32}+X_4S_{21} \end{bmatrix} \begin{bmatrix} a_1 \\ a_3 \end{bmatrix} \qquad (2.12)$$

where

$$X_1 = \frac{S_{41}S_{31} - S_{21}(S_{11} - 1/\Gamma_4)}{(S_{22} - 1/\Gamma_2)(S_{11} - 1/\Gamma_4) - S_{31}^2}$$

$$X_2 = \frac{S_{21}S_{31} - S_{32}(S_{11} - 1/\Gamma_4)}{(S_{22} - 1/\Gamma_2)(S_{11} - 1/\Gamma_4) - S_{31}^2}$$

$$X_3 = \frac{S_{41}(S_{22} - 1/\Gamma_2) - S_{21}S_{31}}{S_{31}^2 - (S_{22} - 1/\Gamma_2)(S_{11} - 1/\Gamma_4)} \qquad (2.13)$$

$$X_4 = \frac{S_{21}(S_{22} - 1/\Gamma_2) - S_{32}S_{31}}{S_{31}^2 - (S_{22} - 1/\Gamma_2)(S_{11} - 1/\Gamma_4)}$$

If the hybrid is assumed to have perfect match and infinite isolation, then

$$S_{11} = S_{22} = 0 \quad \text{and} \quad S_{31} = 0 \tag{2.14}$$

Eqn. (2.10) then reduces to

$$\begin{bmatrix} b_1 \\ b_3 \end{bmatrix} = \begin{bmatrix} (S_{21}^2\Gamma_2 + S_{41}^2\Gamma_4) & (S_{32}S_{21}\Gamma_2 + S_{21}S_{41}\Gamma_4) \\ (S_{32}S_{21}\Gamma_2 + S_{21}S_{41}\Gamma_4) & (S_{32}^2\Gamma_2 + S_{21}^2\Gamma_4) \end{bmatrix} \begin{bmatrix} a_1 \\ a_3 \end{bmatrix} \tag{2.15}$$

For the ideal 180° hybrid

$$\begin{aligned} S_{21} &= \frac{1}{\sqrt{2}} \angle -\phi^\circ \\ S_{41} &= \frac{1}{\sqrt{2}} \angle -\phi^\circ \\ S_{32} &= \frac{1}{\sqrt{2}} \angle -\phi - \pi \end{aligned} \tag{2.16}$$

For the ideal 180° hybrid ring $\phi = 90^\circ$ and Eqn. (2.15) reduces to

$$\begin{bmatrix} b_1 \\ b_3 \end{bmatrix} = \begin{bmatrix} -\frac{(\Gamma_2+\Gamma_4)}{2} & \frac{\Gamma_2-\Gamma_4}{2} \\ \frac{\Gamma_2-\Gamma_4}{2} & -\frac{(\Gamma_2+\Gamma_4)}{2} \end{bmatrix} \begin{bmatrix} a_1 \\ a_3 \end{bmatrix} \tag{2.17}$$

At the centre frequency where the added line length to one of the coupled ports is exactly 90°, $\Gamma_2 = -\Gamma_4 = \Gamma$ and above equation simplifies to the following form

$$\begin{bmatrix} b_1 \\ b_3 \end{bmatrix} = \begin{bmatrix} 0 & \Gamma \\ \Gamma & 0 \end{bmatrix} \begin{bmatrix} a_1 \\ a_3 \end{bmatrix} \qquad (2.18)$$

Phase shifter is then characterized by

$$S_{11p} = S_{33p} = 0$$
$$\text{and} \quad S_{31p} = S_{13p} = \Gamma \qquad (2.19)$$

As for ideal 90° hybrids, the transmission coefficient of the phase shifter is equal to magnitude of the reflection coefficients Γ of the termination.

2.2 EFFECT OF HYBRID PARAMETERS ON PERFORMANCE OF PHASE SHIFTERS

The important parameters of hybrids are: VSWR, isolation, and phase and coupling amplitude errors. Suitability of a hybrid for the given application in general depends on all the above parameters, but some parameters are more important in one application than in the other. For example, in a balanced mixer, a coupler having amplitude inequality of 1 dB or phase error of 11° can limit the AM local oscillator noise concellation to 20 dB [23]. While in a balanced duplexer using two identical hybrids, the phase errors in the two couplers cancel out while VSWR's and isolations combine. This section deals with the effect of hybrid parameters on the performance (VSWR, insertion loss and error in phase shift) of reflection type phase shifters using quadrature hybrids.

2.2.1 Effect of Finite Isolation and VSWR on Phase Shifter Characteristics

Practical hybrids are never ideal (Eqns. 2.6 and 2.8 are not satisfied) even at the centre frequency. Assuming a lossless hybrid and applying the unitary condition to the scattering matrix of the hybrid, it can be easily shown [22] that for $|S_{21}| = |S_{31}|$ we get

$$|S_{11}| = |S_{41}| \tag{2.20}$$

Equations (2.4) and (2.5) can be further simplified when

$$|S_{21}| = |S_{31}| = \frac{1}{\sqrt{2}} \tag{2.21}$$

and

$$\theta_2 - \theta_3 = 90^\circ \tag{2.22}$$

where θ_2 and θ_3 are the phases of S_{21} and S_{31}, respectively.

Above approximations (Eqns. 2.21 and 2.22) are in general true for all 90° hybrids as long as the magnitudes of S_{11} and S_{41} are much smaller than unity. Using these approximations, we may write

$$S_{21}^2 + S_{31}^2 = 0 \tag{2.23}$$

Using the unitary property of the scattering matrices for lossless 4-port networks, we get

$$|S_{11}|^2 + |S_{21}|^2 + |S_{31}|^2 + |S_{41}|^2 = 1$$

Since $|S_{21}| = |S_{31}|$ and $|S_{11}| = |S_{41}|$, this relation reduces to

$$|S_{21}|^2 = \frac{(1-2|S_{11}|^2)}{2} \tag{2.24}$$

By substituting Eqns. (2.23) and (2.24) into Eqns. (2.4) and (2.5) we get,

$$S_{11p}=S_{11} + \frac{|S_{11}|(1-2|S_{11}|^2)\Gamma^2 e^{j(\theta_2+\theta_3+\theta_4)}}{(1-S_{11}\Gamma)^2 - S_{41}^2\Gamma^2} \tag{2.25}$$

$$S_{41p}=S_{41} + \frac{\Gamma(1-2|S_{11}|^2)(1-S_{11}\Gamma)e^{j(\theta_2+\theta_3)}}{(1-S_{11}\Gamma)^2 - S_{41}^2\Gamma^2} \tag{2.26}$$

Thus, the characteristics of the phase shifter can be evaluated from the knowledge of S_{11} and S_{41} for a particular hybrid and the value of Γ.

In the general case of all 90° hybrids Eqns. (2.25) and (2.26) can further be simplified (when $|S_{11}|$ and $|S_{41}| \ll 1$) by ignoring the terms containing $|S_{11}|^3$ and $|S_{41}|^3$.
We get,

$$S_{11p}=|S_{11}|[e^{j\theta_1}+\Gamma^2 e^{j(\theta_2+\theta_3+\theta_4)}+2|S_{11}|\Gamma^3 e^{j(\theta_1+\theta_2+\theta_3+\theta_4)}] \tag{2.26}$$

$$S_{41p}=\Gamma e^{j(\theta_2+\theta_3)}+|S_{11}| e^{j\theta_4} +\Gamma^2 |S_{11}| e^{j(\theta_1+\theta_2+\theta_3)} -2\Gamma|S_{11}|^2 e^{j(\theta_2+\theta_3)}-3\Gamma^3|S_{11}|^2 e^{j(2\theta_1+\theta_2+\theta_3)} +\Gamma^3|S_{11}|^2 e^{j(\theta_2+\theta_3+2\theta_4)} \tag{2.27}$$

where θ_1 and θ_4 are the phases of S_{11} and S_{41}, respectively.

Since generally the phase values associated with S_{11}, S_{21}, S_{31} and S_{41} in an imperfect hybrid depend upon the specific cause of imperfection, exact values of phase shifter reflection and transmission coefficients are difficult to evaluate. Thus, it is useful to determine the worst case values of VSWR, insertion loss and differential phase shift error of the phase bit as the function of isolation (or VSWR) of the hybrid.

The worst case value of VSWR is obtained by choosing θ_1 and θ_4 such that the different terms in Eqn. (2.26) add to yield maximum amplitude of S_{11p}. Taking $\Gamma = e^{j\phi}$, we get

$$S_{11p} = |S_{11}| \left[e^{j\theta_1} + e^{j2\phi}\, e^{j(\theta_2+\theta_3+\theta_4)} \left\{ 1 + 2 |S_{11}|\, e^{j\phi}\, e^{j\theta_1} \right\} \right] \qquad (2.28)$$

The worst case value of $|S_{11p}|$ turns out to be independent of Γ and is given by

$$|S_{11p}|_{wc} = 2 |S_{11}| \left[1 + |S_{11}| \right] \qquad (2.29)$$

Since the two port phase shifter considered is lossless, worst case value of transmission coefficient may be written in terms of worst case value of S_{11p} as

$$|S_{41p}|_{wc} = \sqrt{1 - |S_{11p}|^2_{wc}} \qquad (2.30)$$

Worst case for the phase error is obtained from the transmission coefficient S_{41p} given by Eqn. (2.27). This is obtained by arbitrarily choosing θ_1 and θ_4 such that the vectors other than the main vector (the first term on RHS) are aligned in the same direction and are in quadrature to the first term. This would lead to the maximum deviation in phase of S_{41p} for two values of Γ(viz. $e^{j\phi}$ and $e^{-j\phi}$). Taking $\Gamma = e^{j\phi}$, Eqn. (2.27) reduces to

$$S_{41p} = e^{j(\phi+\theta_2+\theta_3)}[1+|S_{11}|\, e^{j(\theta_4-\phi-\theta_2-\theta_3)} + |S_{11}|\, e^{j(\phi+\theta_1)} - 2|S_{11}|^2 - 3|S_{11}|^2\, e^{j2(\phi+\theta_1)} + |S_{11}|^2\, e^{j2(\phi+\theta_4)}] \quad (2.31)$$

By choosing $\phi+\theta_1 = \pi/2$ and $\theta_4 = \pi/2 + (\phi+\theta_2+\theta_3)$, Eqn. (2.31) reduces to

$$S_{41p} = e^{j(\phi+\theta_2+\theta_3)}[1+2j|S_{11}| + |S_{11}|^2 - 3|S_{11}|^2\, e^{j2(2\phi+\theta_2+\theta_3)}] \quad (2.32)$$

Eqn. (2.32) gives the worst case value of phase when $2\phi+\theta_2+\theta_3 = 0$ and above Eqn. reduces to

$$S_{41p}\Big|_{wc} = e^{j(\phi+\theta_2+\theta_3)}[1+2j\,|S_{11}|] \quad (2.33)$$

Phase shifter performance may be specified by differential phase shift (in two states) defined as $\Delta\phi = \phi_R - \phi_F$. From Eqn. (2.33) worst value of $\Delta\phi$ is obtained as

$$\Delta\phi\Big|_{wc} = \pm\, 2\tan^{-1}\left[\, 2\,|S_{11}|\,\right] \quad (2.34)$$

worst case values of VSWR, insertion loss and phase shift error, computed from Eqns. (2.29), (2.30) and (2.34), respectively, are plotted in Figs. 2.4 to 2.6 as function of isolation of the hybrid. For a 90° hybrid having an isolation of 20 dB the input VSWR of the phase shifter may even go as high as 1.56, insertion loss to 0.215 dB and phase error to approximately $\pm$ 22.8°.

Above results are compared with a particular case of a 90° two-branch hybrid. Values for sample realistic conditions are plotted in these figures for different terminating conditions (Γ= 1, -1, j and -j). In this case the imperfections considered arise from a small shift in centre design frequency. Scattering parameters for such a case are derived using ABCD matrices for even and odd mode excitations. For small deviations from the centre frequency, the frequency dependent parameter t, ($t=\tan \beta \ell/2$) and t^2, t^3 etc. can be expanded in a Taylor series upto second term. This method simplifies the evaluation of scattering parameters. Eqns. (2.25) and (2.26) are used for calculation of phase shifter characteristics. Figures 2.4 and 2.5 indicate that VSWR and insertion loss are minimum when Γ values are 1 and -1 whereas the phase error is minimum when Γ values are j and -j,(Fig. 2.6). It is seen that, for VSWR insertion

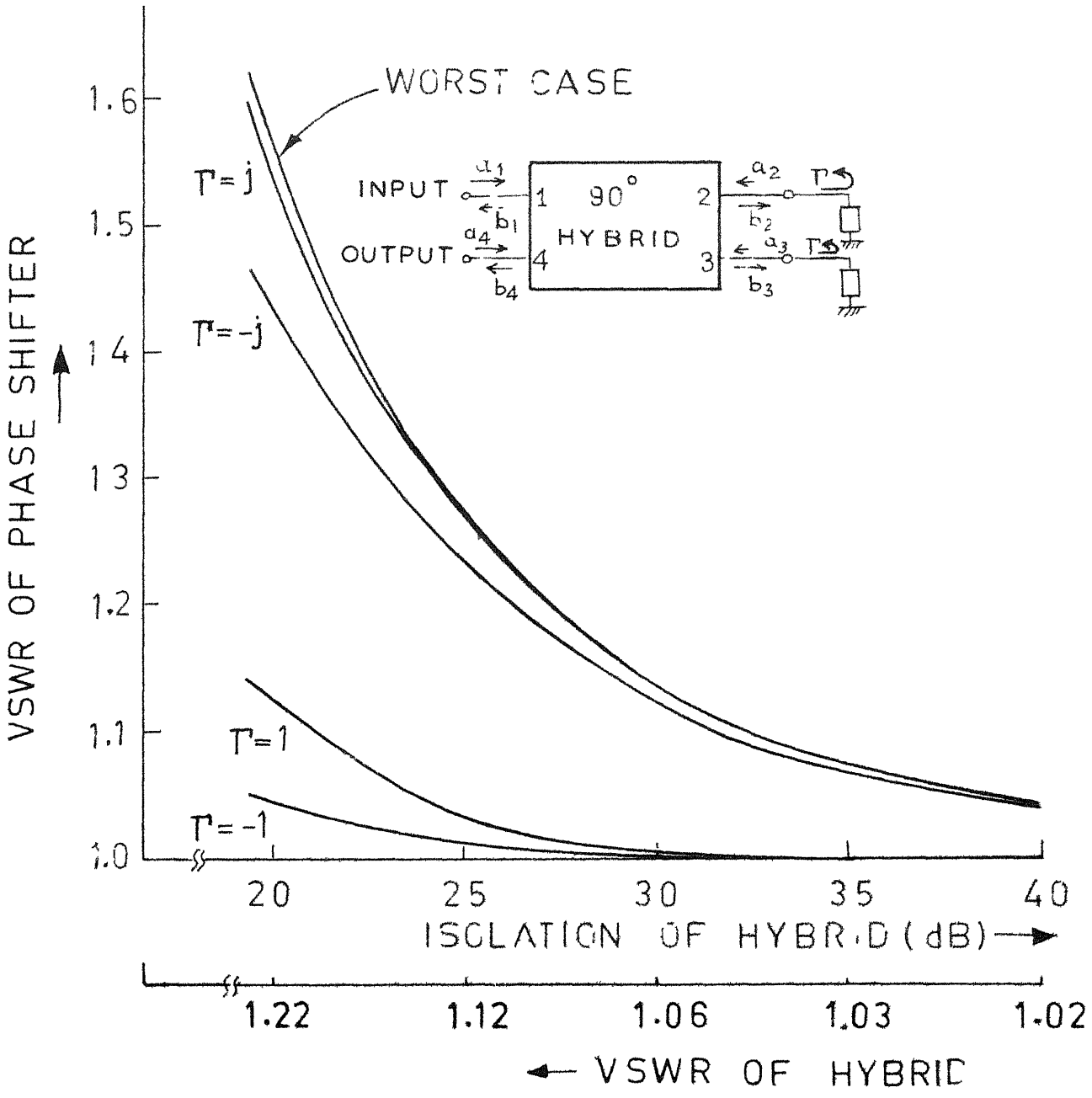


FIG. 2.4 VSWR OF PHASE SHIFTER AS A FUNCTION OF ISOLATION OF THE HYBRID.

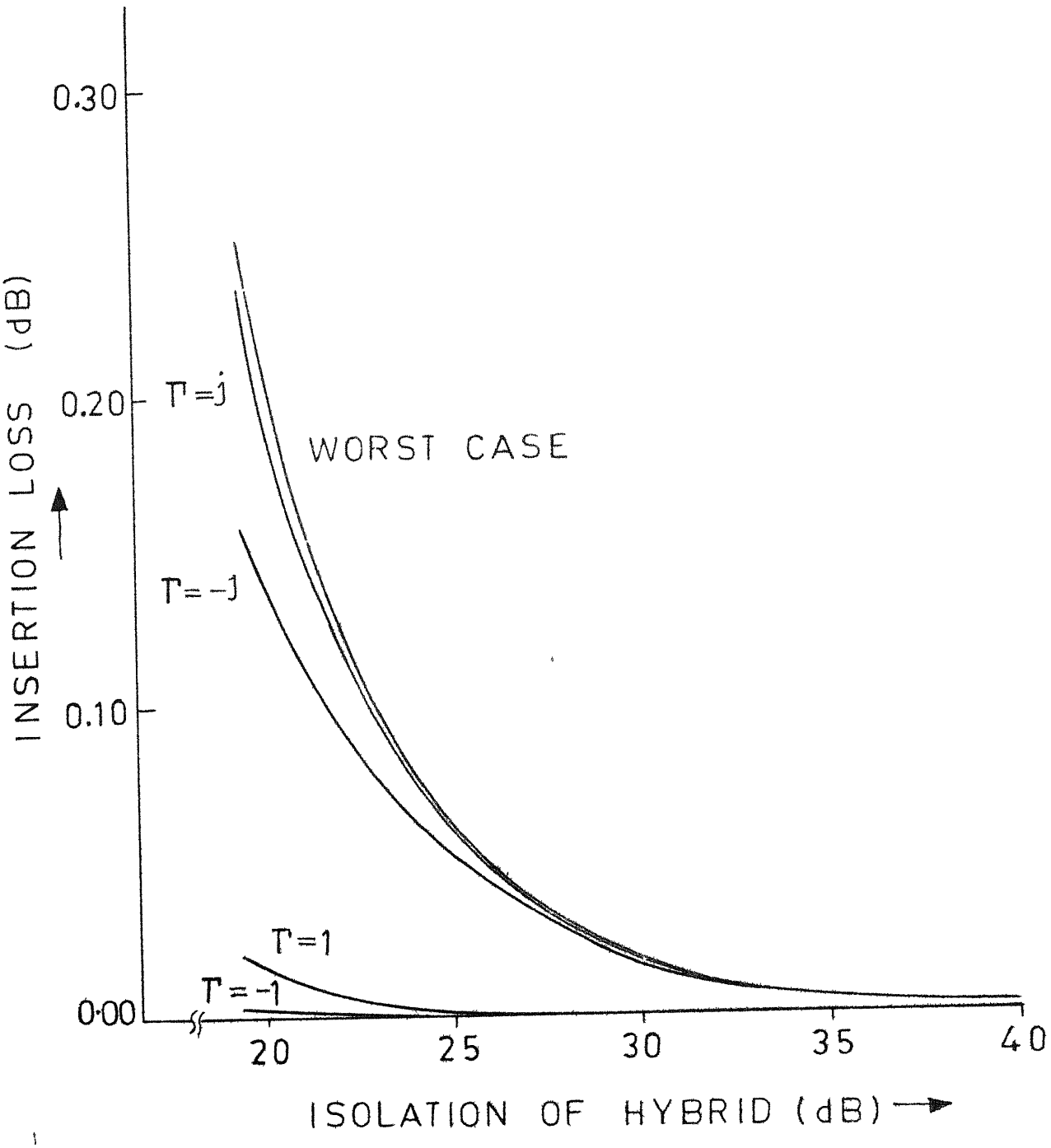


FIG. 2.5 VARIATION OF INSERTION LOSS OF THE [illegible] PHASE SHIFTER WITH ISOLATION OF THE HYBRID.

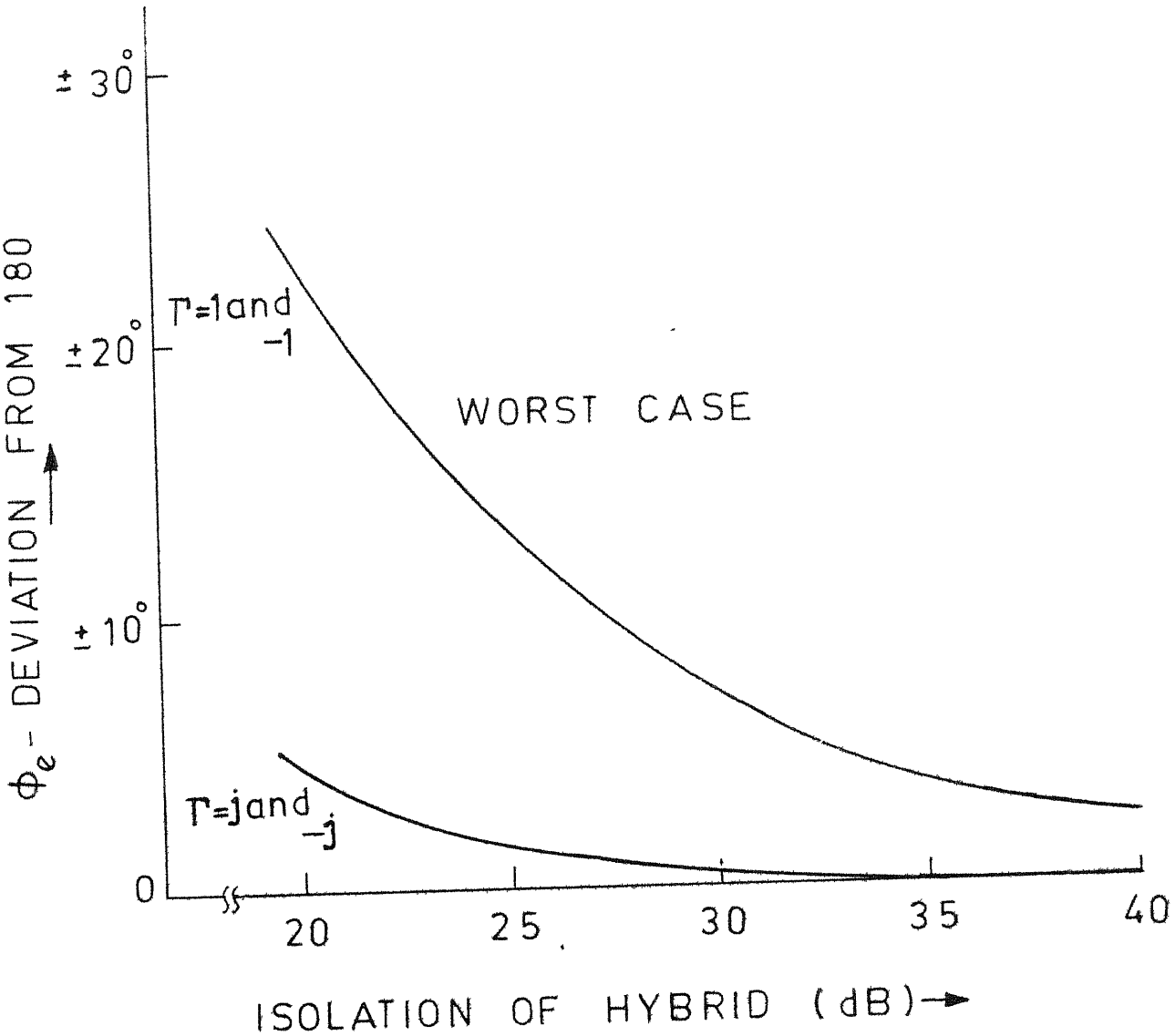


FIG. 2.6 VARIATION OF PHASE ERROR OF THE TRANSMITTER WITH ISOLATION OF THE HYBRID.

loss and phase shift error, the maximum of these values could be predicted reasonably by worst case results.

Garver [24] has reported phase error caused in specific case where a finite isolation value results from the mismatch between the coupled load and the terminating reflection. An error of $\pm 22.8^{\circ}$ is reported for 20 db isolation. This result agrees precisely with the worst case error value arrived at in the present paper. It may be recalled that worst case value calculated here does not depend upon the specific cause of imperfection.

2.2.2 Effect of Imperfect Coupling

The phase shifter performance is affected by imperfect couplings to the two coupled ports. This condition may be stated as

$$|S_{21}| \neq |S_{31}| \quad \text{and}$$

$$\theta_2 - \theta_3 = 90^{\circ} \pm \Delta\theta$$

In this case, we take the hybrid to be perfectly matched and isolation to be infinite, i.e. $S_{11} = S_{41} = 0$. The expressions for reflection and transmission coefficients for the phase shifter given in Eqn. (2.7) may be rewritten as

$$S_{11p} = r\left[|S_{21}|^2 - |S_{31}|^2 \; e^{\pm j2\Delta\theta}\right] e^{j2\theta_2} \qquad (2.35)$$

$$S_{41p} = 2r|S_{21}||S_{31}| \; e^{j(\theta_2+\theta_3)} \qquad (2.36)$$

The case of unequal amplitudes and phase error are considered seperately.

CASE I Effect of unequal coupling amplitudes:

If the phase error in the hybrid is negligible i.e. $\Delta\theta = 0$, then Eqn. (2.35) reduces to

$$S_{11p} = \Gamma[|S_{21}|^2 - |S_{31}|^2]\, e^{j2\theta_2} \qquad (2.37)$$

Hence

$$|S_{11p}| = \left||S_{21}|^2 - |S_{31}|^2\right| \qquad (2.38)$$

Equation (2.38) gives the magnitude of the reflection coefficient for the phase shifter when the error only due to amplitude coupling is considered. The transmission coefficient of the phase shifter is given by Eqn. (2.36). Also from Eqn. (2.36) we note that the differential phase shift for the phase shifter does not depend on the amplitudes of signals at the coupled ports. Variation of these parameters as a function of the ratio of powers in the coupled ports (in dB's) are given in Fig. 2.7. It may be noted that Eqns. (2.36) and (2.37) and hence the conclusions derived therefrom do not depend upon the type of the 90° hybrid.

CASE II Effect of phase error in coupled signals:

In this case the amplitudes at two coupled ports are considered to be equal but phase difference deviates from the ideal 90° value.

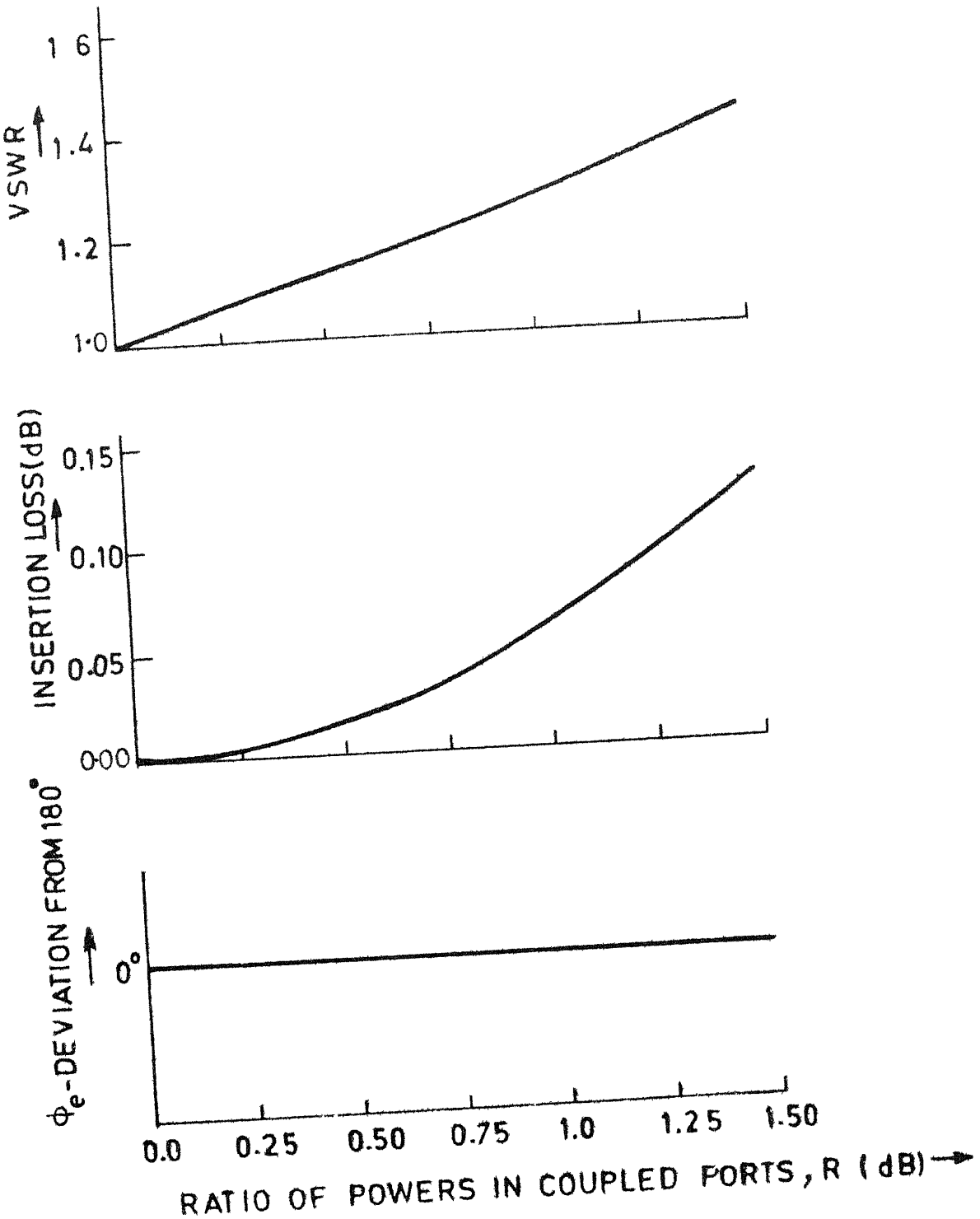


FIG. 2.7 VARIATION OF PHASE SHIFTER CHARACTERISTICS WITH RATIO OF POWERS IN COUPLED PORTS.

$$|S_{21}| = |S_{31}| = \frac{1}{\sqrt{2}} \tag{2.39}$$

Then Eqns. (2.35) and (2.36) reduce to

$$S_{11p} = \frac{\Gamma}{2}\left[1 - e^{\pm j2\Delta\theta}\right] e^{j2\theta_2} \tag{2.40}$$

$$S_{41p} = 2\Gamma|S_{21}|^2 \; e^{j(\theta_2+\theta_3)} = \Gamma e^{j(\theta_2+\theta_3)} \tag{2.41}$$

Magnitude of S_{11p} may be written as

$$|S_{11p}| = \frac{1}{2}\left|1 - e^{\pm j2\Delta\theta}\right| \tag{2.42}$$

Variation of VSWR of the phase shifter with phase error in coupled signals is shown in Fig. 2.8. It is seen that coupler phase error of 10° makes the VSWR of the phase shifter as large as 1.42.

From Eqn. (2.41) we see that the differential phase shift of the phase shifter is independent of the coupling phase error.

The calculations presented above indicate that the hybrid parameters could affect the performance of reflection type phase shifters significantly. The most important hybrid parameters in this connection is directivity (and hence the input VSWR).

It is found that an isolation of 20 dB in a 90° hybrid can cause, in the worst case, an input VSWR of the

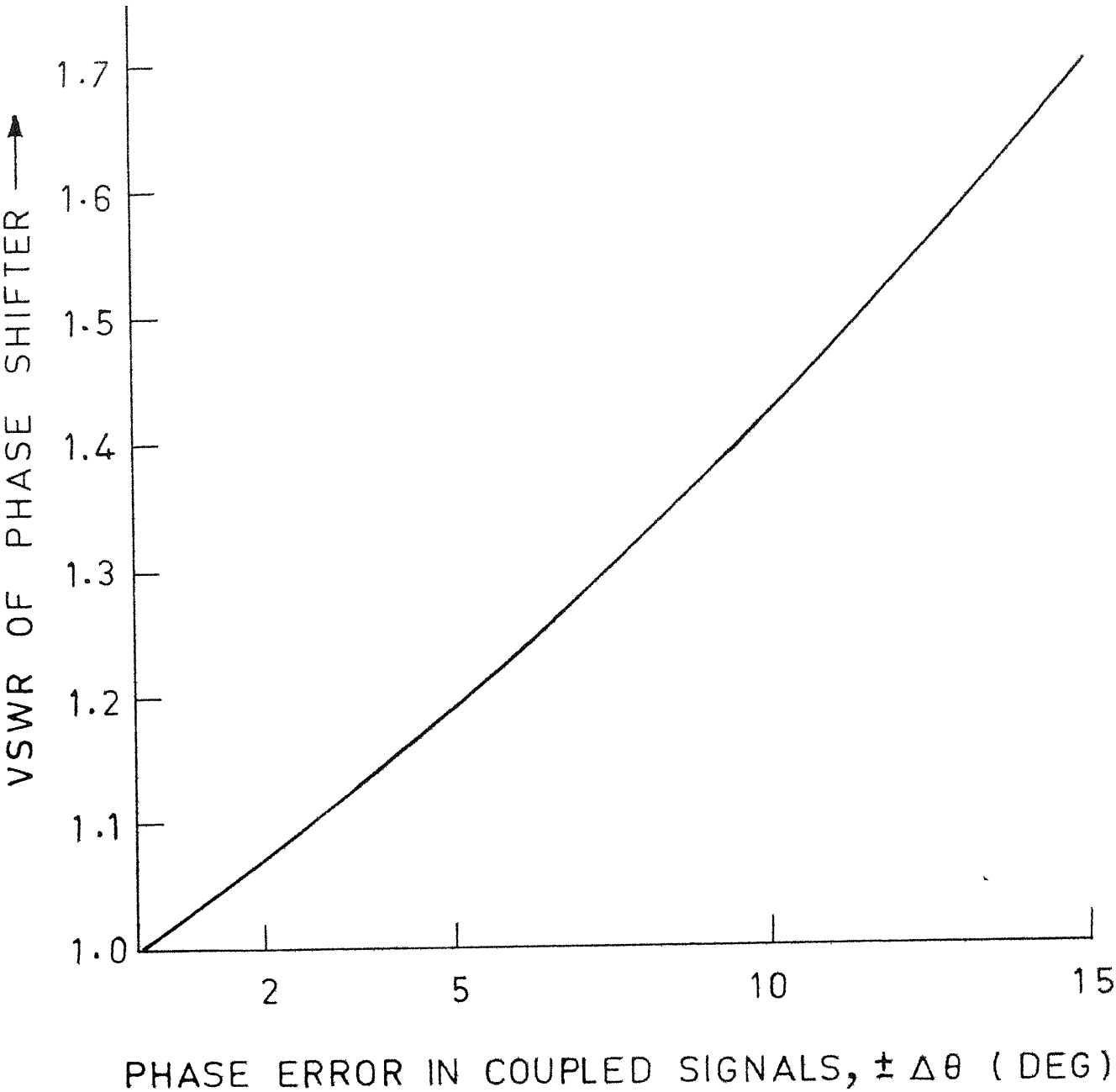


FIG. 2.8 VARIATION OF VSWR OF PHASE SHIFTER WITH PHASE ERROR IN COUPLED SIGNALS ($\pm\Delta\theta$).

phase shifter to be 1.56, insertion loss of 0.215 dB and phase error as high as $\pm 22.8^{\circ}$. Unequal amplitude coupling of 1.0 dB in the hybrid leads to input VSWR of the phase shifter to 1.26 and phase error of the phase shifter is found to be independent of the amplitude coupling. Phase error in the coupled signals of the hybrid of 10° gives rise to input VSWR of 1.42.

The analysis presented is applicable to phase shifter using any 90°, 3 dB hybrid (branch line, parallel coupled, etc.

The results presented in this section would be useful in specifying the performance of hybrids for use in reflection type phase shifters.

CHAPTER 3

PERFORMANCE OF PHASE SHIFTERS USING IDEAL SWITCHES

3.1 GENERAL CONSIDERATIONS 42

3.2 BANDWIDTH OF HYBRIDS 44

3.3 PHASE SHIFTERS USING BRANCH LINE HYBRIDS 44

3.3.1 Circuit Using Two-Branch Hybrid 46

3.3.2 Circuit Using Three-Branch Hybrid 56

3.4 PHASE SHIFTERS USING RAT-RACE HYBRID 67

3.5 BANDWIDTH OF PHASE SHIFTERS USING IDEAL SWITCHES 75

3.5.1 Phase Shifters Using Two-Branch Hybrid 75

3.5.2 Phase Shifters Using Three-Branch Hybrid 78

3.5.3 Phase Shifters Using Rat-Race Hybrid 81

3.6 PHASE SHIFTERS USING PARALLEL COUPLED LINE HYBRIDS 85

3.6.1 Phase Shifters Using Single Section Parallel Coupled Hybrid 87

3.6.2 Phase Shifters Using Tandem Connection of Two Single Section Hybrids. 90

CHAPTER 3

PERFORMANCE OF PHASE SHIFTERS USING IDEAL SWITCHES

Performance of a phase shifter can be specified by its VSWR, insertion loss and the error in differential phase shift. Insertion loss is mainly contributed by the transmission line losses and the diode losses. For low loss diodes, the line losses become important. Bandwidth of a phase shifter can be specified in terms of phase shifter VSWR and phase error. Performance of phase shifters using various hybrids and ideal switches are discussed in this chapter. Hybrids commonly used in phase shifter circuits are: branch line hybrids (with two or more branches) [25,26], rat-race hybrids [25], and parallel coupled transmission line hybrids [27,28] . Several other designs for hybrid couplers are available; for example, De Ronde Strip Slot Coupler[29,30],Lange's interdigitated strip line quadrature hybrid [31] , Chua's slot line rat-race coupler[32] et

Performance of phase shifters using ideal switches with various types of hybrids, namely, two-branch, three-branch, rat-race,parallel coupled and tandem connection of parallel coupled hybrids is evaluated in this chapter. Phase shifters using two-branch, three-branch and rat-race hybrids are studied for their bandwidth.

3.1 GENERAL CONSIDERATIONS

Ideal Switches

For discussions in this chapter ideal 180° and 90° switches are considered in place of PIN diodes commonly used for 180° and 90° phase bits. An ideal 180° or 90° switch is a one port device with zero reflection loss and differential phase shift of 180° or 90°, respectively, for reflected signals in two states over all the frequencies. Ideal PIN diode is a device similar to the 180° switch. There is no device existing for the ideal 90° switch. Out of possible infinite number of switching impedances for 90° switch, the one selected set has impedance values as $\bar{Z}_1 = \infty$ and $\bar{Z}_2 = j$.

The analysis for 180° and 90° bit is carried out using the following conditions:

i) ideal switches (180° or 90°) are connected to the coupled ports of the hybrid

ii) junction reactances are neglected, and

iii) transmission line loss is taken to be 0.2 dB/λ for 50 ohm lines and proportionate to the square root of the normalized impedance for other impedance lines.

Use of ideal 180° and 90° switches allows one to study phase shifter circuits independent of the PIN diode characteristics and thus enables one to investigate the limitations in performance imposed by the characteristics of the hybrid. Phase

shifter performance using nonideal diodes as well as including the junction reactances are presented in later chapters.

Bandwidth of phase shifters

The bandwidth of a phase shifter is defined as the frequency range over which the maximum phase error and the maximum VSWR is less than the specified values. The bandwidth in percentage is defined as

$$\text{Bandwidth (Percent)} = \frac{2\,|f_o - f_b|}{f_o} \times 100 \qquad (3.1)$$

where f_o is the centre frequency and f_b is the nearest frequency at which at least one of the specifications (phase error or VSWR) is violated.

Phase error is defined as

$$\phi_e = \text{Max}(\Delta\phi_{max.} - \Delta\phi_{nom.}),\ (\Delta\phi_{nom.} - \Delta\phi_{min.}))$$

Limits on maximum phase error and VSWR depend upon the type of application and the overall response desired from the multibit phase shifter circuit. Even for a single phase bit, the maximum phase error allowed may depend on the bit size.

Specifications for bandwidth: In the present study bandwidths have been calculated for two different values of phase errors (namely $\leq \pm 2.5°$ and $\leq \pm 5°$). The VSWR is taken to be less than 1.2 in both the cases.

3.2 BANDWIDTH OF HYBRIDS

The bandwidth of a hybrid is defined as the frequency range over which (i) the maximum VSWR (ii) the maximum phase difference error in the signals at the coupled ports and (iii) the maximum amplitude differences are less than the specified values and (iv) the minimum isolation is greater than the set limit. Since there are four constraints to define the bandwidth, there can be many possible specifications for bandwidth. Specifications considered in this study are indicated in Table 3.1. These give the type of constraints one would like to have for the hybrids used in phase shifters. Corresponding bandwidth values of 2-branch, 3-branch and ratrace hybrids are also given in the table. Two-branch hybrid is found to have less isolation and VSWR bandwidth as compared to the three-branch and the rat-race hybrids. In Chapter 2, it has been pointed out that isolation of the hybrid has significant effect on the phase shifter characteristics. Hence, the phase shifters using two-branch hybrid are expected to have narrower bandwidths than phase shifters using three-branch and rat-race hybrids.

3.3 PHASE SHIFTERS USING BRANCH LINE HYBRID

Branch line directional couplers are the most commonly used couplers for various applications. The two-branch coupler is the simplest in this type of couplers. These

TABLE 3.1. Comparison of hybrid bandwidths

Hybrid type	Bandwidth (%) Amplitude difference < 0.2 dB	Amplitude difference < 0.4 dB	Phase Difference Error < ±4°	Isolation > 20 dB	VSWR < 1.2
* Two-branch	11	16	30	10	9
Three-branch	15	21	48	31	28
* Rat-race	10	20	12	31	26

*Bandwidth data for two-branch and ratrace hybrids are taken from reference [33] .

couplers can be constructed in waveguide, coaxial line and other types of transmission line configurations. Bandwidth is smallest for two-branch coupler and increases as the number of branches is increased. In stripline and microstrip configurations, it is difficult to fabricate a coupler with more than three branches due to high impedances of shunt branches.

In this section performances of phase shifter circuits using two-branch and three-branch hybrids are evaluated. Both 180° and 90° phase bits are considered.

3.3.1 Circuit Using Two-Branch Hybrid

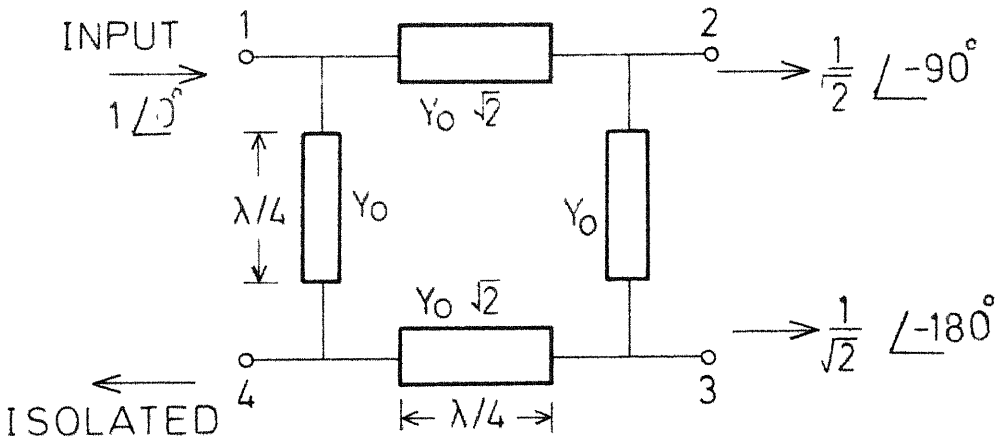
Figure 3.1(a) shows a two branch hybrid. At the centre frequency the input at port 1 divides equally between ports 2 and 3 and no signal comes out of port 4. Also, signals emerging out of ports 2 and 3 have a phase difference of 90°.

Figure 3.1(b) shows a reflection phase shifter using a two-branch hybrid. Ideal switches are connected to the coupled ports 2 and 3. Signals emerging out at these ports are reflected back and they combine at port 4, while they cancel out at the input port. Coupler characteristics change with the deviation from the centre frequency. Phase shifter performance as a function of frequency is evaluated for both 180° and 90° bits.

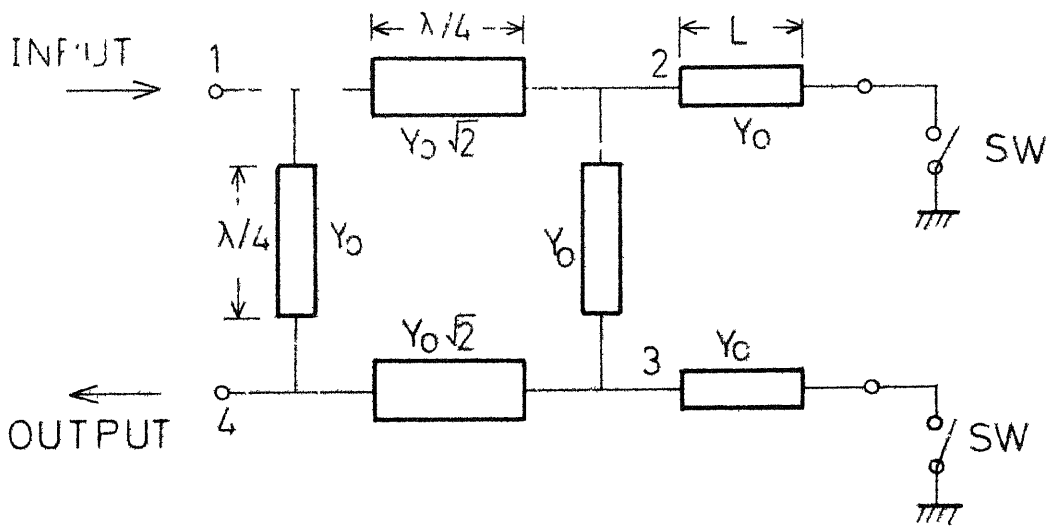
180° bit

A 180° bit is realized by connecting 180° ideal switches to the coupled ports of the hybrid with transmission line length L between the hybrid port and the switch as shown in Fig. 3.1(b).

The circuit is analyzed using the method of even and odd mode analysis [23]. This method reduces a symmetrical n-port network into two n/2-port networks. When ports 2 and 3 of the hybrid are terminated by ideal switches, the four port hybrid network becomes a two-port network. By taking even and odd mode symmetry, it reduces to a single port network as shown in Fig. 3.2.



(a)



(b)

FIG. 3.1 ELECTRICAL EQUIVALENT CIRCUIT FOR
(a) TWO-BRANCH HYBRID, AND
(b) TWO-BRANCH HYBRID PHASE BIT USING IDEAL SWITCHES.

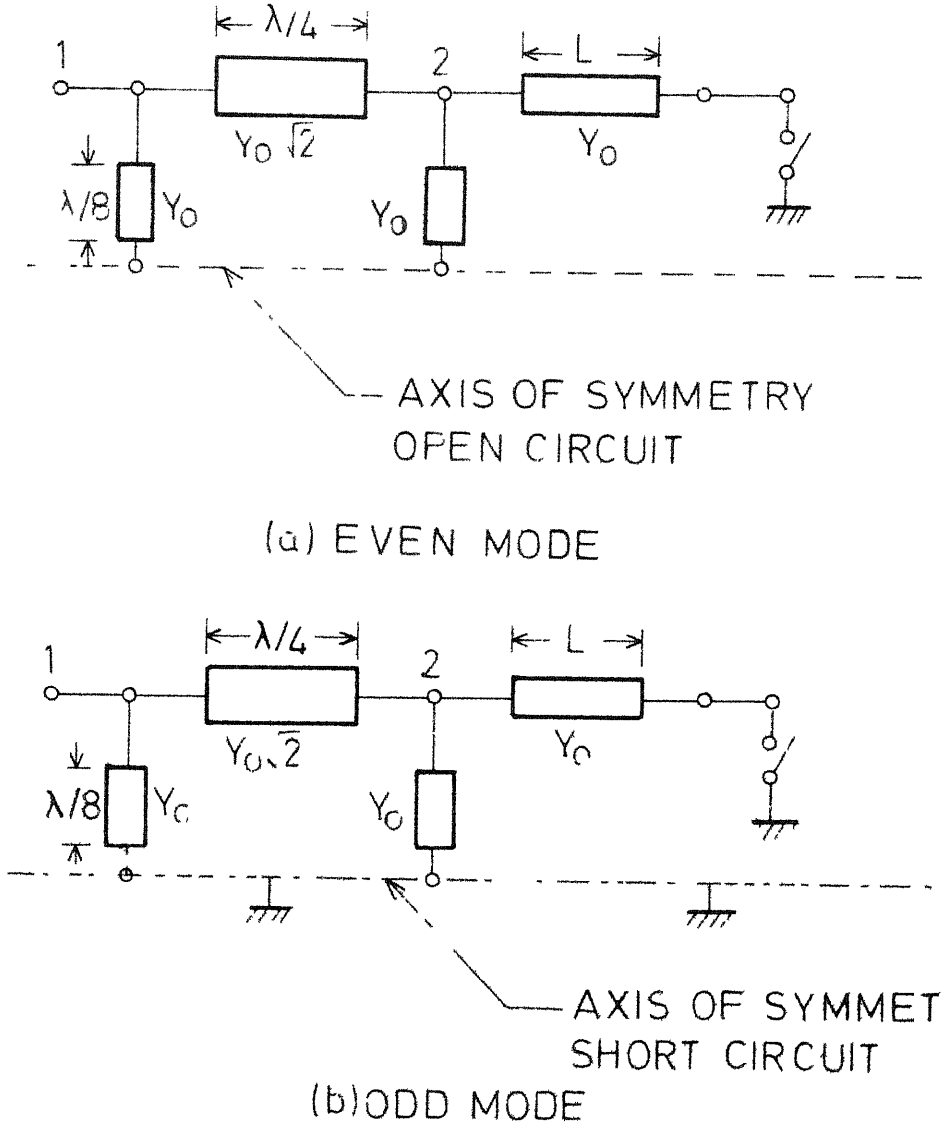


FIG. 3.2 EVEN MODE AND ODD MODE REPRESENTATIONS FOR THE CIRCUIT OF FIG. 3.1(b).

The even mode equivalent circuit shown in Fig. 3.2(a) consists of an open one eighth wavelength long shunt connected stub of admittance Y_o, a series quarter wave transmission line of admittance $Y_o\sqrt{2}$, an open one eighth wavelength shunt connected stub of admittance Y_o, a transmission line of length L of admittance Y_o and the ideal switch. This equivalent circuit consists of two port circuit elements connected in cascade between a generator and load (switch). The overall ABCD matrix for the cascade of two-port elements can be written as

$$[M_{e1}] = [M_1] \cdot [M_2] \cdot [M_1] \cdot [M_3] \qquad (3.2)$$

with

$$[M_1] = \begin{bmatrix} 1 & 0 \\ \tanh(\gamma_1 \ell_1/2) & 1 \end{bmatrix}$$

$$[M_2] \equiv \begin{bmatrix} \cosh \gamma_2 \ell_1 & \frac{1}{\sqrt{2}} \sinh \gamma_2 \ell_1 \\ \sqrt{2} \sinh \gamma_2 \ell_1 & \cosh \gamma_2 \ell_1 \end{bmatrix}$$

$$[M_3] = \begin{bmatrix} \cosh \gamma_1 L & \sinh \gamma_1 L \\ \sinh \gamma_1 L & \cosh \gamma_1 L \end{bmatrix}$$

where, M_1 denotes the normalized ABCD matrix of open stub of length $\ell_1/2$ having propagation constant γ_1 and admittance Y_o.

M_2 denotes the normalized ABCD matrix of transmission line of length ℓ_1 having propagation constant γ_2 and admittance $Y_o/2$. M_3 is the normalized ABCD matrix of line of length L having propagation constant γ_1 and admittance Y_o.

The equivalent circuit for the odd mode is shown in Fig. 3.2(b). The only difference between the even and odd mode circuits is that the shunt stubs eighth wavelength long are short circuited in odd mode case and open circuited in even mode case. Hence the overall ABCD matrix for the two port circuit elements is given as

$$[M_{o1}] = [M_1'] \cdot [M_2] \cdot [M_1'] \cdot [M_3] \qquad (3.3)$$

with

$$[M_1'] = \begin{bmatrix} 1 & 0 \\ \coth(\gamma_1 \ell_1/2) & 1 \end{bmatrix}$$

where M_1' is the normalized ABCD matrix of shorted stub of length $\ell_1/2$ having propagation constant γ_1 and admittance Y_o.
The even mode and odd mode matrices given by Eqns. (3.2) and (3.3) do not change with the change in switch state.

The input impedance can be evaluated from overall ABCD matrix using the following relation

$$Z_{in} = \frac{AZ_L+B}{CZ_L+D} \qquad (3.4)$$

where Z_L is the load impedance (switch impedance). By knowing Z_{in}, reflection coefficients for the even and odd modes can be evaluated.

By superimposing the solutions for the even and odd modes, the response to the source of unit amplitude connected at port 1 is given by

$$S_{11} = \frac{\Gamma_e + \Gamma_o}{2}$$

$$S_{41} = \frac{\Gamma_e - \Gamma_o}{2} \qquad (3.5)$$

These equations for the two states of the switches may correspondingly be written.

Phase shifter performance can be evaluated as follows:

Insertion loss of the circuit in dB's is given by

$$\text{I.L. (dB)} = -20 \log_{10} |S_{41}| \qquad (3.6)$$

Input VSWR of the phase bit is written as

$$\text{VSWR} = \frac{1 + |S_{11}|}{1 - |S_{11}|}$$

Phase of the transmission coefficient S_{41} is given by

$$\phi = \tan^{-1} \left[\frac{\text{Imaginary part of } S_{41}}{\text{Real part of } S_{41}} \right] \qquad (3.7)$$

and differential phase shift $\Delta\phi$ is given by

$$\Delta\phi = \phi_2 - \phi_1 \qquad (3.8)$$

where ϕ_2 and ϕ_1 are the phases of the transmission coefficients when the diodes are in states 2 and 1, respectively.

Input VSWR, insertion loss and differential phase shift are computed for different values of the line length L. Results obtained for 180° bit are similar to that reported in reference [15] . It is to be noted that one gets minimum phase error over a band of frequencies for L=45° which corresponds to the normalized impedances at the hybrid ports in the two switch states as j and -j (symmetrical to X=0 line on the Smith chart).

90° bit

For 90° bit, ideal 90° switches terminate the hybrid ports. Using terminating impedances $\bar{Z}_1$ and $\bar{Z}_2$, the analysis of this phase bit is carried the same way as for 180° bit discussed earlier.

Input VSWR, insertion loss and differential phase shift are computed for different values of the line length L and are plotted as a function of percentage frequency deviation in Figs. 3.3 to 3.5, we observe that L=22.5° gives the minimum phase error in this case. This corresponds to the normalized impedances at the hybrid ports in the two states as j2.4143 and -j2.4143 (symmetrical to X=0 line on the Smith chart).

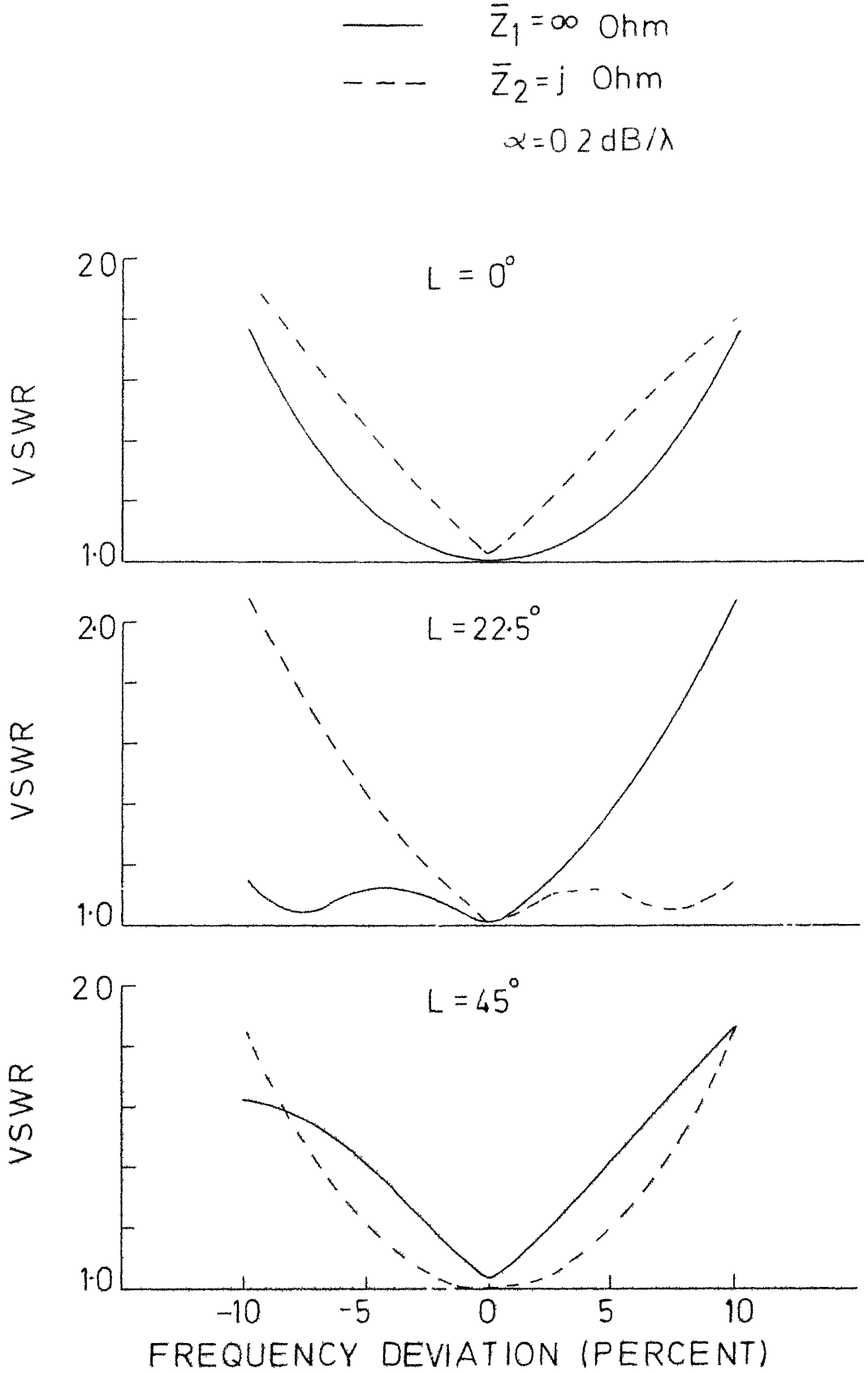


FIG. 3.3 CALCULATED VSWR PLOT FOR 90° PHASE BIT USING TWO-BRANCH HYBRID.

— $\bar{Z}_1 = \infty$ Ohm

--- $\bar{Z}_2 = j$ Ohm

$\alpha = 0.2$ dB/λ

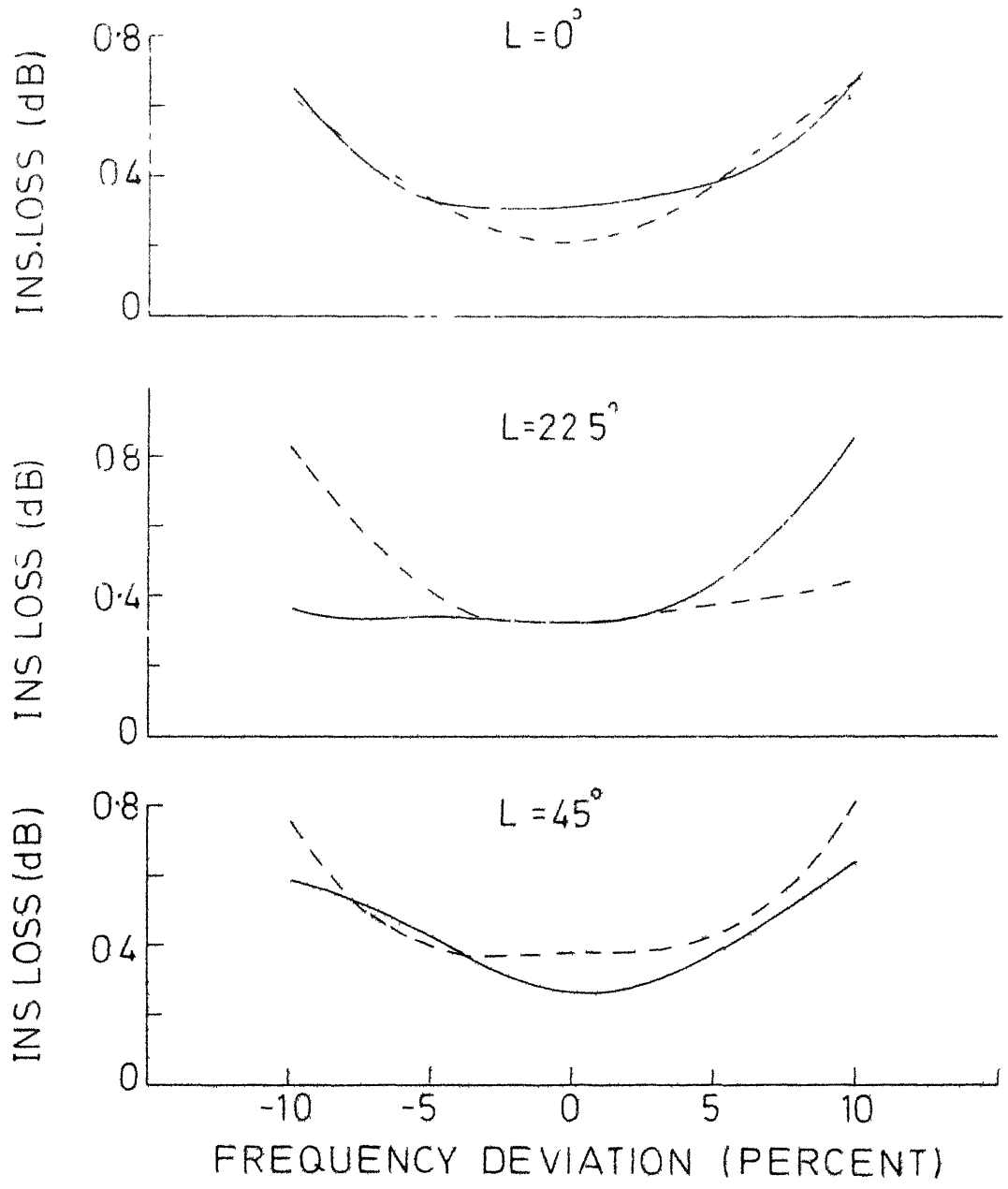


FIG. 3.4 CALCULATED INSERTION LOSS PLOT FOR 90° PHASE BIT USING TWO-BRANCH HYBRID.

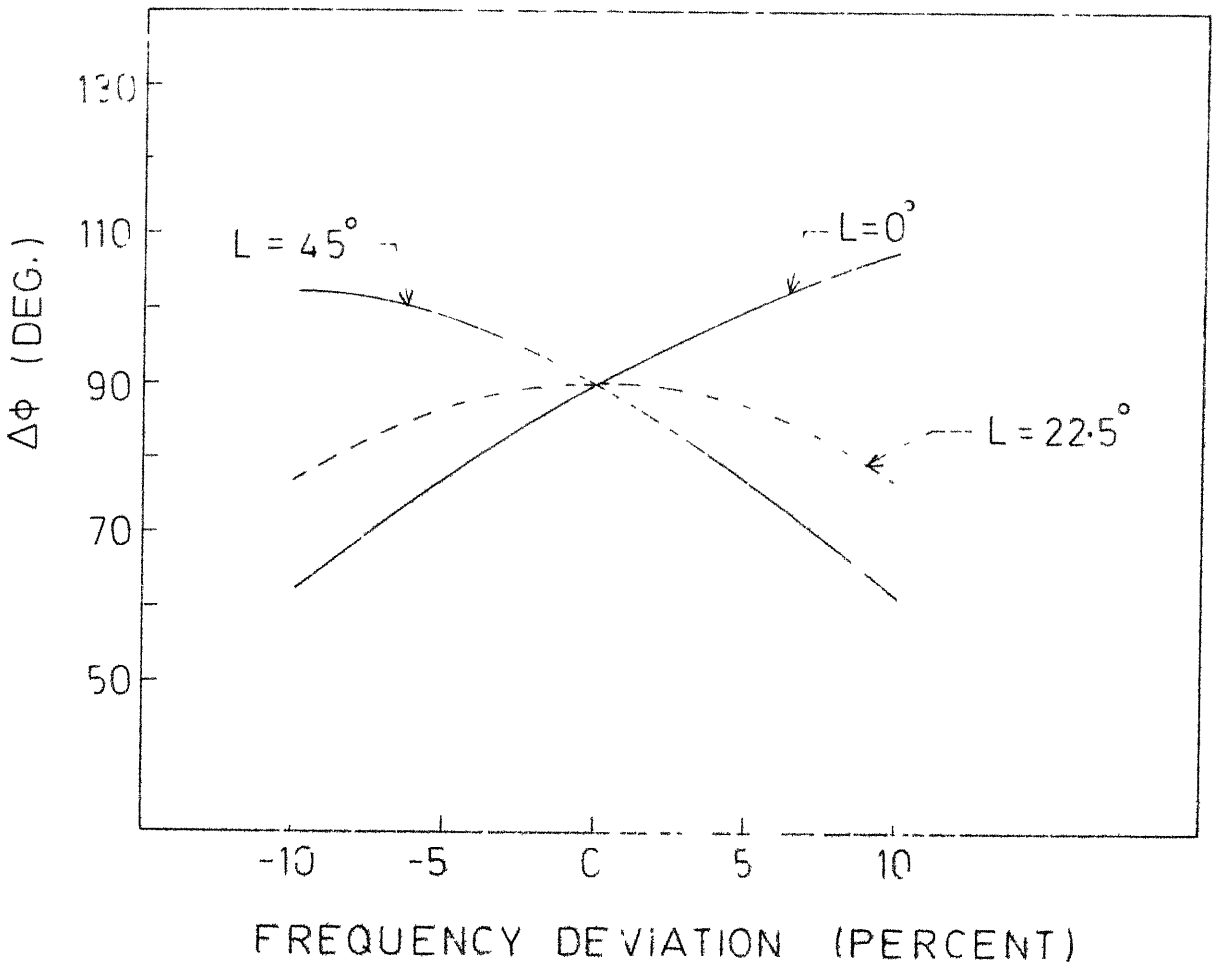


FIG. 3.5 CALCULATED DIFFERENTIAL PHASE SHIFT ($\Delta \phi$) PLOT FOR 90° PHASE BIT USING TWO-BRANCH HYBRID.

3.3.2 Circuit Using Three-Branch Hybrid

Figure 3.6(a) shows a three-branch hybrid and the corresponding phase shifter circuit using this hybrid is shown in Fig. 3.6(b). In this circuit also the switches are connected to the coupled ports with equal line lengths (L) of admittance Y_o between the switches and the hybrid ports.

180° bit

In this case 180° ideal switches are connected to the hybrid ports. Analysis of this circuit is also carried out in the same manner as in the two-branch case.

Overall ABCD matrix for the even mode circuit shown in Fig. 3.7(a) can be written as

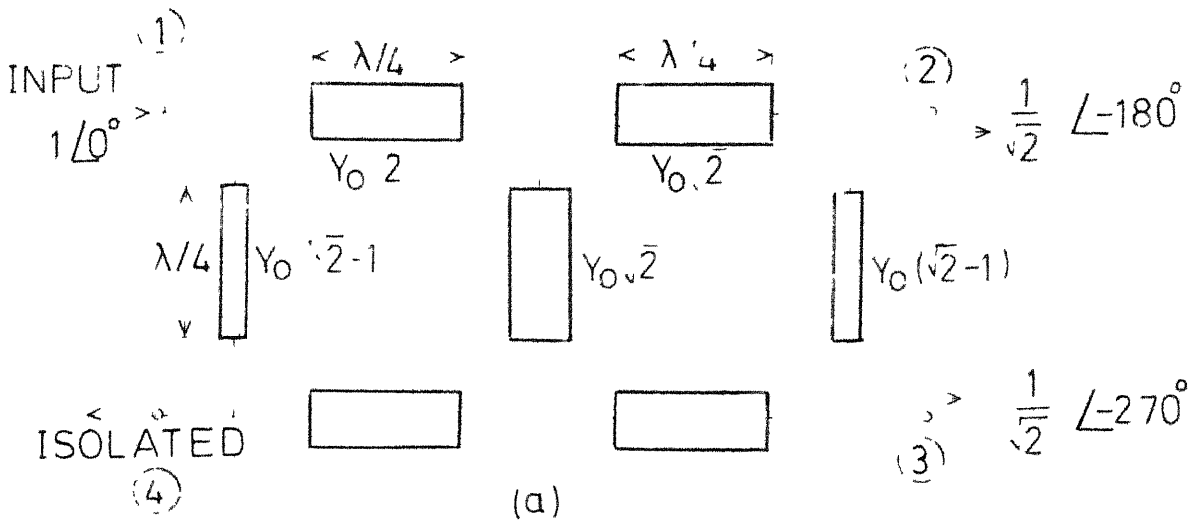
$$[M_{e1}] = [M_1] \cdot [M_2] \cdot [M_3] \cdot [M_2] \cdot [M_1] \cdot [M_4] \qquad (3.9)$$

with

$$[M_1] = \begin{bmatrix} 1 & 0 \\ (\sqrt{2}-1)\tanh(\gamma_3 \ell_1/2) & 1 \end{bmatrix}$$

$$[M_2] = \begin{bmatrix} \cosh \gamma_2 \ell_1 & \frac{1}{\sqrt{2}} \sinh \gamma_2 \ell_1 \\ \sqrt{2} \sinh \gamma_2 \ell_1 & \cosh \gamma_2 \ell_1 \end{bmatrix}$$

$$[M_3] = \begin{bmatrix} 1 & 0 \\ \sqrt{2} \tanh(\gamma_2 \ell_1/2) & 1 \end{bmatrix}$$



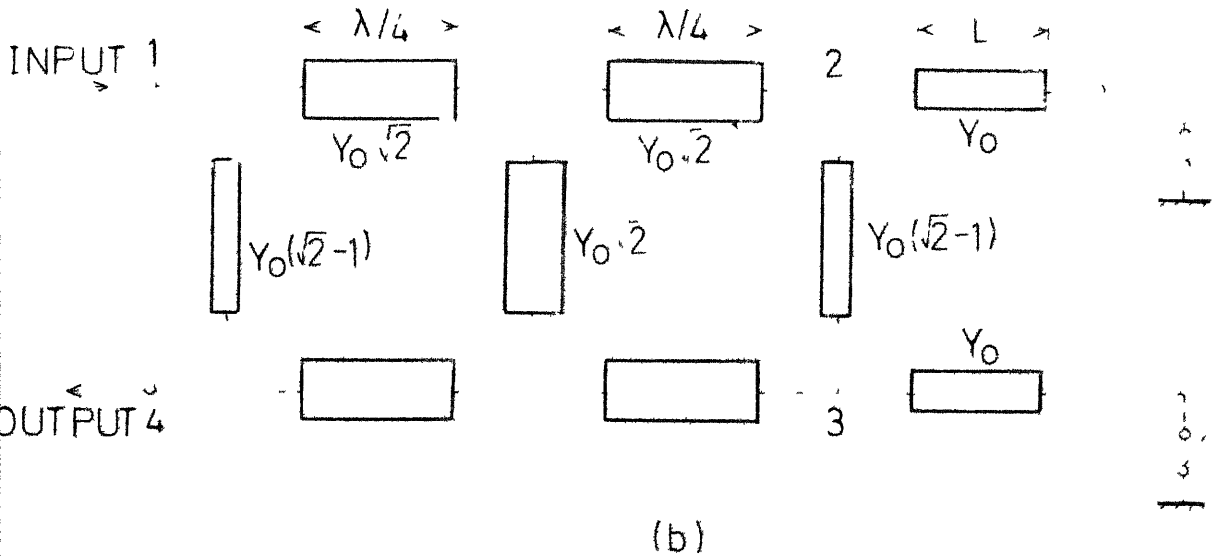
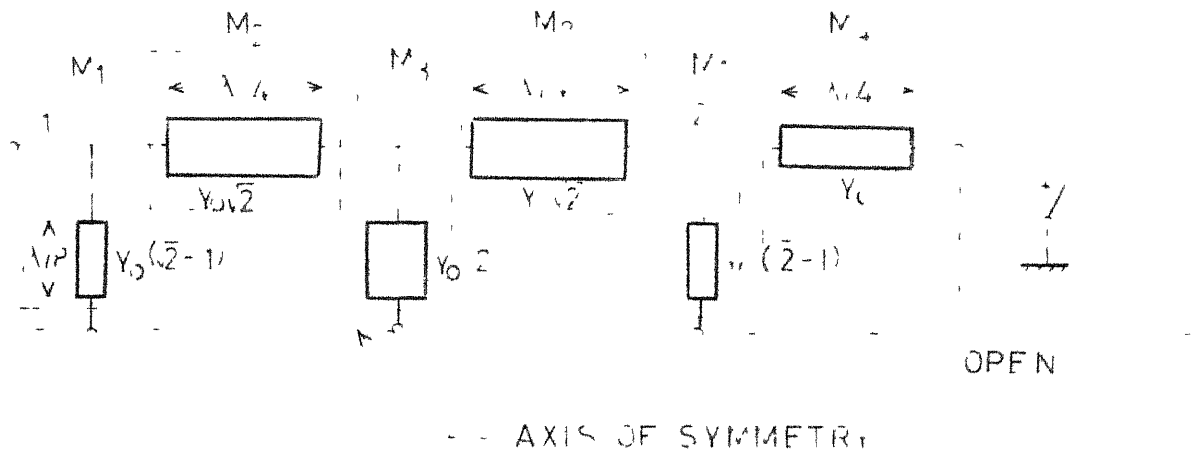
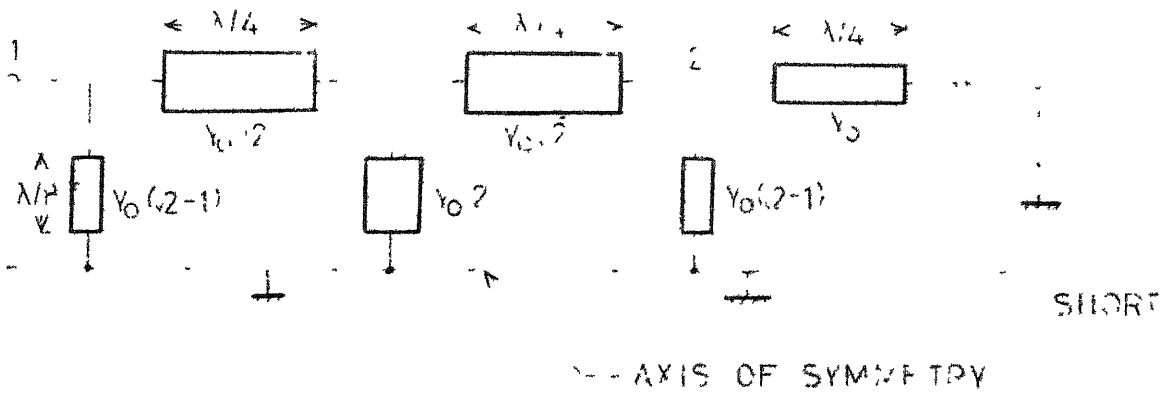


FIG. 3.6 ELECTRICAL EQUIVALENT CIRCUIT FOR
(a) THREE-BRANCH HYBRID, AND
(b) THREE-BRANCH HYBRID PHASE BIT USING IDEAL SWITCHES.



(a) EVEN MODE



(b) ODD MODE

FIG. 3.7 EVEN MODE AND ODD MODE REPRESENTATIONS FOR THE CIRCUIT OF FIG. 3.6(b).

where M_1, M_2, M_3 and M_4 are ABCD matrices for various elements as shown in Fig. 3.7(a).

Even mode matrix when the switches are in the other state (state 2) is obtained by changing the load impedance Z_L of the switch.

The odd-mode circuit is shown in Fig. 3.7(b). The shunt elements in this case are short circuited instead of being open in the even mode circuit and the corresponding matrices are represented by dashed matrices (M_1' and M_3'). The odd mode matrix can be written as

$$[M_{o1}] = [M_1'] \cdot [M_2] \cdot [M_3'] \cdot [M_2] \cdot [M_1'] \cdot [M_4] \qquad (3.10)$$

with

$$[M_1'] = \begin{bmatrix} 1 & 0 \\ (\sqrt{2}-1)\coth(\gamma_3 \ell_1/2) & 1 \end{bmatrix},$$

$$[M_3'] = \begin{bmatrix} 1 & 0 \\ \sqrt{2}\coth(\gamma_2 \ell_1/2) & 1 \end{bmatrix},$$

where M_1' and M_3' are ABCD matrices for the elements shown in Fig. 3.7(b).

Once the overall matrices for the even and odd mode for both the states of the switches are known circuit performance

can be evaluated by using Eqns. (3.4) through (3.8). Figs. (3.8) to (3.10) give the plot of VSWR, insertion loss and differential phase shift of the phase shifter as a function of percentage frequency deviation for different line lengths (L) between the switch and the hybrid port. From these plots we observe that bandwidth of more than 20% can easily be achieved from this phase bit. The effect of line length L is not very significant on the phase error, still L=45° gives the minimum phase deviation around the nominal phase shift $\Delta\emptyset$. Phase variation around the centre frequency is symmetrical for L=45°. It reduces with frequency deviations on either side of the centre frequency.

90° bit

For 90° bit ideal 90° switches terminate the hybrid ports. The analysis of this phase bit is carried out the same manner as for 180° bit.

Input VSWR, insertion loss and differential phase shift are computed for different values of the line length L and are plotted as a function of percentage frequency deviation in Figs. 3.11 to 3.13. We note that L=22.5° gives the minimum phase error and the phase variation is symmetrical about the centre frequency. The overall performance of 90° bit is found to be better than that of 180° bit.

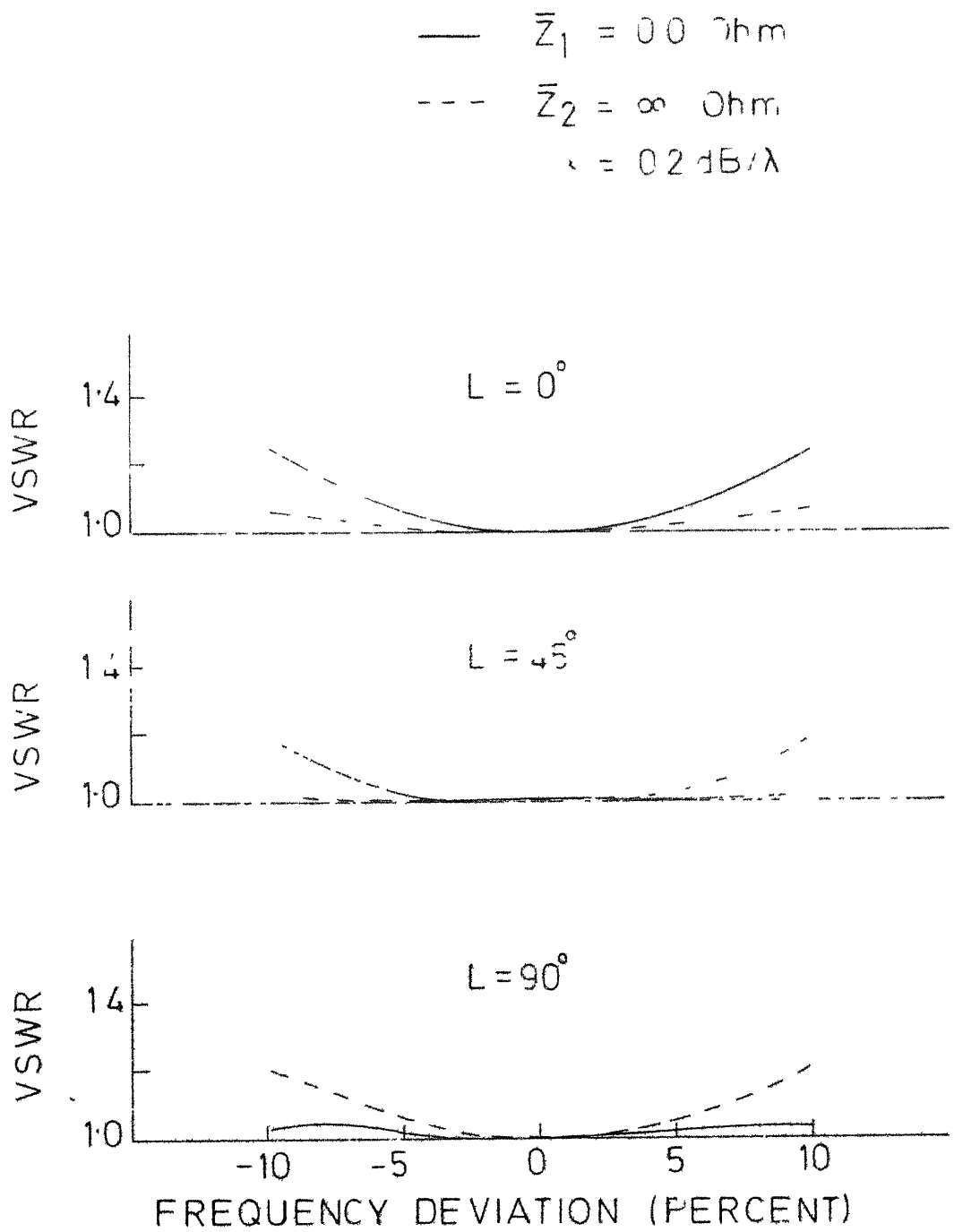


FIG. 3.8 CALCULATED VSWR PLOT FOR 180° PHASE BIT USING THREE-BRANCH HYBRID.

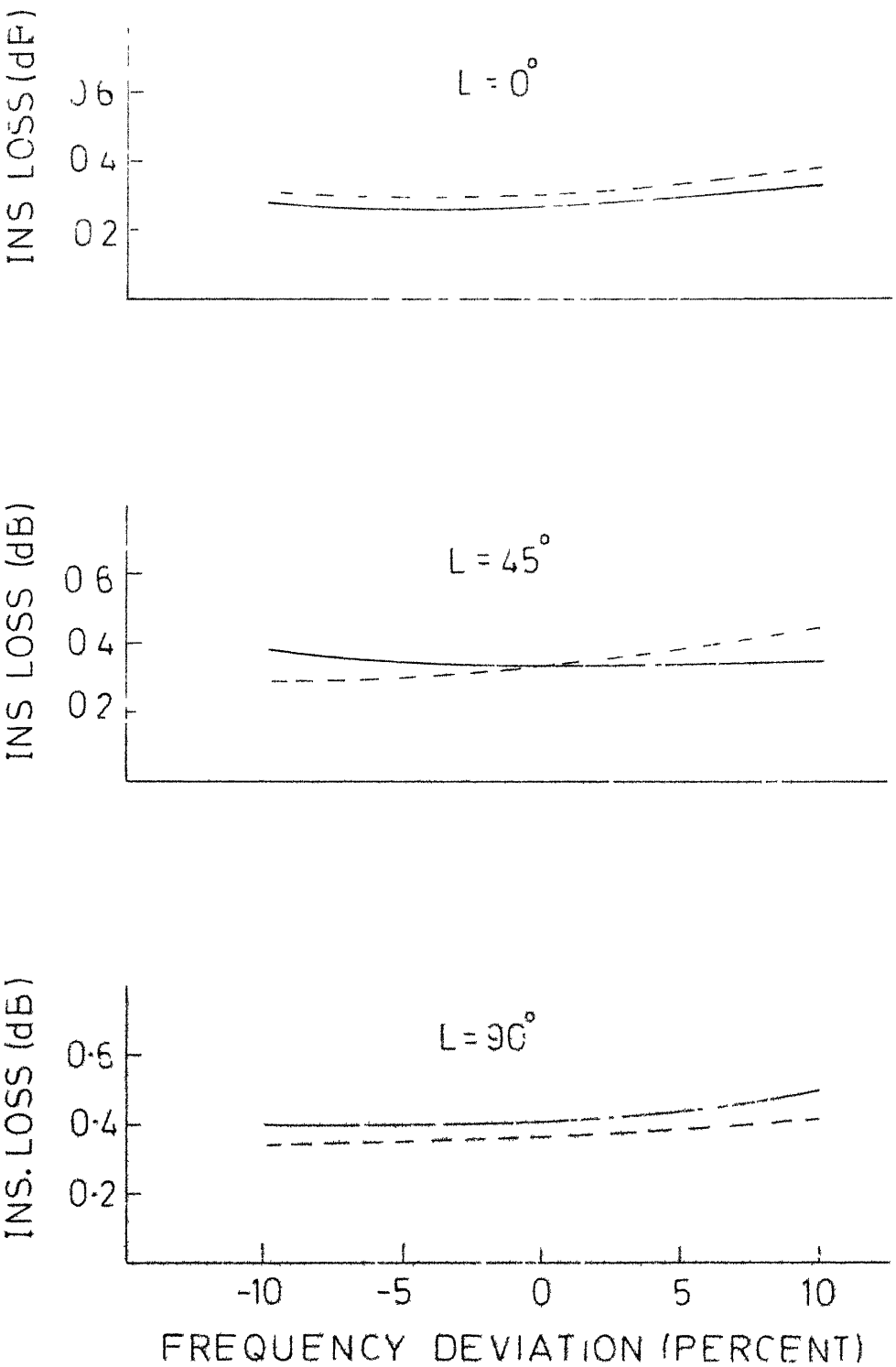


FIG. 3.9 CALCULATED INSERTION LOSS PLOT FOR 180° PHASE BIT USING TIRED-BRANCH HYBRID.

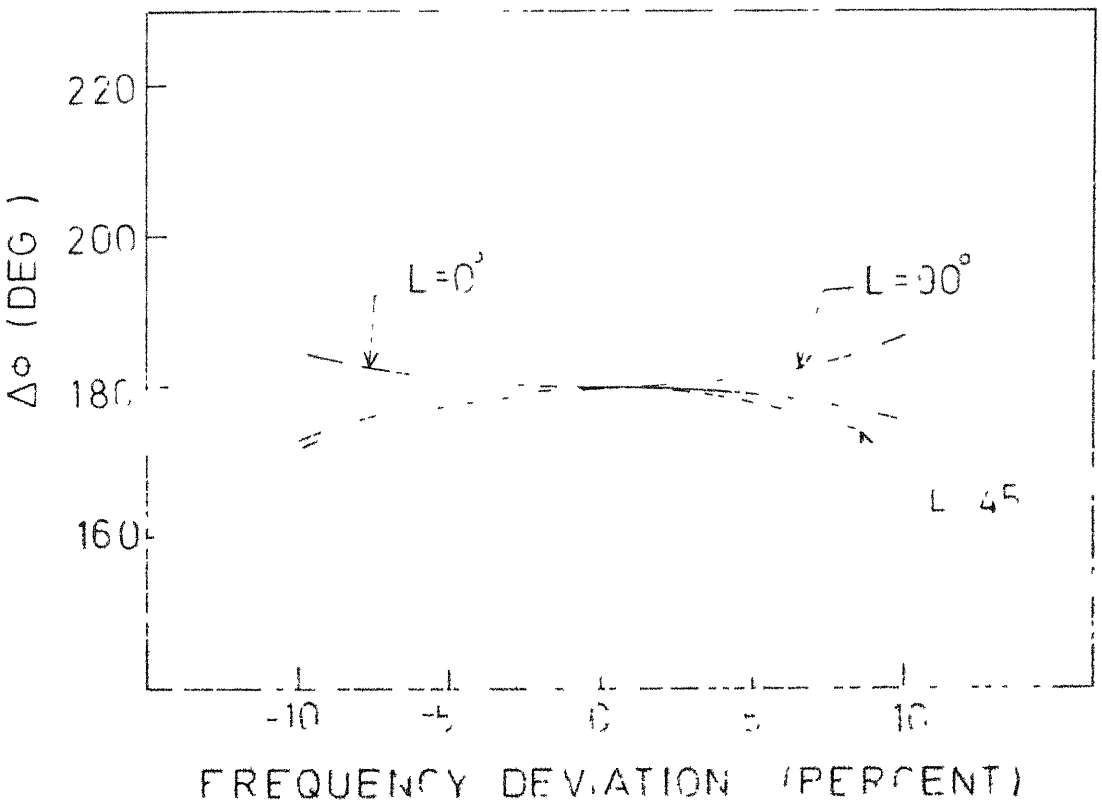


FIG. 3.10 CALCULATED DIFFERENTIAL PHASE SHIFT ($\Delta\phi$) PLOT FOR 180° PHASE BIT USING THREE-BRANCH HYBRID.

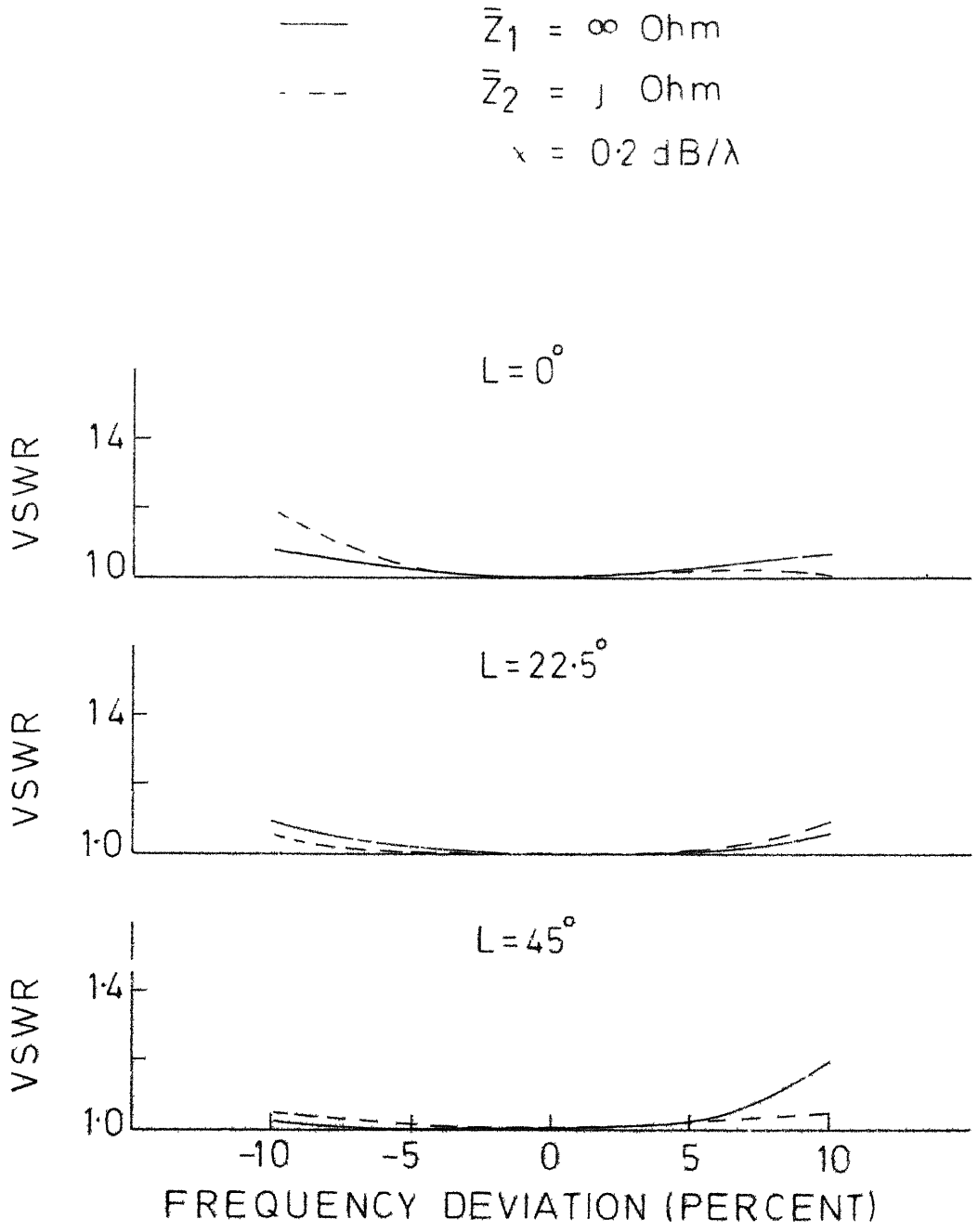


FIG. 3.11 CALCULATED VSWR PLOT FOR 90° PHASE BIT USING THREE-BRANCH HYBRID.

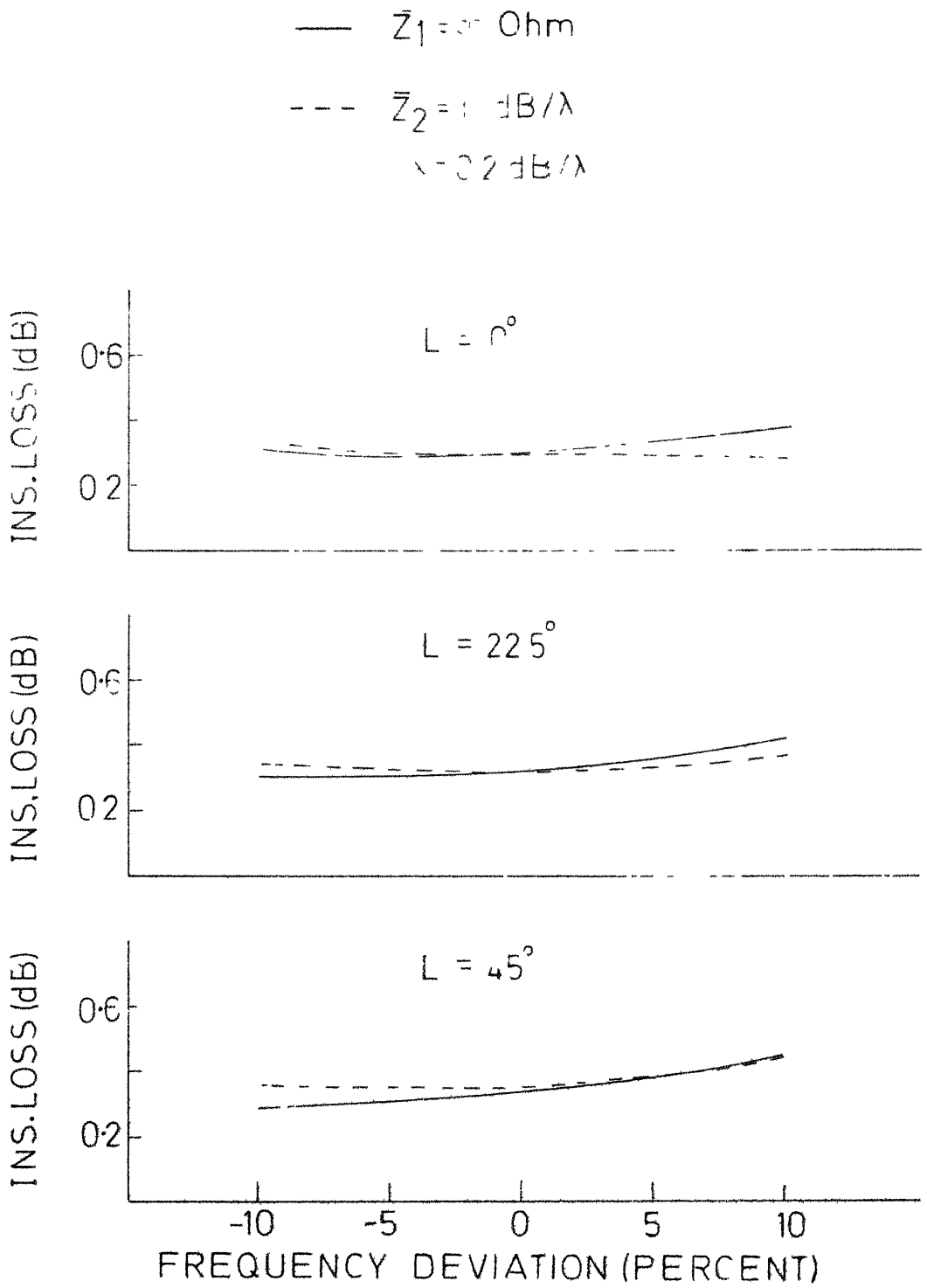


FIG. 3.12 CALCULATED INSERTION LOSS PLOT FOR 90° PHASE BIT USING THREE-BRANCH HYBRID.

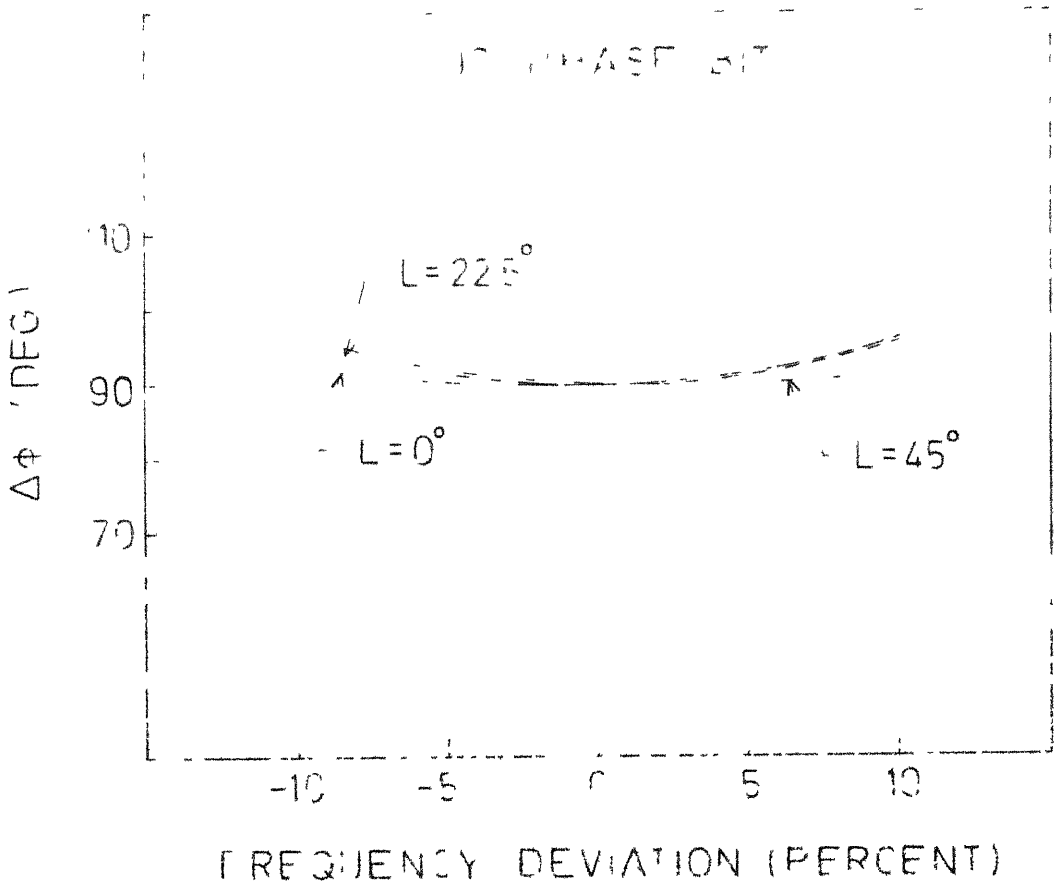


FIG. 3.13 CALCULATED DIFFERENTIAL PHASE SHIFT ($\Delta\phi$) PLOT FOR 90° PHASE BIT USING THREE-BRANCH HYBRID.

3.4 PHASE SHIFTERS USING RAT-RACE HYBRID

Rat-race coupler is a 180° hybrid. It consists of a ring of $3\lambda/2$ circumference. Figure 3.14(a) shows a ratrace coupler. If the power is fed at port 1, it emerges out from ports 2 and 4 in the same phase and port 3 acts as an isolated port. If the input is at port 2 power couples to ports 1 and 3 with phase difference of 180°, and port 4 becomes the isolated port.

Isolation and VSWR bandwidths for the rat-race hybrid are about three times that of two-branch hybrid and are comparable to three-branch hybrid (Table 3.1). Phase bandwidth for rat-race is poor (about 12%). Bandwidth for amplitude coupling for ratrace is better than two-branch and is about the same as for three-branch.

Figure 3.14(b) shows a phase shifter using ratrace hybrid. The extra quarter wavelength line may be placed either in port 2 or port 4. If it is placed in port 2 the resulting bandwidth is narrow [22] due to extra distance (one wavelength) travelled by the wave reflected from port 2 than the wave reflected from port 4. The waves while recombining at port 3 should not only have the same phase but also have travelled the same length which is possible by placing it in port 2.

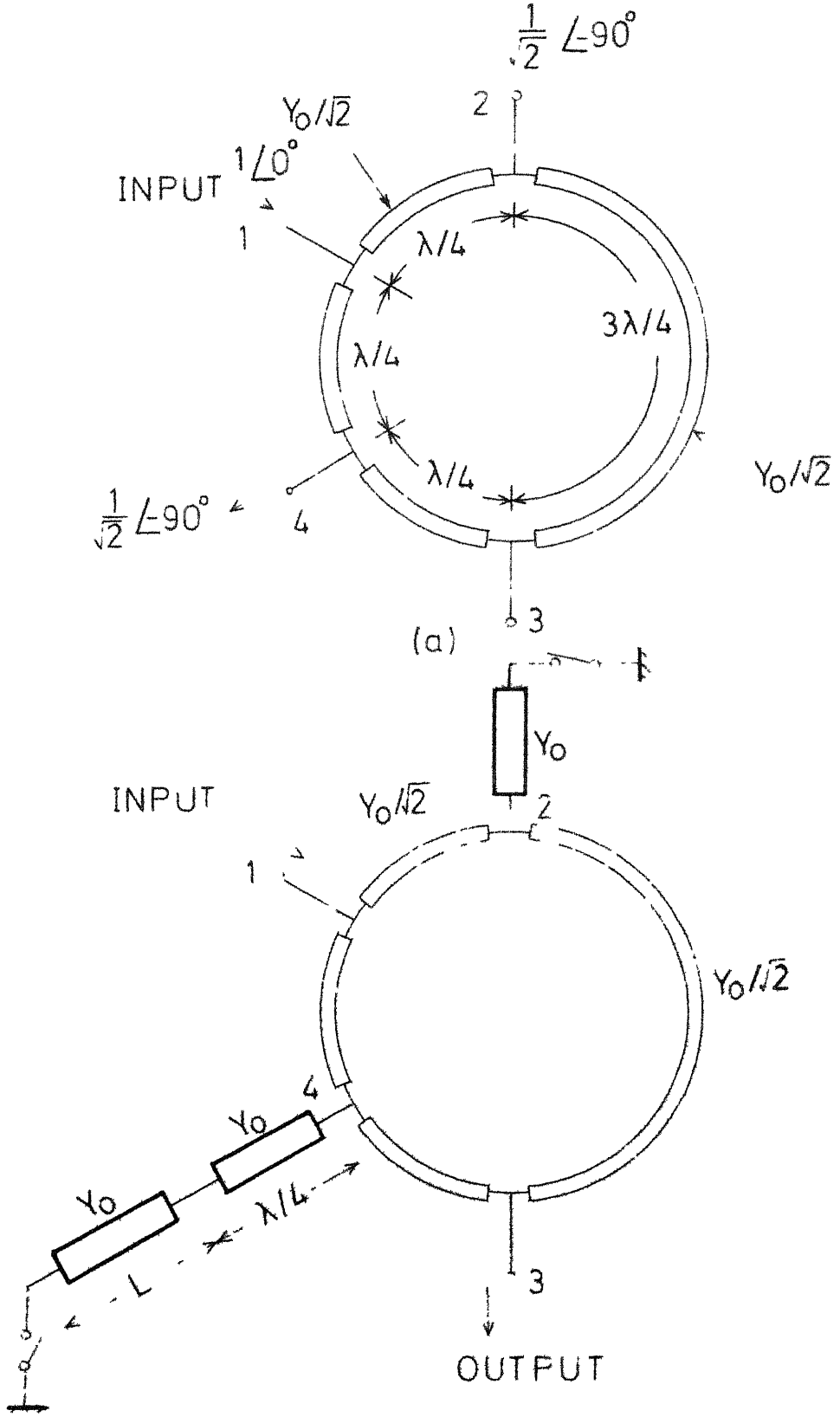
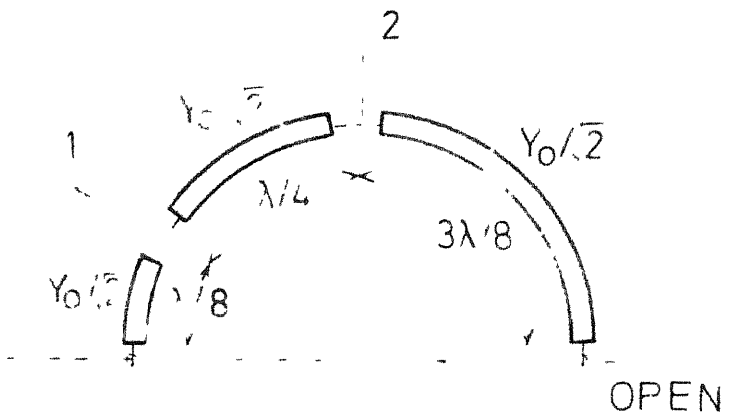


FIG. 3.14 ELECTRICAL EQUIVALENT CIRCUIT FOR
(a) RAT-RACE HYBRID AND
(b) RAT-RACE HYBRID PHASE BIT USING IDEAL SWITCHES

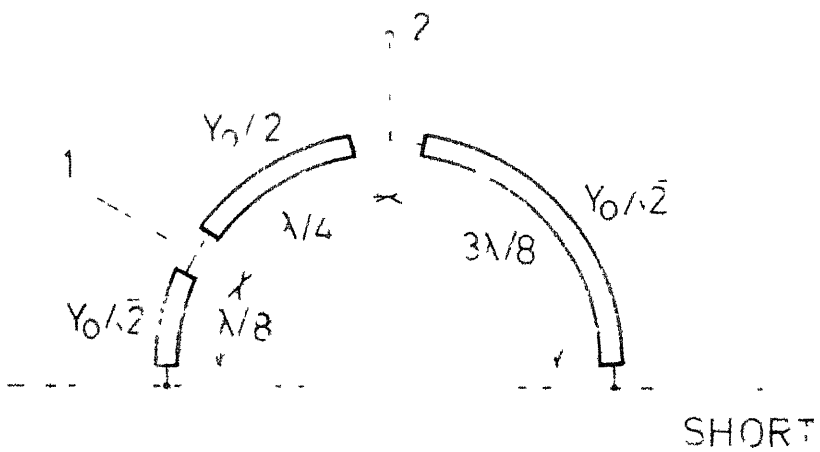
Phase shifter circuits using ratrace hybrid do not possess a plane of symmetry (although ratrace hybrid is symmetrical), hence even and odd mode analysis cannot be used for analyzing this circuit. The analysis is carried out by scattering matrix approach.

The scattering matrix of the ratrace hybrid is given by Eqn. (2.10). If the reflection coefficients at port 2 and 4 are Γ_2 and Γ_4, respectively, then the scattering matrix of the phase shifter is given by Eqn.(2.11)and Eqn. (2.12).

To evaluate the phase shifter performance using Eqn. (2.12), the scattering parameters of the rat-race hybrid and the reflection coefficients Γ_2 and Γ_4 are needed. Scattering parameters for the rat-race hybrid can be calculated by analyzing the hybrid using even and odd mode symmetry. Figure 3.15 gives the equivalent circuit for rat-race hybrid for the even and odd mode excitations. Analysis similar to what has been used in Section 3.3 is carried out to evaluate even and odd mode matrices. Reflection and transmission coefficients for the even and odd modesare found using Eqns.(3.2)&(3.3).Scattering parameters for the hybrid are calculated using the following relations:



(a) EVEN MODE



(b) ODD MODE

FIG. 3.15 EVEN MODE AND ODD MODE REPRESENTATION FOR THE CIRCUIT OF FIG. 3.14(a).

$$
\begin{aligned}
S_{11} &= (S_{11e} + S_{11o})/2 \\
S_{22} &= (S_{22e} + S_{22o})/2 \\
S_{21} &= (S_{21e} + S_{21o})/2 \\
S_{31} &= (S_{21e} - S_{21o})/2 \\
S_{41} &= (S_{11e} - S_{11o})/2 \\
S_{32} &= (S_{22e} - S_{22o})/2
\end{aligned}
\qquad (3.11)
$$

Knowing the scattering parameters of the hybrid reflection and transmission coefficients for the phase shifter are calculated. Phase shifter performance can easily be evaluated from S_{11p} and S_{31p}.

By making the corresponding changes in the reflection coefficients Γ_2 and Γ_4 for the two states of the switch and for both 90° and 180° bits, performances for both the phase bits are computed. Results for 180° are similar to those available in [15] and are not included here. For 90° phase bit these results are plotted in Figs. 3.16 to 3.18. These plots give the variation of input VSWR, insertion loss and differential phase shift ($\Delta\phi$) as a function of percentage frequency deviation for different values of L and for two switch states. In this case also the line length of 22.5° gives the minimum phase error.

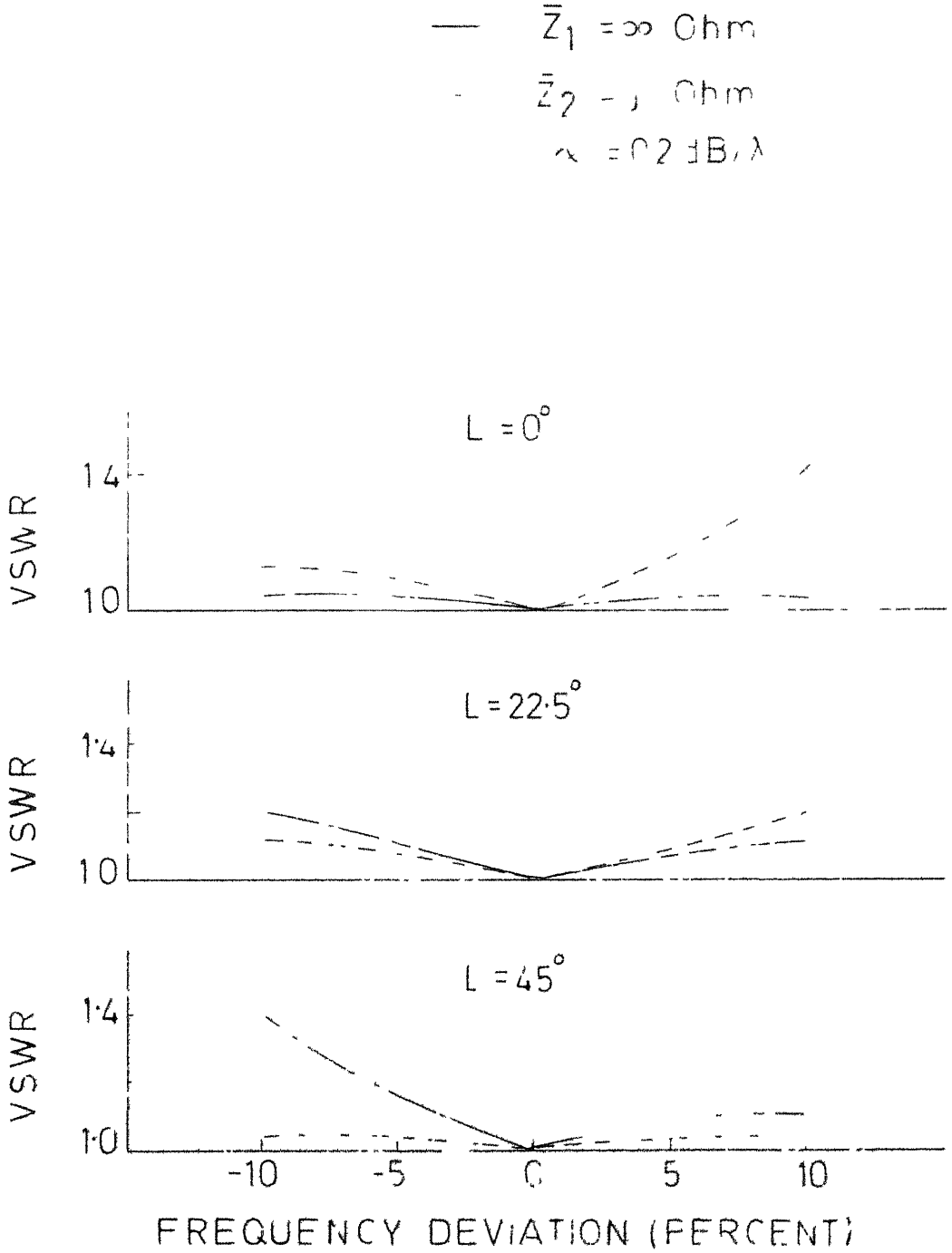


FIG. 3.16 CALCULATED VSWR PLOT FOR 90° PHASE BIT USING RAT-RACE HYBRID.

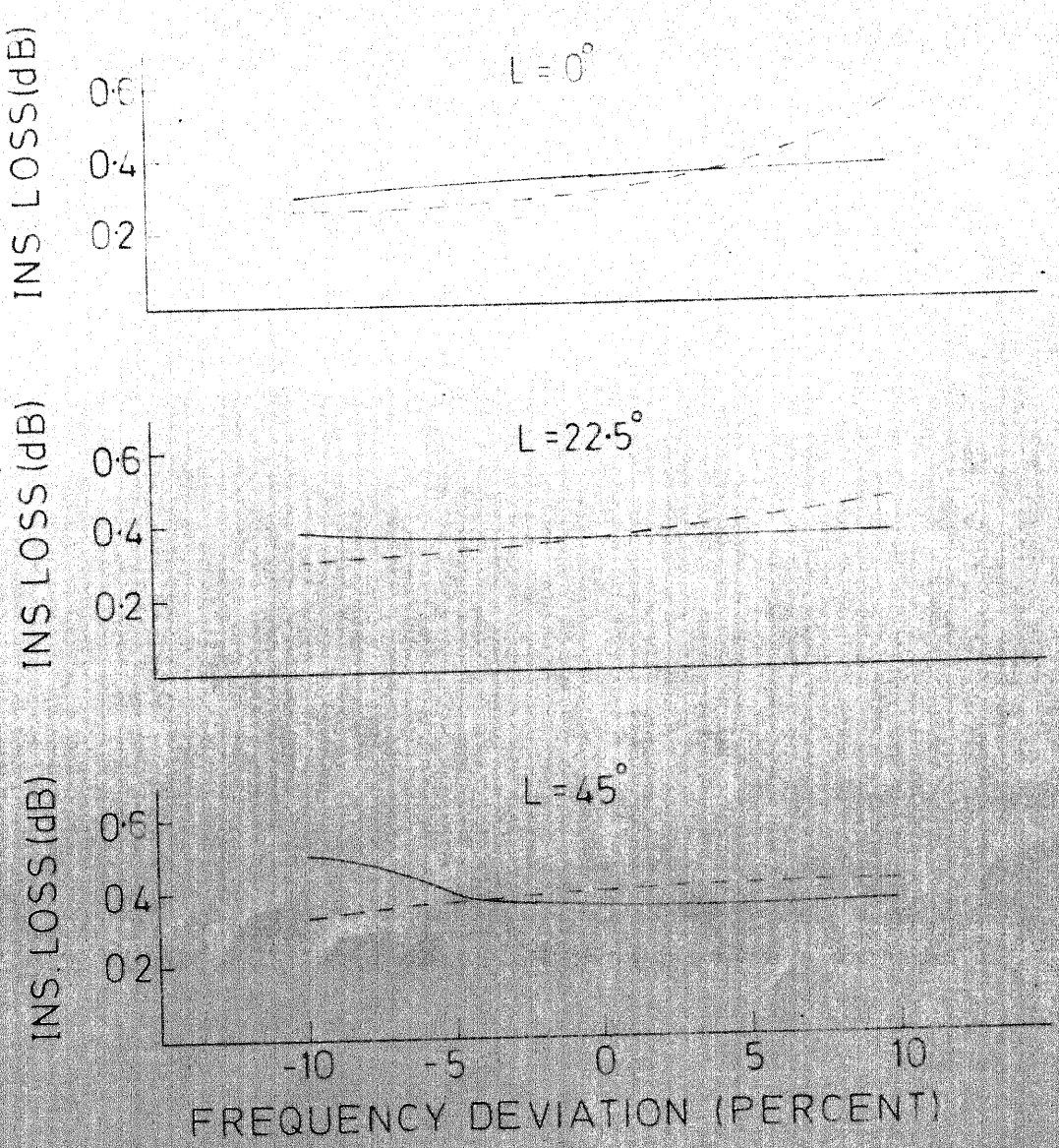


FIG. 3.17 CALCULATED INSERTION LOSS PLOT FOR 90° PHASE BIT USING RAT-RACE HYBRID.

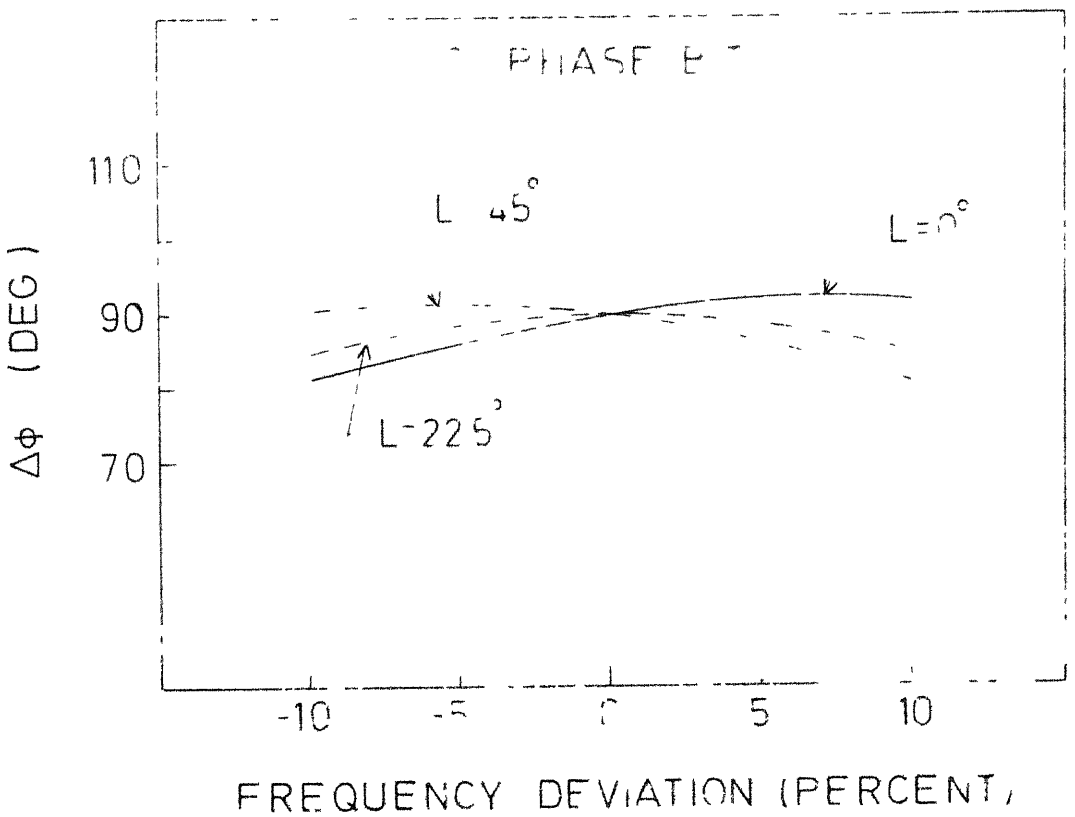


FIG. 5.18 CALCULATED DIFFERENTIAL PHASE SHIFT ($\Delta\phi$) PLOT FOR 90° PHASE BIT USING RAT-RACE HYBRID.

3.5 BANDWIDTH OF PHASE SHIFTERS USING IDEAL SWITCHES

Phase shifter bandwidth has been defined in Section 3.1 and the two specifications considered are used for computing phase shifter bandwidth using ideal switches and two-branch, three-branch and rat-race hybrids.

3.5.1 Phase Shifter Using Two-Branch Hybrid

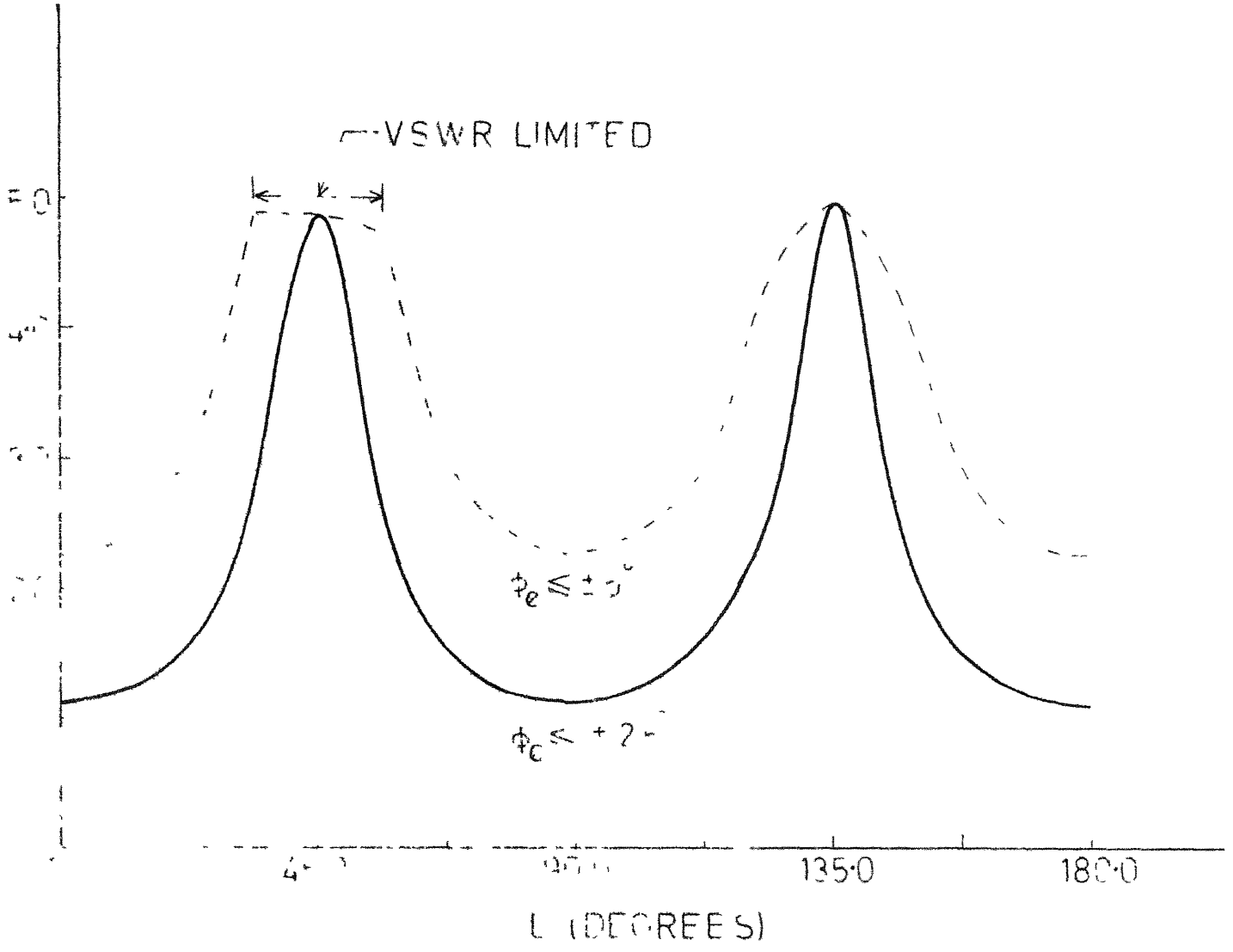
Using the analysis method described in Section 3.3.1, we calculate the nearest frequency f_b at which at least one of the specifications (namely phase error or VSWR) is violated. Bandwidths for both 180° and 90° bits are computed using Eqn. (3.1).

Figures 3.19 and 3.20 give the plot of bandwidth as a function of line length L for both 180° and 90° bits. The continuous curves are for the bandwidth defined for VSWR $\leq$ 1.2 and phase error $(\phi_e) \leq \pm$ 2.5° and the dotted curves are for VSWR $\leq$ 1.2 and phase error $\leq$5°.

For 180° bit, the maximum bandwidth for the two specifications is found to be the same (approx. 5%) and it occurs when the transmission line length L is either 45° or 135°. Both these line lengths place the two switch impedances symmetrical to the Δ=0 line on the Smith chart. It is to be noted that the flattening of the dotted curve ($\phi_e \leq$5°) around

$\bar{Z}_1 = 0\,0$ Ohm

$\bar{Z}_2 = \infty$ Ohm



VARIATION OF PHASE SHIFTER BANDWIDTH WITH LINE LENGTH L FOR 10 DB HYBRID AND 3-BRANCH HYBRID AND IDEAL SWITCHES.

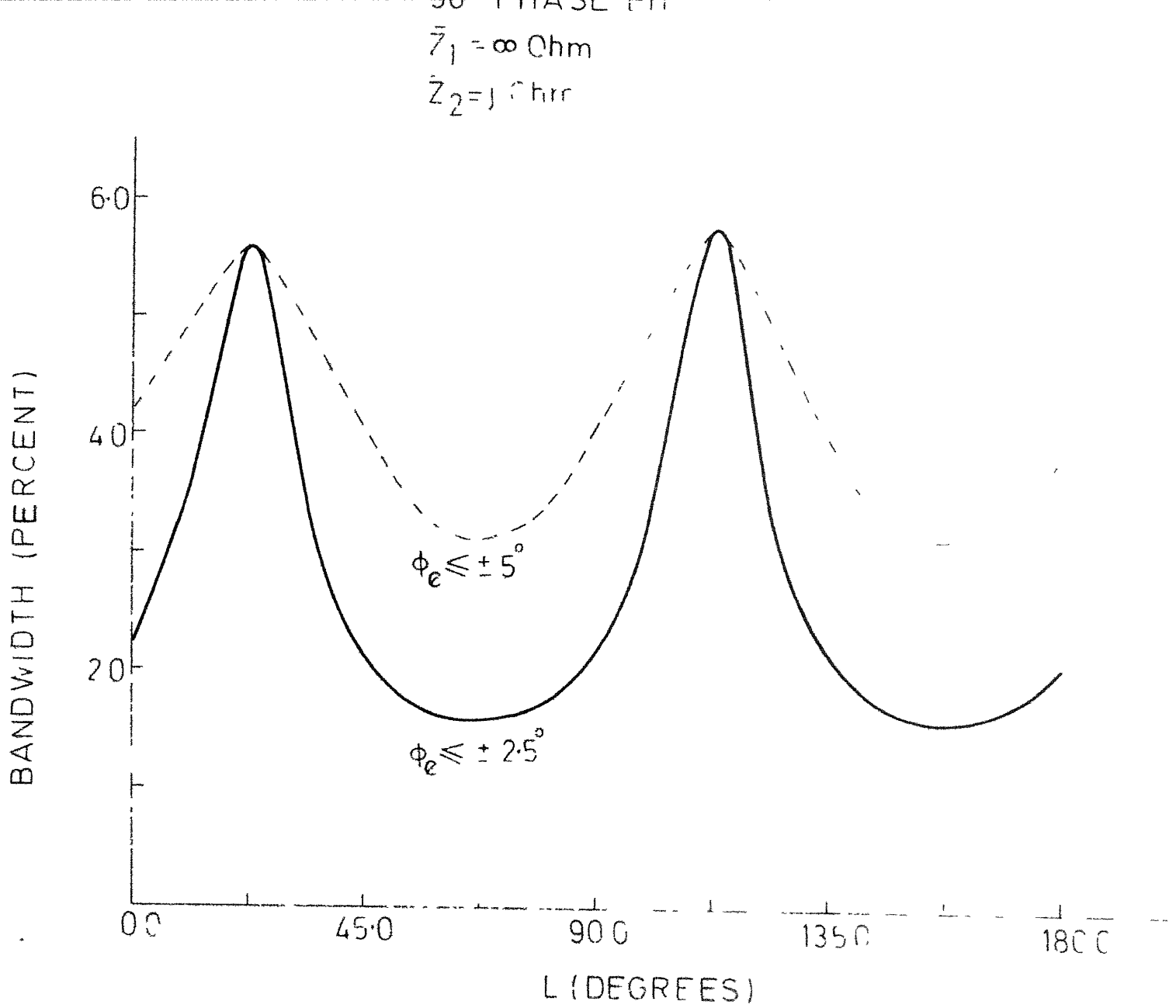


FIG. 3.20 VARIATION OF PHASE SHIFTER BANDWIDTH WITH LINE LENGTH L FOR

L=45° is due to the VSWR limitation (i.e. Bandwidth gets limited due to VSWR specification being violated first).

For 90° bit, the maximum bandwidth is achieved when L=22.5° and 112.5°. The two bandwidths are 5.6% and 5.8% and are approximately equal. L=22.5° places the two switch impedances symmetrically about the open circuit point on the Smith chart, while L=112.5° places them symmetrical to the short circuit point on the Smith chart.

3.5.2 Phase Shifter Using Three-Branch Hybrid

The analysis method described in Section 3.3.2 is used and the bandwidth is calculated using Eqn. (3.1). Computed bandwidths are plotted in Figs. 3.21 and 3.22 for 180° and 90° bits, respectively.

For 180° bit, the maximum bandwidths achieved for the two specifications are not same, as in two-branch hybrid. From the figure we note that the maximum bandwidth is achieved when L=0° for both the bandwidth specifications. Referring Fig. 3.10, which gives the variation of $\Delta\phi$ for L = 0°, 45° and 90°, it may be noted both L=0° and L=90° give less phase error than L=45°. But the total phase deviation ($\Delta\phi_{max} - \Delta\phi_{min}$) is more than for the case of L=45°.

90° bit using three-branch hybrid does not give the unique optimum line length when one considers the phase error

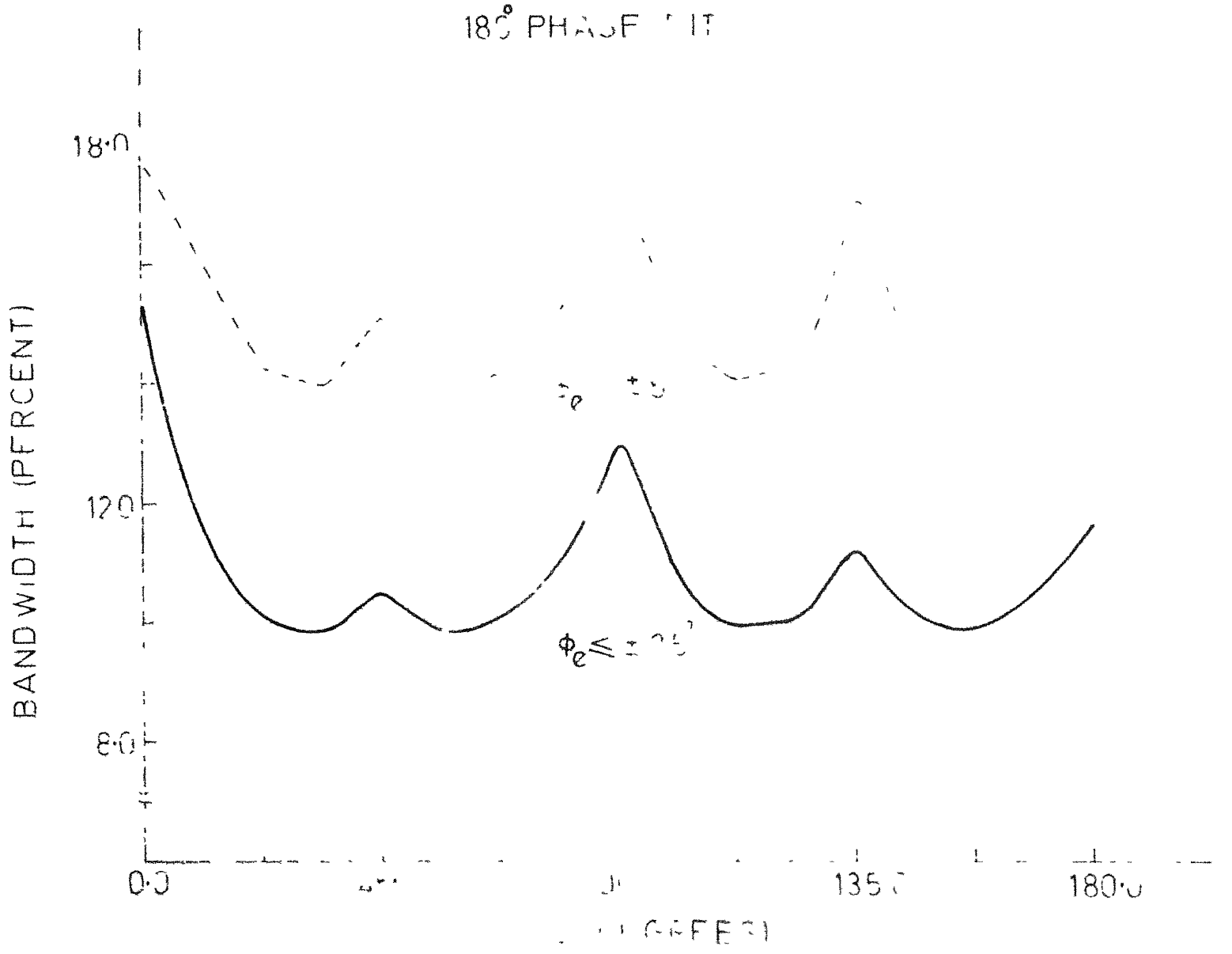


FIG. 3.21 VARIATION OF [illegible] BANDWIDTH WITH LINE LENGTH L FOR [illegible] HYBRID AND IDEAL SWITCHES.

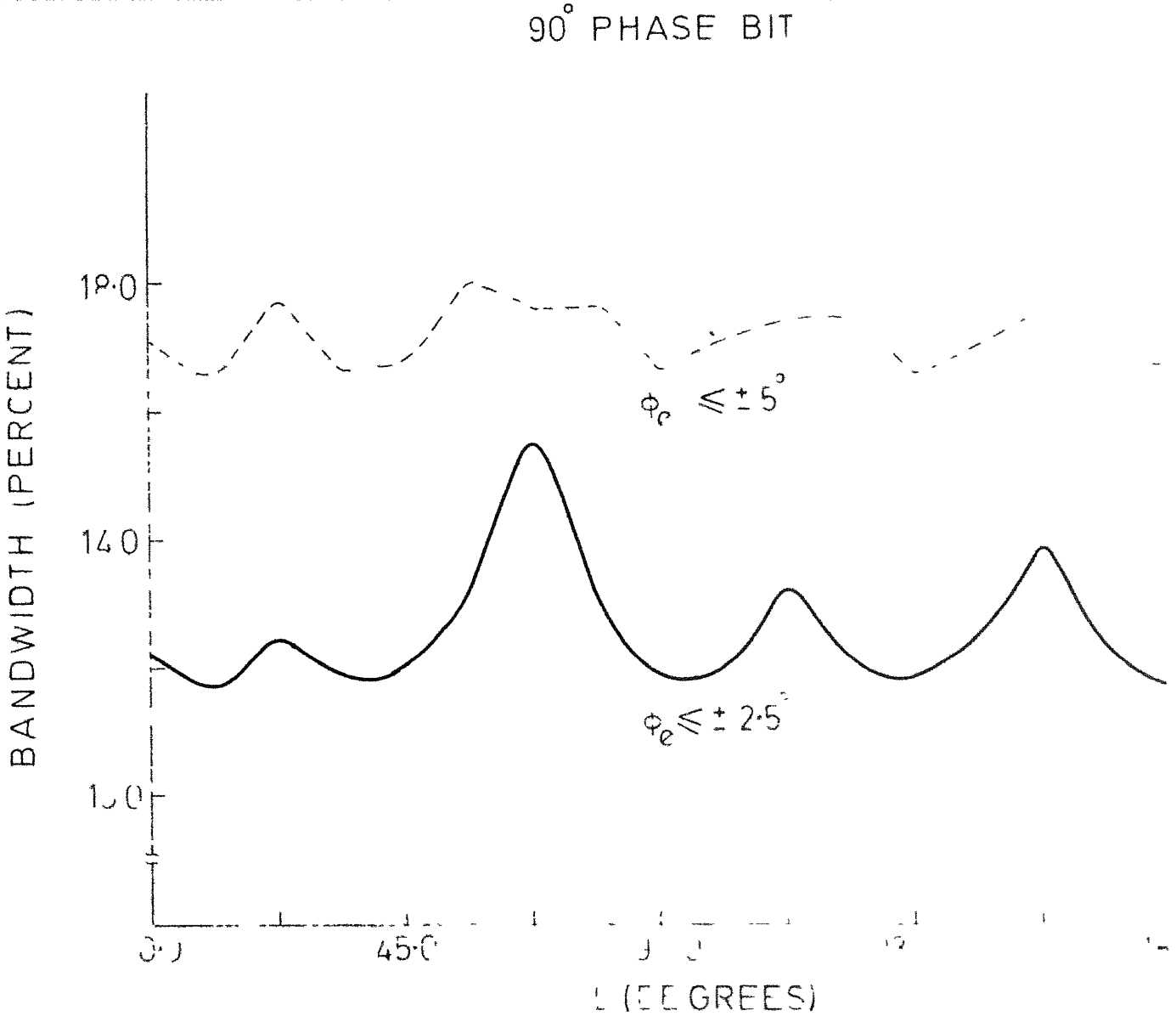


FIG. 3.22 VARIATION OF [illegible] 90° BIT USING THREE-BRANCH HYBRID [illegible]

However an optimum is obtained when the total phase deviation is considered. Table 3.2 gives the maximum phase deviation in a phase bit using three-branch hybrid for ±10% frequency deviation. It is noted that the minimum phase deviation for 180° bit is obtained when L=45° and 135° as was predicted. Similarly, for 90° bit minimum phase deviation is obtained for L= and 112.5°. The effect of line length L on phase shifter bandwidth (or phase error) using three-branch hybrid is not as pronounced as in two branch case.

3.5.3 Phase Shifter Using Rat-race Hybrid

Bandwidth of phase shifter using a rat-race hybrid and ideal switches has also been calculated. Analysis given in Section 3.4 is used for these calculation. Figures 3.23 and 3.24 show the plot of bandwidth for 180° and 90° bits for the two specifications of the bandwidth. As expected the 180° phase bit gives bandwidth peaks for L=45° and 135°. The peak at L=45° gives 10.2% bandwidth while for L=135° the bandwidth peaks to 8.6%. The probable reason for this difference is that as the line length (L) increases the frequency sensitiveness of the phase bit also increases and the bandwidth starts getting limited by the VSWR of the phase bit. This becomes more pronounced because of the additional $\lambda/4$ line length being used with one of the coupled ports.

TABLE 3.2 Maximum phase deviation for ±10% frequency deviation for three-branch hybrid.

L(in deg.) / Phase Bit	0	22.5	45	67.5	90	112.5	135	157.5	180
180°	8.95	9.67	8.06	9.92	14	10.65	5.88	11.95	17.69
90°	6.66	6.06	6.94	9.10	7.00	4.56	7.94	11.95	8.94

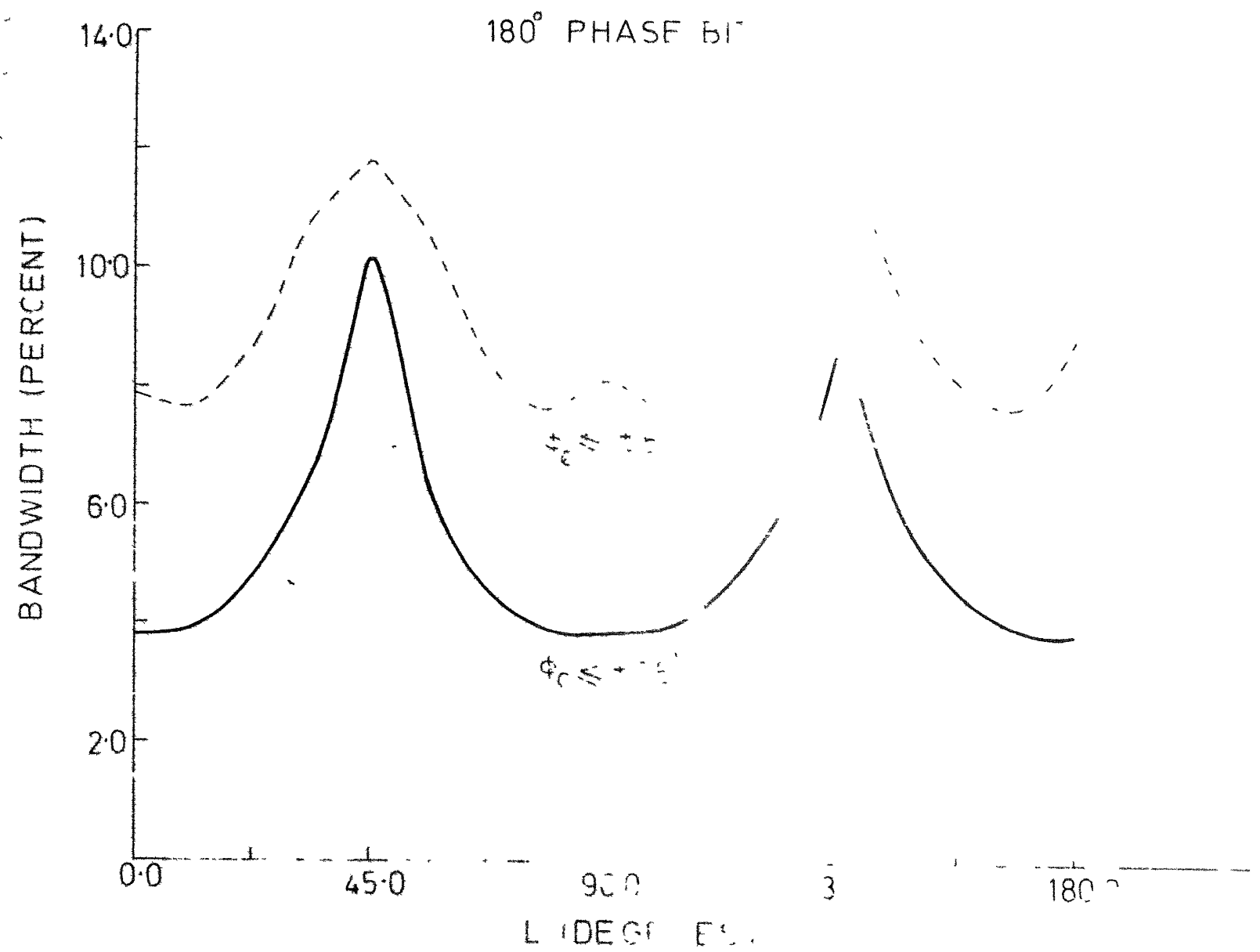


FIG. 3.23 VARIATION OF [illegible] WITH [illegible] FOR 180° BIT CODING RATIO [illegible]

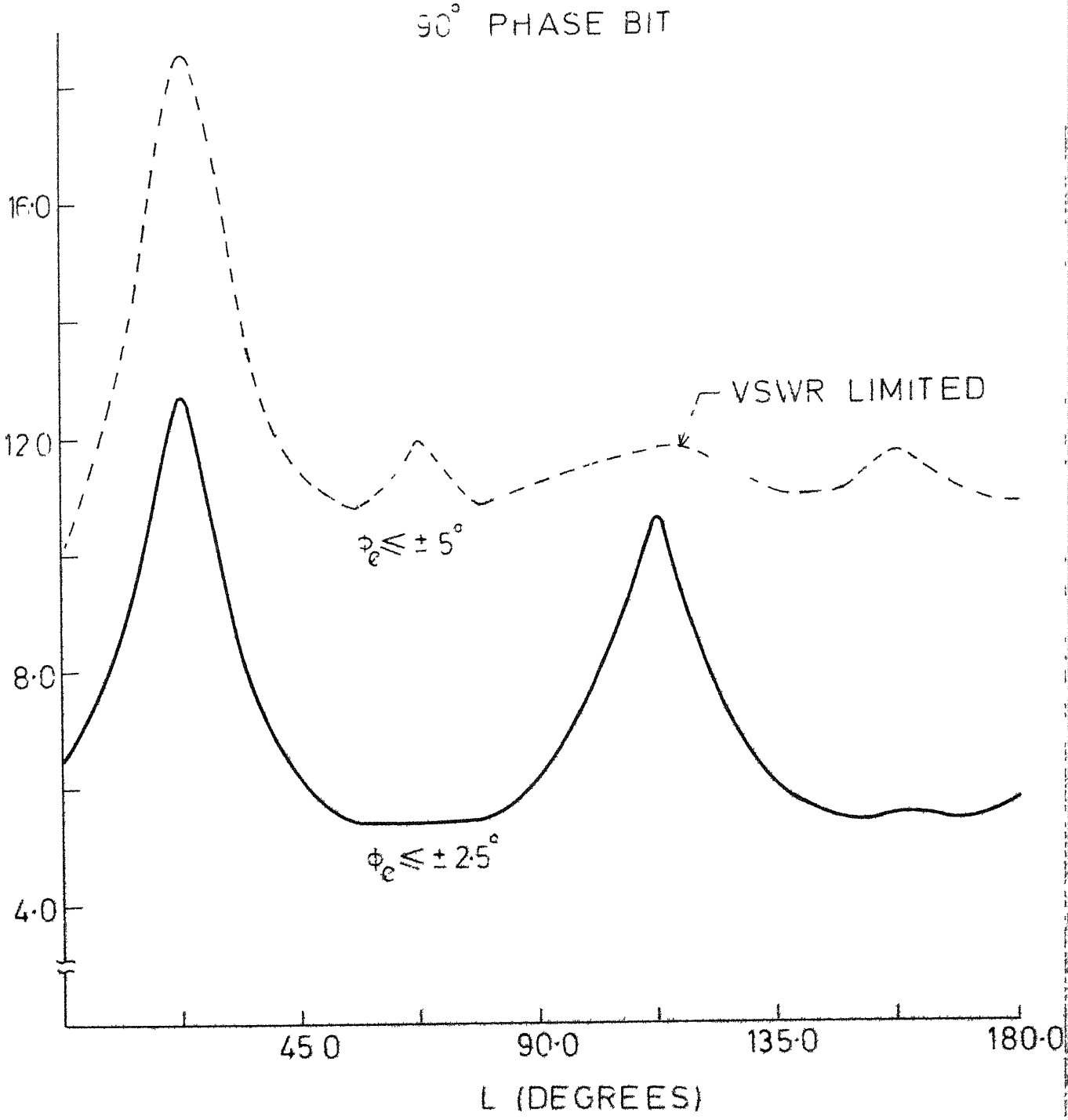


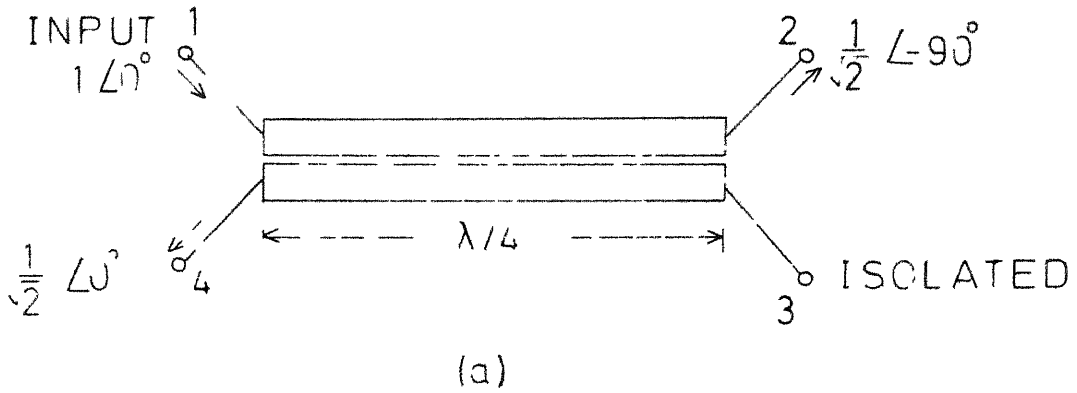
FIG. 3.24 VARIATION OF PHASE SHIFTER BANDWIDTH WITH LINE LENGTH L FOR 90° BIT USING RAT-RACE HYBRID AND IDEAL SWITCHES.

For 90° bit, the peaks occur for L=22.5° and 112.5° as expected. For $\phi_e \leq \pm 5°$ the second peak at L=112.5° got supressed due to VSWR limitation. For $\phi_e \leq \pm 2.5°$ both peaks are present but peak at L=45° gives bandwidth of 12.7% while the one at L=112.5° gives bandwidth of 10.6%. The same reasoning as for 180° bit can be attributed to this difference in bandwidths.

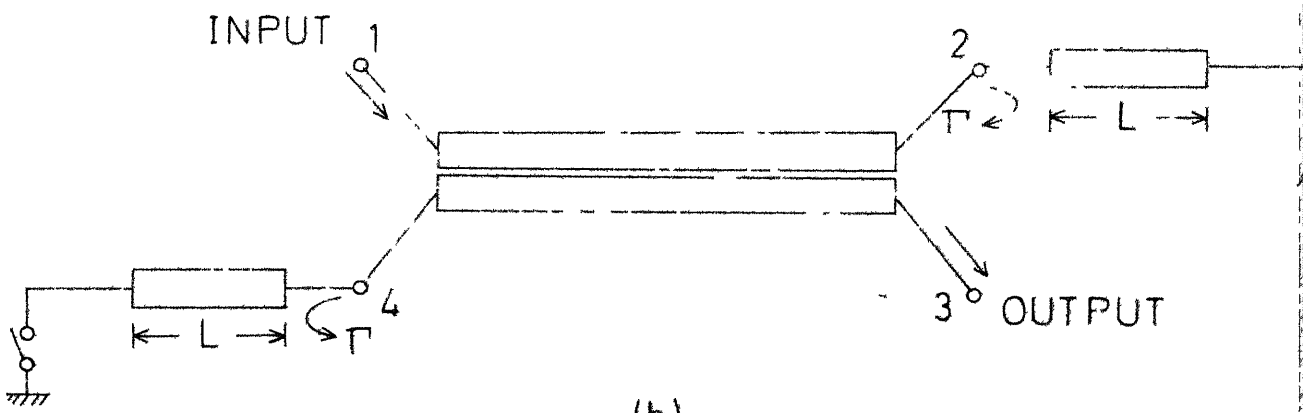
3.6 PHASE SHIFTERS USING PARALLEL COUPLED LINE HYBRIDS

A parallel coupled hybrid consists of two identical quarterwave long lines placed parallel and in close proximity to each other. Figure 3.25(a) gives the schematic of this hybrid. An input at port 1 divides equally between ports 2 and 4 with a phase difference of 90°, while there is no output at port 3. Such couplers are very broad band, usable bandwidth of a single section quarterwave coupler is approximately one octave [34] . 3 dB power split in these couplers is realized only at the centre frequency but the 90° phase difference between the output arms, the input match and the isolation are ideally independent of frequency.

To achieve broader bandwidths, multisection couplers are used. In multisection or single section 3 dB couplers, the main problem is the practical realization of the narrow gap between the lines. This difficulty can be alleviated by



(a)



(b)

FIG. 3.25 ELECTRICAL EQUIVALENT CIRCUIT FOR
(a) PARALLEL COUPLED HYBRID
(b) PARALLEL COUPLED HYBRID PHASE SHIFT.

connecting two or more couplers appropriately to achieve tight coupling from loose couplers. Such an arrangement is known as 'tandem' connection of couplers [28].

Phase shifters using single section parallel coupled hybrid and tandem connection of two such hybrids are considered. As in previous sections, a transmission line loss of 0.2 dB per wavelength at the centre frequency is assumed. Since these couplers operate over large bandwidths, the line loss is assumed to vary proportional to the square root of the normalized frequency.

3.6.1 Phase Shifters Using Single Section Parallel coupled Hybrid

Figure 3.25(b) shows the parallel coupled hybrid phase bit. Ideal 180° switches are connected to the coupled ports 2 and 4. Parallel coupled hybrid is symmetrical but when the switches are connected to ports 2 and 4, this symmetry is no more present. Hence, the phase shifter circuit using this hybrid is analyzed as a four port circuit. Eqn. (2.8) gives the scattering parameters for the phase shifter using this hybrid and, in the present case (with port numbers modified as shown in Fig. 3.25(a)) may be written as

$$\begin{bmatrix} b_1 \\ b_3 \end{bmatrix} = \begin{bmatrix} (S_{21}^2 + S_{41}^2)\Gamma & 2\,S_{21}\,S_{41} \\ 2\,S_{21}\,S_{41} & (S_{21}^2 + S_{41}^2)\Gamma \end{bmatrix} \begin{bmatrix} a_1 \\ a_3 \end{bmatrix} \qquad (3.12)$$

Reflection coefficient Γ may be evaluated as

$$\Gamma = \frac{Y_o - Y_{in}}{Y_o + Y_{in}} \tag{3.13}$$

where

$$Y_{in} = \frac{Y_s \cosh \gamma L + (1/Z_T)\sinh \gamma L}{\cosh \gamma L + Y_L Z_T \sinh \gamma L} \tag{3.14}$$

Y_s is switch admittance

Z_T is impedance of transmission line length L.

Transmission coefficients for the hybrid can be determined by using the concept of even mode and odd mode symmetry and are given as [35]

$$S_{21} = \frac{\sqrt{1-k^2}}{\sqrt{1-k^2}\cosh \gamma \ell + \sinh \gamma \ell} \tag{3.15}$$

$$S_{41} = \frac{k \sinh \gamma \ell}{\sqrt{1-k^2}\cosh \gamma \ell + \sinh \gamma \ell} \tag{3.16}$$

Using Eqns. (3.13), (3.14), (3.15) and (3.16), scattering parameters for the phase shifter can be evaluated from Eqn. (3.12). From these parameters performance of the phase shifter can be evaluated. Fig. 3.26 shows the plot of VSWR, insertion loss and phase shift ($\Delta\phi$) as a function of percentage frequency deviation. VSWR of the phase shifter is found to be independent of the switch state and the line length L. Insertion loss is also independent of switch

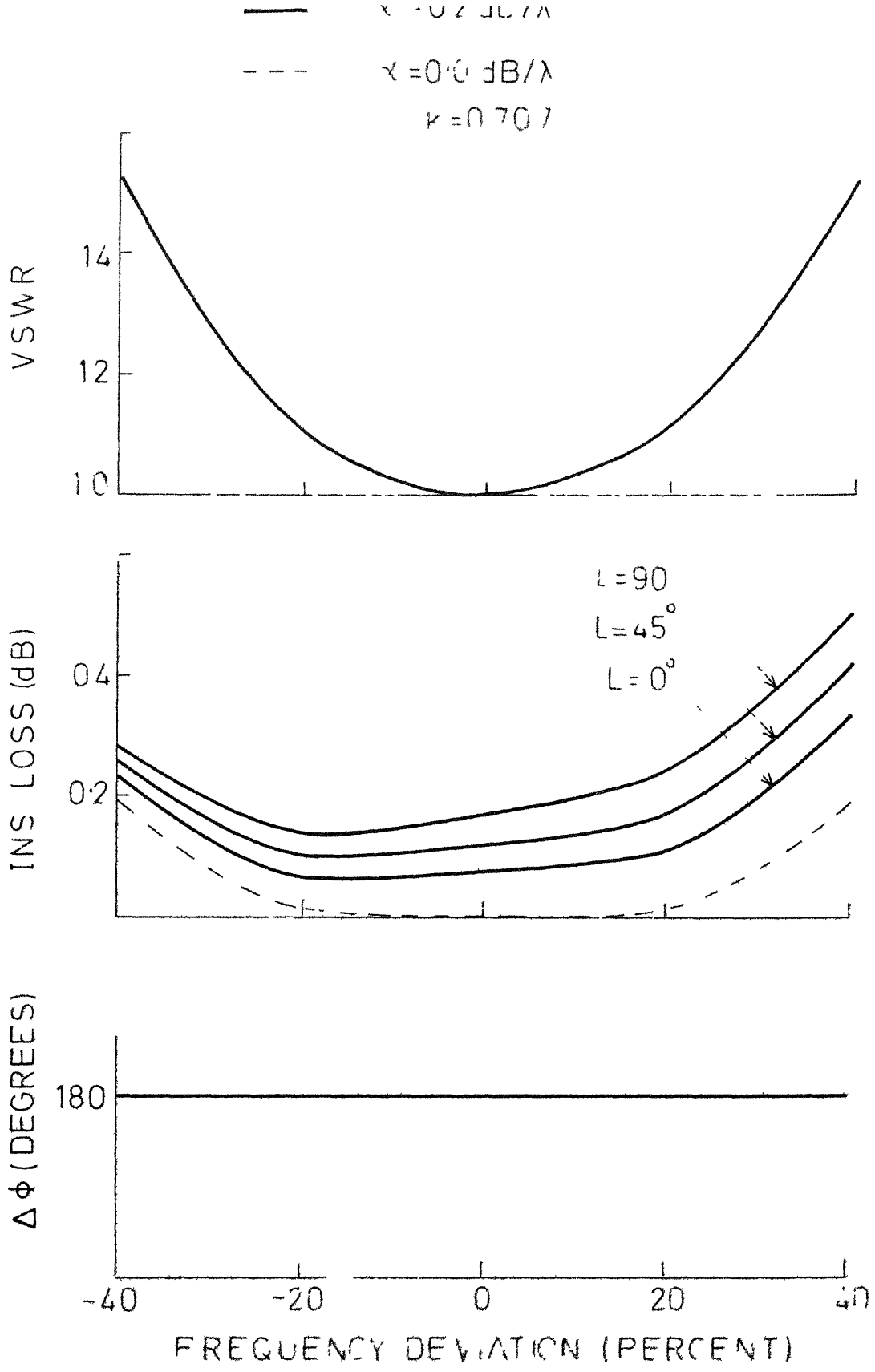


FIG. 3.26 CALCULATED PERFORMANCE OF 180° PHASE BALANCED [illegible] COUPLED HYBRID.

states but depends on the line length L to the extent of the loss of the line only. If the transmission line is assumed lossless (α = 0.0 dB/λ) then the insertion loss curves for all lengths coincide. The differential phase shift is found to be independent of frequency. This is due to the fact that the isolation of this hybrid is infinite and is independent of frequency.

3.6.2 Phase Shifters Using Tandem Connection of Two Single Section Hybrids

A tandem connection of two 8.34 dB (k=0.3828) couplers shown in Fig. 3.28(a) yields a 3 dB coupler [28]. Individual couplers of the tandem will have cross-over so that direct and coupled ports are on the same side and can be fed to the next coupler. Figure 3.27(a) shows a tandem connection of two single section parallel coupled line couplers. If the input is fed to port 1, ports 5 and 6 are coupled ports and port 2 is the isolated port.

Figure 3.27(b) shows a phase shifter using tandem hybrid. Ports 5 and 6 are terminated in ideal switches through an arbitrary line length L. To evaluate the performance of the phase shifter using this coupler, the scattering matrix for the tandem hybrid is to be found out first. Then by terminating ports 5 and 6 into switches with reflection

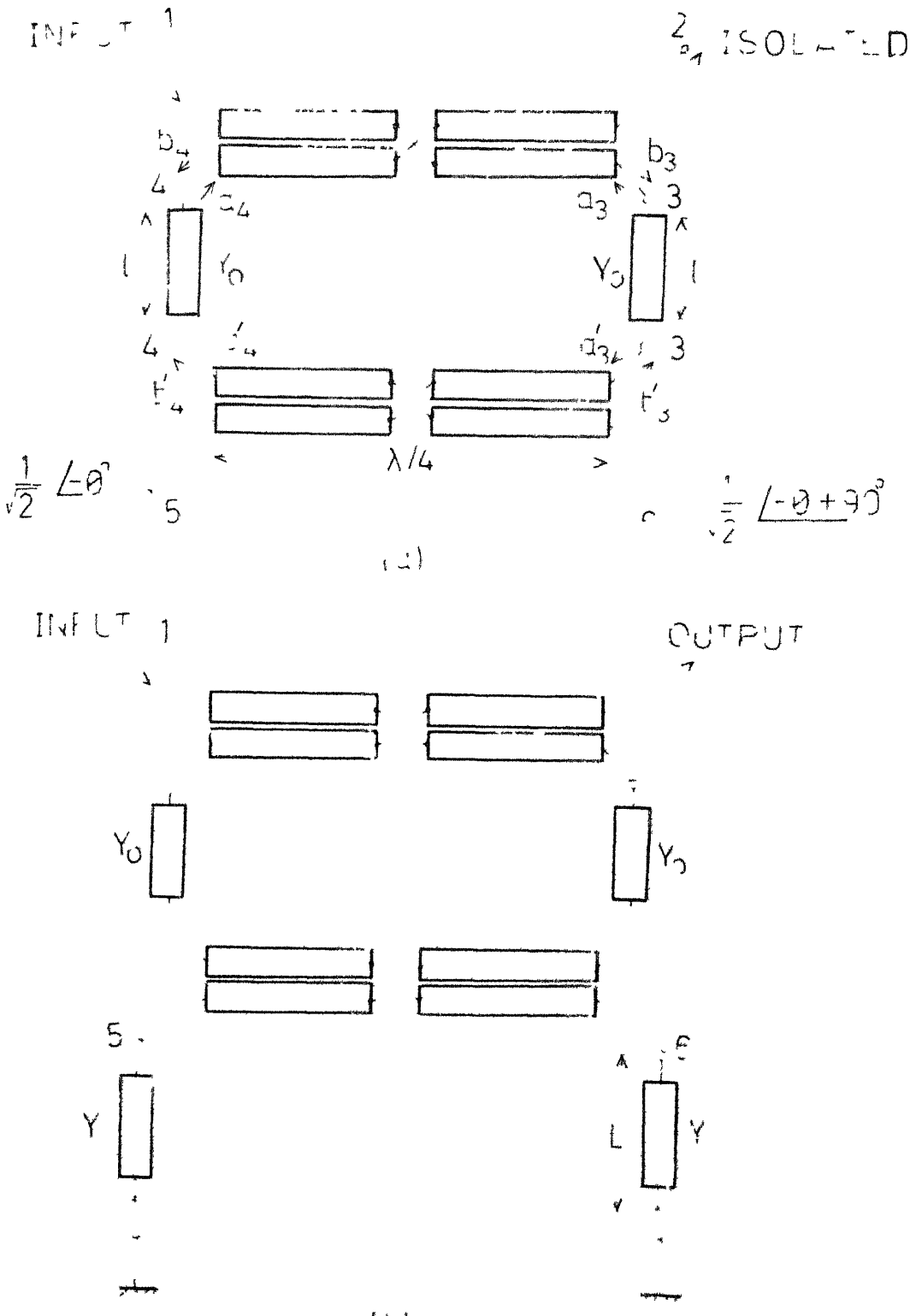


FIG. 3.27 ELECTRICAL EQUIVALENT CIRCUIT FOR

(a) TANDEM CONNECTION OF TWO SINGLE SECTION PARALLEL COUPLED HYBRIDS

(b) PARALLEL HYBRID STRIP LINE

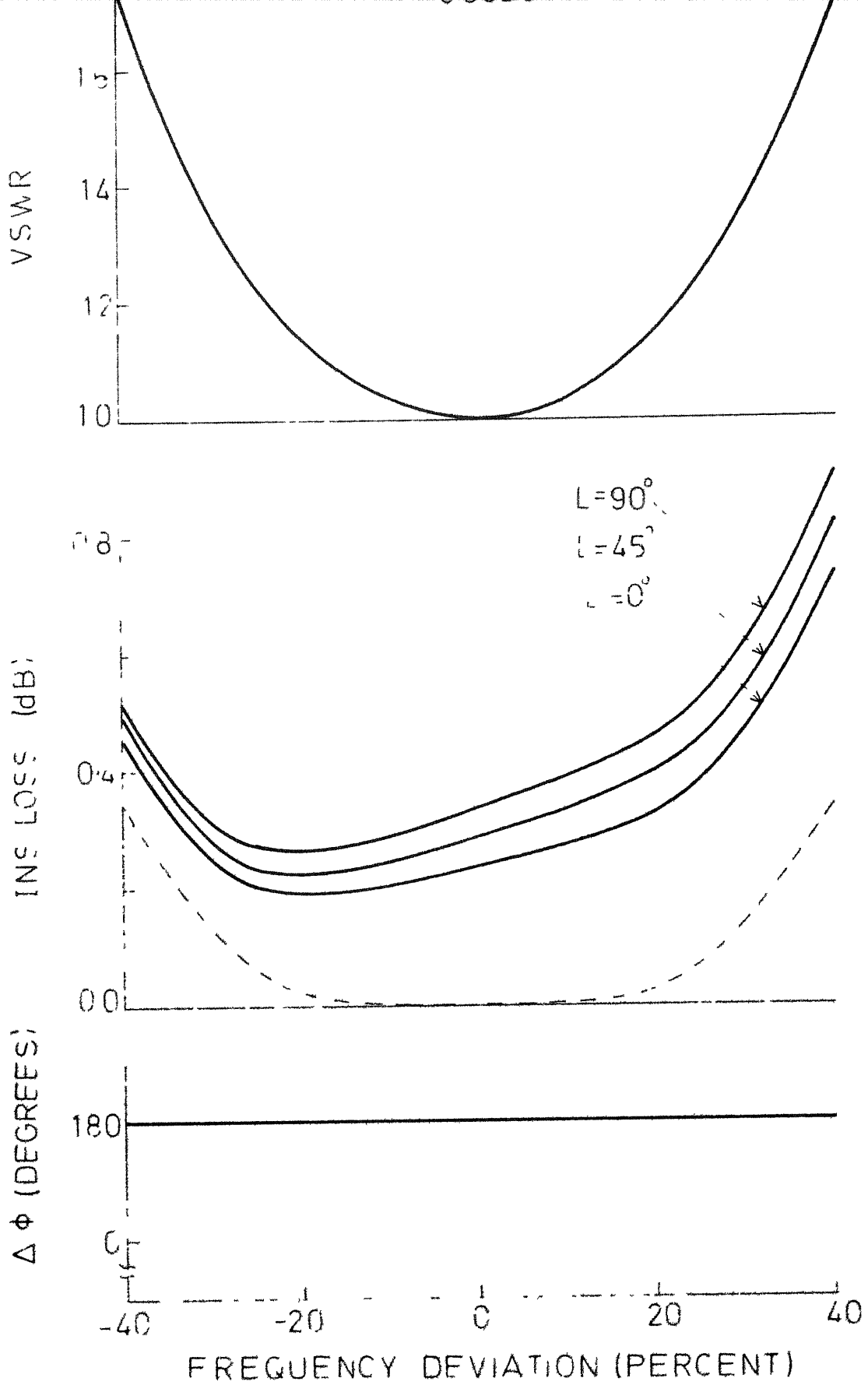


FIG. 3.28 CALCULATED PERFORMANCE OF [illegible] WAVEGUIDE TANDEM COUPLER WITH TWO [illegible] CAVITIES COUPLED VIA A GRID.

coefficients Γ, the scattering matrix for the reduced two-port phase shifter network can be evaluated.

By writing the scattering matrices for the individual couplers and the transmission lines interconnecting them, the scattering matrix for the tandem hybrid is obtained by eliminating the appropriate wave variables. We get the scattering matrix for the tandem hybrid as

$$\begin{bmatrix} b_1 \\ b_2 \\ b_5 \\ b_6 \end{bmatrix} = \begin{bmatrix} 0 & 0 & T_D & T_C \\ 0 & 0 & T_C & T_D \\ T_D & T_C & 0 & 0 \\ T_C & T_D & 0 & 0 \end{bmatrix} \begin{bmatrix} a_1 \\ a_2 \\ a_5 \\ a_6 \end{bmatrix} \tag{3.17}$$

where

$$T_D = \frac{T_c^2 + T_d^2}{x}$$

$$T_C = 2\frac{T_c\, T_d}{x} \tag{3.18}$$

$$x = e^{\gamma \ell}$$

and T_c and T_d are the transmission coefficients for the individual couplers.

Now if the ports 5 and 6 are terminated in reflection coefficient Γ, then the scattering matrix for the phase

shifter can be evaluated, and is written as:

$$\begin{bmatrix} b_1 \\ b_2 \end{bmatrix} = \begin{bmatrix} (T_D^2 + T_C^2)\Gamma & 2T_DT_C \\ 2T_DT_C & (T_D^2 + T_C^2)\Gamma \end{bmatrix} \begin{bmatrix} a_1 \\ a_2 \end{bmatrix} \qquad (3.19)$$

As the reflection coefficient Γ, and the transmission coefficients of the tandem hybrid are known phase shifte performance can be evaluated.

Figure 3.28 gives the plot of VSWR, insertion loss and differential phase shift as a function of percentage frequency deviation. As in the case of phase shifter using parallel coupled hybrid, the VSWR of the phase shifter is independent of the switch state as well as the line length L. Insertion loss also does not depend on the switch state but depends on line length L. This dependence is only due to increase in line loss as L increases. The variation of insertion loss is also found to be unsymmetrical about the centre frequency. This is due to assumed frequency dependence of line loss. Insertion loss variation with $\alpha = 0.0$ dB/λ is also plotted. Here the variation is symmetrical about the centre frequency and is independent of switch state as well as line length L. Differential phase shift is found to be

independent of frequency. This is due to the infinite isolation of the hybrid, not only at the centre frequency but throughout the band.

VSWR bandwidth of this circuit is only slightly less than that obtained by using a single section parallel coupled hybrid. For VSWR ≤ 1.2, the two values are 46% and 52% respectively.

CHAPTER 4

DESIGN OF REFLECTION-TYPE PHASE SHIFTERS

4.1 REVIEW OF AVAILABLE DESIGN PROCEDURES 99

4.2 GENERAL CONSIDERATIONS FOR THE DESIGN OF TRANSFORMING NETWORKS 104

4.2.1 Impedance Required at the Diode Plane 104

4.2.2 Design for Equal VSWR in Two States and Minimum Phase Error. 105

4.3 DESIGN OF THREE TYPES OF TRANSFORMING NETWORKS 108

4.3.1 Network for Use with Impedance Transforming Hybrids. 109

4.3.2 Quarter Wave Transforming Network 110

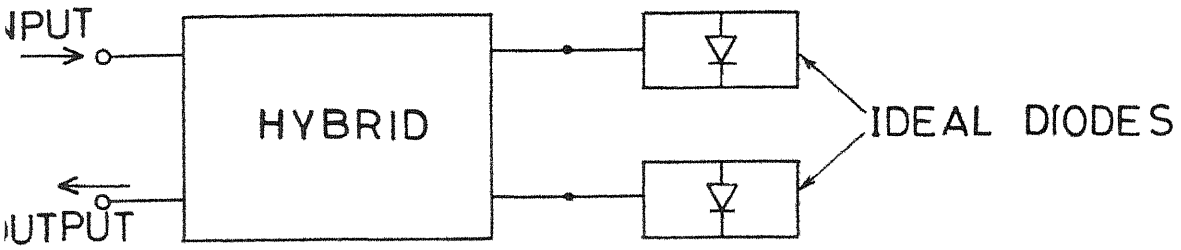
4.3.3 Single Section Transforming Network 114

CHAPTER 4

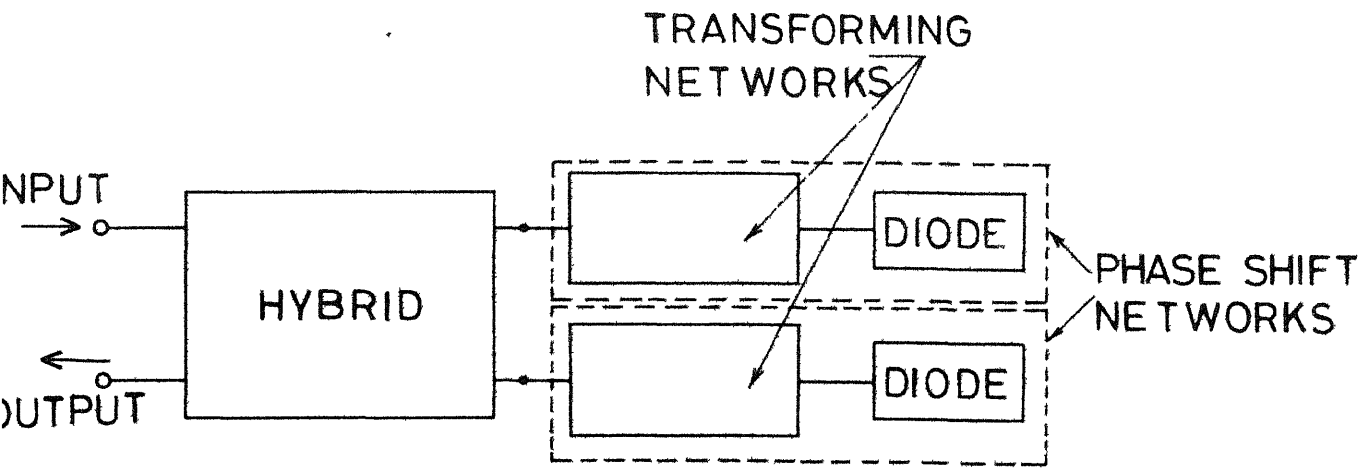
DESIGN OF REFLECTION TYPE PHASE SHIFTERS

A 180° reflection phase bit using ideal PIN diodes (ideal 180° switches) consists of a hybrid and two PIN diodes connected to the coupled ports (Fig. 4.1(a)). As discussed in Chapter 3, if the nonideal hybrid and ideal PIN diodes are considered, a line length between the hybrid port and diode is needed to reduce the mismatch error of the coupler [3] and hence the overall phase error of the phase shifter. If both the hybrid and the PIN diodes are nonideal, a network is to be introduced between the hybrid ports and the diodes to obtain desired phase shift at the centre frequency and the minimum phase error over the band of frequencies. Figure 4.1(b) shows the schematic of such a phase bit. It consists of a hybrid, two transforming networks, and two PIN diodes connected to the coupled ports of the hybrid. Networks terminating the hybrid ports (transforming network and diode) may be called phase shift networks as they are responsible for the required phase shift. The transforming networks may be designed to obtain the desired phase shift for a given set of diode impedances in the forward and reverse bias states.

In this chapter three types of transforming networks (transmission line type) considered are: (i) single line length (to be used with impedance transforming hybrids) (ii) quarter



(a)



(b)

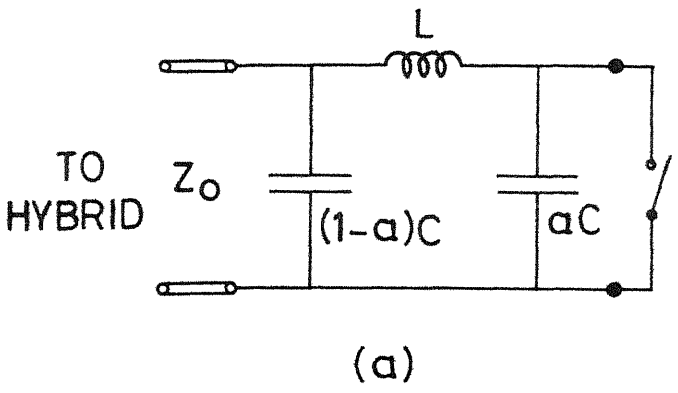
FIG. 4.1 A REFLECTION PHASE BIT
(a) USING IDEAL SWITCHES
(b) USING NONIDEAL SWITCHES

wave transformer and (iii) a single stub. The latter two are used with ordinary hybrids(with equal impedances). Closed form design equations for the above mentioned networks are derived. These design equations also include the design of optimum line length (for maximizing the bandwidth) placed between the hybrid port and the diode. Design curves giving transmission line lengths and impedances of the transforming network for given diode reactances are also included.

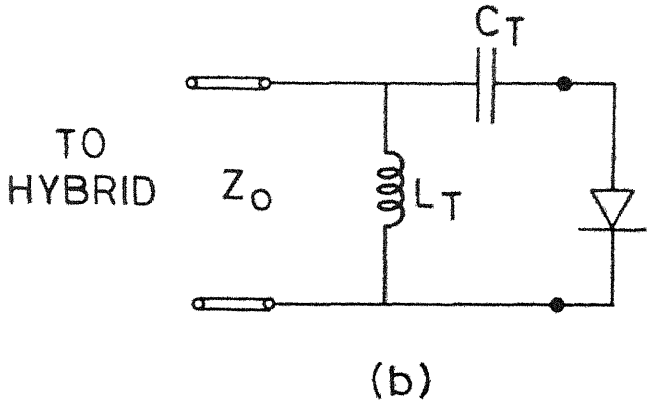
4.1 REVIEW OF AVAILABLE DESIGN PROCEDURES

The design of the transforming network is the key step in the design of reflection phase shifters using imperfect diodes. Five types of such networks have been reported in literature. Two out of these networks use lumped elements only. The third uses series inductance along with transmission line transformer. Fourth is a transmission line section alone and fifth proposes use of stubs.

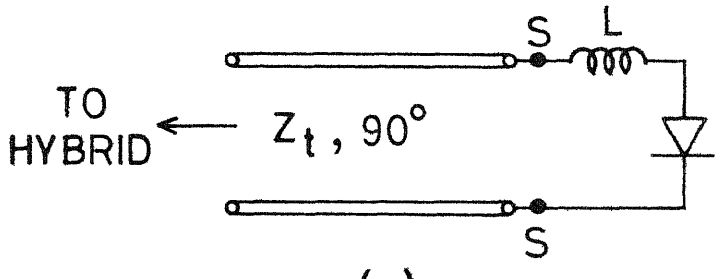
Design of 180° reflection-type phase shifters using imperfect diodes has been first considered by Garver [2,10,11]. Transforming network consists of lumped elements L and (1-a)C as shown in Fig. 4.2(a). This network operates over an octave bandwidth and thus the phase shifter bandwidth is limited by the hybrid. In this circuit, 'aC' is mainly the junction capacitance of the diode and (1-a)C is mainly the package



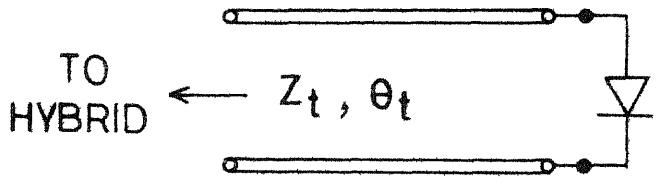
(a)



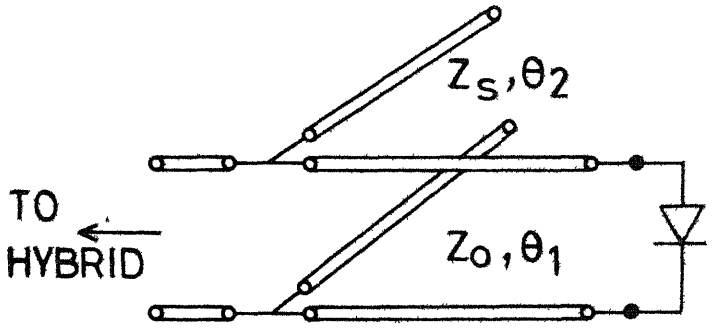
(b)



(c)

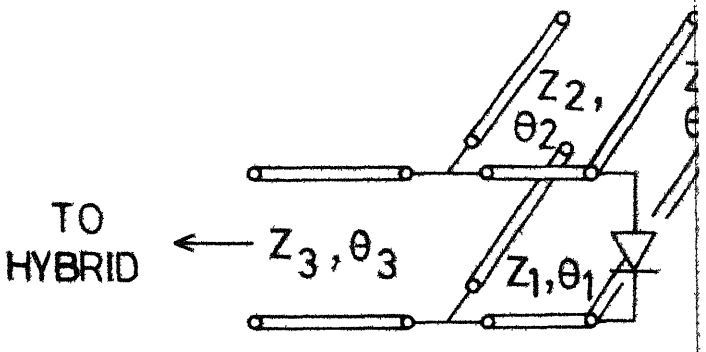


(d)



SINGLE STUB

(e)



DOUBLE STUB

(f)

FIG. 4.2 VARIOUS TRANSFORMING NETWORKS

capacitance. The parameters L and C are expressed in terms of an impedance Z_o' [10] such that

$$Z_o' = \sqrt{\frac{L}{C}} \qquad (4.1)$$

Parameters K (the ratio of Z_o' to the line impedance Z_o) and 'a' are computed for a given phase shift, the desired phase accuracy and the bandwidth.

Burns and Stark [1,4,12] have reported the design for series and parallel resonant type of phase shift network shown in Fig. 4.2(b). In this method tuning elements L_T and C_T are added to obtain series and parallel resonance in the forward bias and the reverse bias states, respectively. The condition for the magnitudes of the reflection coefficients to be equal is

$$Z_o = X_c \sqrt{\frac{R_R}{R_F}} \qquad (4.2)$$

where X_c is the diode's capacitive reactance. If $R_F=R_R$, Z_o becomes equal to X_c. Thus, for equal reflection coefficients in the two states, the characteristic impedance of the line to which diode is connected should be equal to the capacitive reactance of the diode for $R_F=R_R$. This also provides a constant phase shift $\Delta\phi$ for small frequency deviations around f_o.

The lower phase bits are obtained by the 'transformed switch' method [12] . This circuit uses 45° line length

between the 180° bit and ideal transformer. Transformer converts the 50 ohm impedance of hybrid port to the desired value for the given phase bit. These impedance levels for 90°, 45° and $22\frac{1}{2}^{\circ}$ are 2.4 Z_o, 5.0 Z_o and 10.0 Z_o respectively[12].

The third type of phase shift network named as transformed LC network is described by White [3]. This uses both lumped and distributed circuit elements as shown in Fig.4.2(c). In this case,a lumped inductance L is added so that the reactances switched at plane SS are $\pm$ j X_s (for 180° bit). A quarter-wave transformer can be used such that the normalized reactances switched at the coupler port are $\pm$j1.0.

To design lower phase bits the coupler impedance is to be transformed to higher 'socket impedance' Z_s. 90° and 45° phase bits are obtained by selecting $X_s/Z_s = \pm 0.41$ for 90° bit and $X/Z_s = \pm 0.20$ for a 45° bit [3].

Phase shift networks consisting of only transmission lines can be designed in different ways. Such a network using a single transmission line length shown in Fig. 4.2(d) has been described by Starski [19]. The design presented in this reference finds the optimum value of transmission line length and impedance (θ_t and Z_t) to get the minimum phase error over the band.

Phase shift network using single stub has been described by Camisa [20]. In the circuit reported, MIS varactors are used. The design for 180° bit proceeds as follows. The forward and reverse bias reactances of the diode are plotted on the Smith chart. A line of electrical length θ_1 (say) is used to move the reverse bias impedance point to the (R=0, X=0) point. The forward bias reactance point would also move correspondingly. A shunt capacitance (or open stub < $\lambda/4$) of suitable value would move the new forward bias reactance point to ($R = \infty$, $X = \infty$) point. The new reverse bias point which was brought to the short circuit point would not be effected by the shunt capacitance.

A double stub type of transforming network has been reported by Yahara and others [16] and is used with inter-digitated coupler. Design details of this network are not included in this reference.

Transforming networks of lumped element type give wide phase bandwidth and are most suited for wide band phase shifters. Networks using transmission lines are more appropriate for modest bandwidth phase shifters*.

---

*During the course of preparation of this manuscript, another paper by Atwater [49] had appeared. This paper shows how one port circuit having two impedance states can be transformed to exhibit reflection coefficients which have a prescribed phase angle difference and equal magnitude in the two states. Design equations for three types of transforming networks are included. These are: (a) a double stub transformer with quarter wave length spacing (b) line segment of arbitrary length and, (c) a $\lambda/4$ line segment in tandem with a $\lambda/8$ segment of different impedance.

4.2 GENERAL CONSIDERATIONS FOR THE DESIGN OF TRANSFORMING NETWORKS

There are two steps involved in the design of various types of transforming networks. Firstly, a circuit is designed to get the desired phase shift $\Delta\phi$ from the available diode. This involves providing a suitable impedance at the diode plane to ensure that the normalized reactances in two states are located $\Delta\phi$ apart on the Smith chart. The second step in the design is aimed at rotating these reactance locations on the Smith chart so that they are located symmetrically with respect to X = 0 axis.

4.2.1 Impedance Required at the Diode Plane

Consider a diode with forward impedance Z_F and the reverse bias impedance Z_R, looking into an impedance Z_m. The phase difference between reflection coefficients in two states $\Delta\phi$ is related to Z_m by the following relationship

$$Z_F = Z_m \cdot \frac{Z_R + j Z_m \tan(\Delta\phi/2)}{Z_m + j Z_R \tan(\Delta\phi/2)} \qquad (4.3)$$

When diodes are lossless, we may write

$$\begin{aligned} Z_F &= j X_F \\ Z_R &= j X_R \end{aligned} \qquad (4.4)$$

Equation (4.3) then reduces to

$$Z_m^2 \tan(\Delta\phi/2) - Z_m (X_F - X_R) + X_F X_R \tan(\Delta\phi/2) = 0 \qquad (4.5)$$

Equation (4.5) is quadratic in Z_m and its roots are

$$Z_m = \frac{X_F - X_R}{2\tan(\Delta\phi/2)} \pm \sqrt{\left\{\frac{X_F - X_R}{2\tan(\Delta\phi/2)}\right\}^2 - X_F X_R} \qquad (4.6)$$

For 180° bit, $\Delta\phi = 180°$ and we get

$$Z_m = \sqrt{-X_F X_R} \qquad (4.7)$$

For PIN diodes X_R is **negative.**

For 90° bit, $\phi = 90°$ and we get

$$Z_m = \frac{X_F - X_R}{2} + \sqrt{\left\{\frac{X_F - X_R}{2}\right\}^2 - X_F X_R} \qquad (4.8)$$

Variation of Z_m/Z_o with X_R for various values of X_F is given in Figs. 4.3 and 4.4 for 180° and 90° bits. Similarly, for other phase bits, value of Z_m can be calculated from Eqn. (4.6).

Irrespective of the type of transforming network to be used, the circuit impedance appearing across the PIN diode terminals should be equal to Z_m.

Above equations are used later for designing various types of phase shift networks.

4.2.2 Design for Equal VSWR in Two States and Minimum Phase Error

The effect of transmission line length (between ideal diode and hybrid port) on phase shifter bandwidth have been

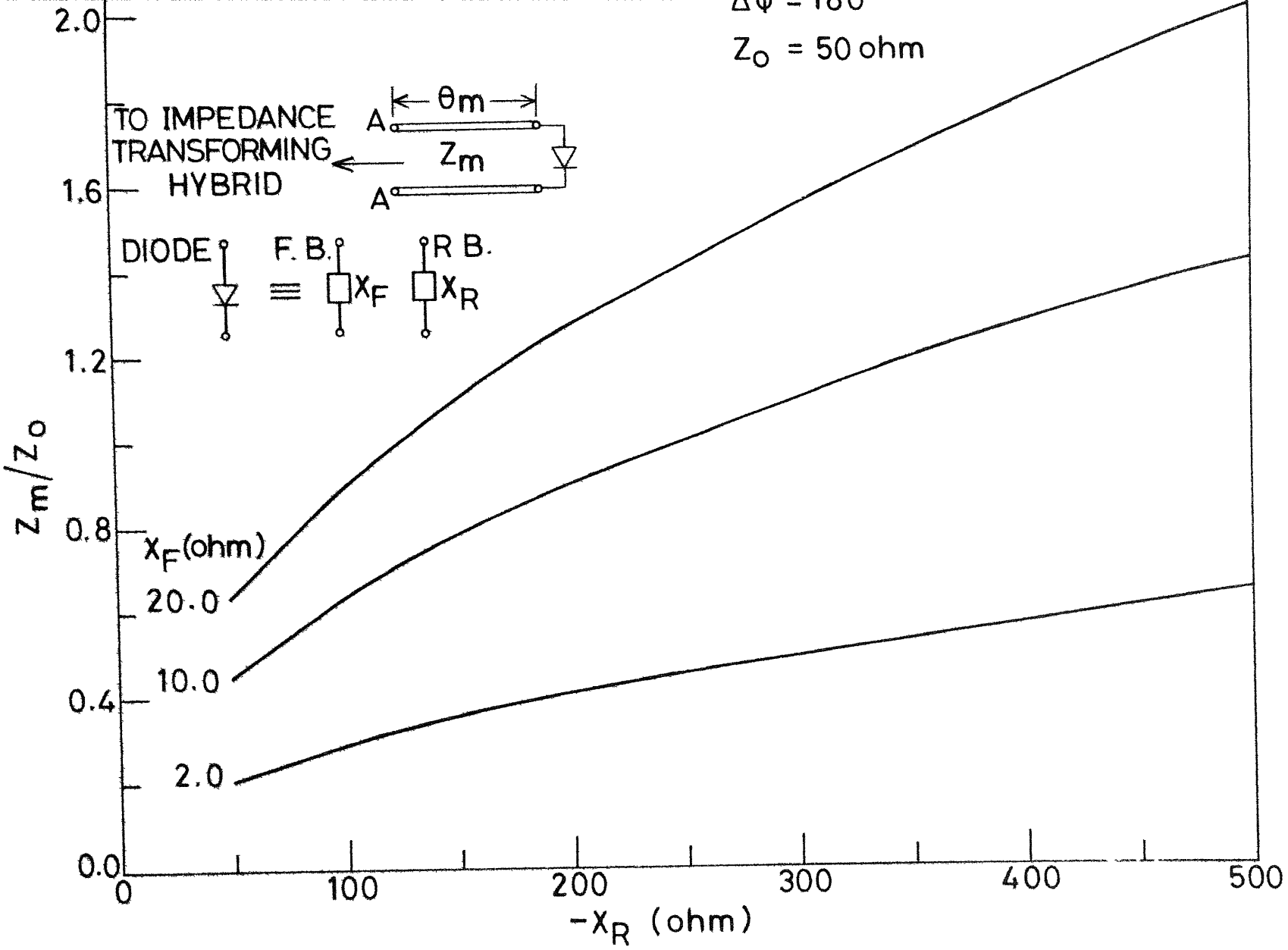


FIG. 4.3 VARIATION OF Z_m/Z_o WITH X_R FOR 180° BIT

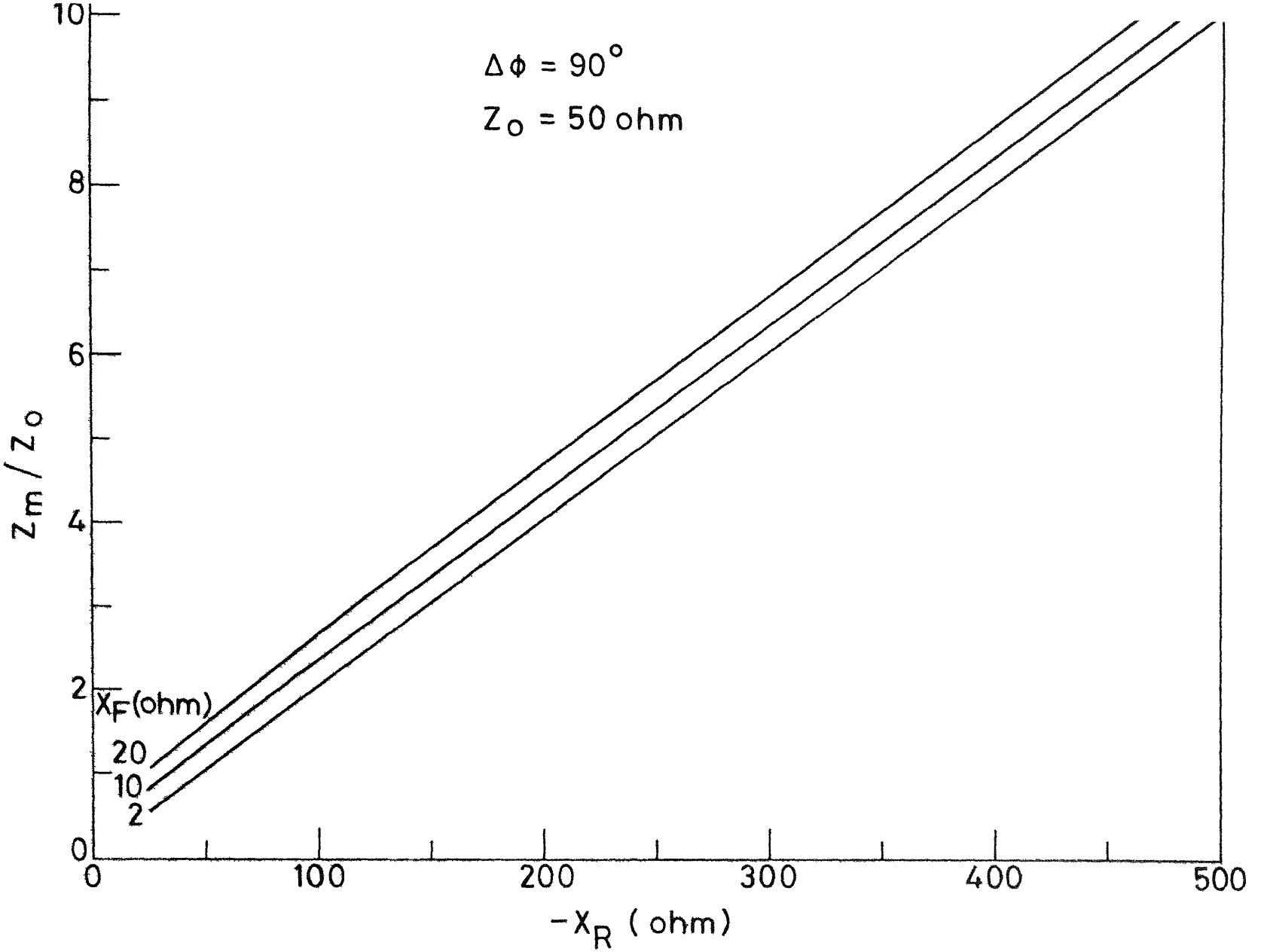


FIG. 4.4 VARIATION OF Z_m/Z_o WITH X_R FOR 90° HIT

discussed in detail in Chapter 3. It was noted that maximum phase bandwidth is obtained when the diode reactances switched in two states are equal and opposite in sign. Similar conclusion is valid even in the case of nonideal diodes. This is due to the fact that when the magnitude of reactances switched in two states are equal, the phase error due to coupler mismatch is greatly reduced [3].

For lower phase bits i.e. 90°, 45°, etc. these reactances may either be placed symmetrically about short circuit or open circuit point on the Smith chart. When the reactance points are symmetrically placed around short circuit, the normalized reactances in two bias states are given by

$$\bar{X}_{ss} = \pm j \tan \left(\frac{\Delta\phi}{4} \right) \qquad (4.9)$$

and when placed around open circuit, reactances are given by

$$\bar{X}_{so} = \pm j \cot \left(\frac{\Delta\phi}{4} \right) \qquad (4.10)$$

This placement of reactance also gives magnitudes of reflection coefficients equal in both bias states and hence equal VSWR.

Equations (4.9) and (4.10) are used in later sections for design of phase shift networks for lower phase bits.

4.3 DESIGN OF THREE TYPES OF TRANSFORMING NETWORKS

Design procedures for three types of transforming networks using transmission lines alone are discussed in this section.

4.3.1 Network for Use with Impedance Transforming Hybrids

This transforming network uses a single line length. To get the desired phase shift, diode should see the impedance Z_m looking into the transforming network, Eqn. (4.6). Impedance transforming hybrids [35,36] can have desired transformation of the impedance level in the hybrid itself. These hybrids have different port impedances. To get the desired phase shift there is no need of transforming network and the diodes can be mounted at the hybrid ports without any intervening line length. To get maximum bandwidth and equal values of the reflection coefficients (at f_o) in the two states, a transmission line of length θ_m and impedance Z_m is used. θ_m depends on the diode parameters. When the diode is forward biased and terminates a transmission line of length θ_m and impedance Z_m (Fig. 4.3(inset)), the input impedance at the plane AA is written as

$$Z_A = j\, Z_m \cdot \frac{X_F + Z_m \tan \theta_m}{Z_m - X_F \tan \theta_m} \qquad (4.11)$$

In order to have equal reflection coefficients in two states for a 180° bit, normalized reactance at AA should be $Z_A/Z_m (= j)$. Hence, the desired line length can be calculated using Eqn.(4.11) and is given by

$$\theta_m\Big|_{180°} = \tan^{-1} \frac{Z_m - X_F}{Z_m + X_F} \qquad (4.12)$$

For 90° bit, $Z_A/Z_m = j0.4142$. Hence

$$\theta_m\Big|_{90^\circ} = \tan^{-1}\left[\frac{Z_m - 2.4142\ X_F}{2.4142\ Z_m + X_F}\right] \qquad (4.13)$$

Variation of electrical length θ_m (in degrees) with X_R for various values of X_F is given in Fig. 4.5 for both 180° and 90° phase bits. For large values of X_R, θ_m becomes independent of X_R. For large values of X_R and small values of X_F, values of θ_m tend asymptotically to 45° and 22.5° for 180° and 90° phase bits respectively. This is in agreement with the discussion for ideal diode cases in Chapter 3.

4.3.2 Quarter Wave Transforming Network

In this case, a quarter wave transformer is used to transform hybrid impedance Z_h to the desired value Z_m needed across the diode. The impedance of this $\lambda/4$ section is given by

$$Z_T = \sqrt{Z_m Z_h} \qquad (4.14)$$

Figure 4.6 shows the variation of Z_T/Z_o with X_R for various X_F values, for both 180° and 90° bits. 90° bits need higher transformer impedances than 180° bits.

To get equal reflection coefficients in the two bias states and minimum phase error, line length θ_T of characteristic impedance 50 ohms is used (Fig. 4.7(inset)). If the diode is assumed to be forward biased, then impedance at the plane BB is given by

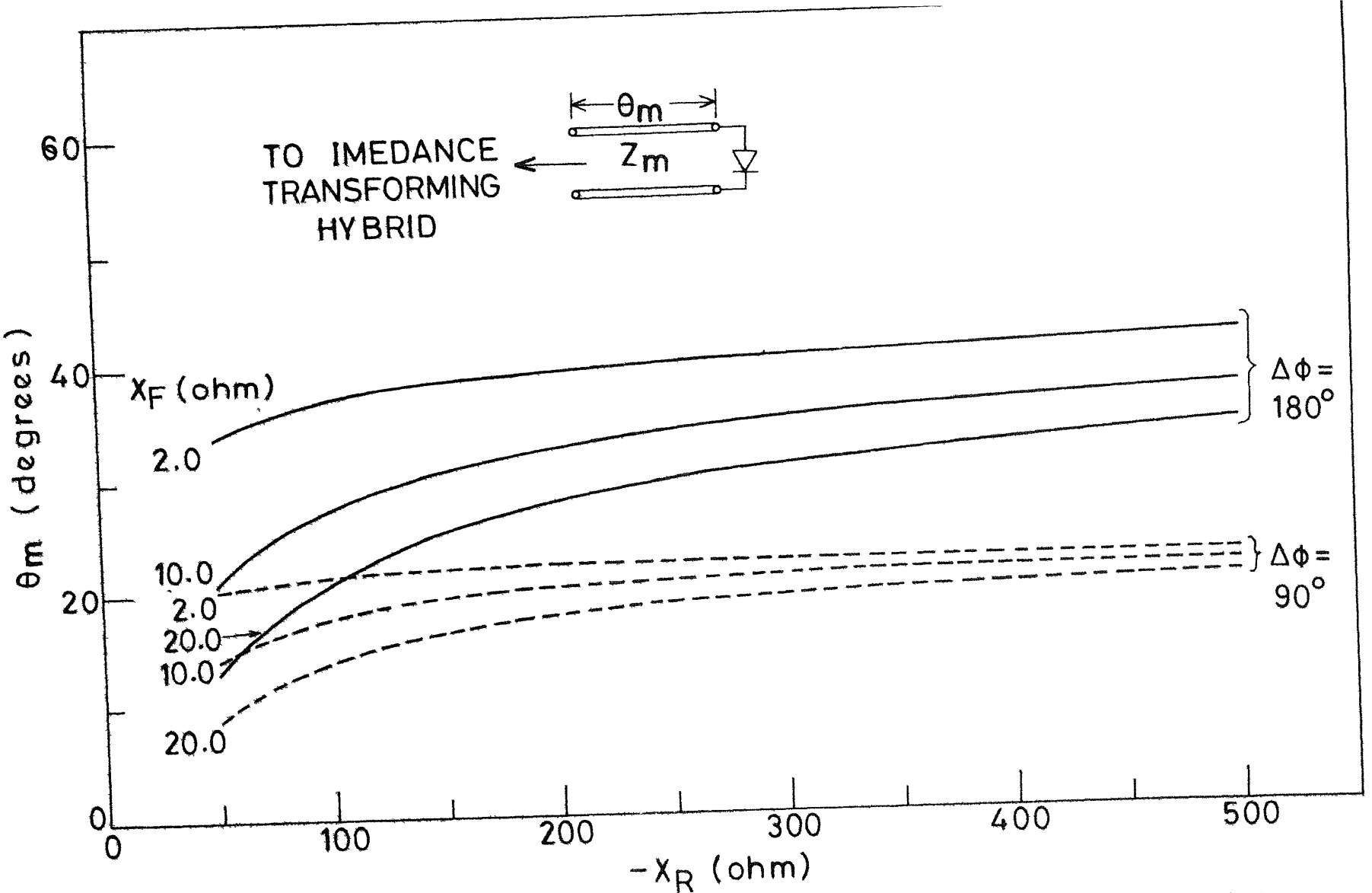


FIG. 4.5 VARIATION OF θ_m WITH X_R FOR 180° AND 90° BITS USING NETWORK FOR USE WITH IMEDANCS TRANSFORMING HYBRID.

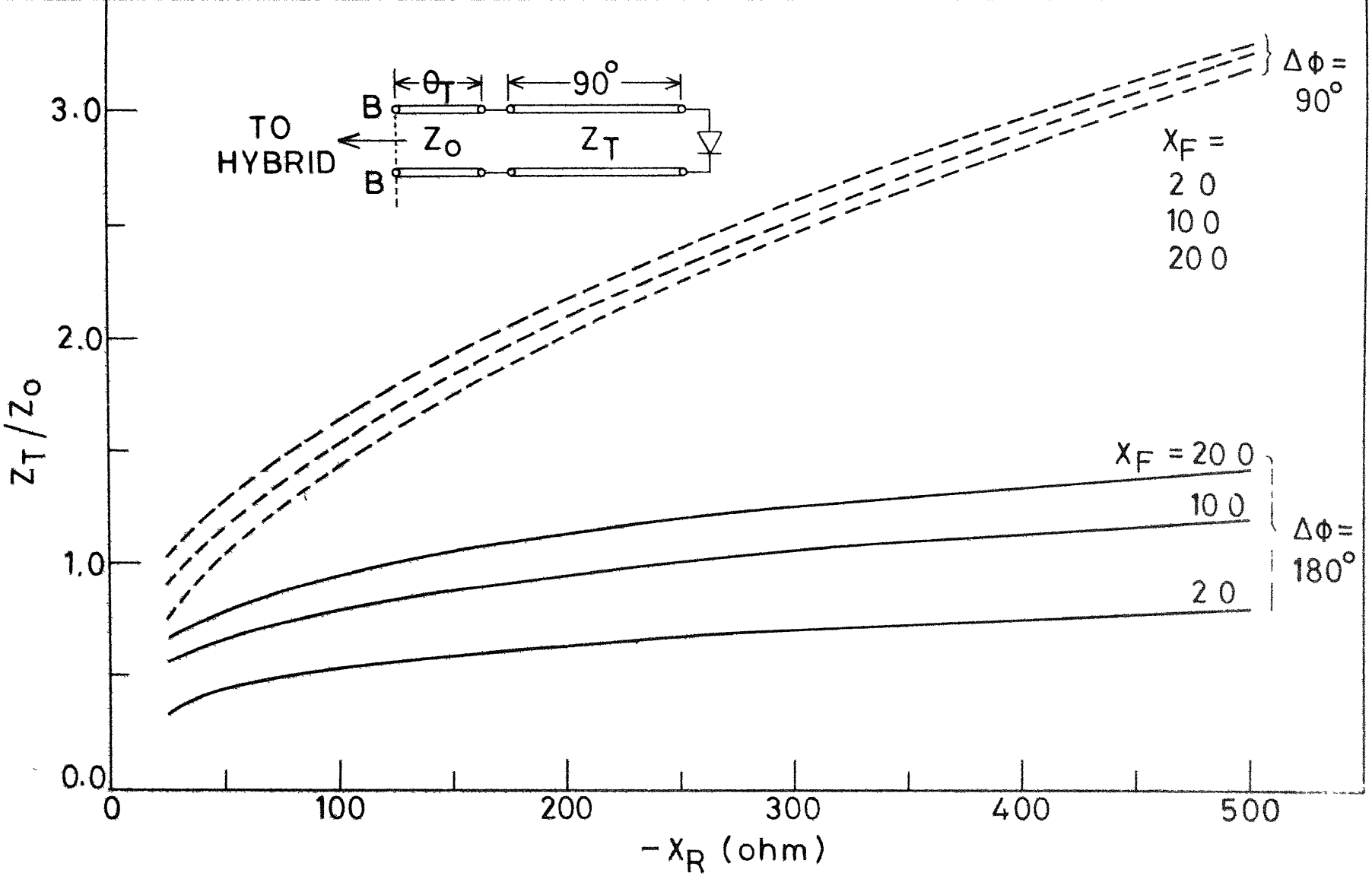


FIG. 4.6 VARIATION OF Z_T/Z_0 WITH X_R FOR 180° AND 90° BITS USING QUARTER WAVE TRANSFORMING NETWORK.

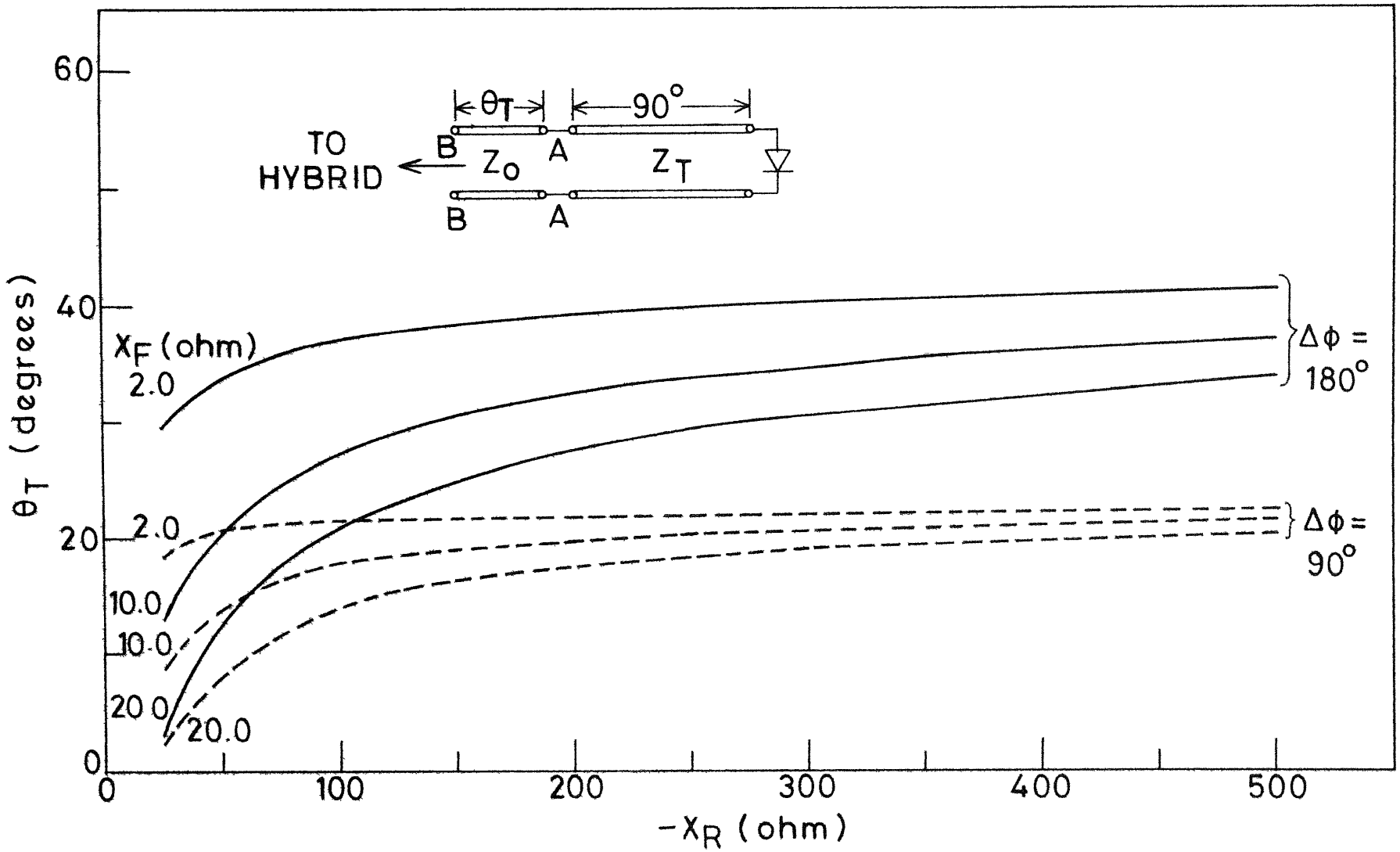


FIG. 4.7 VARIATION OF θ_T WITH X_R FOR 180° AND 90° BITS USING QUARTER WAVE TRANSFORMING NETWORK.

$$Z_B = j\, Z_o \cdot \frac{-Z_T^2/X_F + Z_o \tan \theta_T}{Z_o + Z_T^2/X_F \tan \theta_T} \qquad (4.15)$$

Since X_F point has moved by 180° on Smith chart due to $\lambda/4$ transformer, for 180° bit Z_B/Z_o should be $-j$.

Hence,

$$\theta_T\Big|_{180°} = \tan^{-1}\left[\frac{Z_T^2 - Z_o X_F}{Z_T^2 + Z_o X_F}\right] \qquad (4.16)$$

Similarly, for 90° bit, when the reactance points are chosen to be symmetrical with respect to open circuit point on the Smith chart, Z_B/Z_o should be $-2.4142j$.

Hence,

$$\theta_T\Big|_{90°} = \tan^{-1}\left[\frac{Z_T^2 - 2.4142\, X_F\, Z_o}{Z_o X_F + 2.4142\, Z_T^2}\right] \qquad (4.17)$$

Variation of electrical length θ_T (in degrees) with X_R for various values of X_F is given in Fig. 4.7 for 180° and 90° bits. In this case also θ_T becomes independent of X_R for large X_R values and tends to 45° and 22.5° for 180° and 90° phase bits, respectively.

4.3.3 Single Stub Transforming Network

Transforming network using a single stub has been discussed by Camisa and others [20] . By suitably choosing the stub (open or short) length and its distance from the

diode, desired phase shift can be achieved from practical diodes.

Design for 180° Bit

Figure 4.8 (inset) shows the transforming network of this type. A procedure for the design of 180° bit has been discussed in Section 4.1. Analytical design expressions based on this procedure can be derived as follows. Electrical line length θ_1 (location of the stub from the diode) depends on the reverse bias reactance of the diode and is given as

$$\theta_1 = \tan^{-1}\left[-\frac{X_R}{Z_o}\right] \tag{4.18}$$

By addition of line length θ_1 the reactance X_F gets transformed to a value X_F' (as shown in Fig. 4.8) given by

$$X_F' = Z_o \frac{X_F + Z_o \tan\theta_1}{Z_o - X_F \tan\theta_1} \tag{4.19}$$

Substituting the value of $\tan\theta_1$ from Eqn. (4.18), we get

$$j X_F' = j Z_o^2 \frac{X_F - X_R}{Z_o^2 + X_F X_R} \tag{4.20}$$

An equal reactance of the opposite sign connected in parallel with X_F' would make total reactance infinite. This capacitive reactance can be realized by using open stub of length θ_s given by

$$-j X_F' = -j Z_o \cot\theta_s \tag{4.21}$$

or,

$$\tan \theta_s = \frac{Z_o}{X'_F} \tag{4.22}$$

Substituting for X'_F from Eqn. (4.20) we get

$$\tan \theta_s = \frac{Z_o^2 + X_F X_R}{Z_o(X_F - X_R)} \tag{4.23}$$

From Eqn. (4.23), we see that when $Z_o^2 = -X_F X_R$, $\theta_s = 0$ i.e. no stub length is required and the transforming network reduces to a single line length.

For $Z_o^2 < |X_F X_R|$ the reactance X'_F in Eqn. (4.21) becomes negative (capacitive). Hence the stub length should provide an equal inductive reactance. This is possible by using shorted stub of length less than 90° whose reactance is given by

$$X_{short} = j Z_o \tan \theta_s \tag{4.24}$$

and

$$-j X'_F = j Z_o \tan \theta_s$$

where X'_F is negative

$$\tan \theta_s = -\frac{X'_F}{Z_o} \tag{4.25}$$

Substituting for X'_F, we get

$$\tan \theta_s = -\frac{Z_o(X_F - X_R)}{Z_o^2 + X_F X_R} \tag{4.26}$$

For equalization of the reflection coefficients in the two bias states and for obtaining the minimum phase error, a line length of 45° is desired. Since at the junction point of the

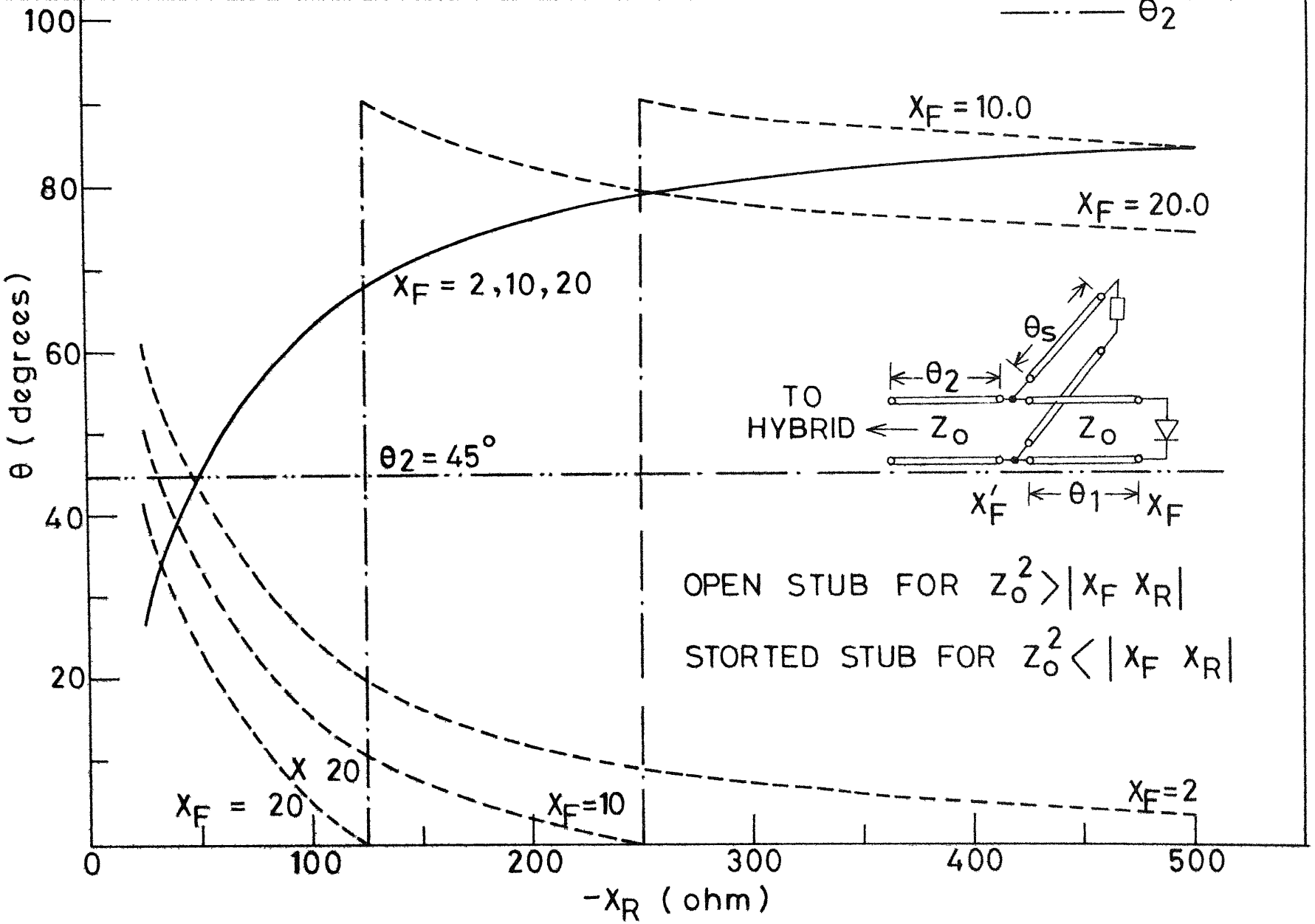


FIG. 4.8 VARIATION OF LINE LENGTHS θ_1, θ_s AND θ_2 WITH X_R FOR 180° HIT USING SINGLE STUB TRANSFORMING NETWORK.

stub, the diode has been idealized having impedances zero and infinite in forward and reverse bias states, respectively.

Figure 4.8 gives the variation of line lengths θ_1, θ_s and θ_2 with X_R for various values of X_F. The electrical length θ_1 depends only on the reverse bias reactance of the diode and the impedance of the line, hence for all values of X_F the curve is same. Stub length θ_s depends on X_F, X_R and Z_o. Plots of θ_s for X_F values of 2, 10 and 20 ohms and X_R values from -50 ohm to -500 ohm are shown in Fig. 4.8. For X_F = 2 ohm, open stub is used for all the ranges of X_R values. For X_F = 10 and 20 ohms, upto certain X_R values given by $Z_o^2 > |X_F X_R|$, an open stub is used, and when $Z_o^2 < |X_F X_R|$, a shorted stub is used. For example, for X_F = 20 ohm and Z_o = 50 ohm ; at X_R = -125 ohm, θ_s = 0° and for X_R values beyond this shorted stub is to be used. The electrical length θ_2 used for equalization of reflection coefficients is independent of X_F and X_R values and is 45°.

Design for 90° Bit

Figure 4.9 (inset) shows the transforming network of single stub type to be used for 90° bit. In this case shorted stub length less than $\lambda/4$ is used for all the diode reactances considered.

The electrical length θ_1 is found in this case also by using Eqn. (4.18). By addition of line length θ_1 the reactance X_F is transformed to a new value X_F' given by Eqn. (4.19). To get 90° phase shift the reactance X_F' point should be modified to a value j Z_o (normalized j1.0). Hence, the reactance X_L needed is given by

$$j Z_o = \frac{j X_F' \; j X_L}{j(X_L + X_F')}$$

or

$$X_L = \frac{Z_o X_F'}{X_F' - Z_o} \tag{4.27}$$

To obtain this inductive reactance, shorted stub of length less than $\lambda/4$ is to be used. Length of the stub is given by

$$\tan \theta_s = -\frac{X_L}{Z_o} \tag{4.28}$$

Substituting for X_L from Eqn. (4.27), we get

$$\tan \theta_s = \frac{X_F'}{X_F' - Z_o} \tag{4.29}$$

Substituting for X_F', we get,

$$\theta_s = \tan^{-1} \left[\frac{1}{1 - \frac{Z_o^2 + X_F X_R}{Z_o (X_F - X_R)}} \right] \tag{4.30}$$

To equalize reflection coefficient in the two bias states a line length of 67.5° is to be used.

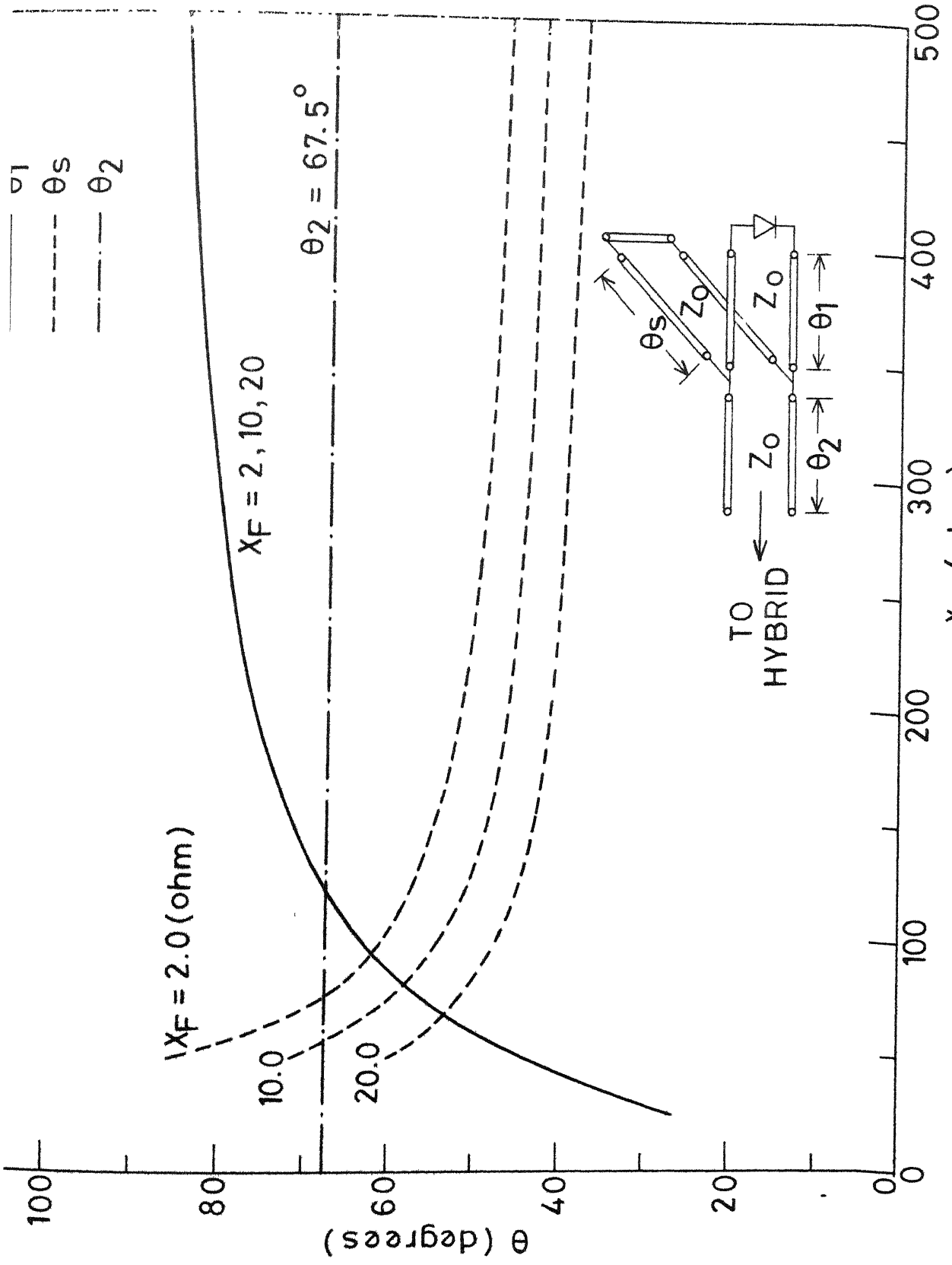


FIG. 4.9 VARIATION OF LINE LENGTHS θ_1, θ_s AND θ_2 WITH X_R FOR 90° BIT USING SINGLE STUB TRANSFORMING NETWORK.

Figure 4.9 gives the variation of line lengths θ_1, θ_s and θ_2 with X_R for various X_F values. In this case also θ_1 does not depend on X_F. Diodes with large X_F and large X_R require shorter stub lengths. For large X_R values stub length becomes independent of X_R.

CHAPTER 5

PERFORMANCE OF REFLECTION-TYPE PHASE SHIFTERS

5.1 BANDWIDTH OF PHASE SHIFTER CIRCUITS 123

5.1.1 Circuit Using Two-Branch Hybrid 124

5.1.1.1 Quarter wave transforming network 125

5.1.1.2 Single stub transforming network 128

5.1.1.3 Network for use with impedance transforming hybrid 132

5.1.2 Circuit Using Three-Branch Hybrid 136

5.1.2.1 Quarter wave transforming network 136

5.1.2.2 Single stub transforming network 139

5.1.3 Circuit Using Rat-Race Hybrid 142

5.1.3.1 Quarter wave transforming network 142

5.1.3.2 Single stub transforming network 145

5.2 INSERTION LOSS OF PHASE SHIFTER CIRCUITS 148

5.2.1 Circuits Using Quarter Wave Transforming Network 148

5.2.2 Circuits Using Single Stub Transforming Network 150

5.2.3 Circuits Using Network for Use with Impedance Transforming Hybrid 159

5.3 COMPARISON OF PHASE SHIFTER CIRCUITS FOR BANDWIDTH, INSERTION LOSS AND SIZE. 159

5.3.1 Bandwidth 161

5.3.2 Insertion Loss 163

5.3.3 Size 163

CHAPTER 5

PERFORMANCE OF REFLECTION-TYPE PHASE SHIFTERS

Performance of reflection phase shifters using ideal switches with various types of hybrids has been discussed in Chapter 3. In this chapter, performance of these phase shifters using three types of transforming networks (discussed in Chapter 4) with two-branch, three-branch and rat-race hybrid, is discussed. Bandwidths for various designs are computed for two specifications of the bandwidth (described in Chapter 3) and for wide range of diode reactances. Insertion loss of phase shifters for the three types of transforming networks are also evaluated. Various designs of these circuits are compared vis-a-vis minimum circuit size, minimum insertion loss and maximum bandwidth.

During the discussions contained in this chapter two typical diodes have been used frequently for illustrating the effects of diode reactances. One of these is called high L-C and has forward and reverse bias reactances around 20 ohm and -62.50 ohm respectively. The other diode called low L-C diode has X_F and X_R as 2 and 400 ohm.

5.1 BANDWIDTH OF PHASE SHIFTER CIRCUITS

Bandwidth of a phase shifter as defined in Chapter 3 can be specified in terms of phase shifter VSWR and phase error. Two specifications of bandwidths considered there are: (i) VSWR $\leq$ 1.2 , Phase error $\leq \pm 2.5^\circ$ and (ii) VSWR $\leq$ 1.2, Phase error $\leq \pm 5^\circ$. These specifications are used for calculating

the BW of various circuits considered in this section.

Bandwidth of phase shifters using two-branch, three - branch and rat-race hybrid with ideal switches has been discussed in section 3.5. In this section, bandwidth of phase shifters using above mentioned hybrids with three types of transforming networks are evaluated and discussed. Transforming networks using quarter wave transformer and single stub are used with normal hybrids (with all port impedances same) while a network using single line length is used with impedance transforming hybrids. Closed form expressions derived in Chapter 4 are used for the design of transforming networks. Phase shifter circuits using these hybrids and transforming networks still have the axis of symmetry as in the case of phase shifters using ideal switches (Chapter 3). Hence, these circuits are also analyzed using the even and odd mode symmetry. To evaluate bandwidth, the nearest frequency point f_b, at which at least one of the specifications (i.e. phase error or VSWR) is violated, is calculated. Bandwidth is computed using Eqn. (3.1). These calculations are carried out for various circuits and for a wide range of diode reactances. In all the cases bandwidths for 180° bit and 90° bit are calculated.

5.1.1 Circuit Using Two-Branch Hybrid

In this section bandwidths of phase shifters using two-branch hybrid and three types of transforming networks are evaluated.

5.1.1.1 Quarter wave transforming network

180° bit

Bandwidth of this circuit is plotted as a function of diode reactance X_R for two values of X_F (2.0 and 20.0 ohms) in Fig. 5.1. The curves with continuous lines are for the bandwidth defined for VSWR $\leq$ 1.2 and phase error $\leq \pm 2.5°$ and the dotted curves denote the BW for VSWR $\leq$ 1.2 and phase error $\leq \pm 5°$.

As mentioned in Section 3.5.1, the maximum bandwidth obtained for 180° bit using two-branch hybrid and ideal switches for both the bandwidth specifications is 5 percent. This maximum bandwidth is obtained in the present case when X_F is large (20.0 ohm) and is independent of the reverse bias reactance (X_R) of the diode. For $|\phi_e| \leq 2.5°$ case, diodes with large X_F give maximum bandwidth when X_R is small and bandwidth decreases with X_R. Diodes with small X_F (2.0 ohm) give lower bandwidth, which increases with increase in X_R. As the value of X_R is increased further, bandwidth approaches to the maximum value of 5%.

90° bit

For the ideal case discussed in Section 3.5.1, the maximum bandwidth of 90° phase bit using two-branch hybrid is approximately 5.8%. In the case of a phase bit using non-ideal diodes the BW is plotted in Fig. 5.2. The bandwidth never approaches the maximum bandwidth value in the ideal

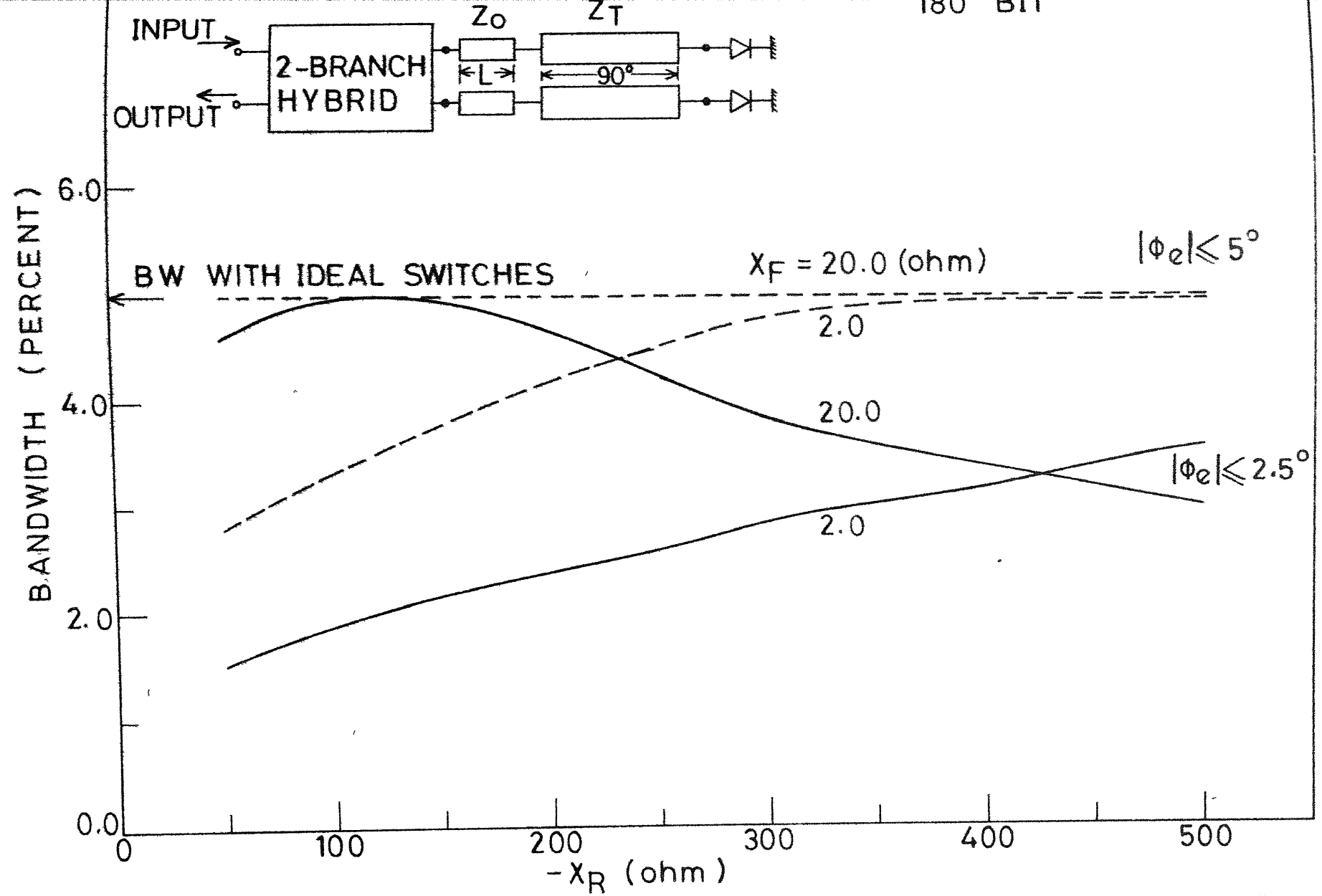


FIG. 5.1 VARIATION OF BANDWIDTH WITH X_R FOR 180° PHASE BIT USING TWO-BRANCH HYBRID AND QUARTER WAVE TRANSFORMING NETWORK.

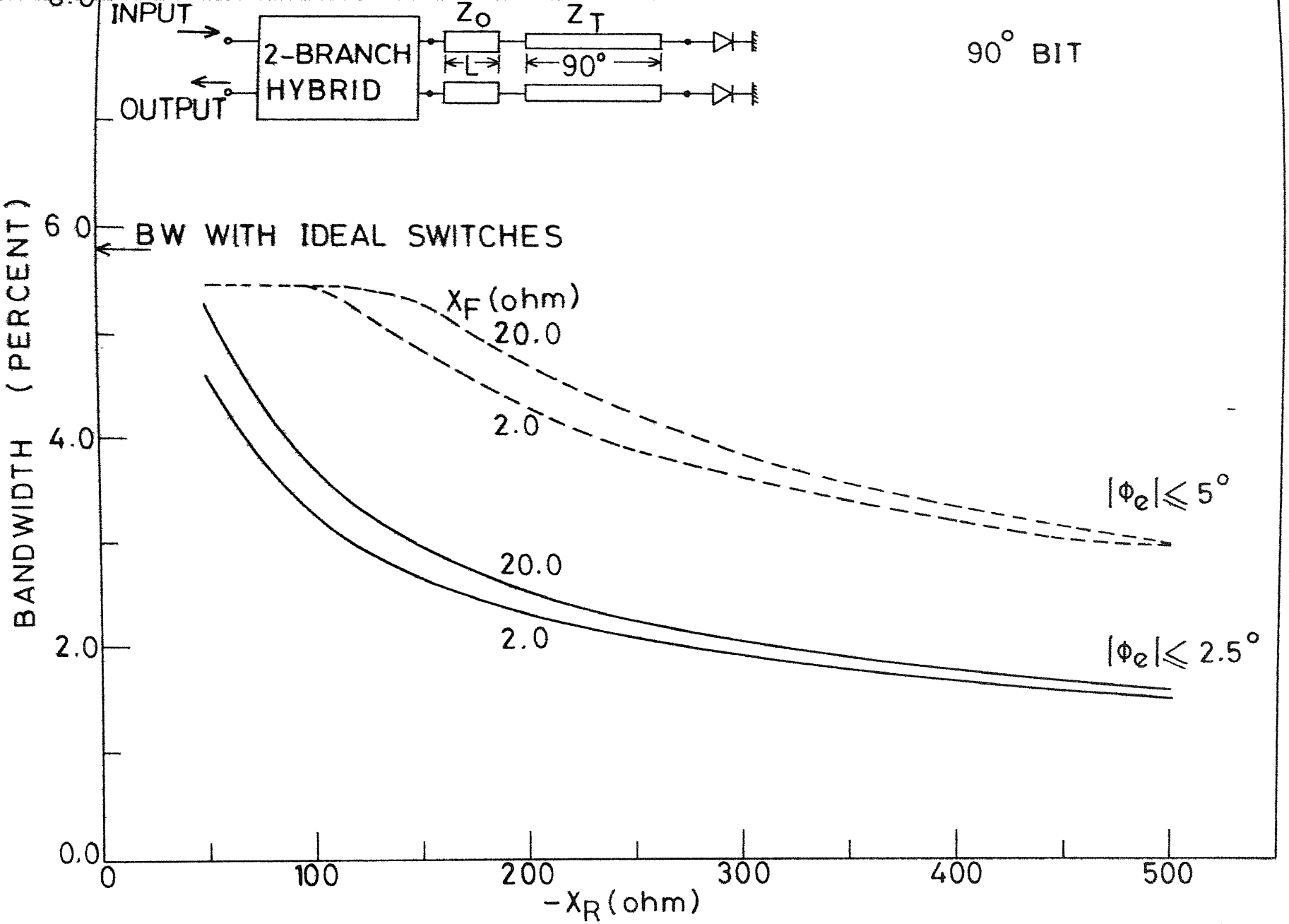


FIG. 5.2 VARIATION OF BANDWIDTH WITH X_R FOR 90° PHASE BIT USING TWO-BRANCH HYBRID

case when X_F values upto 20.0 ohm are considered. Bandwidth is found to decrease with X_R. Diodes having higher X_F value give slightly wider bandwidths. As $|X_R|$ increases the differences in bandwidths reduce. For $|\phi_e| \leq 5°$ and smaller $|X_R|$ values variation of bandwidth with X_R becomes flat for both X_F=2.0 and 20.0 ohms.

For 90° bit of this kind, diodes having large L and C yield wider bandwidths.

5.1.1.2 Single stub transforming network

180° bit

Bandwidth of 180° phase bit is plotted as a function of diode reactance X_R in Fig. 5.3. As before results for two values of X_F (2.0 and 20.0 ohms) are presented. Single stub type of transforming network uses a open stub when $Z_o^2 > |X_F X_R|$ and a shorted stub for $Z_o^2 < |X_F X_R|$. Instead of shorted stub, open stub longer than $\lambda/4$ but less than $\lambda/2$ can also be used. But the latter arrangement is found to give smaller bandwidth. For X_F = 2 ohm, both bandwidths $|\phi_e| \leq 5°$ and $|\phi_e| \leq 2.5°$ increase as $|X_R|$ increases and attain a constant value of 5% for $|X_R| >$ 100 ohm and 150 ohm, respectively.

For X_F = 20 ohm both the bandwidths increase with an increase in $|X_R|$ value and attain a maximum value of 5%. This maximum value of bandwidth is achieved at X_R = -100 ohms. At X_R = - 125 ohm, $Z_o^2 = -X_F X_R$ and the stub length becomes zero. Shorted stub is used beyond this point and its length

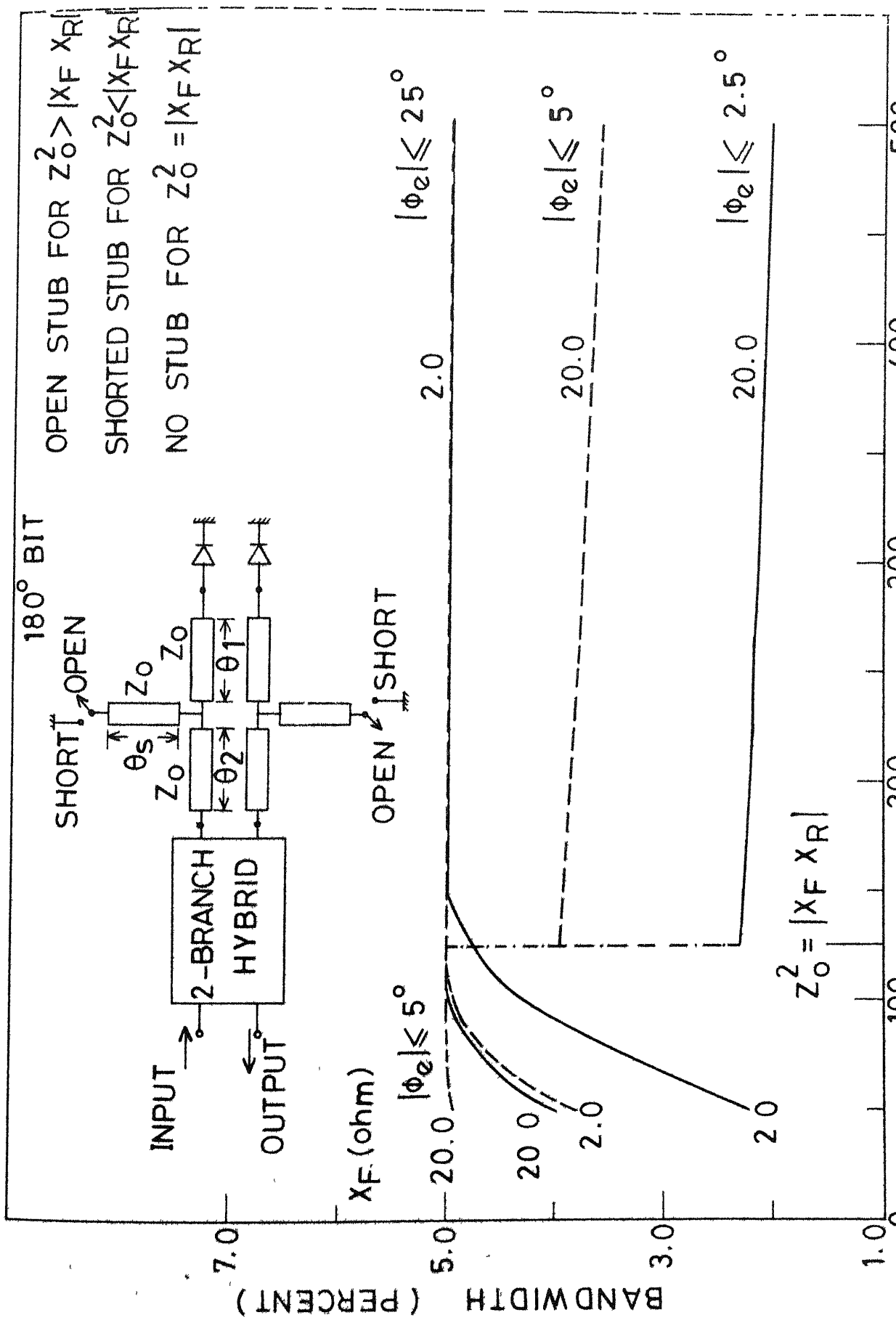


FIG. 5.3 VARIATION OF BANDWIDTH WITH X_R FOR 180° PHASE BIT USING TWO-BRANCH HYBRID AND SINGLE STUB TRANSFORMING NETWORK.

is longer. Hence the bandwidths reduce suddenly to 2.3% for $|\phi_e| \leq 2.5°$ and 3.9% for $|\phi_e| \leq 5°$.

From the above discussion it may be noted that diodes with low L-C yield the maximum bandwidth for this type of phase bit. For these low L-C diodes the length of open stub used is shorter throughout the range of diode reactances considered. This reduces the frequency dependence of the stub reactance and thus increases the bandwidth.

90° bit

This phase bit uses shorted stub (less than quarter wavelength) throughout the range of values of X_F and X_R. Fig.5.4 gives the plot of bandwidth. From this figure we observe that, for X_F=2 and 20 ohms, the bandwidth is independent of the value of the reverse biased reactance (X_R) of the diode and BW for $|\phi_e| \leq 2.5°$ and BW for $|\phi_e| \leq 5°$ are equal.

Bandwidths in this case are limited by the VSWR and not by the phase error. Since VSWR variation of the bit is not so sensitive to variations in diode parameters, bandwidth remains constant throughout the range of reactance values.

The bandwidth obtained in this case for the chosen X_F and X_R values is 5.4% which is comparable to the 5.8% value obtained with ideal switches.

This type of phase bit is most appropriate in the situations where variations in the diode reactances are large and one is aiming to achieve the same bandwidth for a number of similar circuits in a production run.

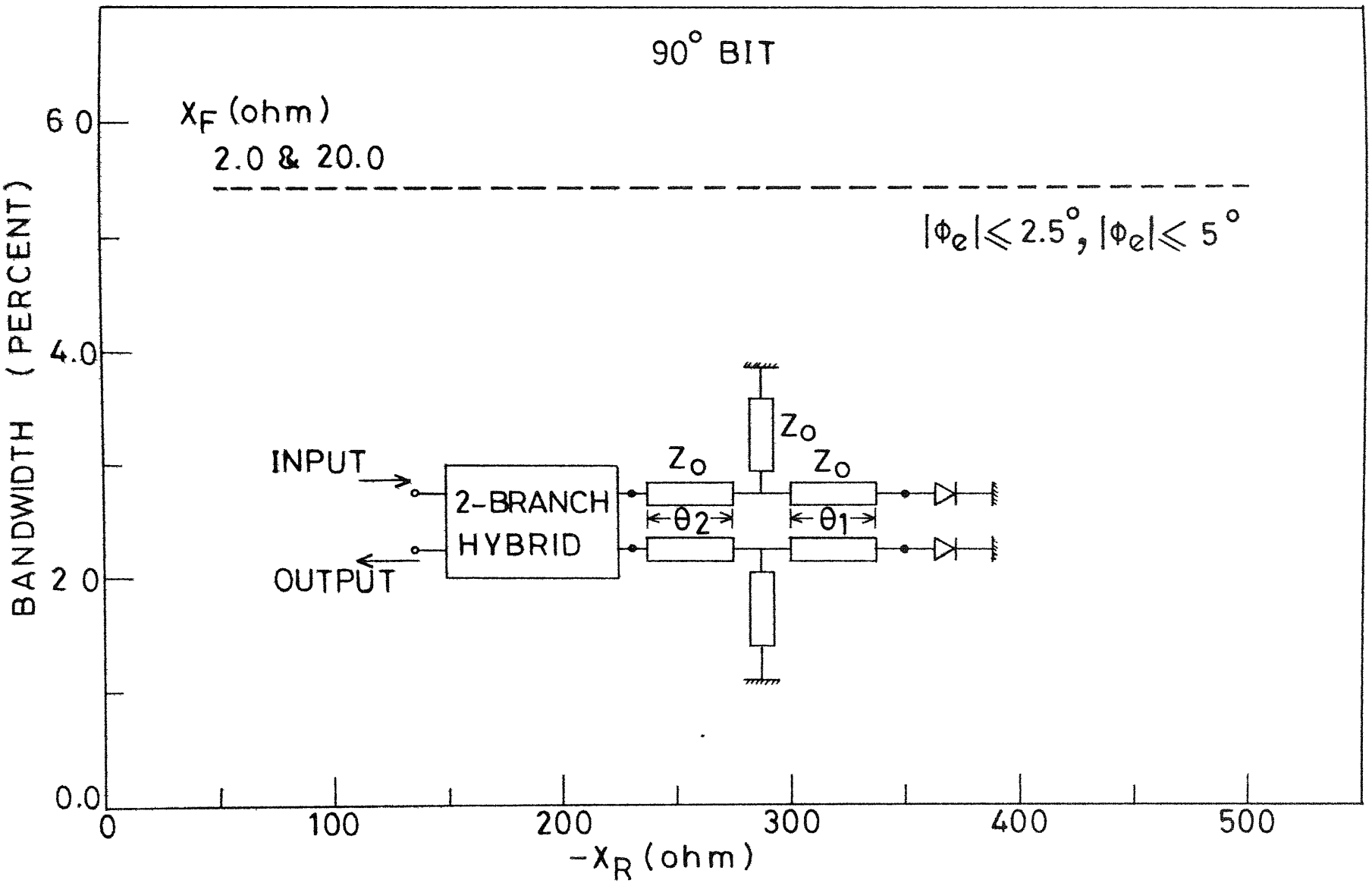


FIG. 5.4 VARIATION OF BANDWIDTH WITH X_R FOR 90° PHASE BIT USING TWO-BRANCH HYBRID AND SINGLE STUB TRANSFORMING NETWORK.

5.1.1.3 Network for use with impedance transforming hybrid

Impedance transforming branch line couplers have been described in the literature [36,37]. These couplers combine the functions of a directional coupler and two impedance transformers connected to coupled branches. Bandwidth of the impedance transforming hybrid is less than that of the normal hybrid. This BW decreases with increase in the value of the ratio of impedance transformation in the hybrid. However, this BW is larger when compared with that of the combination of a normal hybrid and quarter wave transformers at the coupled ports.

Although impedance transforming couplers have unequal input and output port impedances, still the network is symmetrical about XX plane as shown in Fig. 5.5 (inset). The analysis based on even and odd mode symmetry can also be applied to the phase shifter using this hybrid.

180° bit

Figure 5.5 shows the variation of bandwidth as a function of $-X_R$ for two values of X_F(2 and 20 ohms). Results

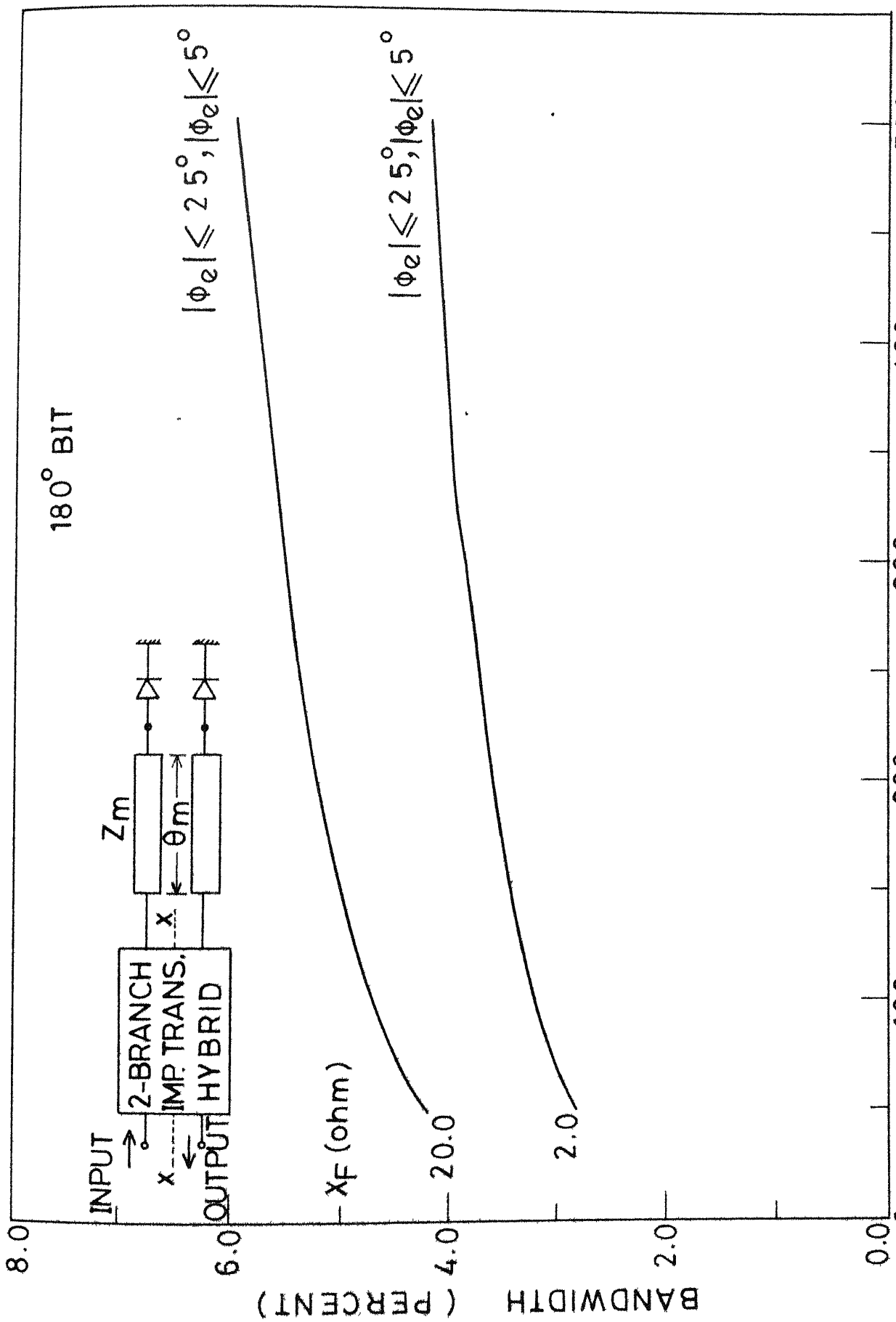


FIG. 5.5 VARIATION OF BANDWIDTH WITH X_R FOR 180° PHASE BIT USING TWO-BRANCH IMPEDANCE TRANSFORMING HYBRID.

are identical for two bandwidth specifications. This is explained by noting that in this case the bandwidth is limited by the VSWR and not by the phase error. For both values of X_F (2 and 20 ohms) the bandwidth is found to increase with $|X_R|$ value.

Diodes with large X_F and X_R values give wider bandwidths. This bandwidth is found to lie in the same range as for the phase bit using ordinary hybrid (Section 5.1.1.1). The maximum bandwidth (for X_F = 20 ohm and X_R = -500 ohm) obtained is about 6%.

90° bit

The variation of bandwidth as a function of $-X_R$ is shown in Fig. 5.6. For $|\phi_e| \leq 2.5°$ and X_F = 2 and 20 ohms, bandwidth is found to decrease with $|X_R|$. Diodes with larger X_F give slightly wider bandwidth. It is found to be limited by the phase error and not by the VSWR.

On the other hand, bandwidth for $|\phi_e| \leq 5°$ is found to increase first (in which range it is limited by VSWR) and attains the value of about 8.5%. As $|X_R|$ increases further this bandwidth gets limited by phase error and starts decreasing. It is worth noting that the maximum bandwidth obtained in this case (8.5%) is larger than for the phase bit using normal hybrid, which is about 5.6%.

Thus, it can be concluded that if the tighter phase error constraints are to be met, diodes with higher X_F and lower $|X_R|$ (high L-C) are suitable for this type of circuit

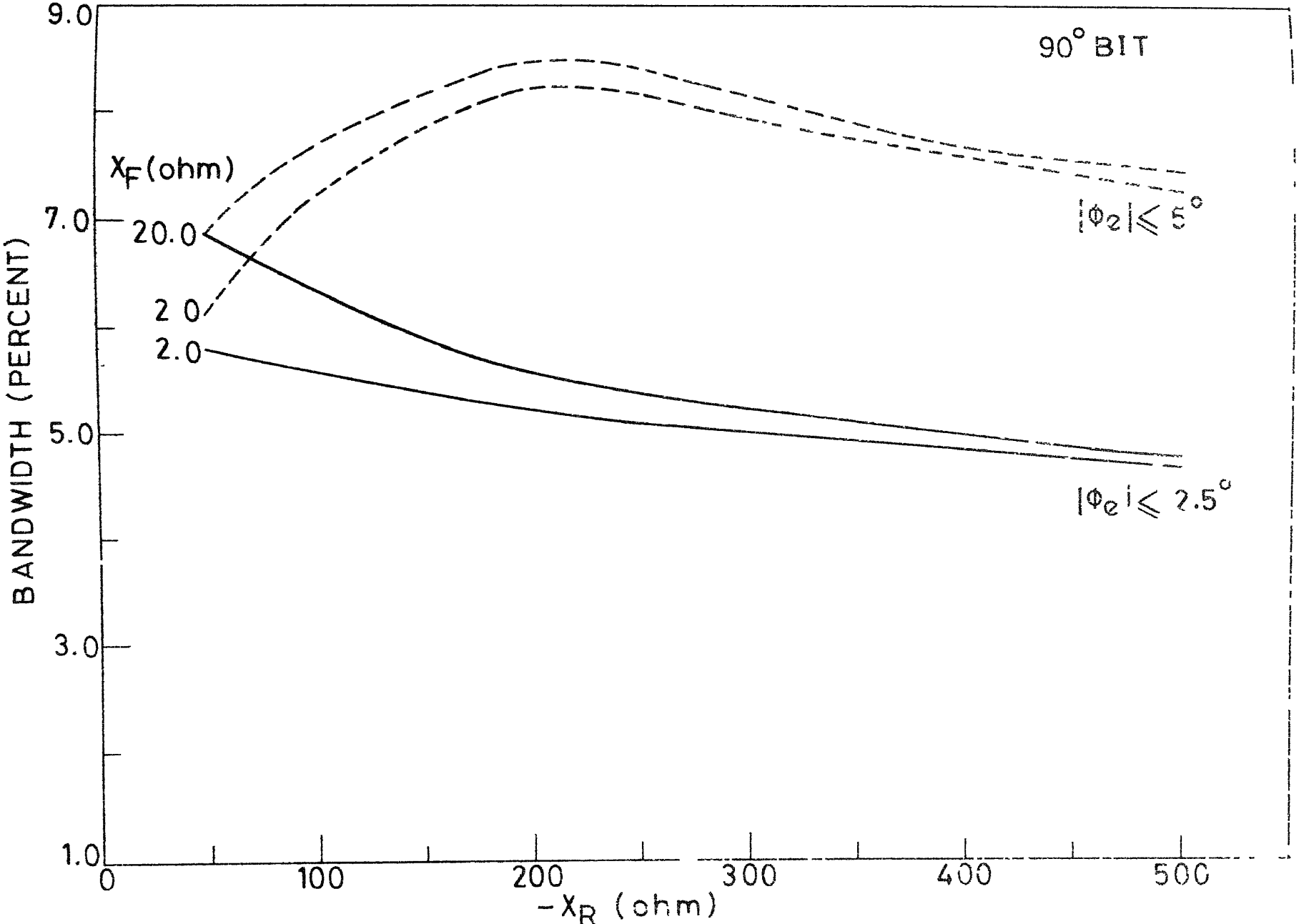


FIG. 5.6 VARIATION OF BANDWIDTH [illegible]

IMPEDANCE TRANSFORMING [illegible]

For the relaxed phase error specifications ($|\phi_e| \leq 5°$), diodes with high X_F and medium value of $|X_R|$ (around 250 ohm) are appropriate.

5.1.2 Circuit Using Three-Branch Hybrid

Two types of transforming networks are considered for phase shifter circuits using three-branch hybrids. These are stub type and quarter wave transformer type.

5.1.2.1 Quarter wave transforming network

180° Bit

Figure 5.7 shows the variation of bandwidth as a function of diode reactance X_R, for two values of X_F (2.0 and 20.0 ohms).

For X_F = 2.0 ohm, bandwidth is found to increase with increase in $|X_R|$ for both $|\phi_e| \leq 2.5°$ and $|\phi_e| \leq 5°$. That is the diodes with smaller capacitance have wider bandwidth. For X_F = 20.0 ohm , bandwidth initially increases with $|X_R|$ and then falls off with further increase in $|X_R|$ value. Behaviour of the curve remains same for both the bandwidth specifications. Bandwidth of this phase bit using ideal switches (Section 3.5.2) is found to be approximately 15% for $|\phi_e| \leq 5°$, and 10.5% for $|\phi_e| < 2.5°$.

90° Bit

The variation of bandwidth as a function of diode reactance X_R for fixed values of X_F is shown in Fig. 5.8. Bandwidth is found to decrease rapidly with increase in $|X_R|$

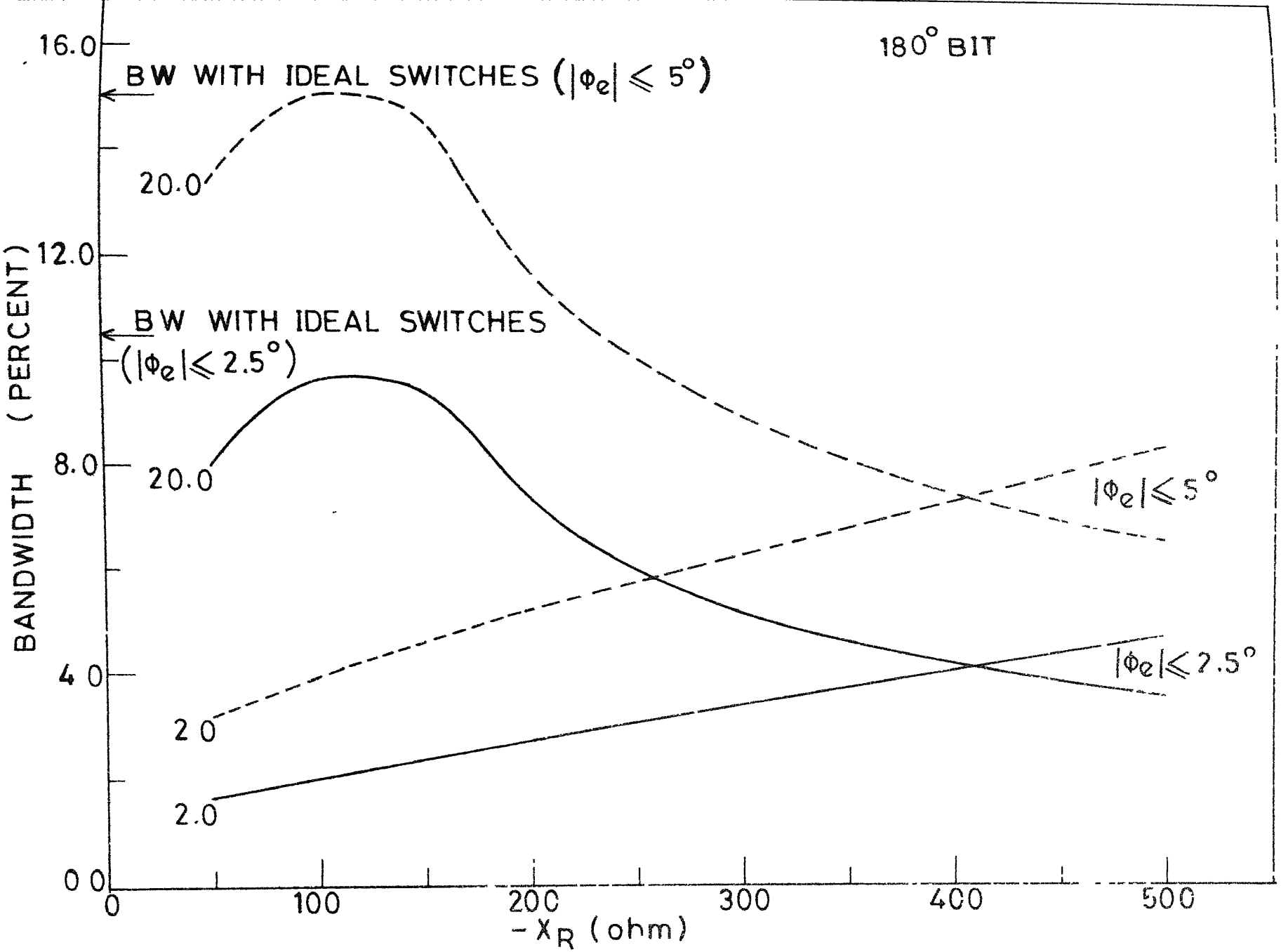
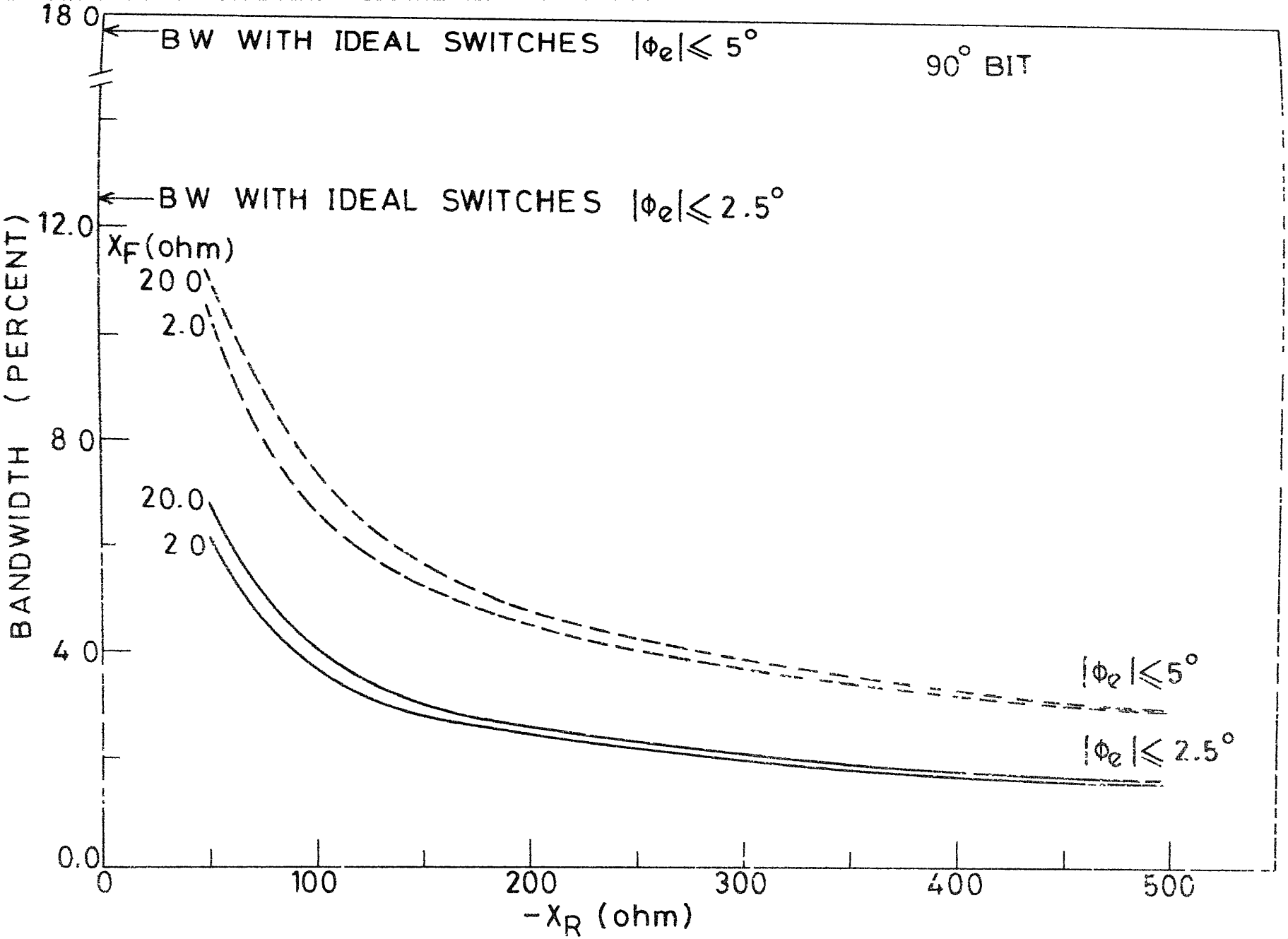


FIG. 5.7 VARIATION OF BANDWIDTH [illegible] FOR 180° [illegible] BIT [illegible]
HYBRID AND QUARTER [illegible] PHASE-SHIFTING NETWORK.



[illegible] VARIATION OF BANDWIDTH WITH X_R FOR OC[illegible] HALF AND QUARTER WAVE TRANSFORMER T-OPE[illegible]

838

value. For X_F = 2 and 20 ohms for $|\phi_e| \leq 2.5°$ bandwidth decreases with $|X_R|$. Similar results (but larger values) for $|\phi_e| \leq 5°$ are obtained. In all the cases bandwidth is found to be limited by the phase error and not by VSWR. Bandwidth using ideal switches (section 3.5.2) is found to be 17.7% for $|\phi_e| \leq 5°$, and 12.5% for $|\phi_e| \leq 2.5°$.

5.1.2.2 Single stub transforming network

180° Bit

Bandwidth of this phase bit is plotted in Fig. 5.9 as a function of diode reactance X_R, for two values of X_F (2.0 ohm and 20.0 ohm). For X_F = 2.0 ohm, and for $|\phi_e| \leq 2.5°$ and $\leq 5°$, it is observed that the bandwidth increases with X_R. Only open stub is used over the given range of X_R. For X_F = 20 ohm, bandwidth increases rapidly with $|X_R|$, till the point $Z_o^2 = -X_F X_R$ is reached. For $Z_o^2 < |X_F X_R|$ shorted stub of longer length is desired and hence the bandwidth becomes low abruptly. Bandwidth is found to be limited by phase error only.

Thus, for this type of circuit, one should use diodes with small X_F and large $|X_R|$ (low L-C) so that only open stubs of shorter lengths are used and wider bandwidths are obtained.

90° Bit

Figure 5.10 shows the variation of bandwidth as a function of X_R. For X_F = 2 ohm, and $|\phi_e| \leq 2.5°$ and $|\phi_e| \leq 5°$, bandwidth remains nearly constant with increase in $|X_R|$.

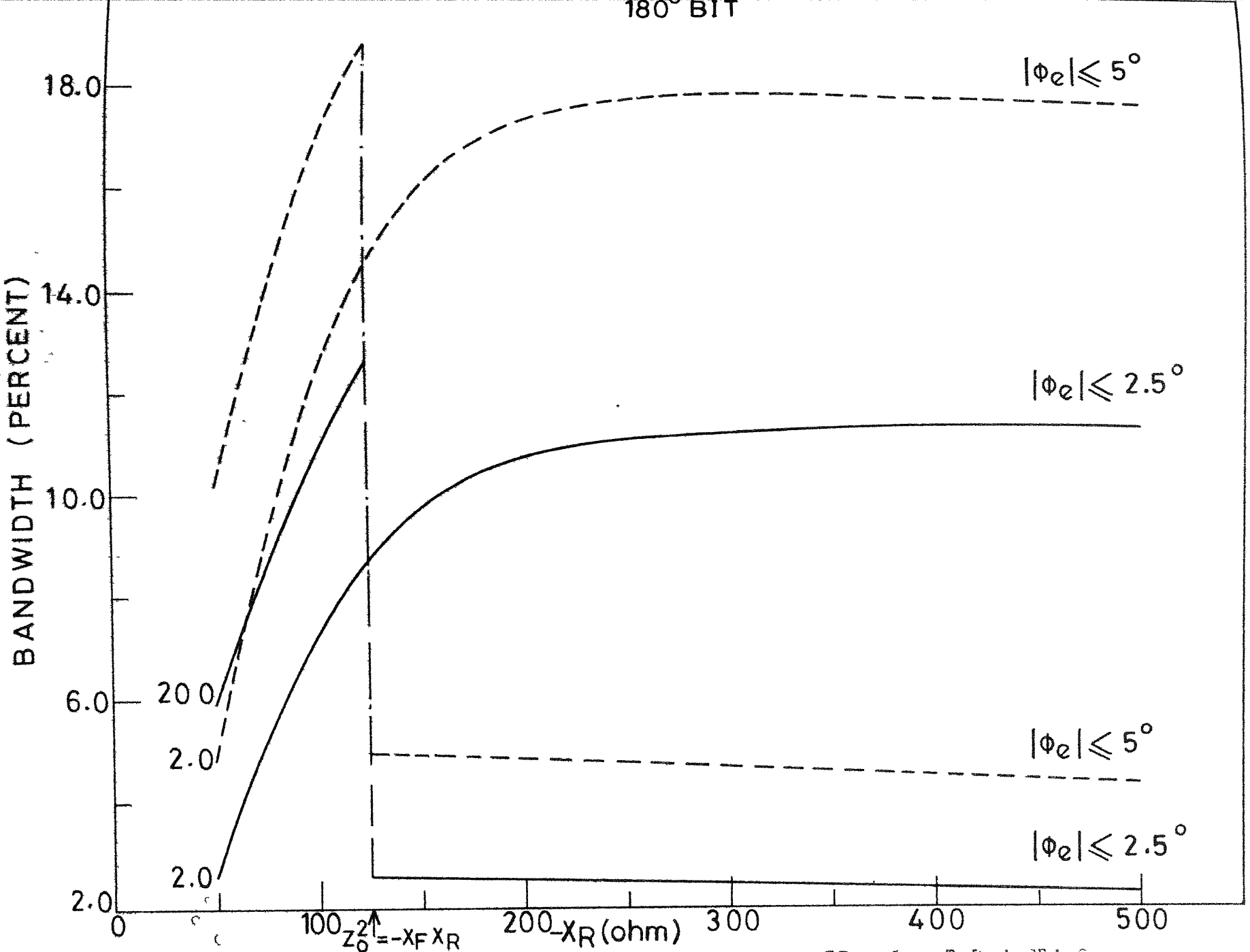


FIG. 5.9 VARIATION OF BANDWIDTH WITH A_R FOR 180° HYBRID RING AND THREE-BRANCH HYBRID AND SINGLE STUB TRANSFORMING NETWORK

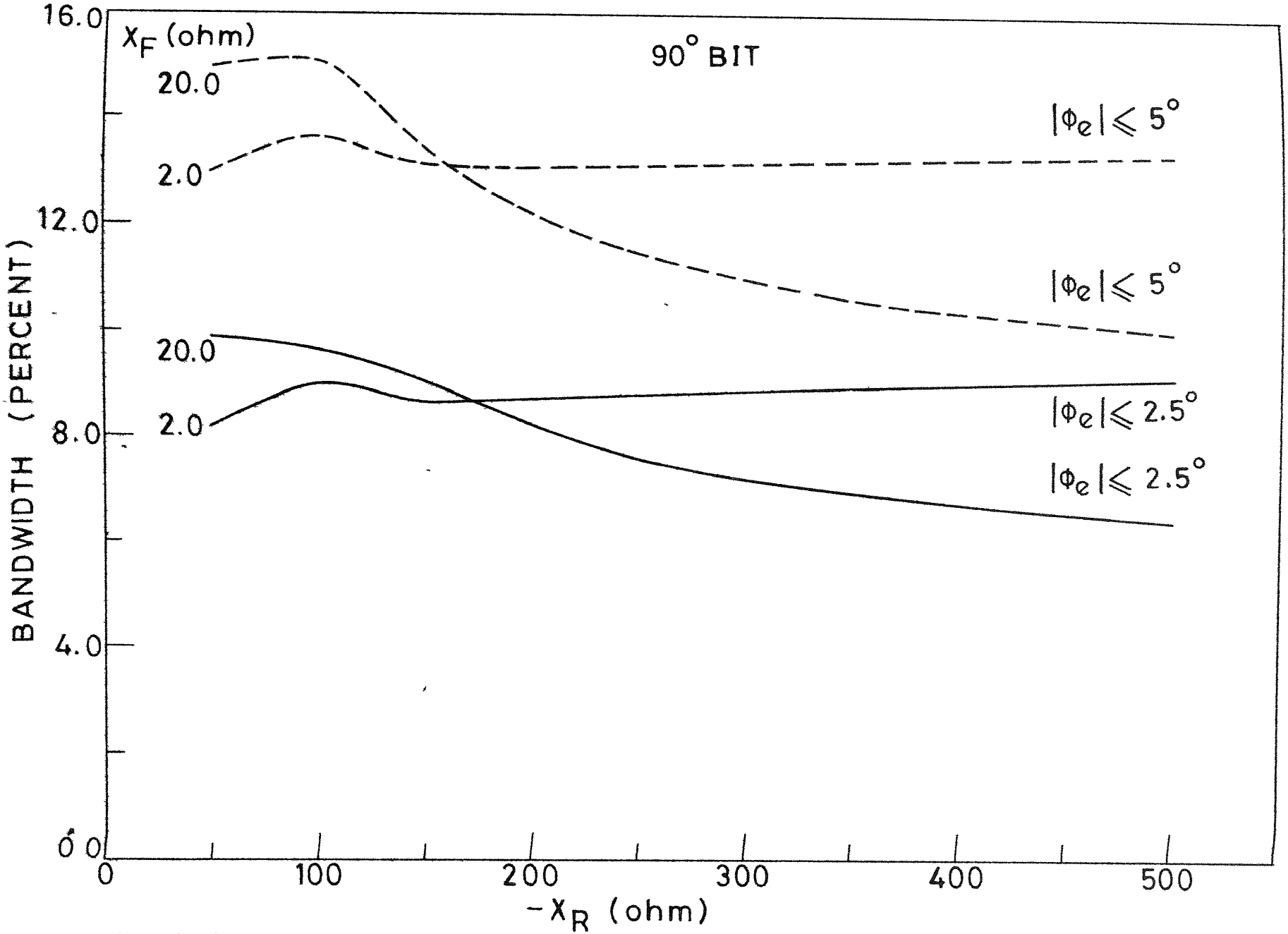


FIG. 5.10 VARIATION OF BANDWIDTH WITH X_R FOR 90° PHASE BIT USING THREE-BRANCH HYBRID AND SINGLE STUB TRANSFORMING NETWORK.

Bandwidth for $|\phi_e| \leq 5°$ is larger than for $|\phi_e| \leq 2.5°$. For X_F = 20 ohm, for both the specifications of bandwidth ($|\phi_e| < 2.5°$ and $|\phi_e| < 5°$), bandwidth is found to decrease with increase in $|X_R|$ value.

5.1.3 Circuit Using Rat-Race Hybrid

In this section phase shifter circuits using rat-race hybrid and two types of transforming networks are considered.

5.1.3.1 Quarter wave transforming network

180° Bit

The variation of bandwidth as a function of diode reactance X_R for fixed values of X_F is shown in Fig. 5.11. The variation of bandwidth in this case is found to be identical to that of three-branch case discussed in Section 5.1.2.1. The maximum bandwidth over the range of the diode reactances considered is more in the three-branch case as compared to rat-race case. For X_F = 20 ohm, the maximum bandwidth $|\phi_e| \leq 5°$ for three-branch hybrid case is approximately 15% compared to that of 11.5% for rat-race hybrid.

90° Bit

Figure 5.12 shows the variation of bandwidth as a function of diode reactance X_R for two values of X_F (2 and 20 ohms). Variation of bandwidth in this case is also found to be similar to that in the three-branch hybrid case (Sec. 5.1.2.1). The maximum and minimum bandwidths for the

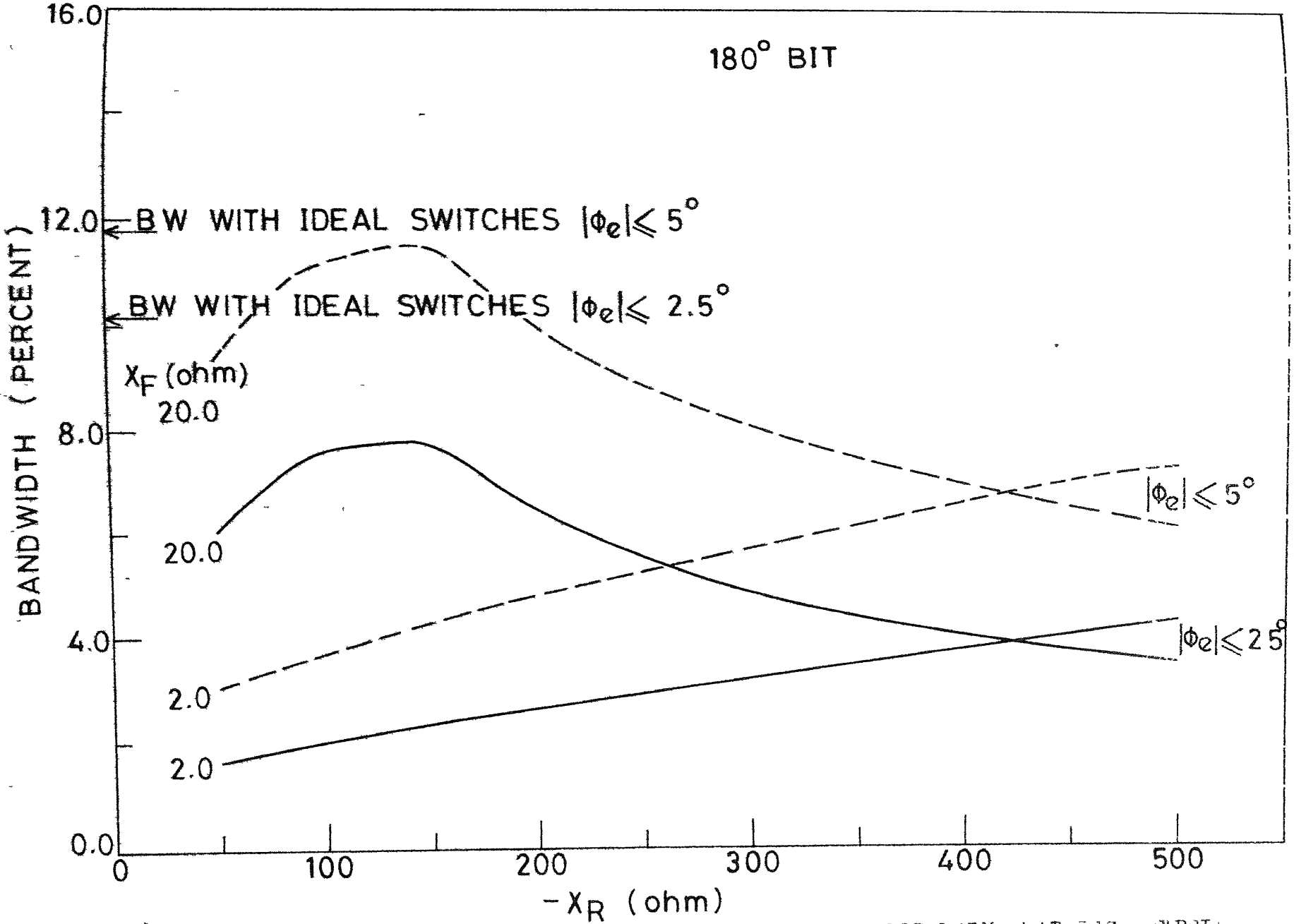


FIG. 5.11 VARIATION OF BANDWIDTH WITH X_R FOR 180° PHASE BIT USING HAT-RACE HYBRID AND QUARTER WAVE TRANSFORMING NETWORK.

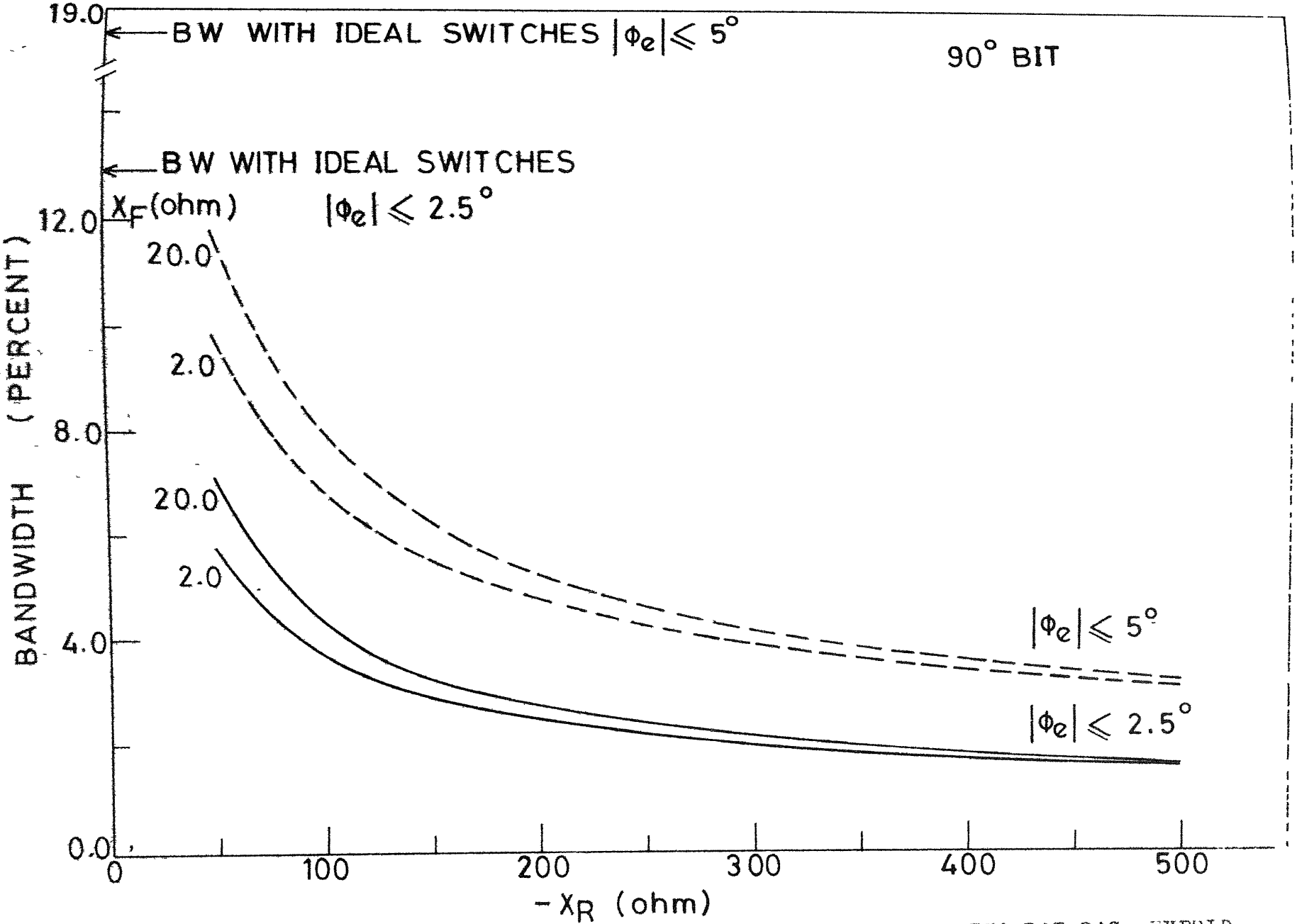


FIG. 5.12 VARIATION OF BANDWIDTH WITH X_R FOR 90° PHASE BIT USING RAT-RACE HYBRID AND QUARTER WAVE TRANSFORMING NETWORK.

given bandwidth specifications are of the same order of magnitude in the two cases.

5.1.3.2 Single stub transforming network

180° Bit

The variation of bandwidth as a function of diode reactance X_R is shown in Fig. 5.13. As in the case of three-branch hybrid (Sec. 5.1.2.2), for X_F = 2 ohm, bandwidth (for both the specifications) increases with $|X_R|$. The maximum bandwidth achieved in this case is less than that achieved in the three-branch case. For example, the maximum bandwidth for $|\phi_e| \leq 5°$ in the case of three-branch hybrid is approximately 18% as compared to approximately 12% in the case of rat-race hybrid. For X_F = 20 ohm, similar variations are obtained in the two cases.

90° Bit

Figure 5.14 shows the variation of the bandwidth in this case as a function of X_R. For X_F = 2 ohm, the bandwidth (both for $|\phi_e| \leq 5°$ and $|\phi_e| \leq 2.5°$) is found to increase with $|X_R|$. For X_F = 20 ohm and $|\phi_e| \leq 2.5°$, bandwidth is found to increase with $|X_R|$ initially and then decreases with $|X_R|$. For X_F = 20 ohm and $|\phi_e| \leq 5°$ bandwidth increases sharply to large value and then decreased slowly with $|X_R|$. The maximum bandwidth achieved is approximately 34%. This value is much larger than that of using ideal switches, in which case the BW is 18.6% (for $|\phi_e| \leq 5°$). This large bandwidth is due to

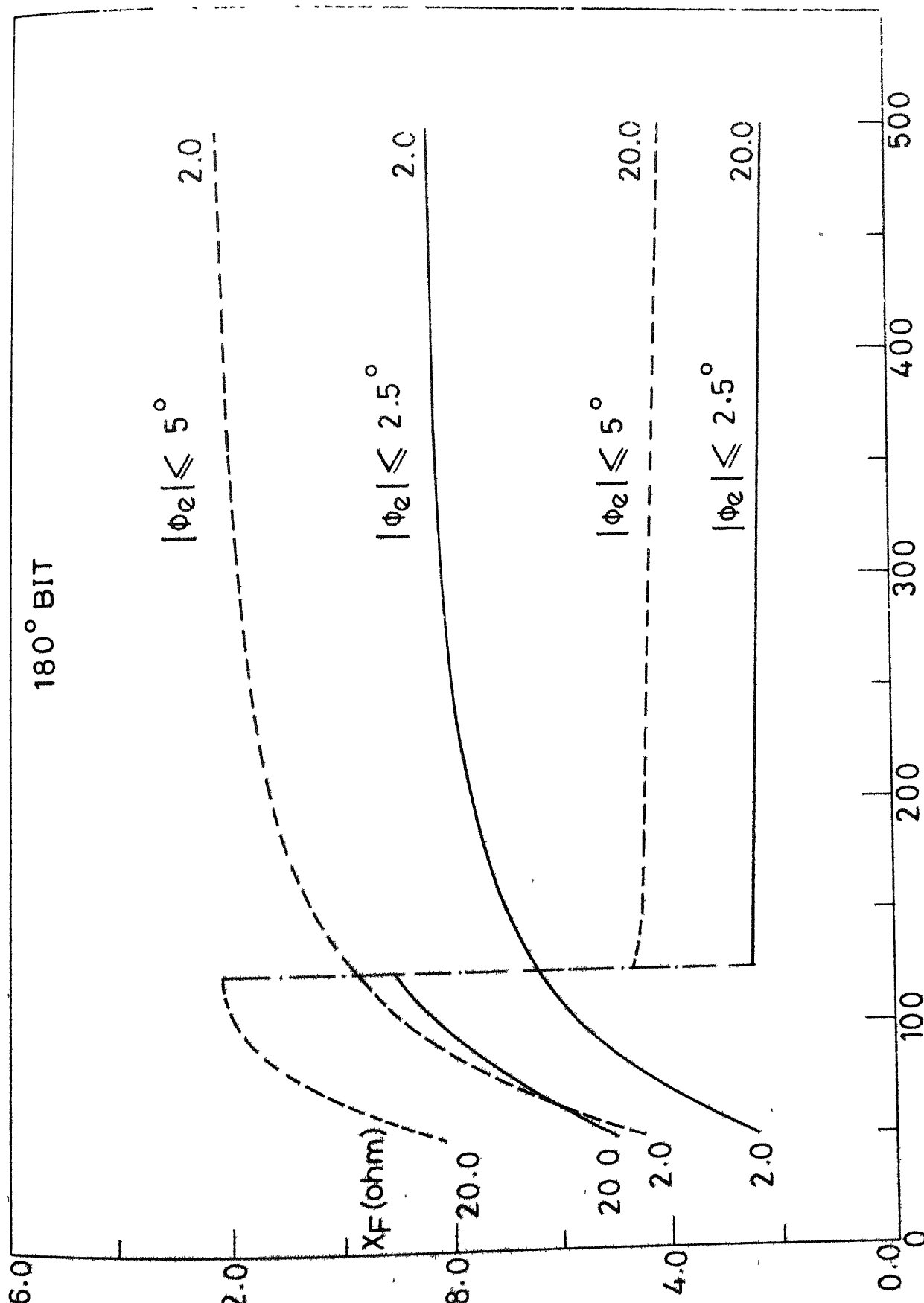


FIG. 5.13 VARIATION OF BANDWIDTH WITH X_R FOR 180° PHASE BIT USING RAT-RACE HYBRID AND SINGLE STUB TRANSFORMING NETWORK.

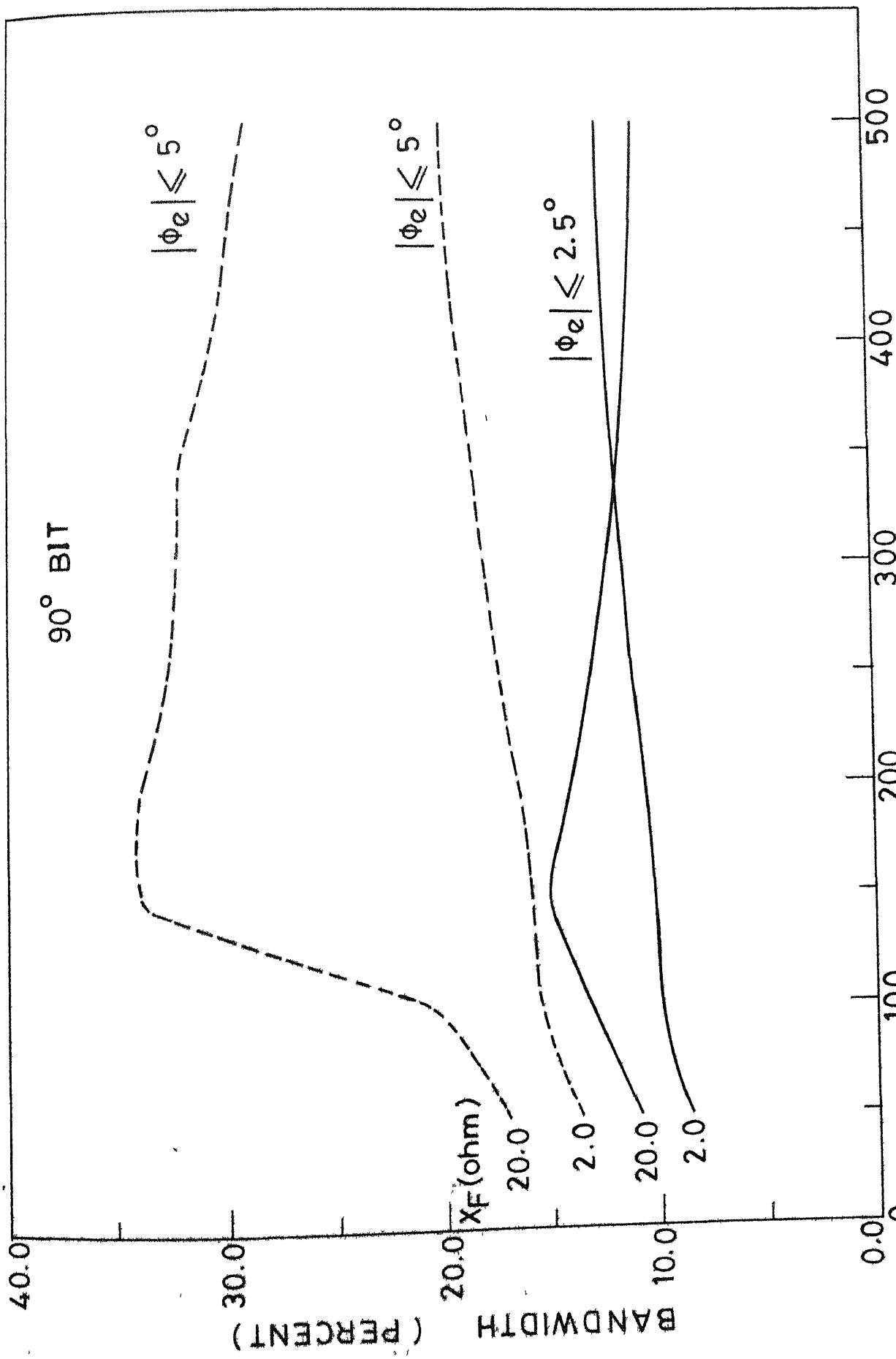


FIG. 5.14 VARIATION OF BANDWIDTH WITH X_R FOR 90° PHASE BIT USING RAT-RACE HYBRID AND SINGLE STUB TRANSFORMING NETWORK.

the ripple type behaviour in the phase error versus frequency plot. The phase error increases but starts decreasing before reaching 5° magnitude. Subsequently,the frequency where it becomes 5° on the other side of the nominal value determines the bandwidth.

5.2 INSERTION LOSS OF PHASE SHIFTER CIRCUITS

The insertion loss of a phase shifter depends on (i) series resistance of the diode (ii) other parameters of the diode and (iii) the type of transforming network and the hybrid used. For computing the insertion loss of the phase bit, the method of analysis discussed in Chapter 3 is used. For insertion loss computation,lossy diodes (with $R_F=R_R=0.5$ ohm) are considered. The values of the insertion loss have been computed only at the centre frequency. If the transmission line losses are ignored, the insertion loss at centre frequency becomes independent of the hybrid type (all hybrids are considered ideal at the centre frequency) and depends only on the diodes and the transforming networks.

In this section losses in phase shift networks for both 180° and 90° bits are computed for $\alpha = 0$ dB/λ and $\alpha = 0.2$ dB/λ. Insertion loss of phase bits using two-branch hybrid with three types of transforming networks, three-branch and rat-race hybrids with two types of transforming networks, are discussed.

5.2.1 Circuits Using Quarter Wave Transforming Network

Figure 5.15 shows the variation of insertion loss as a

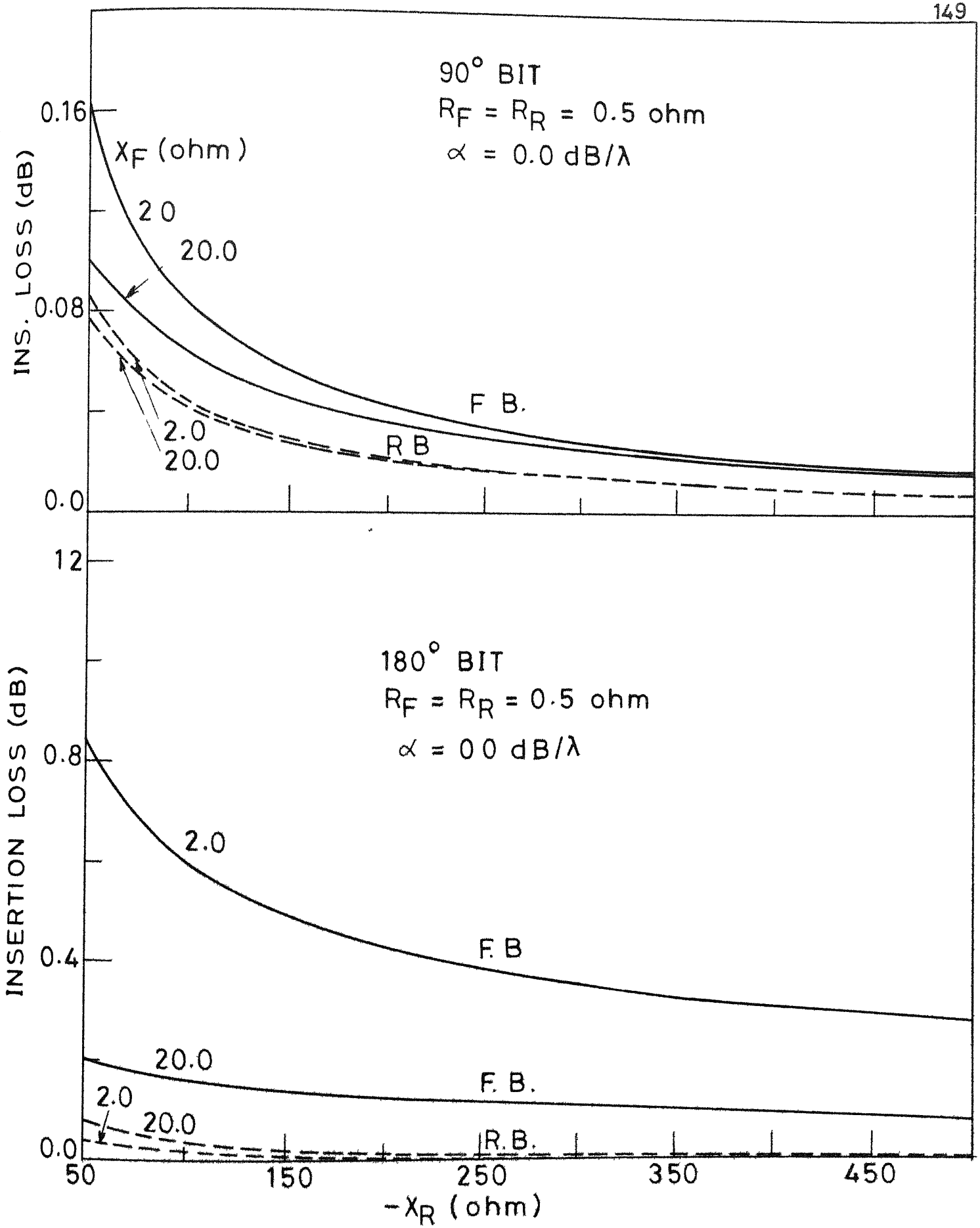


FIG. 5.15 VARIATION OF INSERTION LOSS WITH X_R FOR 180° AND 90° PHASE BITS USING QUARTER WAVE TRANSFORMING NETWORK

function of reverse bias reactance X_R for two values of X_F (2 and 20 ohms). Transmission line losses are ignored in this case. Hence, this represents the losses of the two phase shift networks (transforming networks and diodes). Insertion loss is found to decrease with increase in reverse bias reactance $|X_R|$ for both 90° and 180° phase shifts. In the forward bias state the insertion loss is more than that in the reverse bias state. Typical loss values are 0.161 dB for 90° bit and 0.836 dB for 180° bit (for $R_F = R_R = 0.5$ ohm and $X_F = 2$ ohm, $|X_R| = 50$ ohm). Diodes with larger X_F values give smaller loss in the forward bias state.

Figures 5.16 to 5.18 present the insertion loss of the phase bits using two-branch, three-branch and rat-race hybrids including line losses (0.2 dB/λ) for both 90° and 180° bits. These plots display the total loss of the phase bit. Both line losses and diode losses are dependent on the diode reactances. Line losses change because of the change in line lengths and impedances of the transforming network for the given set of diode reactances.

As seen from Figs. 5.16 to 5.18, the 180° bit gives high loss for small X_F value (2.0 ohm). Hence diodes with larger X_F values should be used in this type of phase shift network.

5.2.2 Circuits Using Single Stub Transforming Network

Insertion loss of a phase shifter circuit using single

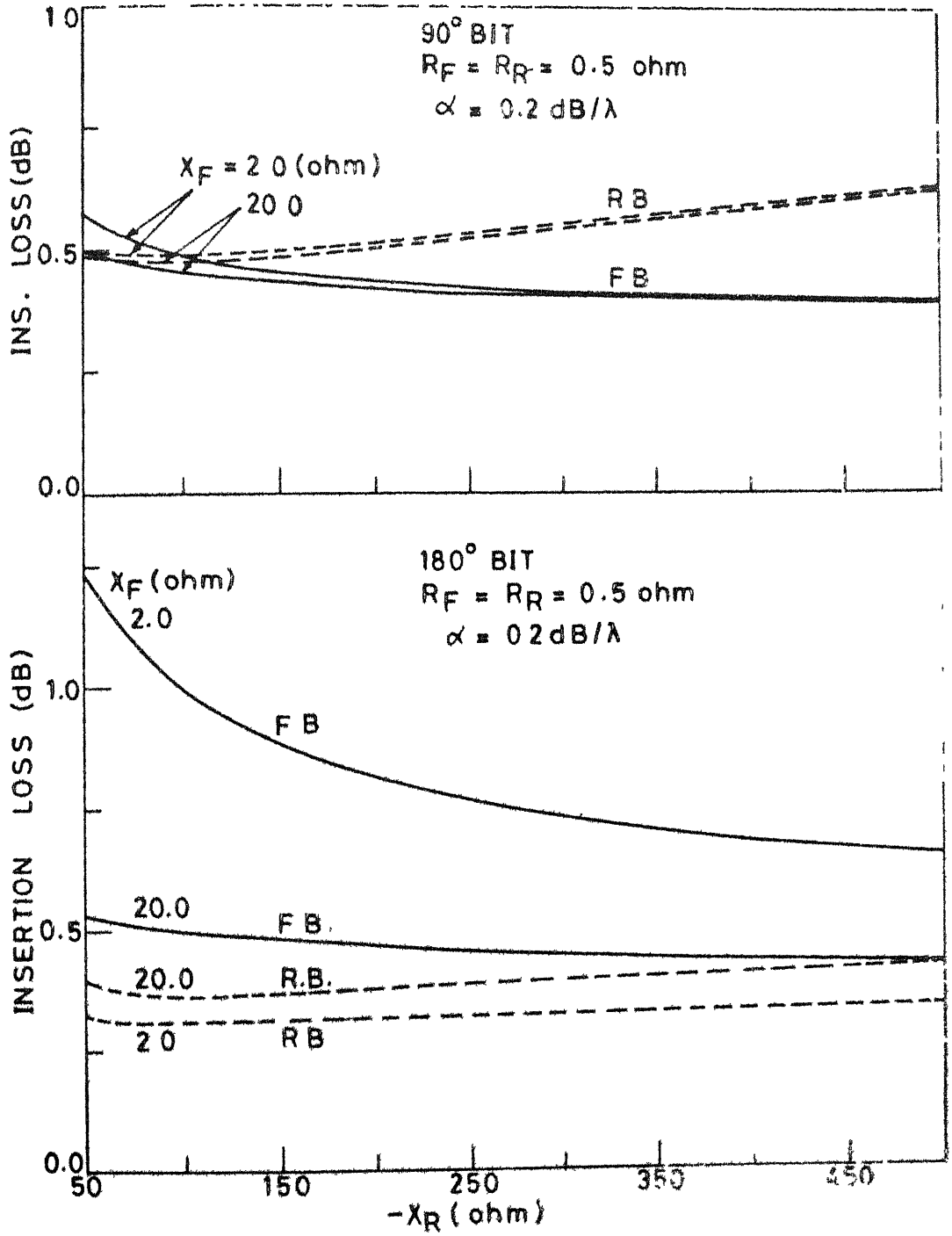


FIG. 5.16 VARIATION OF INSERTION LOSS WITH X_R FOR 180° AND 90° PHASE BITS USING TWO-BRANCH HYBRID AND QUARTER WAVE TRANSFORMING NETWORK

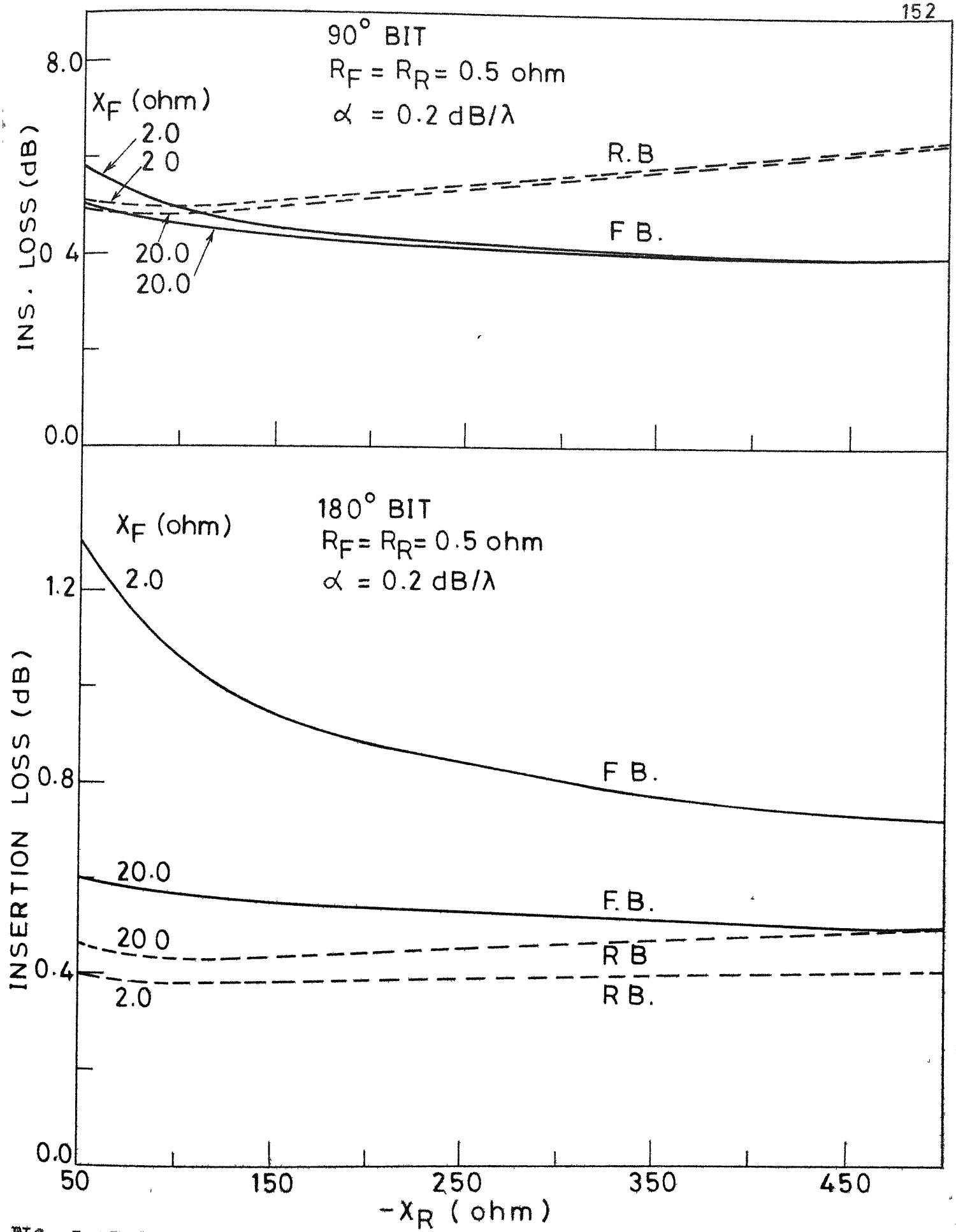


FIG. 5.17 VARIATION OF INSERTION LOSS WITH X_R FOR 180° AND 90° PHASE BITS USING THREE-BRANCH HYBRID AND QUARTER WAVE TRANSFORMING NETWORK

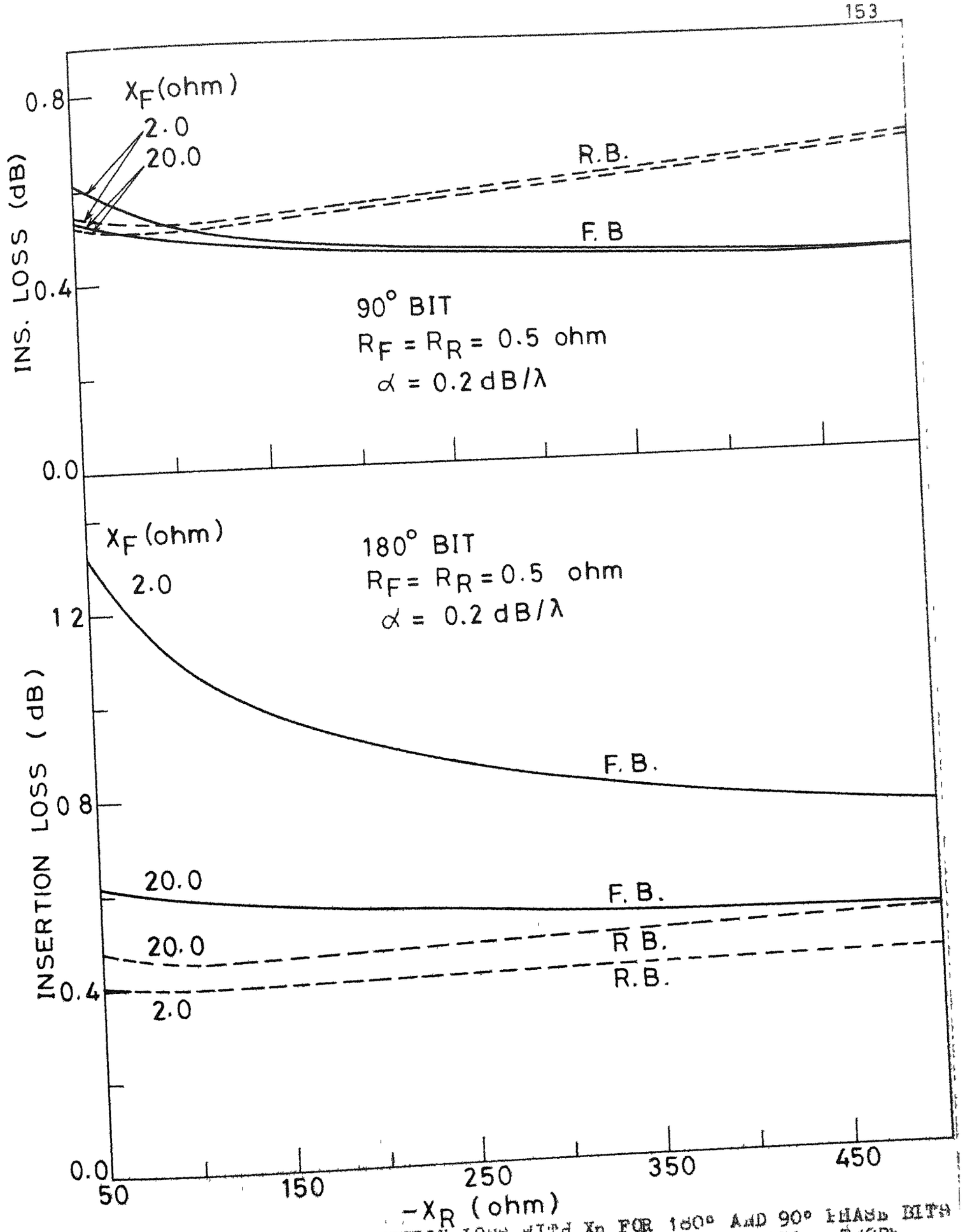


FIG. 5.18 VARIATION OF INSERTION LOSS WITH X_R FOR 180° AND 90° PHASE BITS USING RAT-RACE HYBRID AND QUARTER WAVE TRANSFORMING NETWORK

stub transforming network is computed for different diode parameters. When the line losses are ignored ($\alpha = 0$ dB/λ), the insertion loss of the phase shifter becomes independent of the hybrid type and the loss is only due to the phase shift network used.

Variation of insertion loss as a function of X_R for different X_F values (2 and 20 ohms) is given in Fig. 5.19. Diodes with large $|X_R|$ and large X_F give lower values of the insertion loss. Insertion loss in the reverse bias state becomes independent of X_F. Loss in the reverse bias state is found to be much lower than in the forward bias. As with the quarter wave transforming network, phase bit of 180° gives more loss as compared to 90° phase bit. For 180° phase bit and X_F = 20 ohm, the stub length becomes zero at X_R= -125 ohm. For $|X_R| < 125$ ohm, an open stub is used and for $|X_R| > 125$ ohm a shorted is being used. It is to be noted that stub type of transforming network is found to give less loss than quarter wave transformer type of network (Section 5.2.1).

Figures 5.20 to 5.22 show the variation of insertion loss in the particular cases of two-branch, three-branch and rat-race hybrid using single stub type network for a line loss $\alpha = 0.2$ dB/λ . It is to be noted that line losses become dominant and there is not much variation in insertion loss due to diode reactances. Phase bits using three-branch and rat-race hybrid have nearly identical loss characteristics while circuit using two-branch has little lower loss.

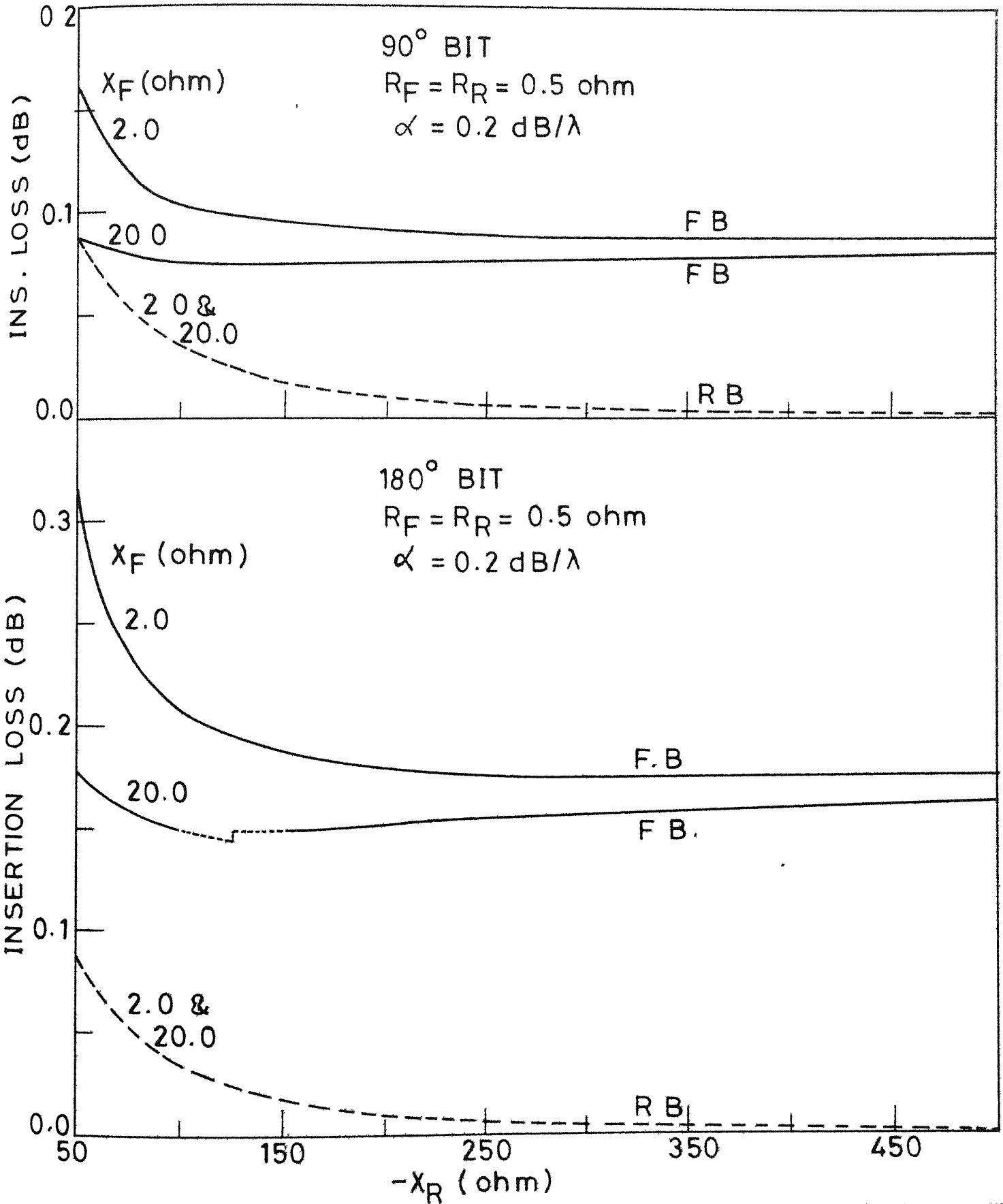


FIG. 5.19 VARIATION OF INSERTION LOSS WITH X_R FOR 180° AND 90° PHASE BITS USING SINGLE STUB TRANSFORMING NETWORK

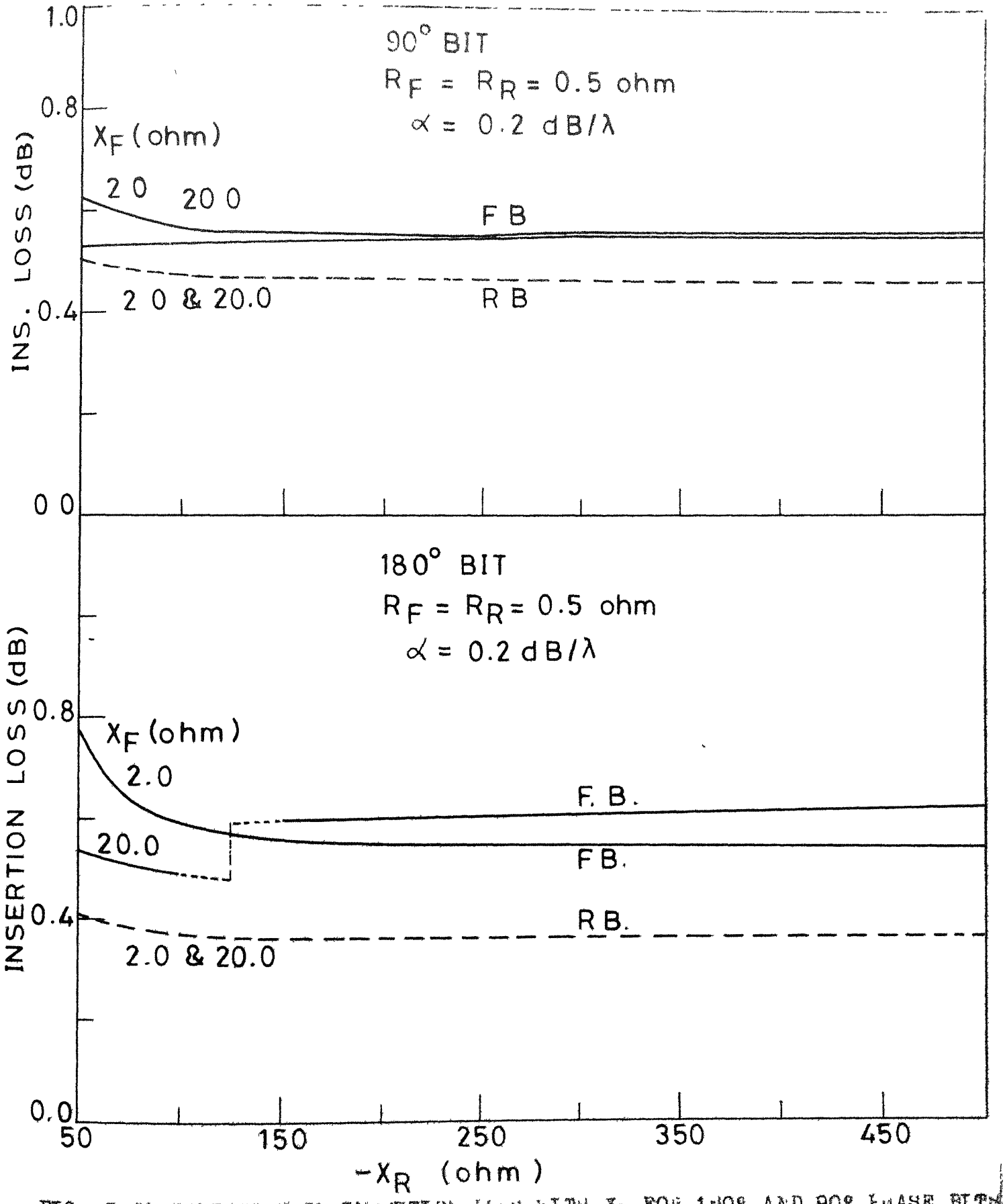


FIG. 5.20 VARIATION OF INSERTION LOSS WITH X_R FOR 180° AND 90° PHASE BITS USING TWO-BRANCH HYBRID AND SINGLE STUB TRANSFORMING NETWORK

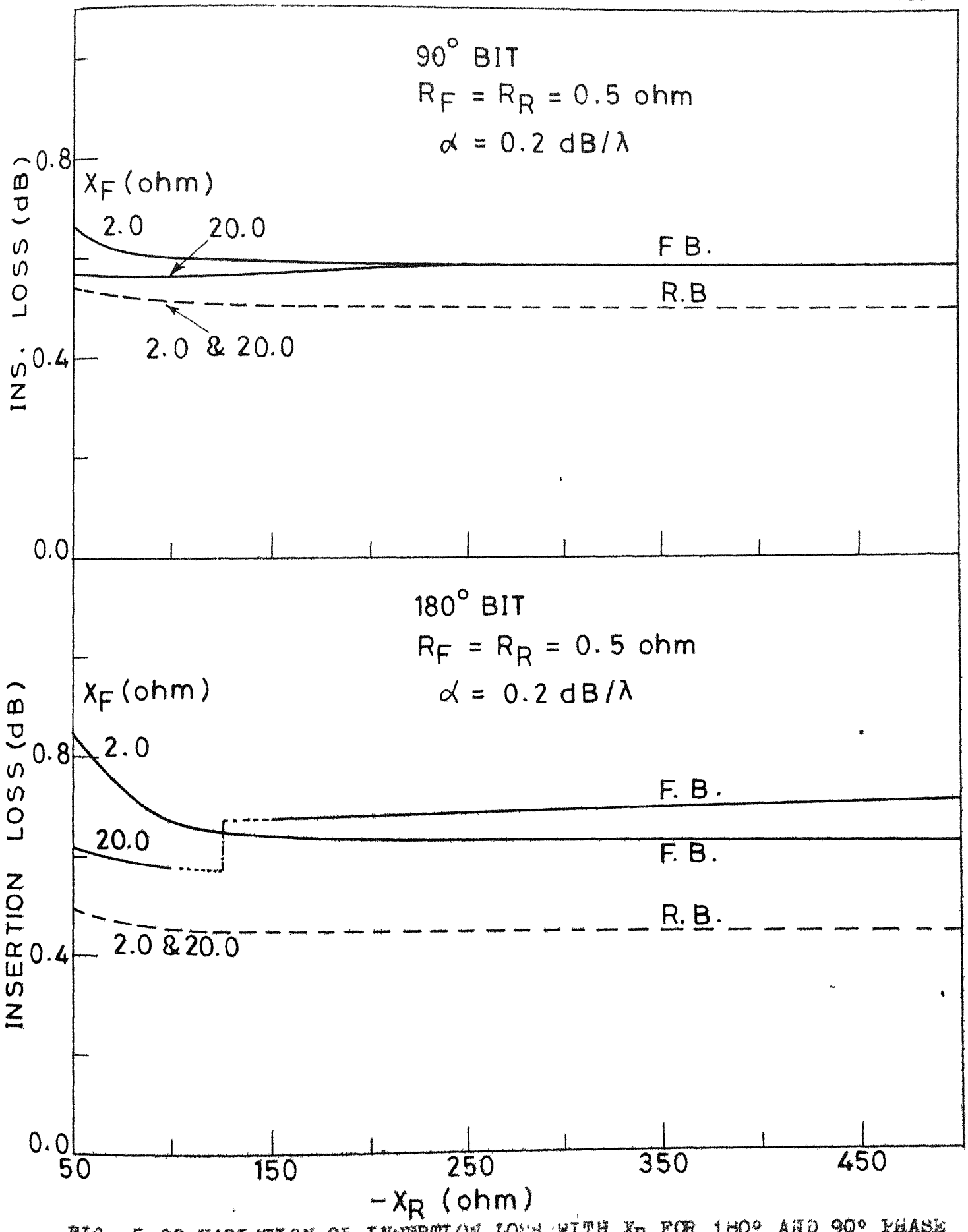


FIG. 5.22 VARIATION OF INSERTION LOSS WITH X_R FOR 180° AND 90° PHASE [illegible] RAT-RACE HYBRID AND SINGLE STUB TRANSFORMING

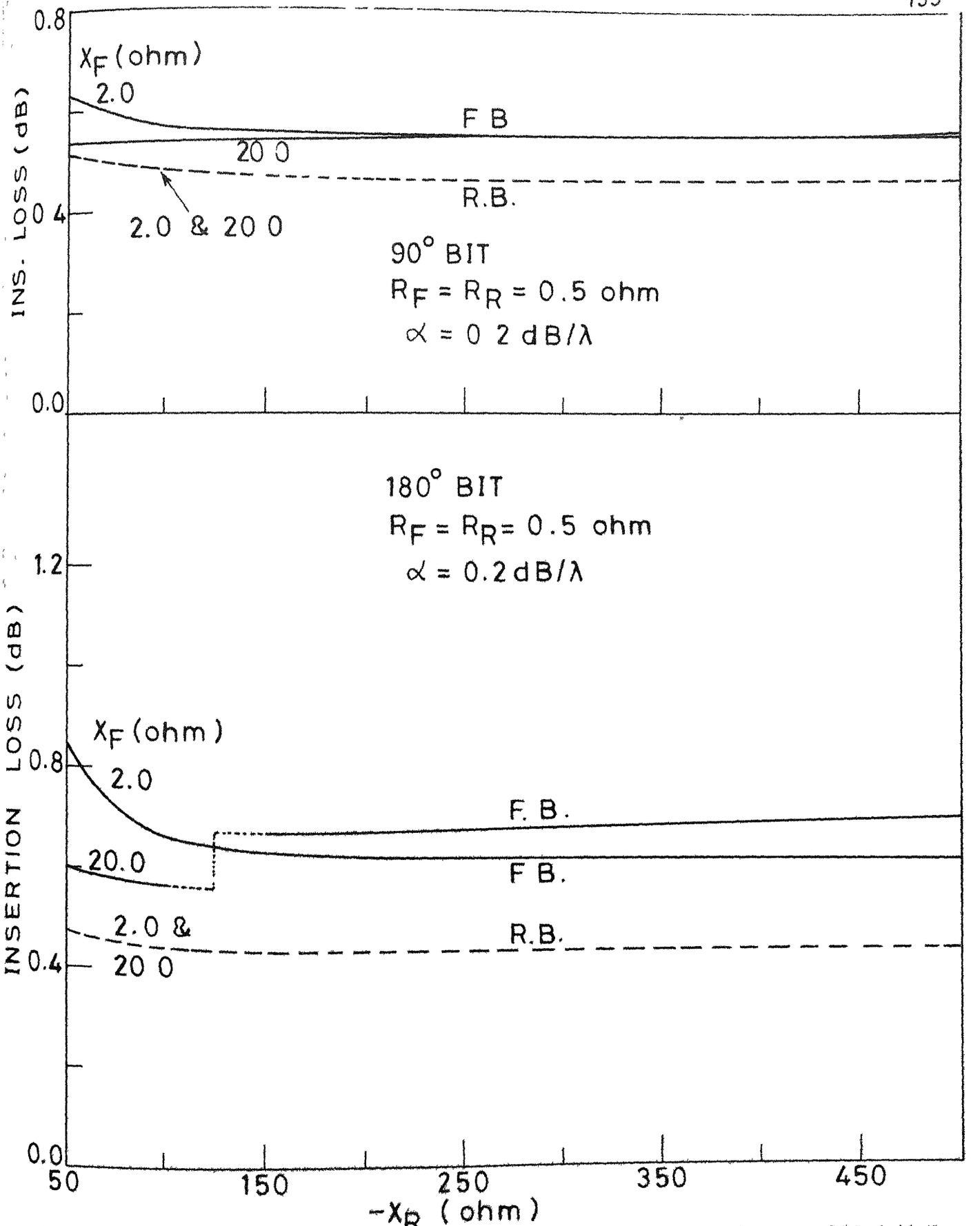


FIG. 5.21 VARIATION OF INSERTION LOSS WITH X_R FOR 180° AND 90° PHASE BITS USING THREE-BRANCH HYBRID AND SINGLE STUB TRANSFORMING NETWORK

5.2.3 Circuit Using Impedance Transforming Hybrid

Insertion loss variation of the phase shift network of this type with zero line loss is found to be exactly same as for the phase shift network using quarter wave transformer (Section 5.2.1). This is due to the fact that the equal RF currents flow through diodes in both of these circuits at the centre frequency. Thus, the discussion of Section 5.2.1 applies here.

For a typical phase bit using two-branch impedance transforming hybrid with line loss 0.2 dB/λ and the above mentioned network, the plot of insertion loss as the function of diode reactance is given in Fig. 5.23. Both 90° and 180° bits are found to have less loss as compared to the phase shifter circuits using normal two-branch hybrid and quarter wave or single stub type transforming networks. The reason being that the shorter line lengths are needed for the phase bit using impedance transforming hybrid. Size of the circuit also becomes smaller in the latter case.

5.3 COMPARISON OF PHASE SHIFTER CIRCUIT FOR BANDWIDTH, INSERTION LOSS AND SIZE

Bandwidth and insertion loss of phase shifter circuits using two-branch, three-branch and rat-race hybrids with three types of transforming networks have been studied in Sections 5.1 and 5.2. This section presents a comparison of these phase shifter circuits for bandwidth insertion loss and size. Table 5.2 and 5.3 give bandwidth and insertion

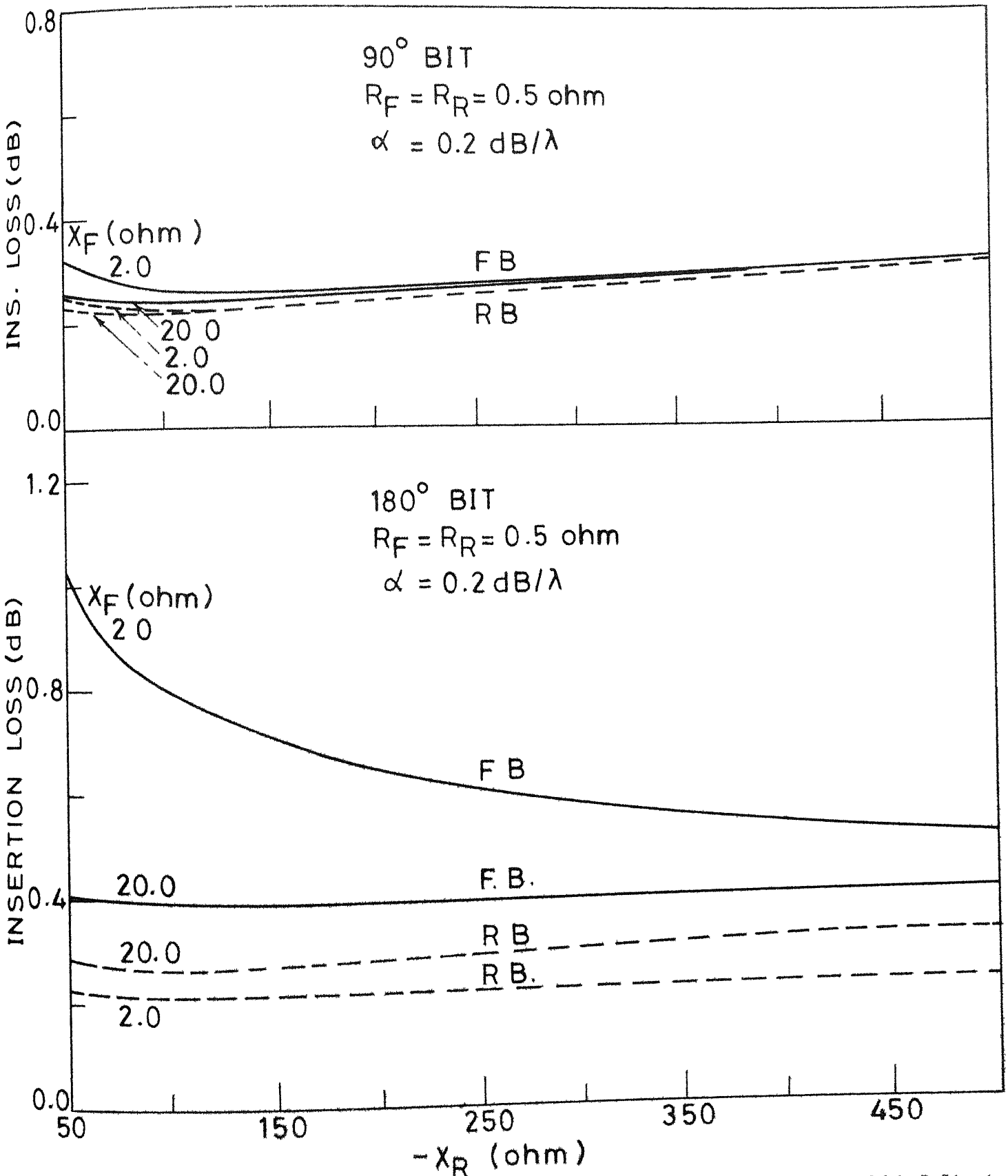


FIG. 5.3 VARIATION OF INSERTION LOSS WITH X_R FOR 180° AND 90° BITS OF E. CRIM. 2-ELEMENT IMPEDANCE TRANSFORMER [illegible]

loss performance for the typical diode parameters. Two sets of typical diode parameters (one with low L-C and the other with high L-C) are selected in each case.

5.3.1 Bandwidth

Phase shifter circuits using two-branch hybrids for 180° bits, both transformer type and stub type transforming networks are appropriate if diodes with low L and C are used for $|\phi_e| \leq 5°$. If tighter phase variations are desired (say $|\phi_e| \leq 2.5°$) stub type transforming network is the best choice. For diodes with high L and C, quarter wave transforming network is the better choice. Phase bits using impedance transforming hybrid and its associated network give wide bandwidths when diodes with large X_F and large X_R are used as compared to the circuits using normal two-branch hybrid and other transforming networks (quarter wave transformer and stub type). For example, diode with X_F = 20 ohm and X_R = -500 ohm gives bandwidth approaching 6% which is independent of the phase error specification (i.e. the BW is limited by VSWR specification).

A 90° bit using two-branch hybrid and quarter wave transforming network does not require diodes with low L and C to get wider bandwidths, a diode with large X_F and small $|X_R|$ (high L and C) is most appropriate. For normal two-branch hybrid, stub type network seems to be a better choice. Impedance transforming hybrid with its transforming network gives the widest bandwidth approaching approximately 8.5% for X_F = 20 ohm and X_R = -200 ohm for $|\phi_e| \leq 5°$.

Phase shifter circuits using three-branch and rat-race hybrids with quarter wave transforming networks give narrow bandwidths than for stub type networks (180° bit) using low L-C diodes. When diodes with high L,C are used, bandwidth using stub type network is not much affected, while with quarter wave transformer it is found to improve to a great extent. For 90° bit, using transformer type network only diodes with high L and C give usable bandwidths and it sharply reduces with increase in $|X_R|$. For 90° bit, stub type network is most suited to all diode types. Phase shifters using three - branch hybrids are in general have wider bandwidths than the circuits using rat-race hybrid. Tables 5.1(a) and (b) give bandwidths using 'low L-C' and 'high L-C' diodes, respectively for various types of phase shifter circuits considered in earlier discussions.

For several configurations discussed in this chapter, it has been observed that high L-C diodes yield wider phase shifter BW than low L-C diodes. This is true for all cases except for stub type transforming network where a short length of the stub becomes more significant than diode reactances for obtaining a wide bandwidth.

For high L-C case, the configuration may be compared with lumped-element reflection phase shifter discussed by Garver [10]. Reactance values for a typical 45° bit considered in [10] are: C_D = 8.8 pf and C_C = (1-a)C at 1.0 GHz frequency. This corresponds to X_F = 18 ohm and X_R = -14.55 ohms which

according to our terminology corresponds to a high L-C diode.

5.3.2 Insertion Loss

Insertion loss of the phase shift networks (i.e. when α = 0 dB/λ) is found to decrease in general, with the increase in the reverse bias reactance $|X_R|$ of the diode. In other words, diodes having small reverse bias capacitances would yield lower loss. Forward bias reactance X_F of the diode is found to have considerable effect on the insertion loss for smaller $|X_R|$ values. Insertion loss in the reverse bias state does not depend much on the diode parameters. Diodes having small inductance and large capacitance give very high loss in the forward bias state.

When the transmission line loss of 0.2 dB/λ is considered, the total loss of the phase bit is obtained. The variation of this loss with X_R is mainly governed by the loss due to the change in the transmission line length and not by the variation in diode losses (which are small if R_F and R_R are small). Tables 5.2(a) and (b) give insertion values for 'low L-C' and 'high L-C' diodes for α = 0 dB/λ and 0.2 dB/λ. From the table we see that phase bit using impedance transforming two-branch hybrid gives the lowest total loss, for both 180° and 90° bits, as compared to other circuits.

5.3.3 Size

The substrate area required for a phase shifter circuit

corresponds to θ_ℓ x θ_t where θ_ℓ and θ_t are the electrical lengths in the longitudenal and the transverse directions, respectively. The phase shifter circuits using a quarter wave transforming network and those using impedance transforming hybrid, do not require extra lengths in the transverse direction. The phase shifters using stub type network require lengths in transverse direction. These extra lengths depend on the size of the stubs to be used which in turn depends on the diode parameters.

In the case of transforming networks of quarter wave type and impedance transforming type, the diodes with large X_F and small $|X_R|$ ('high L-C' diodes) require shorter electrical lengths for both 180° and 90° bits. The quarter wave network requires additional 90° length for the transformer while the transforming network used with impedance transforming hybrid does not require this 90° length, since impedance transformation has been incorporated in the hybrid itself. Hence, the circuit using impedance transforming hybrid has smaller size.

Phase shifters using stub type transforming networks are larger in size. When the stubs used in each coupled port can not be accomodated in the space between the coupled ports, dimensions in transverse direction also increase. Hence, stub type circuits are not suitable where small size is the dominating factor.

TABLE 5.1(a). Bandwidth of phase shifters using 'low L-C' diodes (X_F = 2 ohm and X_R = -400 ohm)

Phase Bit	TWO-BRANCH HYBRID						THREE-BRANCH HYBRID				RAT-RACE HYBRID			
	BW_1(%)			BW_2(%)			BW_1(%)		BW_2(%)		BW_1(%)		BW_2(%)	
	TRN_1	TRN_2	TRN_3	TRN_1	TRN_2	TRN_3	TRN_1	TRN_2	TRN_1	TRN_2	TRN_1	TRN_2	TRN_1	TRN_2
180° Bit	3.2	5.0	4.0	4.9	5.0	4.0	4.1	11.4	7.3	17.7	3.8	8.4	6.6	12.0
90° Bit	1.7	5.4	4.9	3.3	5.4	7.6	1.7	6.7	3.2	13.2	1.7	12.2	3.5	19.3

BW_1 - BW for VSWR < 1.2 and $\phi_e < \pm 2.5°$

BW_2 - BW for VSWR < 1.2 and $\phi_e < \pm 5°$

TRN_1 - Quarter wave transformer type network

TRN_2 - Single stub type network

TRN_3 - Network for use with impedance transforming hybrid.

TABLE 5.1(b). Bandwidth of phase shifters using 'high L-C' diodes (X_F = 20 ohm & X_R = 62.5 ohm).

Phase Bit	TWO-BRANCH HYBRID						THREE-BRANCH HYBRID				RAT-RACE HYBRID			
	BW_1(%)			BW_2(%)			BW_1(%)		BW_2(%)		BW_1(%)		BW_2(%)	
	TRN_1	TRN_2	TRN_3	TRN_1	TRN_2	TRN_3	TRN_1	TRN_2	TRN_1	TRN_2	TRN_1	TRN_2	TRN_1	TRN_2
180° Bit	4.7	4.5	4.4	5.0	5.0	4.4	8.6	7.2	14.0	12.0	6.5	6.0	10.0	9.5
90° Bit	4.8	5.5	6.7	5.5	5.5	7.1	6.0	9.9	10.5	15.0	6.0	11.5	10.7	18.0

BW_1, BW_2, TRN_1, TRN_2 and TRN_3 are defined in Table 5.1(a).

TABLE 5.2(a). Insertion loss of phase shifters using 'low L-C' diodes (X_F = 2 ohm & X_R = -400 ohms)

Phase bit	Bias State	Insertion loss (dB) for α = 0.0 dB/λ			Insertion loss(dB) for α = 0.2 dB/λ						
					Two-branch hybrid			Three-branch hybrid		Rat-race hybrid	
		TRN_1	TRN_2	TRN_3	TRN_1	TRN_2	TRN_3	TRN_1	TRN_2	TRN_1	TRN_2
180° Bit	F.B.	0.306	0.175	0.306	0.680	0.541	0.534	0.754	0.610	0.768	0.625
	R.B.	0.001	0.003	0.001	0.331	0.363	0.230	0.400	0.432	0.415	0.447
90° Bit	F.B.	0.021	0.087	0.021	0.401	0.553	0.302	0.406	0.557	0.437	0.590
	R.B.	0.011	0.003	0.011	0.600	0.466	0.291	0.603	0.470	0.635	0.502

TRN_1, TRN_2 and TRN_3 are defined in Table 5.1(a).

TABLE 5.2(b). Insertion loss of phase shifters using 'high L-C' diodes (X_F = 20 ohm & X_R = 62.5 ohm)

Phase bit	Bias State	Insertion loss (dB) for α = 0.0 dB/λ			Insertion loss (dB) for α = 0.2 dB/λ						
					Two-branch hybrid			Three-branch hybrid		Rat-race hybrid	
		TRN_1	TRN_2	TRN_3	TRN_1	TRN_2	TRN_3	TRN_4	TRN_2	TRN_1	TRN_2
180° Bit	F.B.	0.185	0.165	0.185	0.52	0.52	0.40	0.58	0.58	0.61	0.61
	R.B.	0.065	0.067	0.065	0.38	0.40	0.28	0.45	0.46	0.47	0.47
90° Bit	F.B.	0.089	0.082	0.089	0.48	0.53	0.25	0.48	0.54	0.52	0.57
	R.B.	0.065	0.070	0.065	0.48	0.49	0.23	0.47	0.50	0.51	0.53

TRN_1, TRN_2 and TRN_3 are defined in Table 5.1 (a).

CHAPTER 6

EFFECT OF DIODE PARAMETERS ON PHASE SHIFTER PERFORMANCE

6.1 EFFECT OF DIODE REACTANCES 171

6.1.1 Sensitivities of Network for Use with Impedance Transforming Hybrid 171

6.1.2 Sensitivities of Transformer Type Network 175

6.1.3 Sensitivities of Single Stub Type Network 181

6.2 EFFECT OF DIODE RESISTANCES 182

6.2.1 Phase Shift Networks Using Quarter Wave Transformer and Network for Use with Impedance Transforming Hybrid. 183

6.2.2 Phase Shift Network Using Single Stub 187

6.3 EFFECT OF MISMATCHED DIODES 194

6.3.1 Effect on the Reflection Coefficient of the Phase Shifter 197

6.3.2 Effect on the Transmission Coefficient of the Phase Shifter. 199

6.4 DISCUSSIONS 201

CHAPTER 6

EFFECT OF DIODE PARAMETERS ON PHASE SHIFTER PERFORMANCE

Characteristics of PIN diodes used in phase shifters vary from unit to unit because of manfacturing tolerances. These variations can be as large as 10% above or below the nominal specified values. Since a large number of phase shifters are used in a practical phased array system, it is desirable to evaluate the effect of variation in diode parameters on the performance of the phase shifter. A study of this type has been reported [18] for one type of the circuit design which uses a shorted line length behind a shunt mounted diode. Similar study for the other commonly used design (diode mounted at the end of a transmission line) is not available.

This chapter deals with the effect of variations in diode reactances X_F and X_R and diode resistances R_F and R_R on performance of phase shifters based on various designs studied in Chapter 4. As mentioned there, three types of transforming networks are used in these designs. Also, the effect of unmatched diodes ($\Gamma_2 \neq \Gamma_3$) on phase shifter characteristics is evaluated. This study is useful in predicting the maximum deviations in diode parameters which can be tolerated for the given specifications of a phase bit. This investigation also brings out the critical diode parameters effecting the phase shifter performance.

In the study reported in this chapter, changes in the reflection coefficient at the input of the transforming network (caused by the variation in diode parameters) have been evaluated. It may be noted that these results are valid at the design frequency for the complete phase bit (including hybrid) if the mismatch error of the hybrid and the transmission line losses are ignored.

6.1 EFFECT OF DIODE REACTANCES

Nominal values of diode reactance in forward bias may typically range from 1 ohm to 25 ohm. In reverse bias the reactance X_R varies from -50 ohm to -500 ohm. Actual values for a particular diode may differ from the nominal values due to tolerances in diode fabrication process. Effect of these variations can be evaluated by finding sensitivity of differential phase shift $\Delta\phi$ with respect to diode reactances, namely X_F and X_R. These sensitivities are evaluated in this section.

To evaluate the sensitivities of $\Delta\phi$ with respect to X_F and X_R, the phases of reflection coefficients of the phase shift network (transforming network and diode) are first arrived at. From partial derivatives of these phases with respect to X_F and X_R, sensitivities of $\Delta\phi$ can be evaluated. These calculations have been carried out for three types of transforming networks which are commonly used.

6.1.1 Sensitivities of Network for Use with Impedance Transforming Hybrid

Figure 6.1 (inset (a))shows a phase shift network to be

used with impedance transforming hybrid (Chapter 4). It is to be noted that the line length θ_m of impedance Z_m, connected between hybrid port and diode for equalization of reflection coefficients in two states, does not change $\Delta\phi$ and is therefore not considered in the present analysis.

Reflection coefficients at plane AA for the two diode states can be written as

$$\Gamma_F = \frac{(X_F^2 - Z_m^2 + j\,2\,X_F Z_m}{X_F^2 + Z_m^2} \qquad (6.1a)$$

$$\Gamma_R = \frac{(X_R^2 - Z_m^2) + j\,2\,X_R Z_m}{X_R^2 + Z_m^2} \qquad (6.1b)$$

Partial derivatives of the phases of reflection coefficients are:

$$\frac{\partial \phi_F}{\partial X_F} = - \frac{2Z_m}{X_F^2 + Z_m^2} \qquad (6.2a)$$

$$\frac{\partial \phi_R}{\partial X_R} = - \frac{2Z_m}{X_R^2 + Z_m^2} \qquad (6.2b)$$

Derivative of ϕ_F with respect to X_R, and that of ϕ_R with respect to X_F are zero, since phase in one state does not depend on the reactance of the other state. Since the differential phase shift $\Delta\phi = \phi_R - \phi_F$, and

$$\frac{\partial}{\partial X_F}(\Delta\phi) = - \frac{\partial \phi_F}{\partial X_F} \qquad (6.3a)$$

and

$$\frac{\partial}{\partial X_R}(\Delta\phi) = \frac{\partial \phi_R}{\partial X_R} \qquad (6.3b)$$

Now the value of Z_m can be substituted in terms of X_F and X_R for a particular phase bit.

180° Phase Bit

In this case Z_m is given by Eqn. (4.7) as equal to $\sqrt{-X_F X_R}$ and Eqns. (6.2) may be rewritten as

$$\frac{\partial \phi_F}{\partial X_F} = - \frac{2.\sqrt{-\frac{X_R}{X_F}}.\frac{1}{X_F}}{(1 - X_R/X_F)} \qquad (6.4a)$$

$$\frac{\partial \phi_R}{\partial X_R} = - \frac{2.\sqrt{-\frac{X_R}{X_F}}.\frac{1}{X_R}}{(1 - X_R/X_F)} \qquad (6.4b)$$

It may be noted that X_R is negative as in Chapter 4.

Sensitivities of $\Delta\phi$ with respect to X_F and X_R may now be written as

$$S_{X_F}^{\Delta\phi} = \frac{\partial}{\partial X_F}(\Delta\phi).\frac{X_F}{\pi} = \frac{2}{\pi}\frac{\sqrt{-X_R/X_F}}{(1-X_R/X_F)} \qquad (6.5)$$

$$S_{X_R}^{\Delta\phi} = \frac{\partial}{\partial X_R}(\Delta\phi).\frac{X_R}{\pi} = \frac{-2}{\pi}\frac{\sqrt{-X_R/X_F}}{(1-X_R/X_F)} \qquad (6.6)$$

Where S_B^A is the sensitivity of function A with respect to parameter B. It may be noted that sensitivities with respect to X_F and X_R are equal in magnitude.

90° Phase Bit

In this case Z_m is given by Eqn. (4.8) as,

$$Z_m = \frac{X_F - X_R}{2} + \sqrt{\left[\frac{X_F - X_R}{2}\right]^2 - X_F X_R} \qquad (6.7)$$

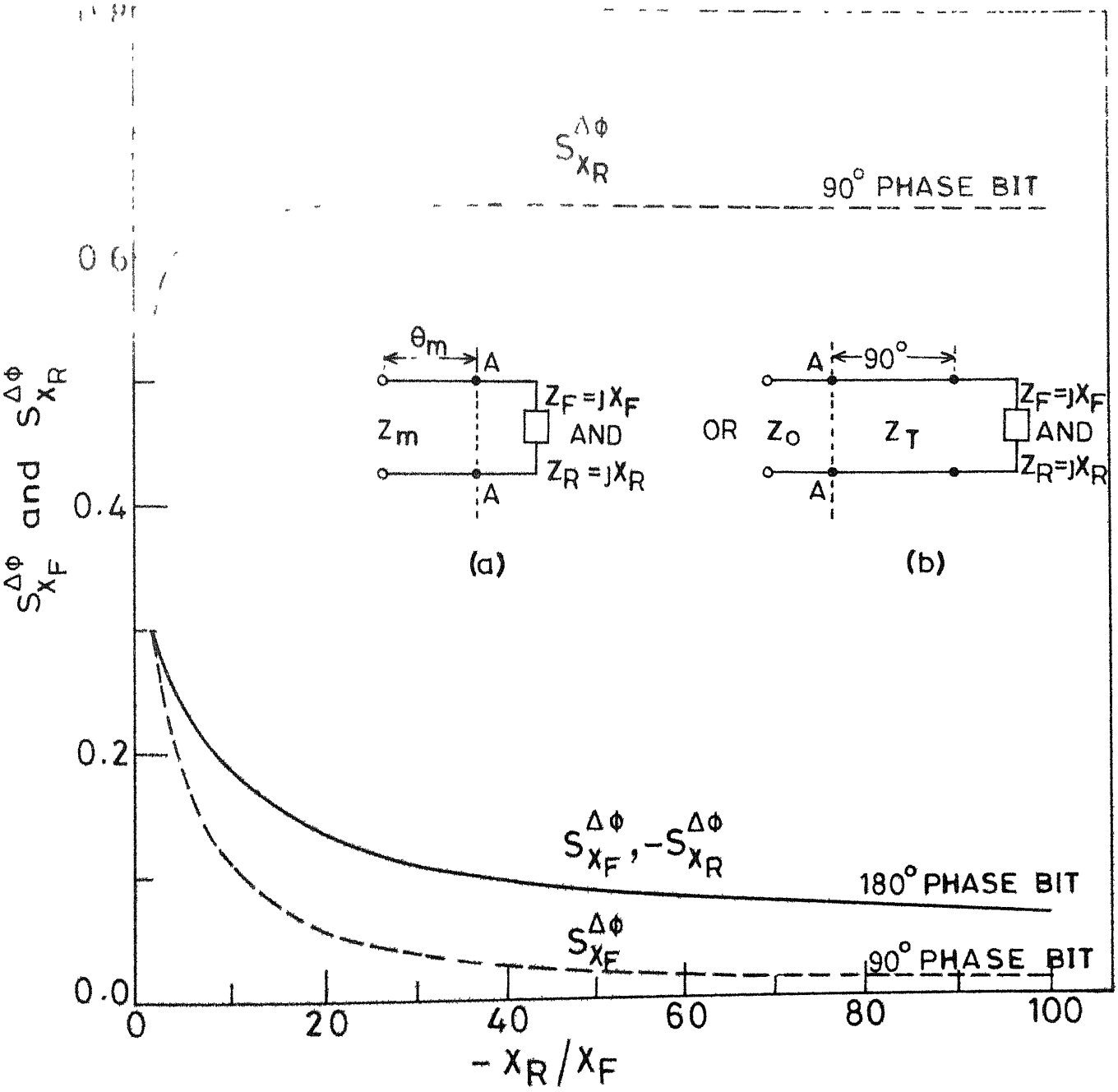


FIG. 3.1 VARIATION OF $S_{X_F}^{\Delta\phi}$ AND $S_{X_R}^{\Delta\phi}$ WITH X_R/X_F FOR 180° AND 90° PHASE BITS USING i) NETWORK FOR USE WITH IMPEDANCE TRANSFORMING HYBRID AND ii) QUARTER WAVE TRANSFORMING NETWORK

Equations (6.2) in this case may be rewritten as

$$\frac{\partial \phi_F}{\partial X_F} = - \frac{2}{X_F} \cdot \frac{Y}{1+Y^2} \tag{6.8a}$$

$$\frac{\partial \phi_R}{\partial X_R} = - \frac{2}{X_R} \left(\frac{X_R}{X_F}\right) \frac{Y}{(Y^2+X_R^2/X_F^2)} \tag{6.8b}$$

where

$$Y = \frac{1}{2} \left(1-X_R/X_F \right) + \sqrt{\frac{1}{4} \left(1-X_R/X_F\right)^2 - X_R/X_F}$$

Sensitivities can be evaluated using Eqns. (6.8) and are given as

$$S_{X_F}^{\Delta \phi} = - \frac{\partial \phi_F}{\partial X_F} \cdot \frac{X_F}{(\pi/2)} = \frac{4}{\pi} \cdot \frac{Y}{(Y^2+1)} \tag{6.9}$$

$$S_{X_R}^{\Delta \phi} = \frac{\partial \phi_R}{\partial X_R} \cdot \frac{X_R}{(\pi/2)} = - \frac{4}{\pi} \left(\frac{X_R}{X_F}\right) \cdot \frac{Y}{(Y^2+X_R^2/X_F^2)} \tag{6.10}$$

6.1.2 Sensitivities of Transformer Type Network

Phase shift network using quarter wave transformer is very commonly used in phase shifter circuits. Figure 6.1(inset (b)) shows the network of this type (discussed in Chapter 4). Reflection coefficients of this network in the two bias states at plane AA may be written as

$$\Gamma_F = - \frac{Z_o X_F + j Z_T^2}{Z_o X_F - j Z_T^2} \tag{6.11a}$$

$$\Gamma_R = - \frac{Z_o X_R + j Z_T^2}{Z_o X_R - j Z_T^2} \tag{6.11b}$$

Knowing ϕ_F and ϕ_R from Eqns. (6.11), $\frac{\partial \phi_F}{\partial X_F}$ and $\frac{\partial \phi_R}{\partial X_R}$ can be

obtained and are given as

$$\frac{\partial \phi_F}{\partial X_F} = - \frac{2Z_o Z_T^2}{Z_T^4 + Z_o^2 X_F^2} \qquad (6.12a)$$

$$\frac{\partial \phi_R}{\partial X_R} = - \frac{2Z_o Z_T^2}{Z_T^4 + Z_o X_R^2} \qquad (6.12b)$$

Value of Z_T depends on diode parameters and desired phase shift (Chapter 4). For 180° phase bit

$$Z_T^2 = Z_o \sqrt{- X_F X_R} \qquad (6.13)$$

and for 90° phase bit

$$Z_T^2 = Z_o \left[\frac{X_F - X_R}{2} + \sqrt{\left[\frac{X_F - X_R}{2}\right]^2 - X_F X_R} \right] \qquad (6.14)$$

When above expressions for Z_T are used in Eqns. (6.12) for a particular phase shift, the Eqns. thus,obtained are identical to Eqns. (6.4) and (6.8). Thus the expressions for sensitivities are same as given by Eqns. (6.5), (6.6), (6.9) and (6.10) for the case of network to be used with impedance transforming hybrid.

Sensitivities of differential phase shift with respect to parameters X_F and X_R, evaluated above, are plotted in Fig. 6.1 for both 180° and 90° phase bits, as a function of X_R/X_F. It is observed that diodes with low X_R/X_F ratio are more sensitive to X_F variations than diodes with higher X_R/X_F ratios. For example, a diode having $X_R/X_F = -60$ has sensitivity of $\Delta\phi$ with X_F for 180° phase shift as 0.08, hence a $\pm$ 5% variation in X_F would give about $\pm$0.4% phase deviation.

Plot of sensitivity with respect to X_R (mainly the capacitive reactance of the diode) as a function of X_R/X_F is also given in Fig. 6.1. For 180° phase bit, sensitivities with X_F and X_R are equal in magnitude. 90° phase bit is more sensitive to X_R variations and the sensitivity does not depend much on the quality of the diode (X_R/X_F ratio) used. Let us again consider a diode with $X_R/X_F = -60$ which has sensitivity of approximately 0.64. A 5% variation in X_R causes about $\pm 3.2\%$ ($\pm 2.9°$) variation in differential phase.

In the above discussion it is assumed that when the variation in one kind of reactance (i.e. X_R or X_F) is considered, the other reactance remains fixed. In a practical situation both the reactances may vary. To obtain the worst case phase variation in $\Delta\phi$ the magnitudes of variations due to individual reactances are added.

6.1.3 Sensitivities of Single Stub Type Network

Figure 6.2 (inset) shows the phase shift network of single stub type, discussed in Chapter 4. In this case also, the additional transmission line length used for equalization of reflection coefficients is not considered since it does not affect the present analysis.

180° Phase Bit

For 180° phase bit, when $Z_o^2 > |X_F X_R|$, an open stub is used (Section 4.3.3). In the present discussion it is assumed that an open stub is always used and the value of Z_o

can accordingly be adjusted to take care that throughout the range of practical diode parameters the above condition is satisfied.

The reflection coefficients Γ_F and Γ_R at plane AA are found to be

$$\Gamma_F = \frac{[(Z_o - X_F \tan\theta_1) - (X_F + Z_o \tan\theta_1)\tan\theta_2] - j(X_F + Z_o \tan\theta_1)}{[(Z_o - X_F \tan\theta_1) - (X_F + Z_o \tan\theta_1)\tan\theta_2] + j(X_F + Z_o \tan\theta_1)} \qquad (6.15)$$

expression for Γ_R can be written by replacing X_F by X_R.

The phases of reflection coefficients ϕ_F and ϕ_R are given by

$$\phi_{F,R} = \tan^{-1}\left[\frac{2(D-\tan\theta_2)}{1-(D-\tan\theta_2)^2}\right] \qquad (6.16)$$

where

$$D = \frac{Z_o - X_F \tan\theta_1}{X_F + Z_o \tan\theta_1} \quad \text{for } \phi_F$$

$$= \frac{Z_o - X_R \tan\theta_1}{X_R + Z_o \tan\theta_1} \quad \text{for } \phi_R$$

To evaluate the sensitivities, partial derivatives of the phases of reflection coefficients with respect to diode reactances are required. These can be evaluated as

$$\frac{\partial \phi_F}{\partial X_F} = -\frac{2Z_o(1+\tan^2\theta_1)}{(X_F + Z_o\tan\theta_1)^2 + [(Z_o - X_F\tan\theta_1) - \tan\theta_2(X_F + Z_o\tan\theta_1)]^2} \qquad (6.17a)$$

$$\frac{\partial \phi_R}{\partial X_R} = -\frac{2Z_o(1+\tan^2\theta_1)}{(X_R + Z_o\tan\theta_1)^2 + [(Z_o - X_R\tan\theta_1) - \tan\theta_2(X_R + Z_o\tan\theta_1)]^2} \qquad (6.17b)$$

The electrical lengths θ_1 and θ_2 depend on diode parameters and the phase shift desired. For 180° phase shift they are given by (Eqns.(4.18) and(4.23))

$$\tan\theta_1 = - X_R/Z_o \qquad (6.18a)$$

$$\tan\theta_2 = \frac{Z_o^2 + X_F X_R}{Z_o(X_F - X_R)} \qquad (6.18b)$$

Substituting for $\tan\theta_1$ and $\tan\theta_2$ into Eqns. (6.17), we get

$$\frac{\partial \phi_F}{\partial X_F} = - \frac{2Z_o(1+X_R^2/Z_o^2)}{X_F^2(1-X_R/X_F)^2} \qquad (6.19a)$$

$$\frac{\partial \phi_R}{\partial X_R} = - \frac{2}{Z_o} \cdot \frac{1}{(1+X_R^2/Z_o^2)} \qquad (6.19b)$$

Sensitivities can now be evaluated using Eqns. (6.19) and are given as

$$S_{X_F}^{\Delta\phi} = - \frac{\partial \phi_F}{\partial X_F} \cdot \frac{X_F}{\pi} = \frac{2}{\pi} \cdot \frac{Z_o}{X_R} \cdot \frac{X_R}{X_F} \cdot \frac{(1+X_R^2/Z_o)}{(1-X_R/X_F)^2} \qquad (6.20)$$

$$S_{X_R}^{\Delta\phi} = \frac{\partial \phi_R}{\partial X_R} \cdot \frac{X_R}{\pi} = - \frac{2}{\pi} \cdot \frac{X_R}{Z_o} \cdot \frac{1}{(1+X_R^2/Z_o^2)} \qquad (6.21)$$

90° Phase Bit

For 90° phase bit, a shorted stub is used instead of the open circuited stub and the evaluation of the reflection coefficients proceeds the same way as for 180° phase bit. The partial derivatives of ϕ_F and ϕ_R with respect to diode reactances are evaluated as

$$\frac{\partial \phi_F}{\partial X_F} = \frac{2Z_o(1+\tan^2\theta_1)}{(X_F+Z_o\tan\theta_1)^2+[(Z_o-X_F\tan\theta_1)+(X_F+Z_o\tan\theta_1)\cot\theta_2]^2} \qquad (6.22a)$$

$$\frac{\partial \phi_R}{\partial X_R} = - \frac{2Z_o(1+\tan^2\theta_1)}{(X_R+Z_o\tan\theta_1)^2 + [(Z_o-X_R\tan\theta_1)+(X_R+Z_o\tan\theta_1)\cot\theta_2]^2} \tag{6.22b}$$

For 90° bit, electrical lengths θ_1 and θ_2 are related to diode reactances (Eqns.(4.18) and (4.30)) and are given as

$$\tan\theta_1 = - X_R/Z_o \tag{6.23a}$$

$$\cot\theta_2 = -\left[\frac{(Z_o^2+X_FX_R)-Z_o(X_F-X_R)}{Z_o(X_F-X_R)}\right] \tag{6.23b}$$

Substituting for $\tan\theta_1$ and $\tan\theta_2$ in Eqns. (6.22), we get

$$\frac{\partial \phi_F}{\partial X_F} = - \frac{Z_o}{X_F^2} \cdot \frac{(1+X_R^2/Z_o^2)}{(1-X_R/X_F)^2} \tag{6.24a}$$

$$\frac{\partial \phi_R}{\partial X_R} = - \frac{2}{Z_o} \cdot \frac{1}{(1+X_R^2/Z_o^2)} \tag{6.24b}$$

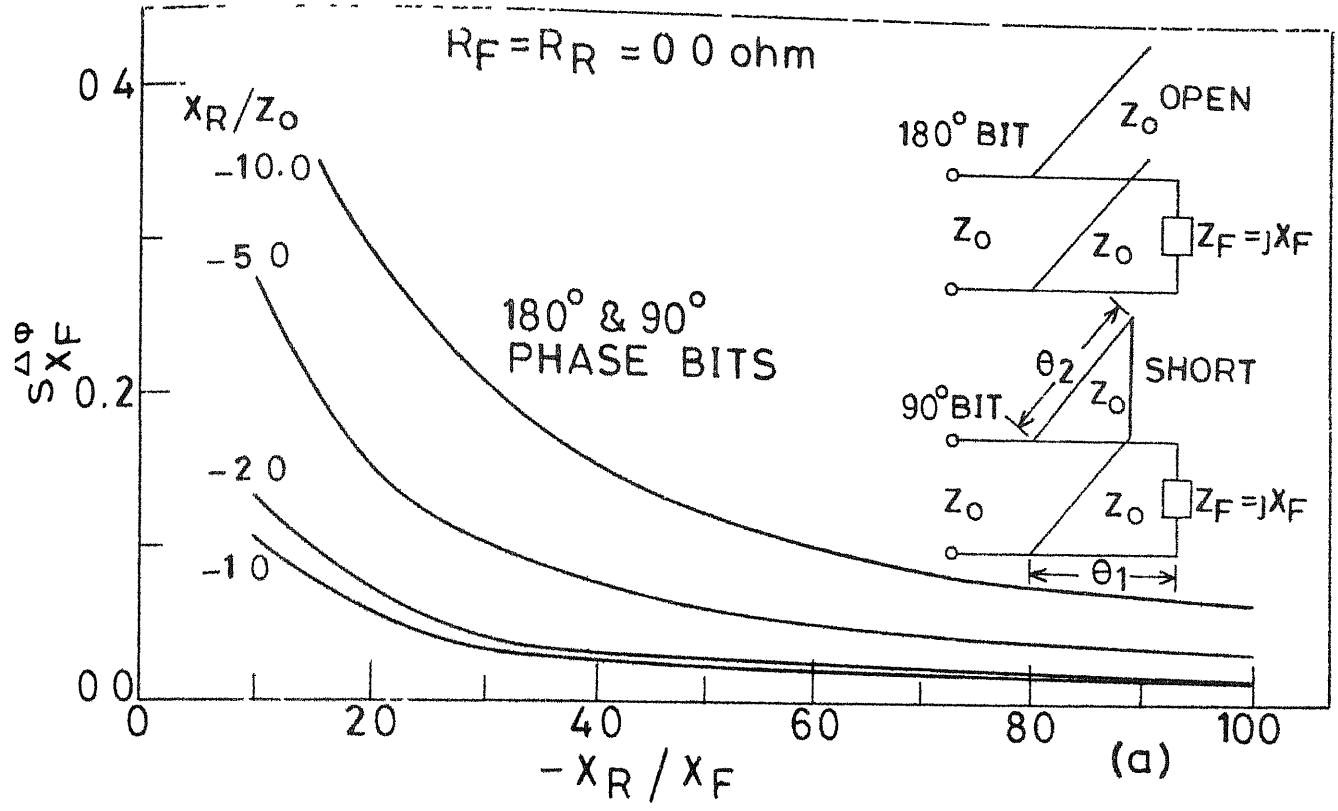
Now the sensitivities can be evaluated as:

$$S_{X_F}^{\Delta\phi} = - \frac{\partial \phi_F}{\partial X_F} \cdot \frac{X_F}{(\pi/2)} = \frac{2}{\pi} \cdot \frac{Z_o}{X_R} \cdot \frac{X_R}{X_F} \cdot \frac{(1+X_R^2/Z_o^2)}{(1-X_R/X_F)^2} \tag{6.25}$$

$$S_{X_R}^{\Delta\phi} = \frac{\partial \phi_R}{\partial X_R} \cdot \frac{X_R}{(\pi/2)} = - \frac{4}{\pi} \cdot \frac{X_R}{Z_o} \cdot \frac{1}{(1+X_R^2/Z_o^2)} \tag{6.26}$$

Equations (6.20), (6.21), (6.25) and (6.26) are plotted in Figs. 6.2(a) and 6.2(b). We observe that additional parameter X_R/Z_o has been introduced in this case.

Figure 6.2(a) gives the sensitivity of $\Delta\phi$ with respect to X_F as a function of diode reactance ratio X_R/X_F for different



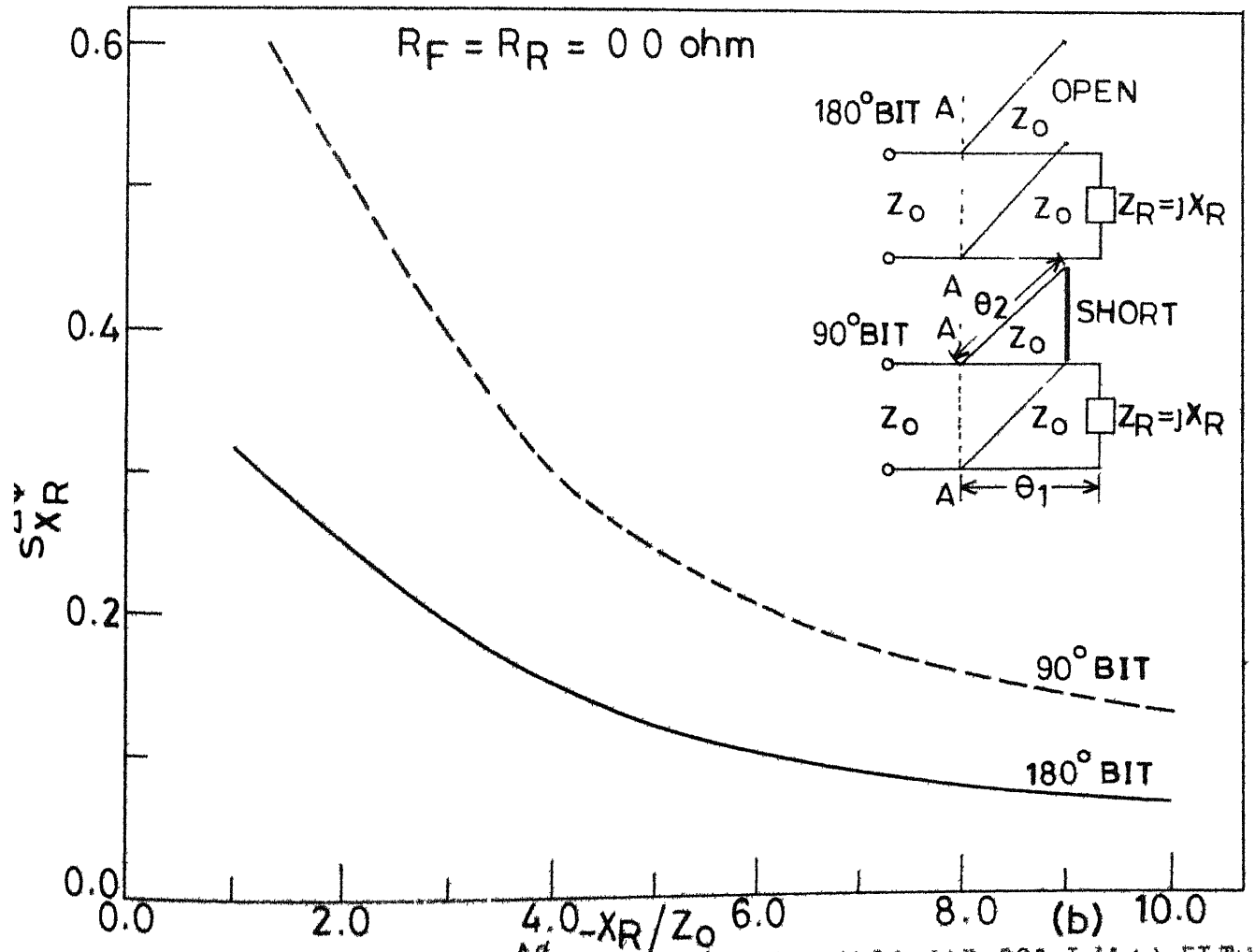


FIG. 6.2 (a) VARIATION OF $S^{\Delta\phi}_{\Delta P}$ WITH X_R/X_F FOR 180° AND 90° PHASE BITS USING SINGLE STUB TRANSFORMING NETWORK (b) VARIATION OF $S^{\Delta\phi}_{X_R}$ WITH X_R/Z_o FOR 180° AND 90° PHASE BITS USING SINGLE STUB TRANSFORMING NETWORK.

values of X_R/Z_o ratios. We note that diodes with large X_R/X_F ratio are less sensitive to variations in X_F. For a fixed X_R/X_F ratio, sensitivity becomes large for higher X_R/Z_o. To consider an example, a diode with $X_R/X_F = -60$ and $X_R/Z_o = -5$ gives sensitivity of approximately 0.05, hence a $\pm$ 5% variation in X_F would give about $\pm$ 0.25% phase deviation. It is to be noted that for both 180° and 90° phase bits the sensitivities are same in this case.

Figure 6.2(b) shows the plot of sensitivities with respect to X_R for both 90° and 180° phase bits. In this case also the 90° phase bit is found to be more sensitive to X_R variations than 180° phase bit. It is to be noted that the parameter X_R/X_F does not appear in the sensitivity expressions and the sensitivities depend only on the reverse bias capacitance of the diode. Let us consider a diode with $X_R = -300$ ohm and if $Z_o = 50$ ohm, X_R/Z_o -6,which gives sensitivity for 180° bit as 0.1. A 5% variation in X_R would give about $\pm$0.5% variation in $\Delta\phi$ for a 180° bit. A 90° bit would give a variation of approximately $\pm$ 1% in $\Delta\phi$.

6.2 EFFECT OF DIODE RESISTANCES

Design equations for the transforming networks described in Chapter 4 assume the diodes to be lossless. This is justified since the change in differential phase shift due to finite diode resistance is very small. In this section this change is studied quantitatively for three types of phase shift networks. Variation of phase shifter characteristics

with the resistances R_F and R_R is evaluated. As the effect of R_F and R_R on $\Delta\phi$ is found to be very small, corresponding sensitivities have not been studied. Variation of insertion loss with R_F and R_R is also reported.

6.2.1 Phase Shift Network Using Quarter Wave Transformer and the Network for Use with Impedance Transforming Hybrid

Figure 6.3 (inset) shows the phase shift networks of the two types. Diode is considered to have non-zero R_F and R_R.

The expressions for the phase shifts ϕ_F and ϕ_R for non-zero R_F and R_R can be derived for network used with impedance transforming hybrid.

$$\phi_F = \tan^{-1}\left[\frac{2X_F Z_m}{R_F^2+X_F^2-Z_m^2}\right] \qquad (6.27a)$$

and

$$\phi_R = \tan^{-1}\left[\frac{2X_R Z_m}{R_R^2+X_R^2-Z_m^2}\right] \qquad (6.27b)$$

180° Phase Bit

In this case Z_m is given by $\sqrt{-X_F X_R}$. Substituting for Z_m in Eqns. (6.27), we get

$$\phi_F = \tan^{-1}\left[\frac{2\sqrt{-X_R/X_F}}{1+X_R/X_F+R_F^2/X_F^2}\right] \qquad (6.28a)$$

and

$$\phi_R = \tan^{-1}\left[\frac{2\sqrt{-X_R/X_F}}{1+\frac{X_R}{X_F}+\frac{R_R^2}{X_R^2}\frac{X_R}{X_F}}\right] \qquad (6.28b)$$

Effects of R_F and R_R on $\Delta\phi$ are studied independently. We define

$$\Delta\phi_{R_F} = \phi_R - \phi_{R_F} \tag{6.29}$$

and $$\Delta\phi_{R_R} = \phi_{R_R} - \phi_F \tag{6.30}$$

where ϕ_R and ϕ_F refer to the lossless diode case. Insertion loss of the phase shift network considered can be evaluated from the reflection coefficients in the two bias states. For 180° phase bit Γ_F and Γ_R are given by

$$\Gamma_F = \frac{(1+X_R/X_F+R_F^2/X_F^2) + j\,2\sqrt{-X_R/X_F}}{(R_F/X_F+\sqrt{-X_R/X_F})^2+1} \tag{6.31a}$$

$$\Gamma_R = \frac{\frac{X_R}{X_F}\cdot\left[1+\frac{X_R}{X_F}\cdot(1+R_R^2/X_R^2)+j2\sqrt{-X_R/X_F}\right]}{\left[\frac{R_R}{X_R}\cdot\frac{X_R}{X_F}+\sqrt{-X_R/X_F}\right]^2+X_R^2/X_F^2} \tag{6.31b}$$

Losses in dB's are given by

$$L_F(dB)=10\log_{10}\frac{\left[\left\{\frac{R_F}{X_F}+\sqrt{-X_R/X_F}\right\}^2+1\right]^2}{(1+X_R/X_F+R_F^2/X_F^2)^2+4\cdot(-X_R/X_F)} \tag{6.32}$$

$$L_R(dB)=10\log_{10}\frac{\left[\left\{\frac{R_R}{X_R}\cdot\frac{X_R}{X_F}+\sqrt{-X_R/X_F}\right\}^2+X_R^2/X_F^2\right]^2}{\left(\frac{X_R}{X_F}\right)^2\left[\left\{1+\frac{X_R}{X_F}(1+R_R^2/X_R^2)\right\}^2+4(-X_R/X_F)\right]} \tag{6.33}$$

As in the case of sensitivity expressions derived in Section 6.1.1 and 6.1.2, expressions for L_F and L_R for circuits

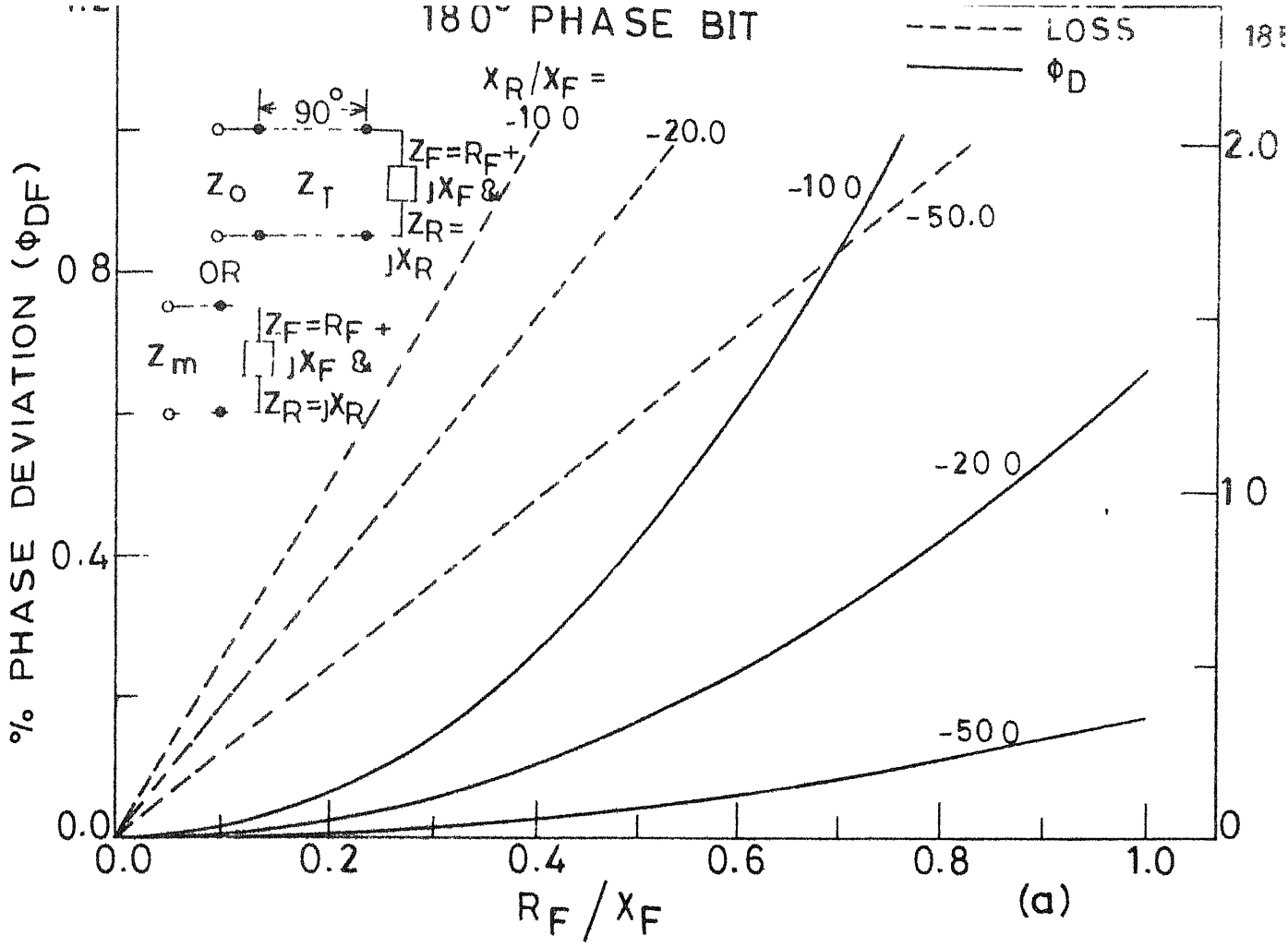
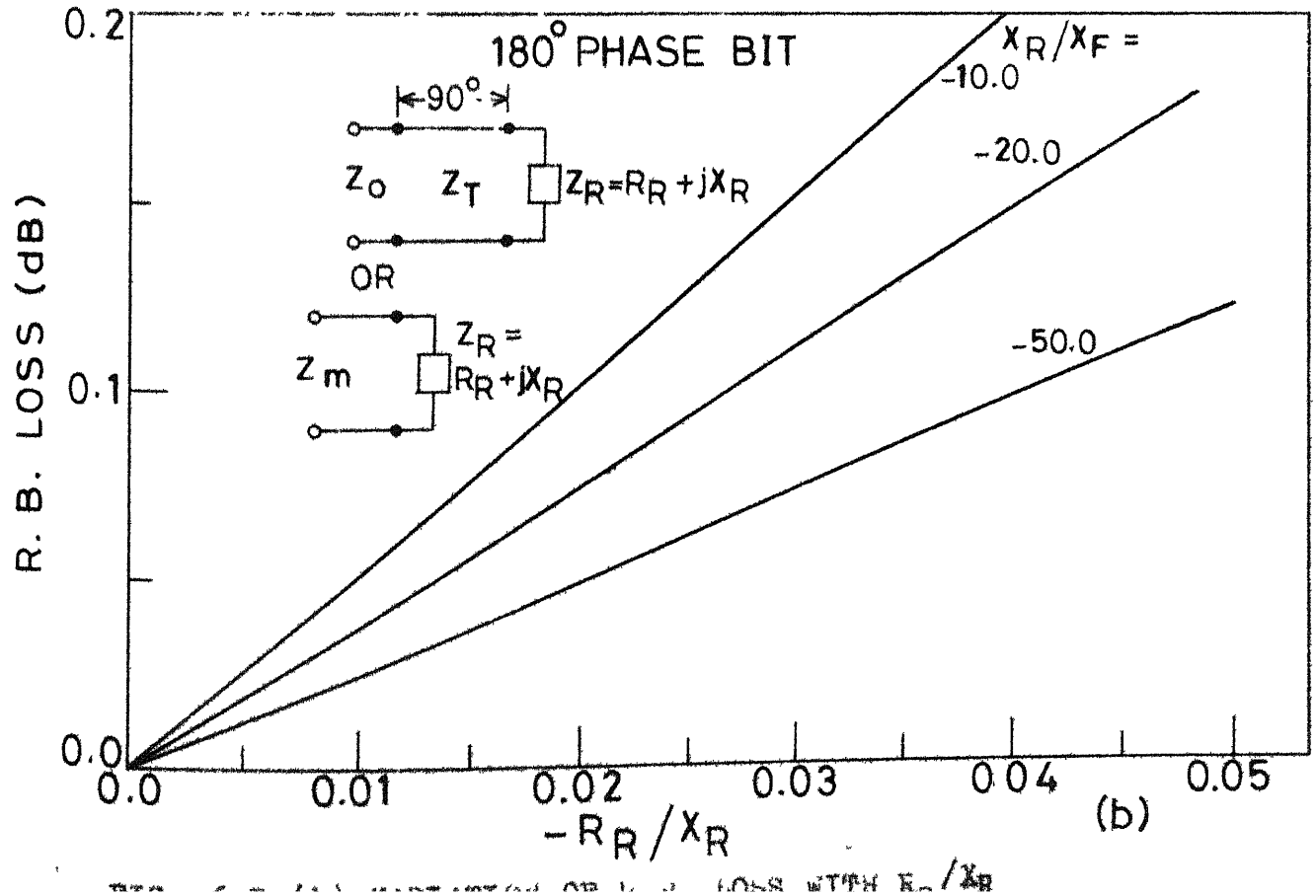


FIG. [illegible] VARIATION OF ϕ_{DF} WITH R_F/X_F



[illegible] VARIATION OF R. B. LOSS WITH R_R/X_R

using quarter wave transformer type network are found to be identical to Eqns. (6.32) and (6.33) above.

Figure 6.3(a) and (b) shows the variations of percentage phase deviation and loss as a function of R_F/X_F and R_R/X_R for different X_R/X_F values. The parameter percentage phase deviation (ϕ_D) is defined as

$$\phi_{D_F}\ (\text{Percent}) = \frac{\Delta\phi_{R_F} - \Delta\phi}{\Delta\phi} \cdot 100 \qquad (6.34)$$

where $\Delta\phi$ is the differential phase shift when both R_F and R_R are zero. We observe that the deviation in phase values due to R_F is typically less than one percent. For example, a diode with $X_R/X_F = -50$ and $R_F/X_F = 0.4$ has values of ϕ_{D_F} and L_F approximately 0.028 percent and 0.96 dB, respectively. ϕ_{D_F} of 0.028 percent corresponds to a phase deviation of about 0.05° in 180° phase bit. Figure 6.3(b) shows the variation of loss as a function of $-R_R/X_R$. Phase deviation ϕ_{D_R} is not plotted in this case, since these values are at least an order of magnitude smaller than the corresponding values in the forward bias case.

90° Phase Bit

For the 90° phase bit the phases and the losses in the forward and reverse bias states are derived to be;

$$\phi_F = -\tan^{-1}\left[\frac{2Y}{Y^2-(1+R_F^2/X_F^2)}\right] \qquad (6.35a)$$

$$\phi_R = \tan^{-1}\left[\frac{-2Y\cdot(X_R/X_F)}{Y^2-\frac{X_R^2}{X_F^2}\cdot(1+R_R^2/X_R^2)}\right] \qquad (6.35b)$$

$$L_F = 10 \log_{10} \frac{\left\{(R_F/X_F+Y)^2+1\right\}^2}{(R_F^2/X_F^2+1-Y^2)^2+4Y^2} \qquad (6.36)$$

$$L_R = 10 \log_{10} \frac{\left[\left\{\frac{R_R}{X_R}\cdot\frac{X_R}{X_F}+Y\right\}^2+X_R^2/X_F^2\right]^2}{\left[\frac{R_R^2}{X_R^2}\cdot\frac{X_R^2}{X_F^2}+\frac{X_R^2}{X_F^2}-Y^2\right]^2+4\,\frac{X_R^2}{X_F^2}\,Y^2} \qquad (6.37)$$

where $Y = \frac{1}{2}(1-X_R/X_F)+\sqrt{\frac{1}{4}(1-X_R/X_F)^2 - X_R/X_F}$

Figures 6.4(a) and (b) show the variations of ϕ_D and the loss with R_F/X_F and R_R/X_R for 90° phase bit. Phase deviations due to finite R_F are much less in this case (typically less than 0.01%) as compared to those for 180° bit. For example, a diode with $X_R/X_F = -50$ and $R_F/X_F = 0.4$ has ϕ_{D_F} of approximately 0.0009% for 90° bit as compared to 0.028% for 180° bit. Forward biased loss (L_F) in this case is also found to be smaller, a value of 0.13 dB as compared to 0.96 dB for 180° bit.

In the reverse bias case, (Fig. 6.4(b)) it is observed that both the phase deviations and the loss do not depend much on X_R/X_F ratio of the diode. It may be because of the fact that typical values of R_R/X_R for practical diodes (as considered in Fig. 6.4(b)) are considerably smaller than the ratio R_F/X_F considered in Fig. 6.4(a).

6.2.2 Phase Shift Network Using Single Stub

This type of phase bit is shown in Fig. 6.5a (inset). For the present discussion the diode impedances in two bias

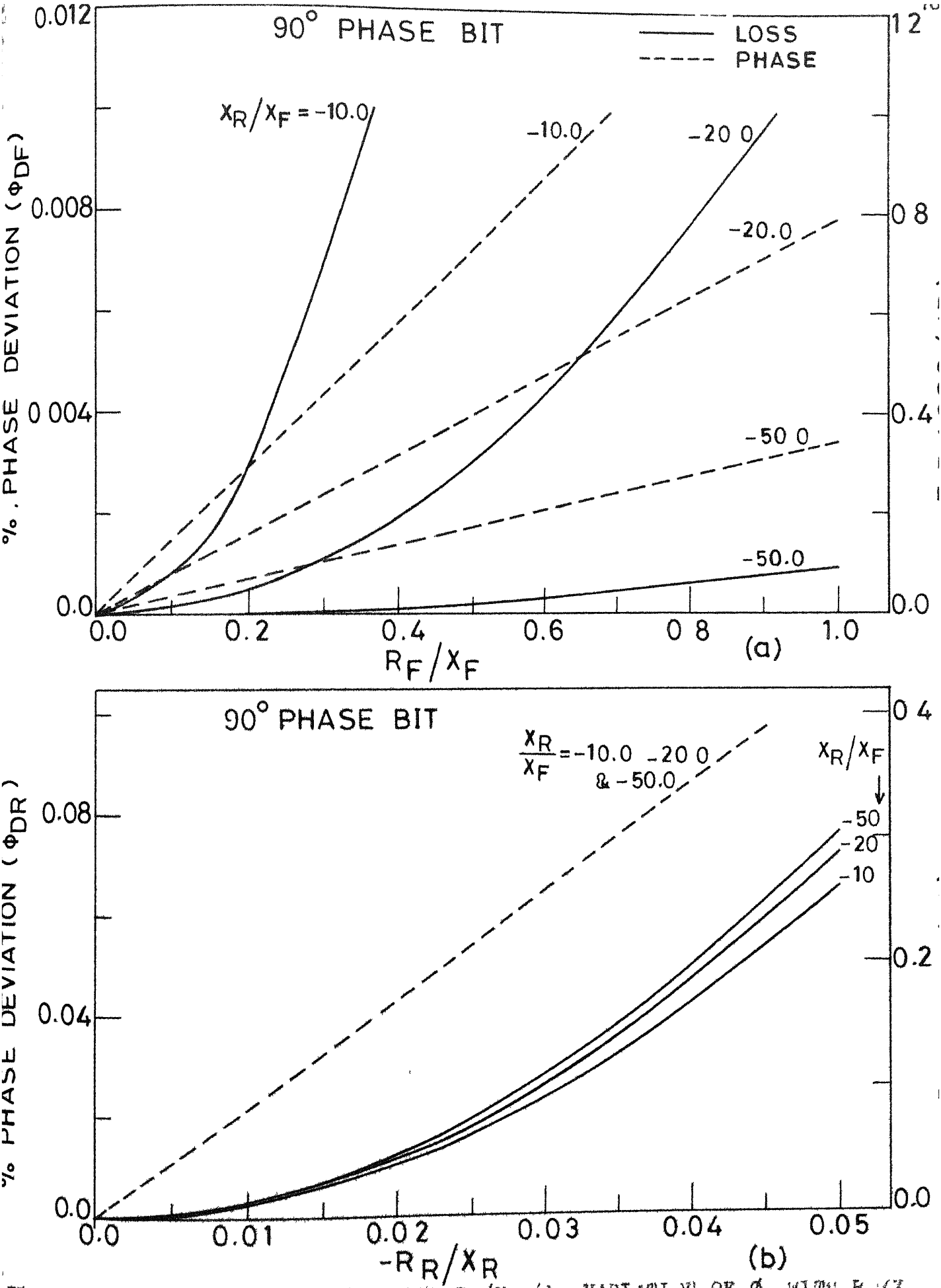


FIG. 6.4 (a) VARIATION OF ϕ_{DF} WITH R_F/X_F (b) VARIATION OF ϕ_{DR} WITH R_R/X_R

states are taken as $Z_F=R_F+jX_F$ and $Z_R=R_R+jX_R$. As before, for calculation of ϕ_D and the loss, the effects of R_F and R_R are considered independently.

180° Phase Bit

As discussed earlier, for 180° bit, an open stub is used. The expressions for Γ_F and Γ_R are derived as:

$$\Gamma_F = \frac{(Z_1-R_F\tan\theta)-j\left[(R_F-Z_o)+X_F\tan\theta+Z_o\tan\theta_1\tan\theta_2\right]}{(Z_1+R_F\tan\theta)+j\left[-(R_F+Z_o)+X_F\tan\theta+Z_o\tan\theta_1\tan\theta_2\right]} \qquad (6.38)$$

where $Z_1 = X_F+Z_o\tan\theta_1$

$\tan\theta = \tan\theta_1 + \tan\theta_2$

The corresponding expression for Γ_R can be obtained by replacing R_F by R_R and X_F by X_R.

Phase of reflection coefficient, ϕ_F and loss(L_F) can be evaluated from Eqn. (6.38) and using the design Eqns.(6.18). For 180° phase bit, we get

$$\phi_F = \tan^{-1}\left[\frac{2K_1(R_F^2/X_F^2)(Z_o/X_R)}{\frac{R_F^2}{X_F^2}\cdot\left\{1-\frac{Z_o^2}{X_R^2}\cdot K_1^2\right\}+(1+X_R/X_F)^2}\right] \qquad (6.39)$$

where $K_1 = \frac{X_R}{X_F}\cdot\frac{(1+X_R^2/Z_o^2)}{(1-X_R/X_F)}$

and

$$L_F(dB)=10\log_{10}\frac{\left[(1-X_R/X_F)^2+K_2\right]^2+\frac{R_F^2}{X_F^2}\cdot(1-X_R/X_F)^2}{\left[(1-X_R/X_F)^2-K_2\right]^2+\frac{R_F^2}{X_F^2}\cdot(1-X_R/X_F)^2} \qquad (6.40)$$

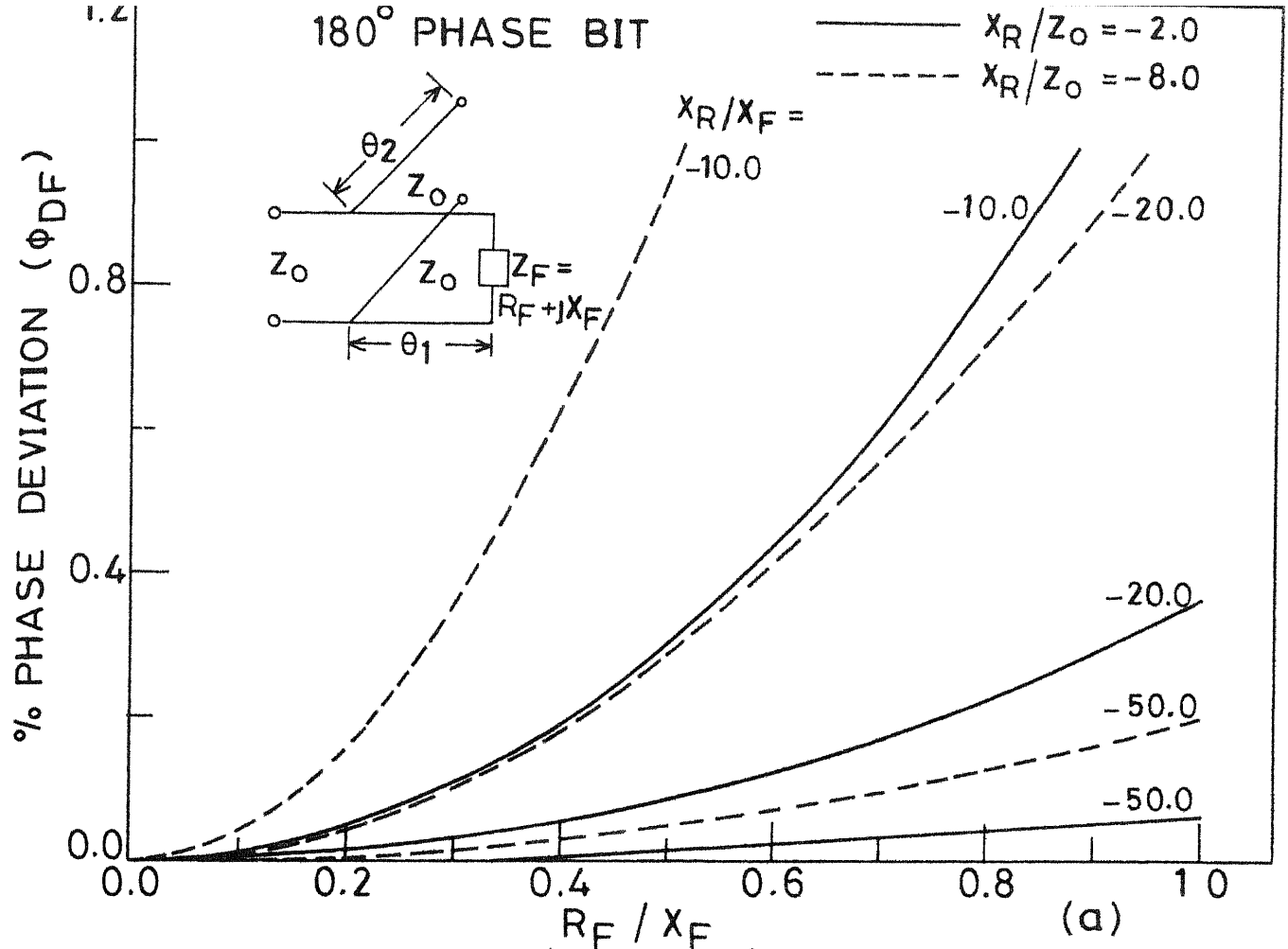


FIG. 6.5 (a) VARIATION OF ϕ_{DF} WITH R_F/X_F.

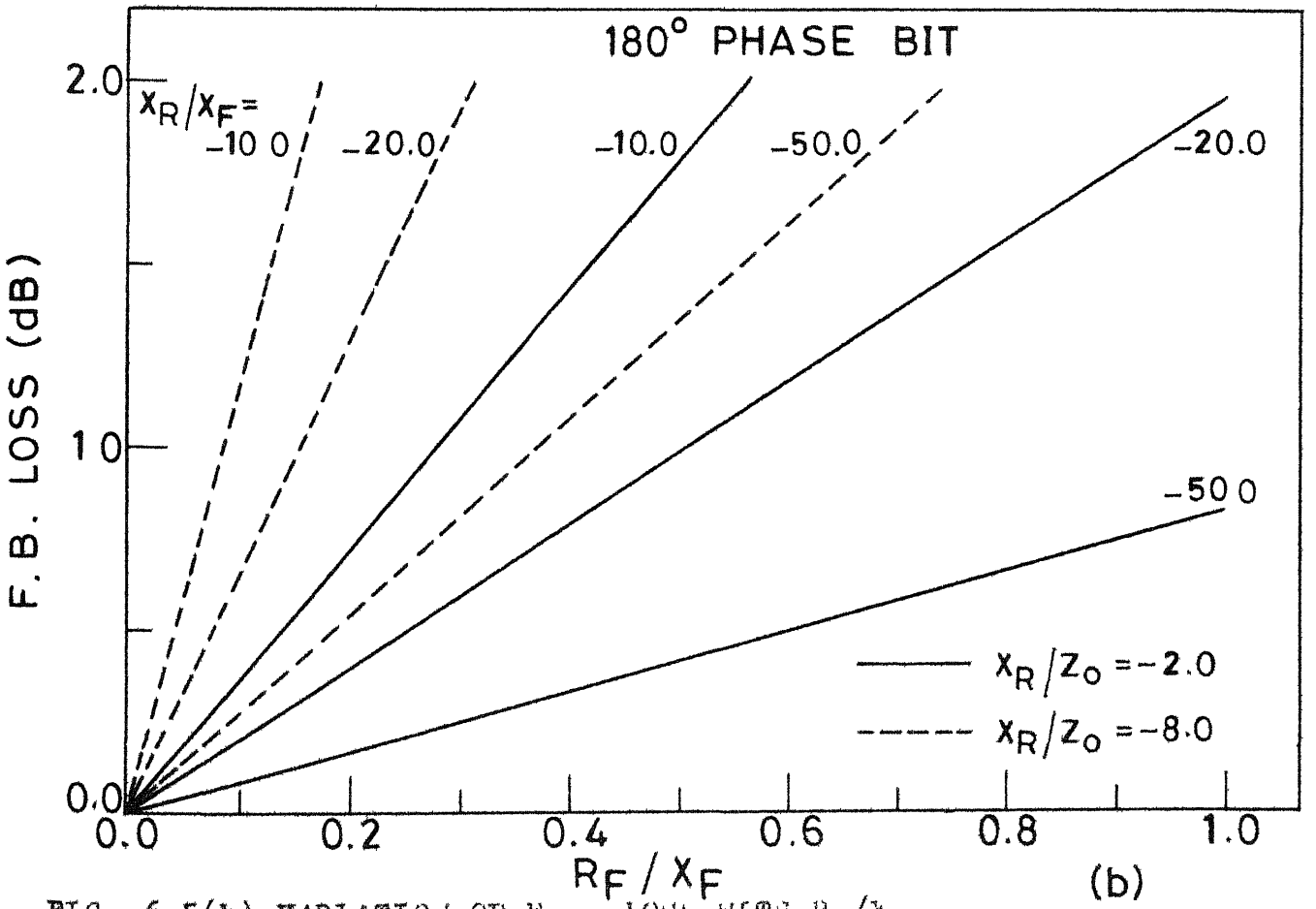


FIG. 6.5(b) VARIATION OF F... LOSS WITH R_F/X_F

where $K_2 = \frac{R_F}{X_F} \cdot \frac{Z_o}{X_R} \cdot \frac{X_R}{X_F} \cdot \left(1+\frac{X_R^2}{Z_o^2}\right)$

Similarly, expressions for ϕ_R and L_R can be derived and are given as follows:

$$\phi_R = \tan^{-1}\left[\frac{2K_1 \frac{R_R^2}{X_R^2} \cdot \frac{X_R}{Z_o}}{\frac{R_R^2}{X_R^2} \cdot \frac{X_R^2}{Z_o^2} \cdot \left\{\frac{Z_o^2}{X_R^2} \cdot K_1^2 - 1\right\} + \frac{X_R^2}{Z_o^2}\left(X_R^2/Z_o^2+2\right)+1}\right] \qquad (6.41)$$

and

$$L_R(dB) = 10 \log_{10}\left[\frac{\frac{R_R^2}{X_R^2} \cdot \frac{Z_o^2}{X_R^2} \cdot K_1^2 + \left\{\frac{R_R}{X_R} + \frac{Z_o}{X_R} + \frac{X_R}{Z_o}\right\}^2}{\frac{R_R^2}{X_R^2} \cdot \frac{Z_o^2}{X_R^2} \cdot K_1^2 + \left\{\frac{R_R}{X_R} - \frac{Z_o}{X_R} - \frac{X_R}{Z_o}\right\}^2}\right] \qquad (6.42)$$

where $K_1 = \frac{X_R}{X_F} \cdot \frac{(1+X_R^2/Z_o^2)}{(1-X_R/X_F)}$ as given before.

Differential phase shift $\Delta\phi_{R_F}$ and $\Delta\phi_{R_R}$ can be evaluated using Eqns. (6.29) and (6.30).

Figures 6.5(a) and (b) show the variations of phase deviations and loss as a function of R_F/X_F. In this case it is necessary to consider another parameter X_R/Z_o and computations are presented for two typical values of X_R/Z_o, namely -2 and -8. We find that both phase deviation and loss are higher for $X_R/Z_o = -8$. This may be clasified as follows. As X_R/X_F is constant, large X_R/Z_o implies a large X_F and hence a large R_F (for same value of R_F/X_F ratio shown along abscissa). Consider a diode with $X_R/Z_o = -8.0$, if $Z_o = 50$ ohm, X_R would be -400 ohm.

For $X_R/X_F = -20$, corresponding X_F is 20 ohm. If R_F/X_F ratio considered is 0.8, R_F is 16 ohm which is a large value.

Figures 6.6(a) and (b) show the plots for ϕ_{D_R} and L_R as a function of R_R/X_R. Both phase deviations and loss are seen to increase with R_R/X_R. Value of X_R/X_F has a very small effect on ϕ_{D_R} and practically no effect on the loss.

90° Phase Bit

For 90° bit shorted stub is used. The expression for Γ_F is derived to be,

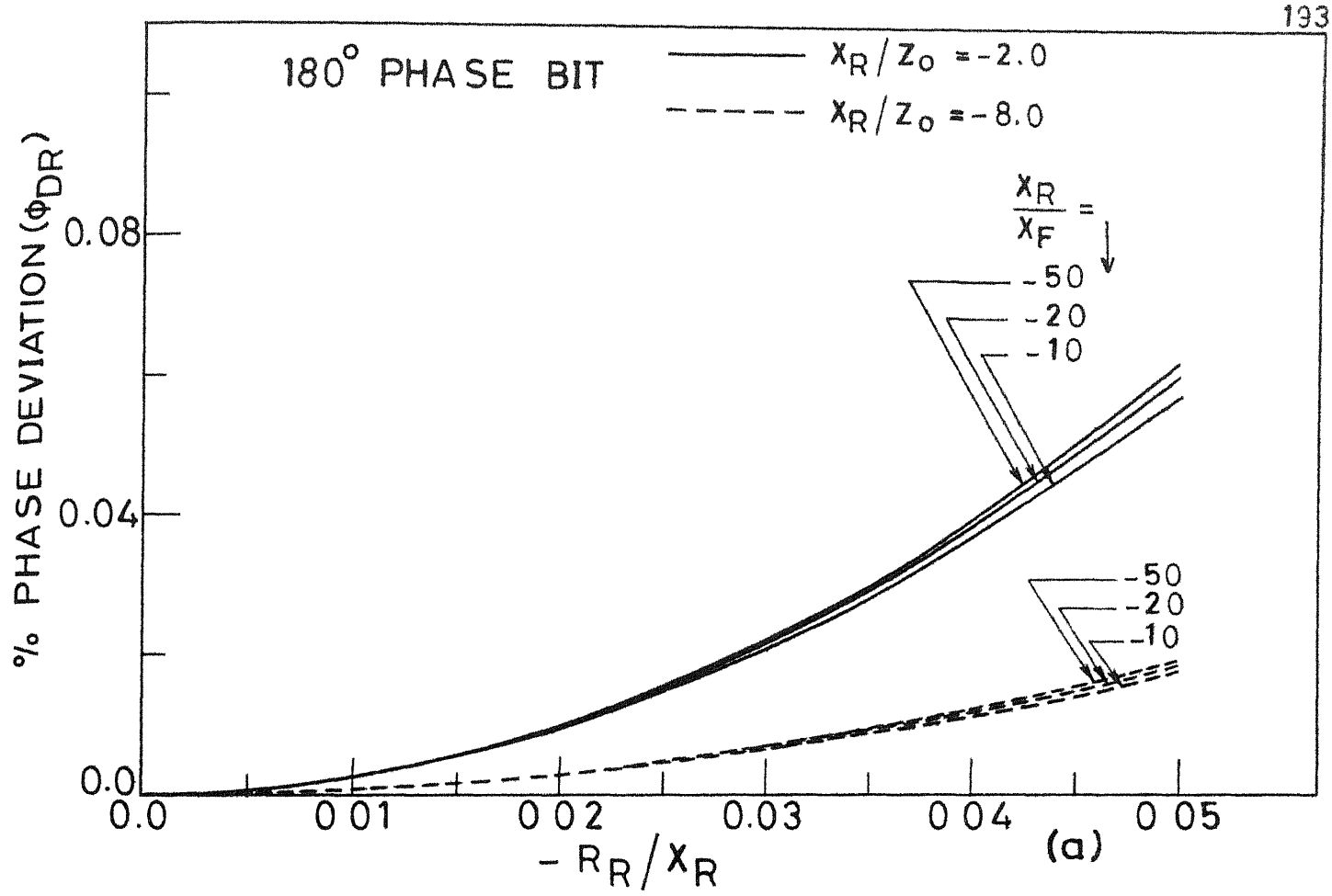
$$\Gamma_F = \frac{[(R_F-Z_o)\tan\theta_1 - X_F - R_F\cot\theta_2] + j\,[R_F - Z_o + X_F\tan\theta_1 - Z_1\cot\theta_2]}{[(R_F+Z_o)\tan\theta_1 - X_F + R_F\cot\theta_2] + j\,[R_F + Z_o - X_F\tan\theta_1 + Z_1\cot\theta_2]} \qquad (6.43)$$

where $Z_1 = X_F + Z_o \tan\theta_1$

Expression for Γ_R can be written by replacing R_F by R_R and X_F by X_R.

Phases ϕ_F and ϕ_R can be calculated Γ_R from Γ_F and $_R$. Line lengths θ_1 and θ_2 are computed from the design equations (6.23) for 90° bit, relating θ_1 and θ_2 to X_R and X_F of the diode. Insertion loss in the two states can be calculated from Γ_F and Γ_R. Expressions for ϕ_F, ϕ_R, L_F and L_R are given by the following equations.

$$\phi_F = -\tan^{-1} \frac{2\left[\frac{R_F^2}{X_F^2}\left\{(1+X_R/Z_o)-K_3\right\}+(1-X_R/X_F)^2\right]}{\frac{R_F^2}{X_F^2}\left[\left\{(1+X_R/Z_o)-K_3\right\}^2 - 1\right]} \qquad (6.44)$$



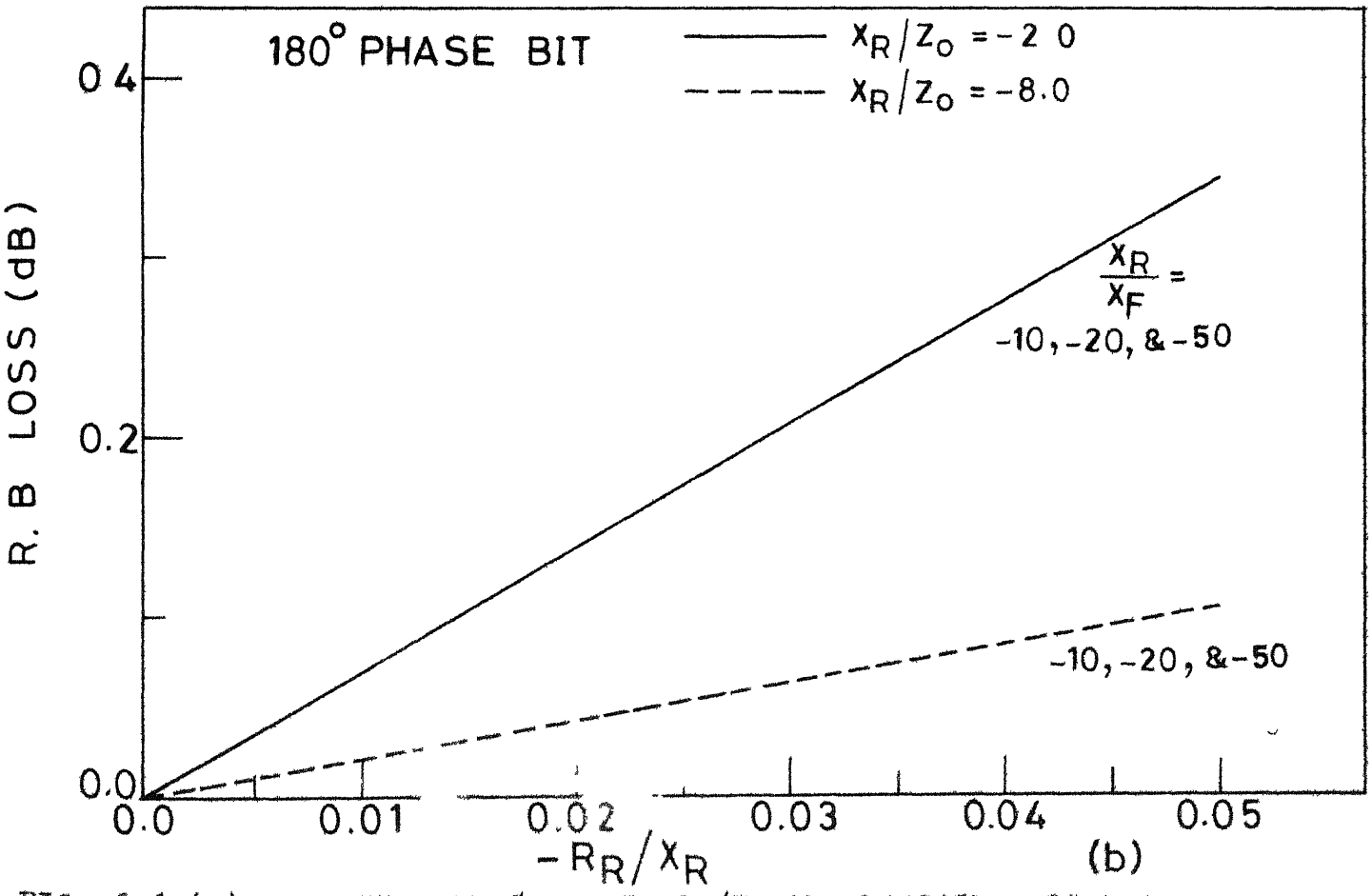


FIG. 6.6 (a) VARIATION OF ϕ_{DR} WITH R_R/X_R (b) VARIATION OF R.B. LOSS WITH R_R/X_R.

$$\phi_R = \tan^{-1} \frac{2\,\frac{R_R^2}{R_R^2}\left[K_3 - (1+X_R/Z_o)\right]}{\frac{R_R^2}{X_R^2}\left[\left\{K_3-(1+X_R/Z_o)\right\}^2-1\right] + \frac{Z_o^2}{X_R^2}(1+X_R^2/Z_o^2)^2} \qquad (6.45)$$

$$L_F=10\log_{10}\frac{\left[-K_3\cdot\frac{R_F}{X_F} -(1-X_R/X_F)+\frac{R_F}{X_F}(1+X_R/Z_o)\right]^2\left[R_F/X_F+(1-X_R/X_F)\right]^2}{\left[K_3\cdot\frac{R_F}{X_F} -(1-X_R/X_F)-\frac{R_F}{X_F}(1+X_R/Z_o)\right]^2+\left[R_F/X_F-(1-X_R/X_F)\right]^2} \qquad (6.46)$$

$$L_R=10\log_{10}\frac{\left[K_3\cdot\frac{R_R}{X_R} - \frac{R_R}{X_R}\cdot(1+X_R/Z_o)\right]^2 + \left[\frac{R_R}{X_R} + \frac{Z_o}{X_R} + \frac{X_R}{Z_o}\right]^2}{\left[K_3\cdot\frac{R_R}{X_R} - \frac{R_R}{X_R}(1+X_R/Z_o)\right]^2 + \left[\frac{R_R}{X_R} - \frac{Z_o}{X_R} - \frac{X_R}{Z_o}\right]^2} \qquad (6.47)$$

where $K_3 = \frac{Z_o}{X_R}\cdot\frac{(X_R/X_F+X_R^2/Z_o^2)}{(1-X_R/X_F)}$

Figures 6.7 and 6.8 show the variations of phase deviations and insertion loss as a function of R_F/X_F and R_R/X_R.

6.3 EFFECT OF MISMATCHED DIODES

If the diodes connected to the coupled ports of the hybrid are not matched, reflections Γ_2 and Γ_3 at the two coupled ports of the hybrid become unequal. All the diodes used in phase shifter circuits are not always characterized individually. They are usually matched within the manufacturing tolerances. In this section, the effect of unequal Γ's on phase shifter performance is discussed.

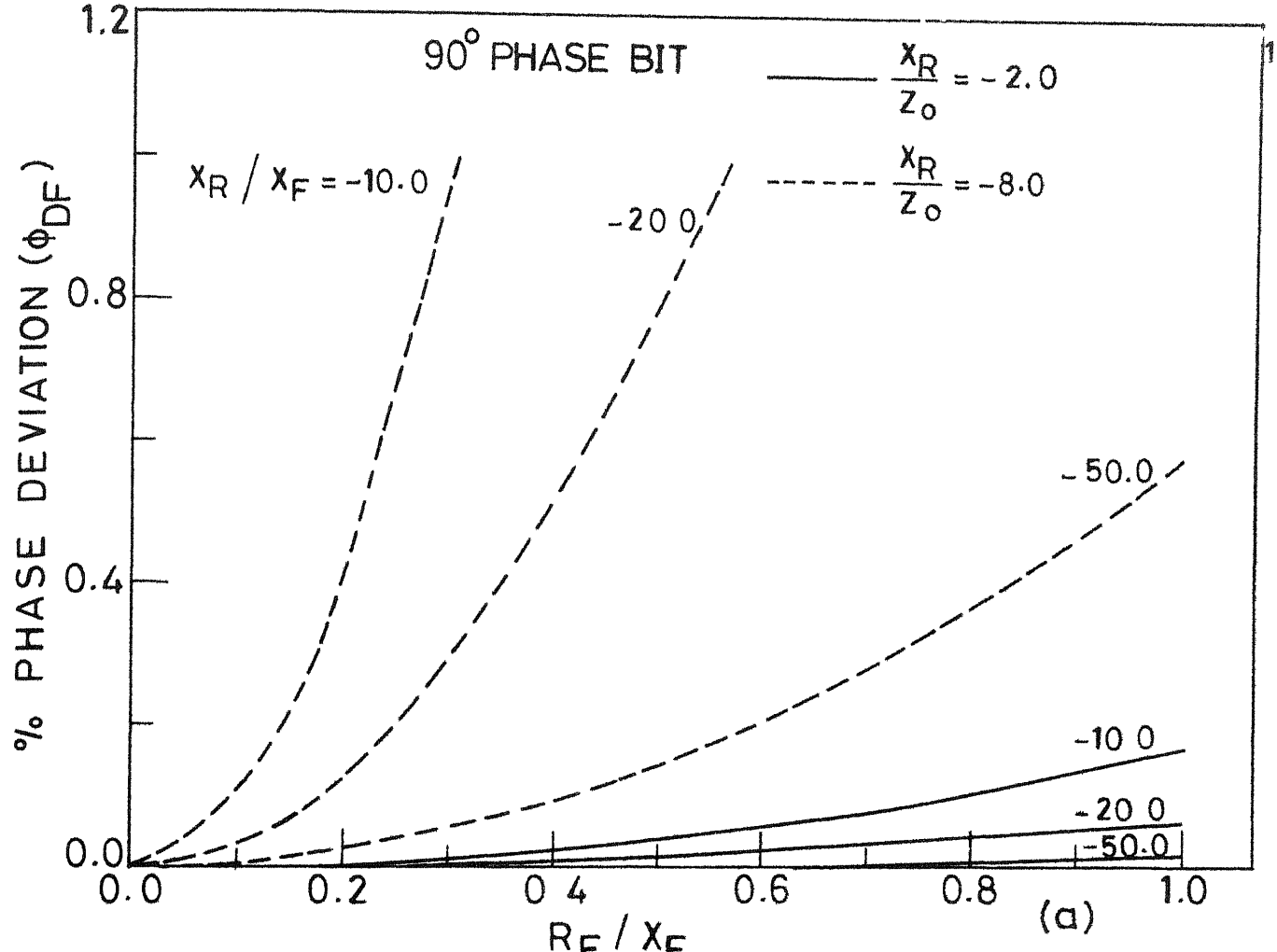


FIG. 6.7(a) VARIATION OF ϕ_{DF} WITH R_F/X_F.

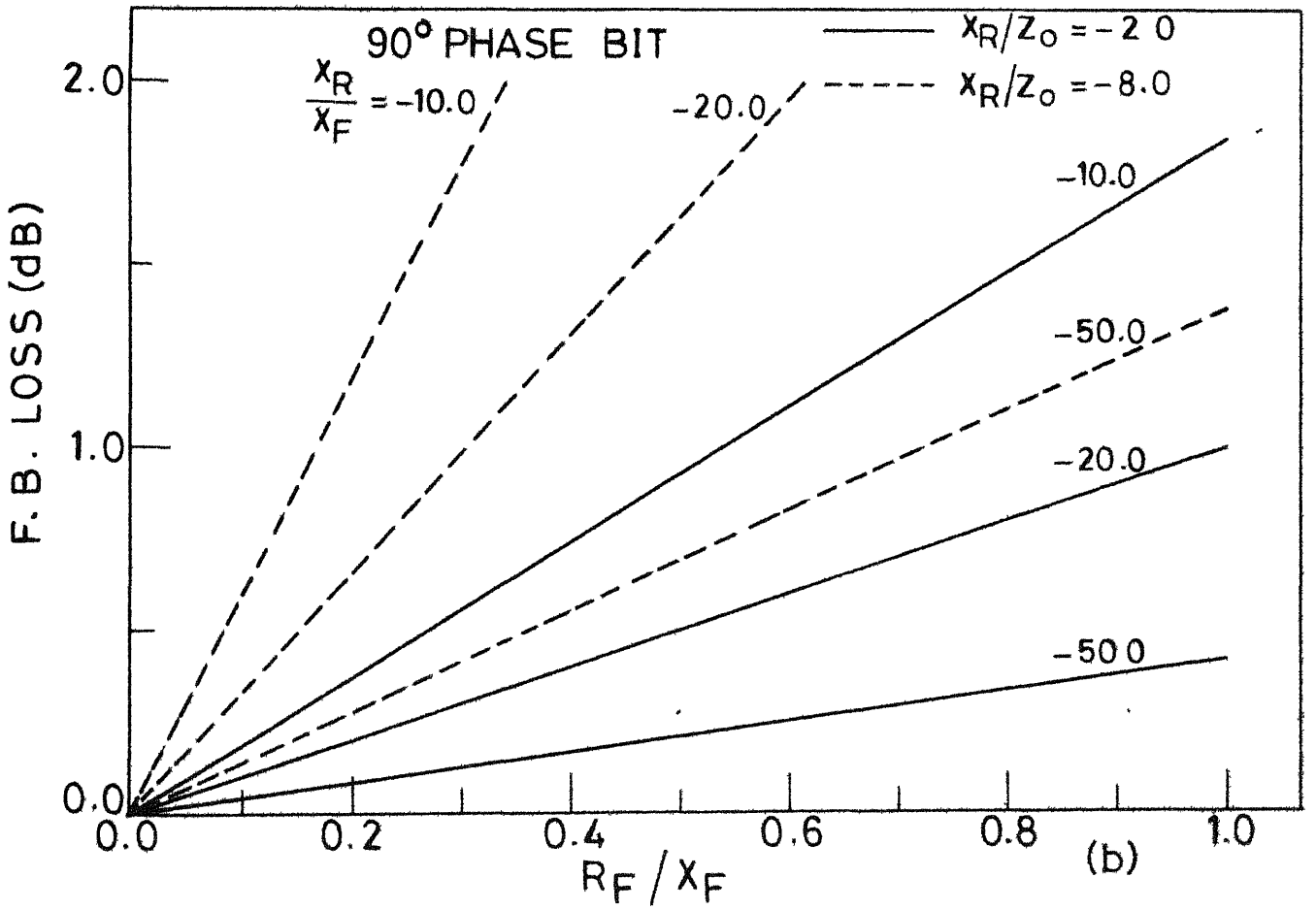
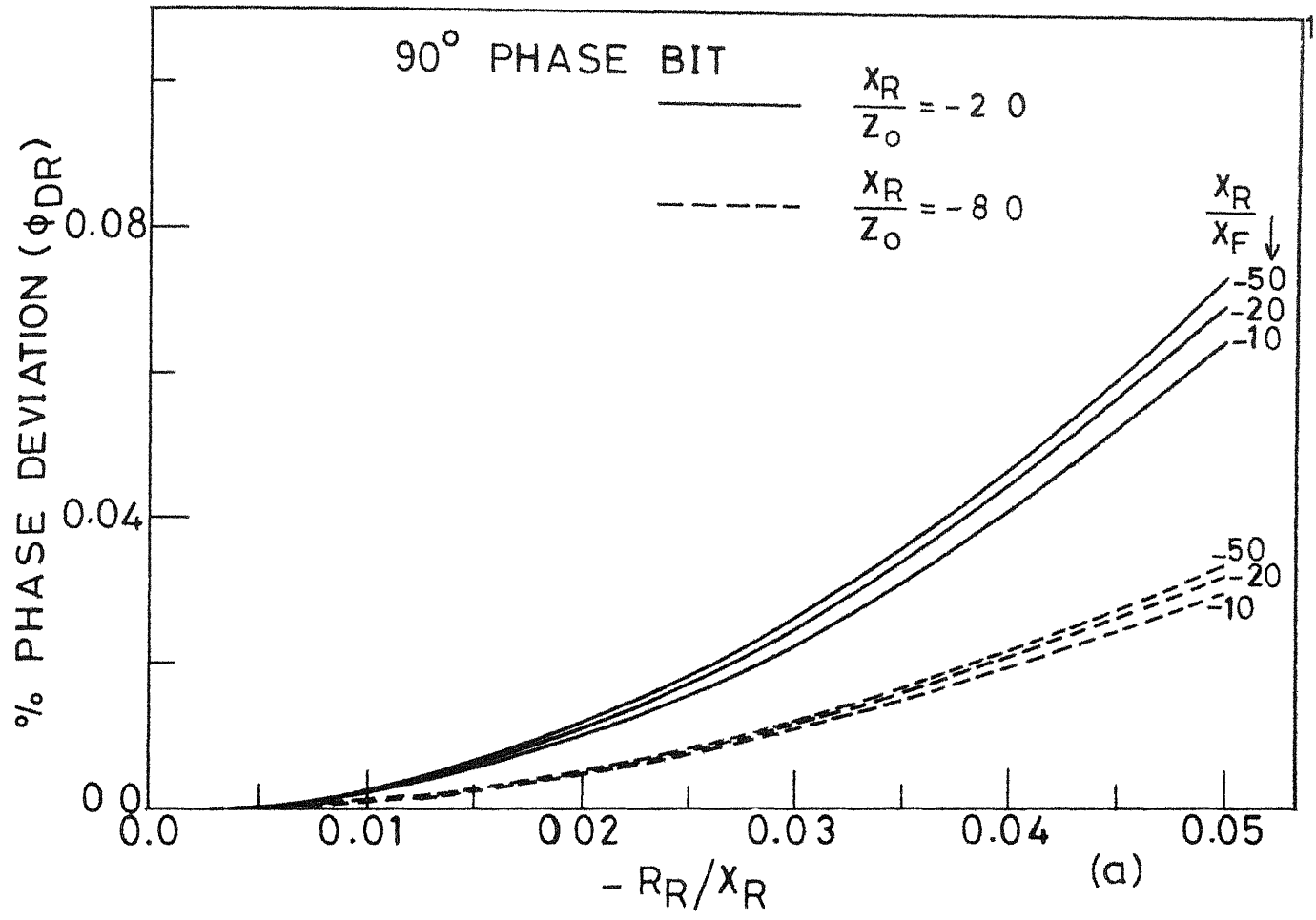


FIG. 6.7(b) VARIATION OF F.B. LOSS WITH R_F/X_F.



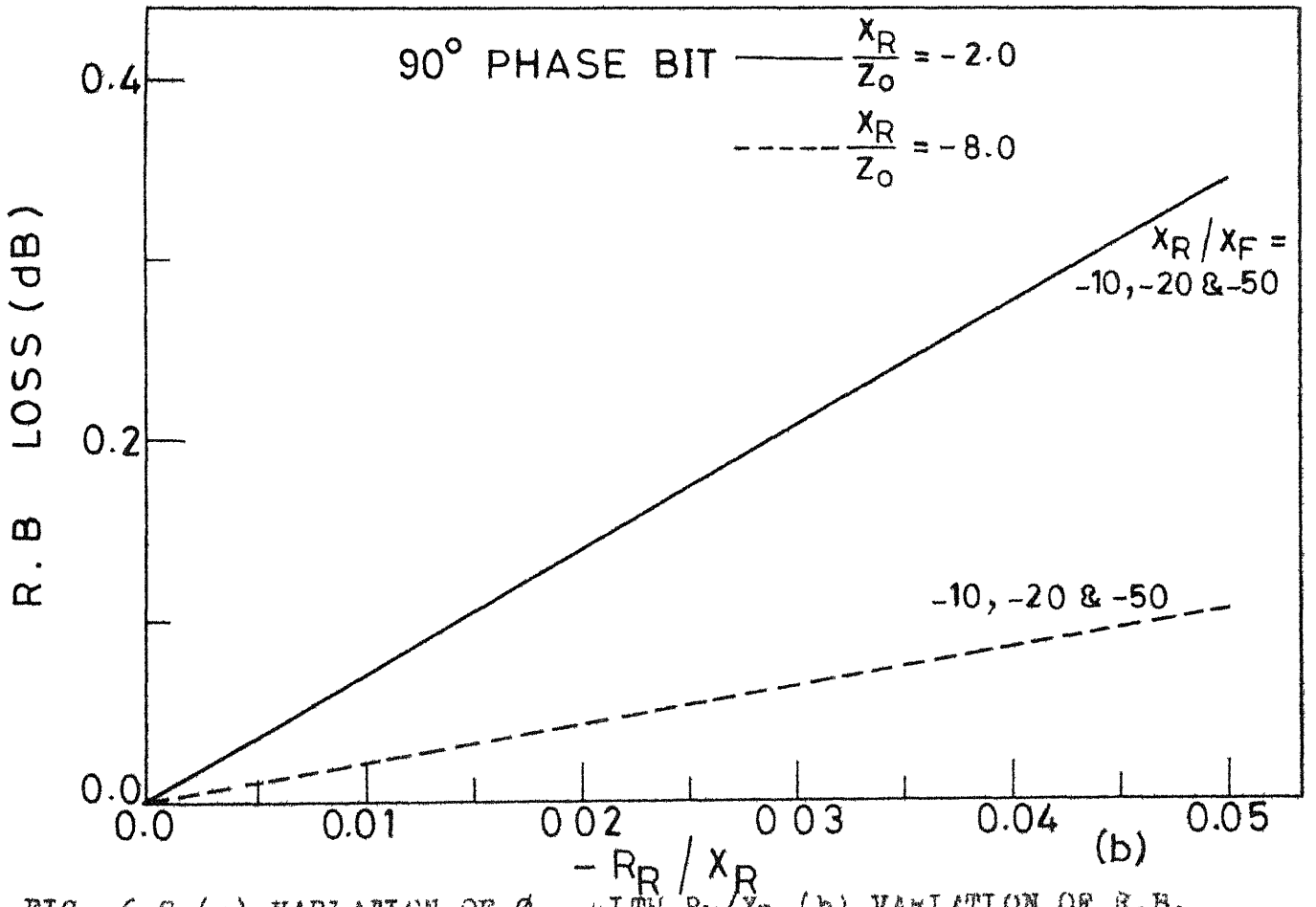


FIG. 6.8 (a) VARIATION OF ϕ_{DR} WITH R_R/X_R (b) VARIATION OF R.B. LOSS WITH R_R/X_R.

The reflection and transmission coefficients of the phase shifter using ideal hybrid ($S_{ii} = 0$, $S_{14}=S_{41}=0$, $|S_{21}| = |S_{31}| = 1/\sqrt{2}$ and $|\phi(S_{21})-\phi(S_{31})| = 90°$) with ports 2 and 3 terminated in reflection coefficients Γ_2 and Γ_3 can be written as (using Eqn. (2.7))

$$S_{11p} = S_{21}^2 \Gamma_2 + S_{31}^2 \Gamma_3 \tag{6.48}$$

$$S_{41p} = S_{14p} = S_{21} S_{31} (\Gamma_2 + \Gamma_3) \tag{6.49}$$

where S_{21} and S_{31} are the scattering parameters of the hybrid and S_{11p} and S_{41p} are the reflection and transmission coefficients of the phase shifter.

The effect of variation in Γ is studied on both S_{11p} and S_{41p} of the phase shifter. Since, Γ's are complex, they may differ in phase and/or amplitude.

6.3.1 Effect on the Reflection Coefficient of the Phase Shifter

This can be either due to difference in phases of Γ or due to differences in amplitudes. These are discussed seperately.

Inequality in Phases of Γ's

Consider the case $|\Gamma_2| = |\Gamma_3| = 1$ and $\angle\Gamma_2 \neq \angle\Gamma_3$.

Let

$$\Gamma_2 = |\Gamma_2| e^{j\phi_2} = e^{j\phi_2} \tag{6.50}$$

$$\Gamma_3 = |\Gamma_3| e^{j\phi_3} = e^{j(\phi_2 \pm \delta\phi)} \tag{6.51}$$

where $\delta\phi$ is the difference in phases of Γ_2 and Γ_3. Substituting for Γ_2 and Γ_3 from Eqns. (6.50) and (6.51) into Eqn. (6.48), we get

$$S_{11p} = \frac{e^{j\phi_2}}{2} \left[e^{j2\theta_2} + e^{j2\theta_3} \cdot e^{\pm j\delta\phi} \right] \qquad (6.52)$$

where θ_2 and θ_3 are the phases of S_{21} and S_{31}, respectively. Values of θ_2 and θ_3 would depend on the type of hybrid used. For the most common quadrature hybrids these are as follows:

(i) For two-branch hybrids, we have $\theta_2 = -90°$ and $\theta_3 = -180°$.

(ii) For parallel coupled hybrids, we have $\theta_2 = -90°$ and $\theta_3 = 0°$.

(iii) And for three-branch hybrids, we have $\theta_2 = -180°$ and $\theta_3 = -270°$.

Substituting the values of θ_2 and θ_3 for the above hybrids into Eqn. (6.52), we get in all the above cases

$$S_{11p} = \frac{e^{j\phi_2}}{2} \left[\mp 1 \pm e^{\pm j\delta\phi} \right] \qquad (6.53)$$

Hence,

$$\left| S_{11p} \right| = \frac{1}{2} \sqrt{(\cos\delta\phi - 1)^2 + \sin^2 \delta\phi} \qquad (6.54)$$

From Eqn. (6.54), VSWR of the phase shifter can be calculated as a function of $\delta\phi$.

Inequality in Magnitudes of Γ

Assuming, $\angle\Gamma_2 = \angle\Gamma_3$ and $|\Gamma_2| \neq |\Gamma_3|$, let,

$\Gamma_2 = |\Gamma_2| e^{j\phi}$ and $\Gamma_3 = |\Gamma_3| e^{j\phi}$

Substituting these into expressions for S_{11p} (Eqn. (6.48)), we get

$$S_{11p} = \frac{1}{2} e^{j\phi} \left[e^{j2\theta_2} |\Gamma_2| + e^{j2\theta_3} |\Gamma_3| \right] \qquad (6.55)$$

Substituting for the values of θ_2 and θ_3 for the most common quadrature hybrids, we get

$$S_{11p} = \frac{e^{j\phi}}{2} \left[\mp |\Gamma_2| \pm |\Gamma_3| \right] \text{ and}$$

$$|S_{11p}| = \frac{||\Gamma_3| - |\Gamma_2||}{2} \qquad (6.56)$$

VSWR of the phase shifter can now be evaluated as a function of $\pm (|\Gamma_2| - |\Gamma_3|)$.

6.3.2 Effect on the Transmission Coefficient of the Phase Shifter Inequality in Phases of Γ's

Substituting the values of Γ_2 and Γ_3 given by Eqns. (6.50) and (6.51) into the equation for the transmission coefficient of the phase shifter (Eqn. (6.49)), we get

$$S_{41p} = \frac{e^{j(\theta_2+\theta_3)} e^{j\phi_2}}{2} \left[1 + e^{\pm j\,\delta\phi} \right] \qquad (6.57)$$

Substituting the values of $(\theta_2 + \theta_3)$ for the common quadrature hybrids, we get

$$S_{41pF} = \cos(\delta\phi/2) \cdot e^{j(\phi_2 \pm \pi/2 \pm \delta\phi/2)} \qquad (6.58a)$$

$$S_{41pR} = \cos(\delta\phi/2) \cdot e^{j(\phi_2 + \Delta\phi \pm \pi/2 + \delta\phi/2)} \qquad (6.58b)$$

From Eqns. (6.58a) and (6.58b) the magnitude of transmission coefficient is given by

$$|S_{41pF}| = |S_{41pR}| = \cos(\pm \delta\phi/2) \qquad (6.59)$$

And the maximum value of differential phase error is given by $\pm \delta\phi$.

Inequality in Magnitudes of Γ's

Substituting, $|\Gamma_2| e^{j\phi}$ and $|\Gamma_3| e^{j\phi}$ for Γ_2 and Γ_3 in Eqn. (6.49), we get,

$$S_{41pF} = \frac{|\Gamma_2| + |\Gamma_3|}{2} e^{j(\phi_2 \pm \pi/2)} \qquad (6.60a)$$

$$S_{41pR} = \frac{|\Gamma_2| + |\Gamma_3|}{2} e^{j(\phi_2 + \Delta\phi \pm \pi/2)} \qquad (6.60b)$$

From Eqns. (6.60) we note that the differential phase shift is independent of differences in magnitudes of Γ_2 and Γ_3.

Magnitude of the transmission coefficient is given by

$$|S_{41pF}| = |S_{41pR}| = \left|\frac{|\Gamma_2| + |\Gamma_3|}{2}\right| \qquad (6.61)$$

Ideally, $|S_{41pF}|$ and $|S_{41pR}|$ should each be unity and hence $|\Gamma_2| + |\Gamma_3|$ should be equal to 2.0. When diodes are lossy both $|\Gamma_2|$ and $|\Gamma_3|$ may be less than unity each. From Eqn. (6.61) we note that loss due to inequality in magnitude depends on how far the sum ($|\Gamma_2| + |\Gamma_3|$) is different from 2.0 and is not an explicit function of $|\Gamma_2| - |\Gamma_3|$. If we assume, $\Gamma_2 = (1 - \Delta\Gamma_2)$ and $\Gamma_3 = (1 - \Delta\Gamma_3)$, then Eqn. (6.61) can be rewritten as

$$|S_{41pF}| = |S_{41pR}| = \frac{2 - (\Delta\Gamma_2 + \Delta\Gamma_3)}{2} \qquad (6.62)$$

The resulting insertion loss of the phase shifter in this case is plotted as a function of $2-(|\Gamma_2|+|\Gamma_3|)$ in Fig. 6.9(c).

Figures 6.9(a) and (b) show the plot of phase shifter characteristics as a function of phase and amplitude difference in Γ's. Maximum differences in the phases of Γ considered are $\pm$ 10° while in amplitudes the maximum difference is 0.05.

An inequality in the phase of Γ's of $\pm 6°$ gives input VSWR of the phase shifter as 1.11, phase error as $\pm 6°$ and insertion loss to be 0.012 dB. Inequality in amplitudes of of 0.03 leads to VSWR of 1.03, but there is no phase error due to this amplitude difference. Figure 6.9(c) shows the plot of insertion loss of the phase shifter as a function of $2 - (|\Gamma_2|+|\Gamma_3|)$.

6.4 DISCUSSIONS

The results presented in this chapter are useful in specifying the tolerances required in diode parameters for the specified phase shifter performance. Some of the significant conclusions that may be drawn are as follows.

1. We observe that 90° phase bit is most sensitive to X_R (mainly diode capacitance) variations. Hence tighter tolerances in diode capacitances are needed for 90° bits than for 180° bits. Stub type transforming network is found to be less sensitive than transformer type network for diodes having small capacitance.

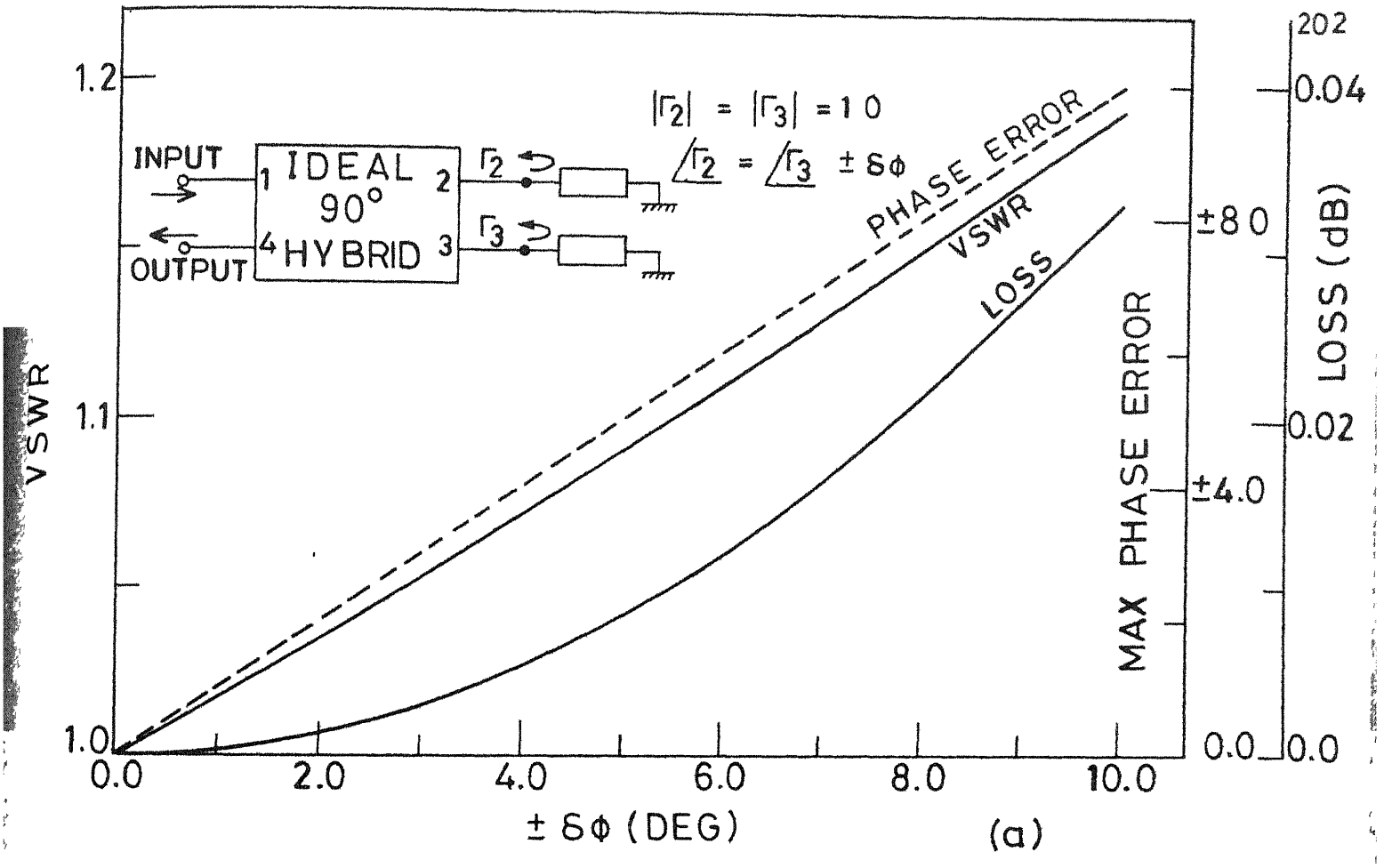


FIG. 6.9(a) PLOT OF PHASE SHIFTER CHARACTERISTICS DUE TO PHASE DIFFERENCE IN Γ's

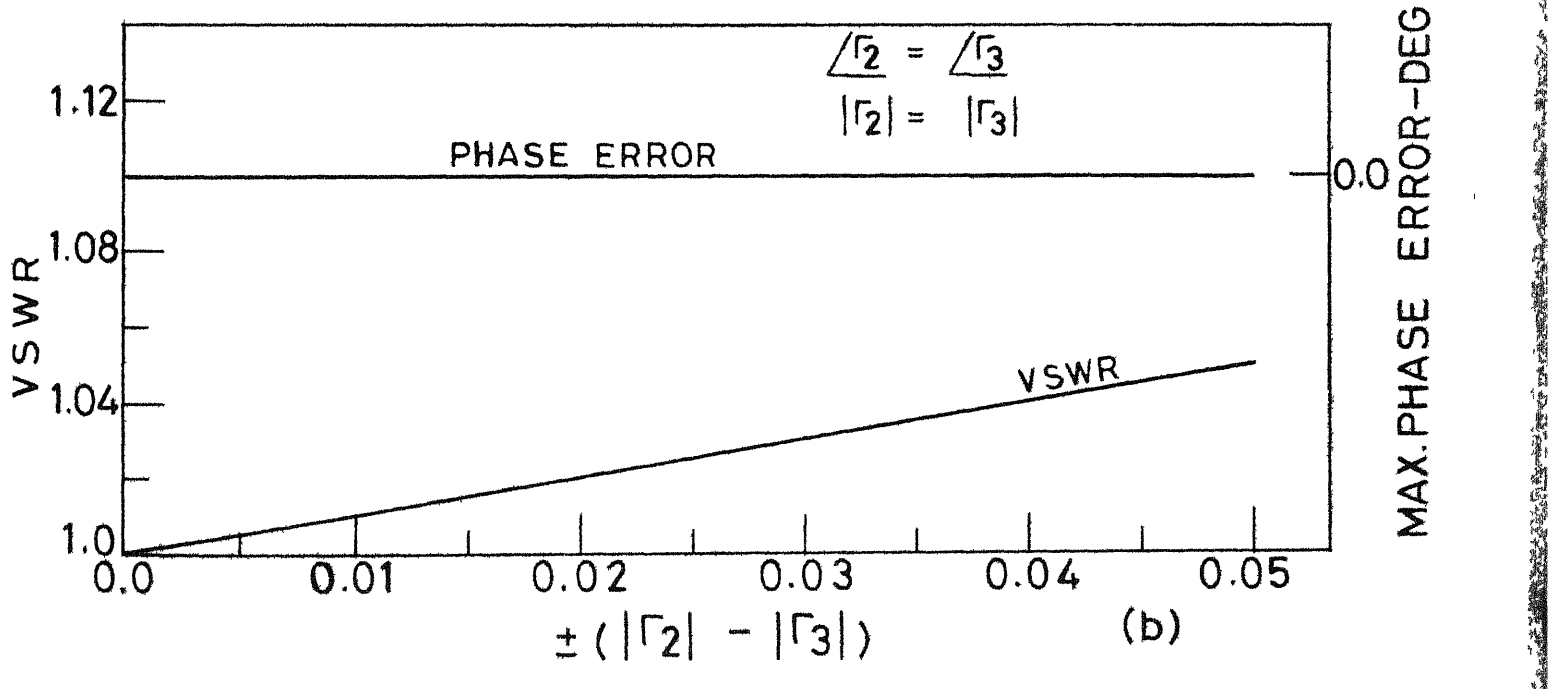


FIG. 6.9(b) PLOT OF PHASE SHIFTER CHARACTERISTICS DUE TO AMPLITUDE DIFFERENCE IN Γ's

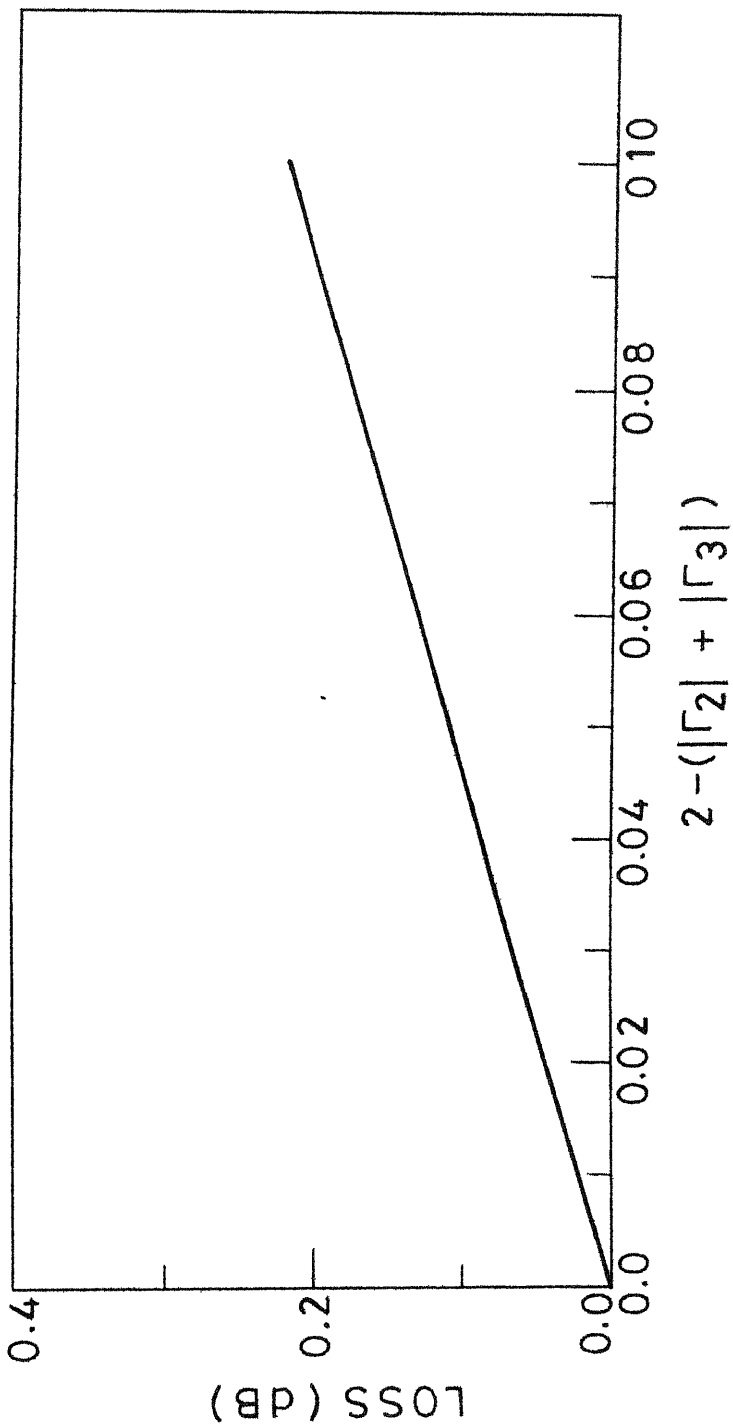


FIG. 6.9(c) ... OF IMPEDANCE ... OF THREE SHIFTER WITH
$2 - (|\Gamma_2| + |\Gamma_3|)$

Effects of forward bias and reverse bias resistances of the diode on the phase shift are small as compared to those of reactances. Hence, the design equations arrived at by considering the lossless diodes (Chapter 4) may be used for the lossy diodes also.

It is to be noted that the phase deviations and loss variations as a function of R_R/X_R do not depend much on the diode reactance ratio X_R/X_F.

Phase shifter performance using mismatched diodes is more sensitive to variations in phase of Γ's than their magnitudes. Phase of Γ depends on diode reactances. Diode capacitance varies the maximum from piece to piece in a production run. Hence, diode capacitance is the most important parameter which should be matched in selecting diodes.

CHAPTER 7

DISCONTINUITY REACTANCES AND OPTIMIZATION OF PHASE SHIFTER CIRCUITS

7.1 EFFECT OF DISCONTINUITY REACTANCES ON PHASE SHIFTER PERFORMANCE 206

7.1.1 Discontinuity Reactance Characterization 207

7.1.2 Phase Bit UsingTwo-Branch Hybrid and Stub Type Network (180° bit) 211

7.1.3 Phase Bit Using Two-Branch Impedance Transforming Hybrid and Length of Line (90° bit) 213

7.2 OPTIMIZATION OF HYBRIDS 219

7.2.1 Optimization by Pattern Search 219

7.2.2 Two-Branch Hybrid 222

7.2.3 Two-Branch Impedance Transfoming Hybrid 227

7.3 OPTIMIZATION OF PHASE SHIFTER CIRCUITS 231

7.3.1 180° Phase Bit Using Two-Branch Hybrid and Stub Type Network 232

7.3.2 90° Phase Bit Using Two-Branch Impedance Transforming Hybrid with Length of Line. 236

7.4 EXPERIMENTS USING OPTIMIZED DESIGN 237

7.4.1 180° Phase Bit 240

7.4.2 90° Phase Bit 240

CHAPTER 7

DISCONTINUITY REACTANCES AND OPTIMIZATION OF PHASE SHIFTER CIRCUITS

Performance of the phase shifter circuits described in Chapter 3 and 5 had been evaluated without considering the effect of discontinuity reactances. Depending upon the substrate height, the dielectric constant and the frequency of operation, effect of discontinuity reactances can be significant. If the characterization of these discontinuities is available, their effects may be compensated either by analytical methods or by computer optimization. The later approach is used in the present investigations.

In this chapter, the effect of discontinuity reactances on 180° and 90° bits using two-branch normal hybrid and two-branch impedance transforming hybrid with suitable transforming networks is discussed. Pattern search, a direct search strategy of Hook and Jeeves has been used for compensation of these discontinuities and later for optimization of phase bits (both 180° and 90°). Experiments carried out to verify optimized results are also described. A good agreement between the optimized and experimental results is achieved.

7.1 EFFECT OF DISCONTINUITY REACTANCES ON PHASE SHIFTER PERFORMANCE

Two types of phase bits have been analyzed for studying the effect of discontinuity reactances. These are: a 180° phase bit using two-branch hybrid and stub type transforming

network, and a 90° bit using two-branch impedance transforming hybrid. In these circuits two types of discontinuity reactances, namely, open ends and T-junctions, are encountered.

7.1.1 Discontinuity Reactance Characterization

Characterization of microstrip discontinuities is well documented in literature [38-43]. However, for continuity of the present discussions, results for the open-end and the T-junction discontinuities are summarized in this section.

Microstrip Open End

A microstrip open end and its equivalent circuit [38] are shown in Fig. 7.1. The equivalent circuit is represented by an excess capacitance C_{oc} (Fig. 7.1(b)) which can be modelled by an equivalent length of transmission line, $\Delta\ell_{oc}$, as shown in Fig. 7.1(c). An empirical expression for $\Delta\ell_{oc}/h$ has been obtained by Hammerstad and Bekadal [39] as follows

$$\frac{\Delta\ell_{oc}}{h} = 0.412 \cdot \frac{\varepsilon_{re} + 0.3}{\varepsilon_{re} - 0.258} \cdot \frac{W/h + 0.262}{W/h + 0.813} \qquad (7.1)$$

This closed-form expression gives maximum relative error (compared to empirical formula of Silvester and Benedek [38]) of 8.7% for $\varepsilon_r = 1$ and for $\varepsilon_r > 1$ the maximum relative error is 2.4%.

Microstrip T-junction

Various equivalent circuits have been proposed for characterization of a microstrip T-junction [39-42]. The

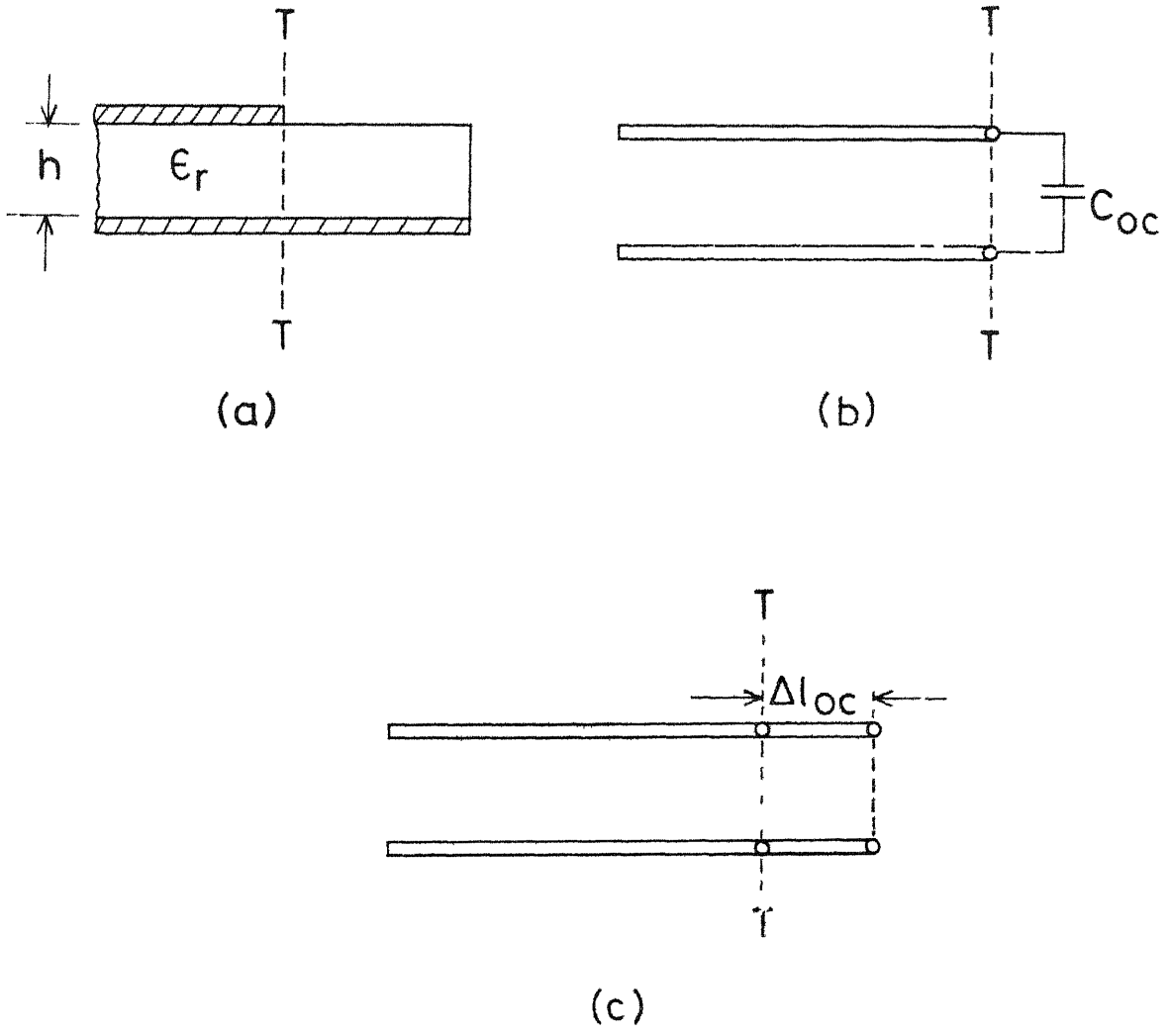


FIG. 7.1 MICROSTRIP OPEN END AND ITS EQUIVALENT CIRCUIT

representation given by Hammerstad and Bekkadal [39] has been of most practical use and is considered in the present discussions. The T-junction equivalent circuit is shown in Fig. 7.2 and the various parameters are as follows:

$$D_1 = \frac{120\,\pi\,h}{\sqrt{\varepsilon_{re_1}}.Z_1} \quad , \quad D_2 = \frac{120\pi h}{\sqrt{\varepsilon_{re_2}}.Z_2} \tag{7.2}$$

$$n = \frac{\sin\left(\frac{\pi}{2} \cdot \frac{2D_1}{\lambda_{g_1}} \cdot \frac{Z_1}{Z_2}\right)}{\frac{\pi}{2} \cdot \frac{2D_1}{\lambda_{g_1}} \cdot \frac{Z_1}{Z_2}} \tag{7.3}$$

$$\frac{d_1}{D_2} = 0.05 \quad \frac{Z_1}{Z_2} \cdot n^2 \tag{7.4}$$

$$\frac{d_2}{D_1} = 0.5 - 0.16 \left[1 + (2D_1/\lambda_{g_1})^2 - 2\,\ell n(Z_1/Z_2)\right] \cdot \frac{Z_1}{Z_2} \tag{7.5}$$

$$\frac{B_T\,\lambda_{g_1}}{Y_1 D_1} = \begin{cases} -(1 - 2D_1/\lambda_{g_1}) \cdot \dfrac{Z_1}{Z_2}, & Z_1/Z_2 < 0.5 \\ (1 - 2D_1/\lambda_{g_1})\left(3.\dfrac{Z_1}{Z_2} - 2\right), & Z_1/Z_2 > 0.5 \end{cases} \tag{7.6}$$

It has been pointed out [39] that Eqns. (7.2) through (7.6) give good results except for $Z_1/Z_2 > 2$ where the calculated values of d_2/D_1 are too high. In this range a better value for d_2 is obtained by replacing Z_1/Z_2 with Z_2/Z_1.

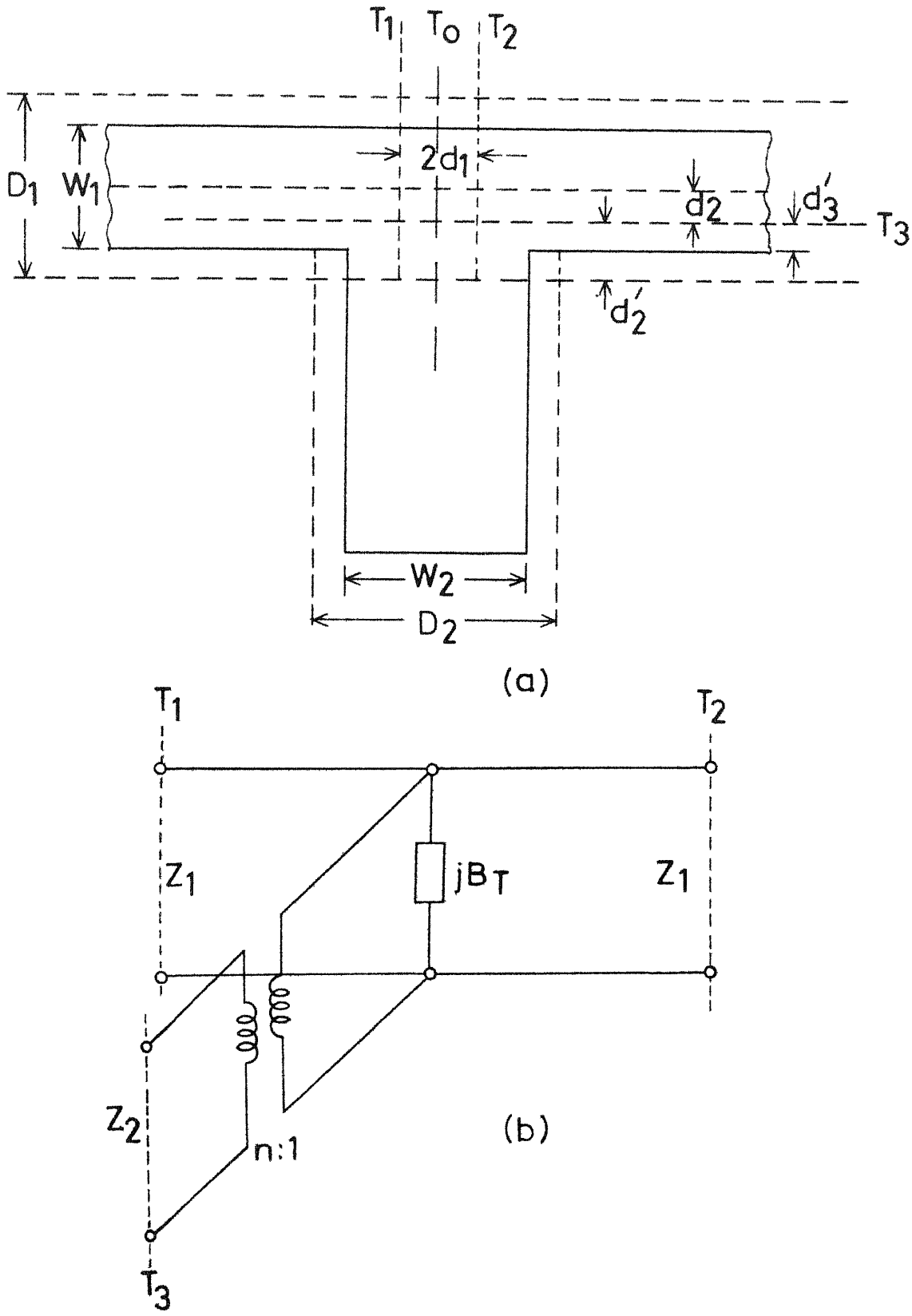


FIG. 7.2 MICROSTRIP T-JUNCTION AND ITS EQUIVALENT CIRCUIT

We see from Fig. 7.2(a), that d_2 is the shift in reference plane of the shunt branch, d_2' is the shift with respect to lower edge of D_1, and d_3' is shift of reference plane T_3 with respect to lower edge of microstrip. Expressions for d_2' and d_3' can be easily written as

$$d_2' = D_1/2 - d_2 \tag{7.7}$$

and

$$d_3' = \frac{D_1 - W_1}{2} - d_2' \tag{7.8}$$

7.1.2 Phase Bit Using Two-Branch Hybrid and Stub-Type Network (180° bit)

Figure 7.3(a) shows the configuration of phase bit of this type. As discussed earlier in Chapter 4, coupled ports of two-branch hybrid are connected to the transforming network of single stub type and PIN diode. It is to be noted that the line lengths in the main branch of the T-junction (e.g. $\lambda_{g_1/4}$ in the figure) are measured from the centre of the junction and the lengths in the shunt branch (e.g. $\lambda_{g_2/4}$) are measured from the microstrip edge.

The equivalent circuit of this phase bit including junction reactances is shown in Fig. 7.3(b). The plane 'SS' represents the plane of symmetry. Blocks labeled 'T-junction' represent the equivalent circuit of the junction (similar to Fig. 7.2) formed by the transmission lines of given impedances. Corresponding T-junction parameters are also indicated in the figure. Other blocks represent the corresponding transmission line lengths and impedances. The block at the

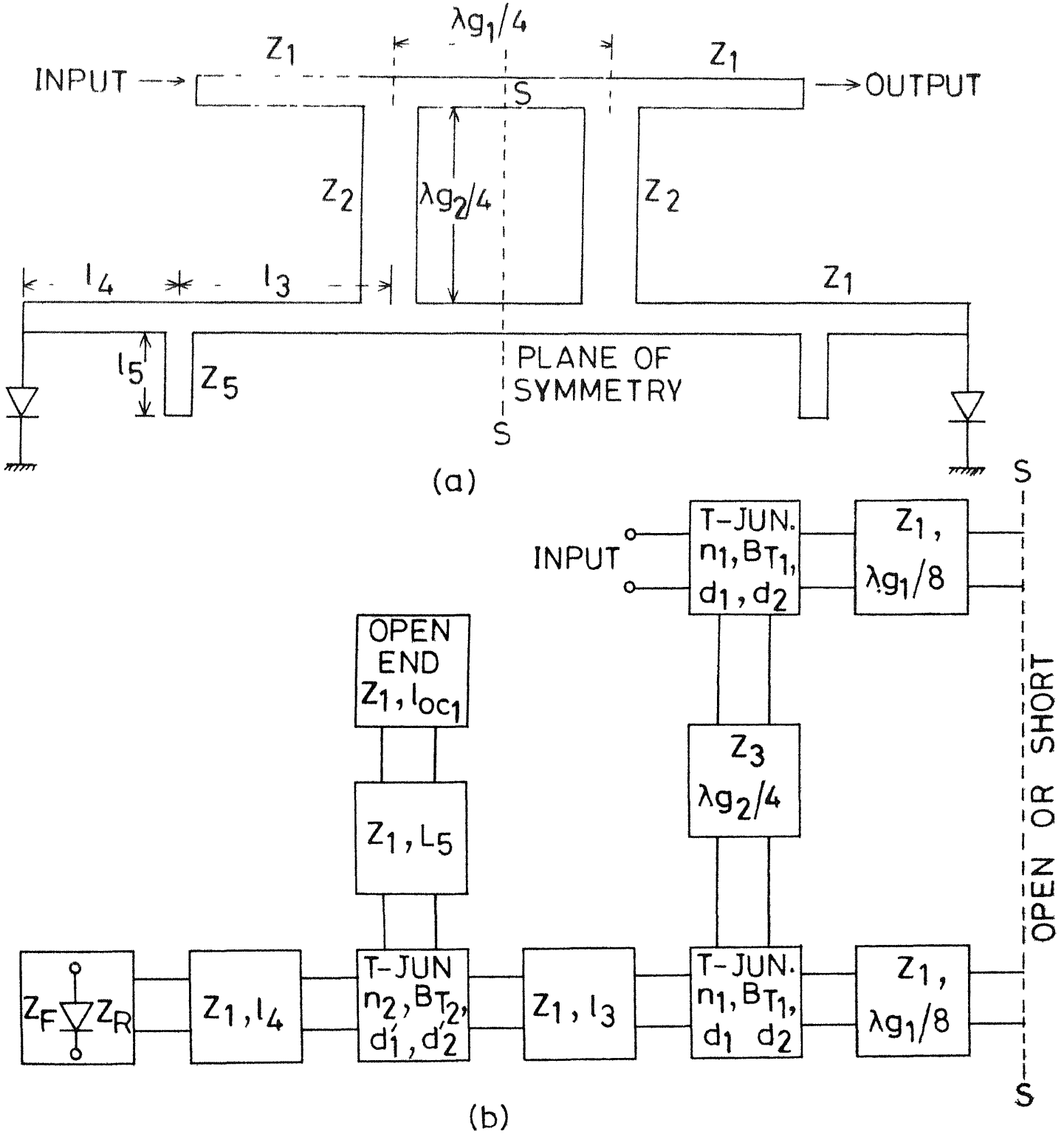


FIG. 7.3 (a) CONFIGURATION OF 180° PHASE BIT USING TWO-BRANCH HYBRID AND STUB TYPE TRANSFORMING NETWORK

(b) EQUIVALENT CIRCUIT OF 7.3(a) INCLUDING DISCONTINUITY REACTANCES

extreme left represents the diode impedances Z_F and Z_R in the two bias states.

Analysis of this circuit using junction reactances is carried out by using even/odd mode symmetry and ABCD matrices. This procedure is similar to that followed in Chapters 3 and 5. Parameters of the diodes used for this circuit were measured at 2.1 GHz. Figure 7.4 gives the equivalent circuit of the diode in the two states along with the measured values of the parameters.

Performance of the phase bit with and without discontinuities is shown in Fig. 7.5. We observe that the parameters VSWR, loss and ϕ of the phase bit exhibit a frequency shift due to discontinuity reactances. VSWR and insertion loss performance has shifted towards higher frequency for both the bias states. Differential phase shift is found to have value of 190° instead of the designed value of 180° at 2.1 GHz. We note that the effect of discontinuities is significant for all the three performance characteristics. This brings out clearly the necessity of considering the effects of discontinuities in the design.

7.1.3 Phase Bit Using Two-Branch Impedance Transforming Hybrid and Length of Line (90° Bit)

Figure 7.6 shows the phase bit using two-branch impedance transforming hybrid. This hybrid performs the required impedance transformation to achieve the desired

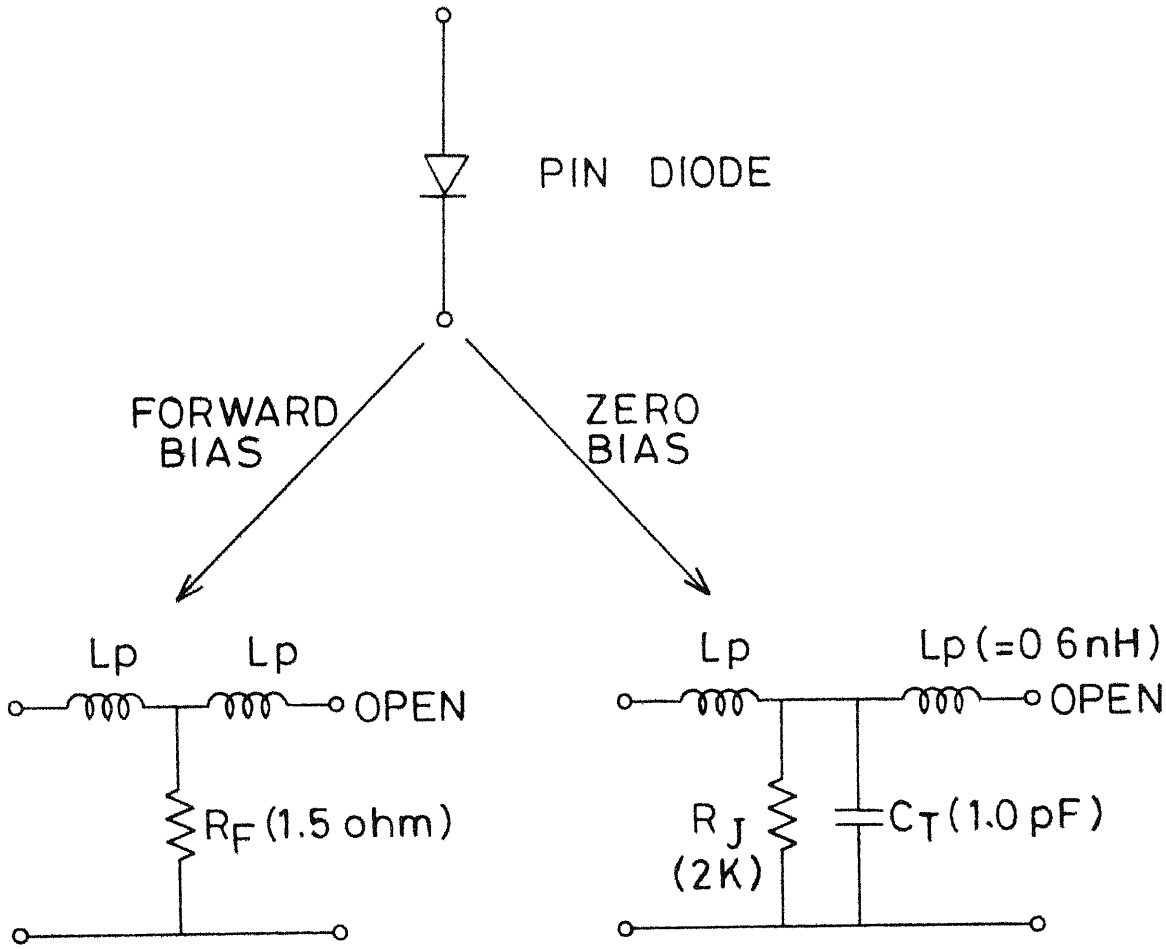


FIG. 7.4 EQUIVALENT CIRCUIT OF PIN DIODE IN FORWARD AND REVERSE BIAS WITH MEASURED PARAMETERS

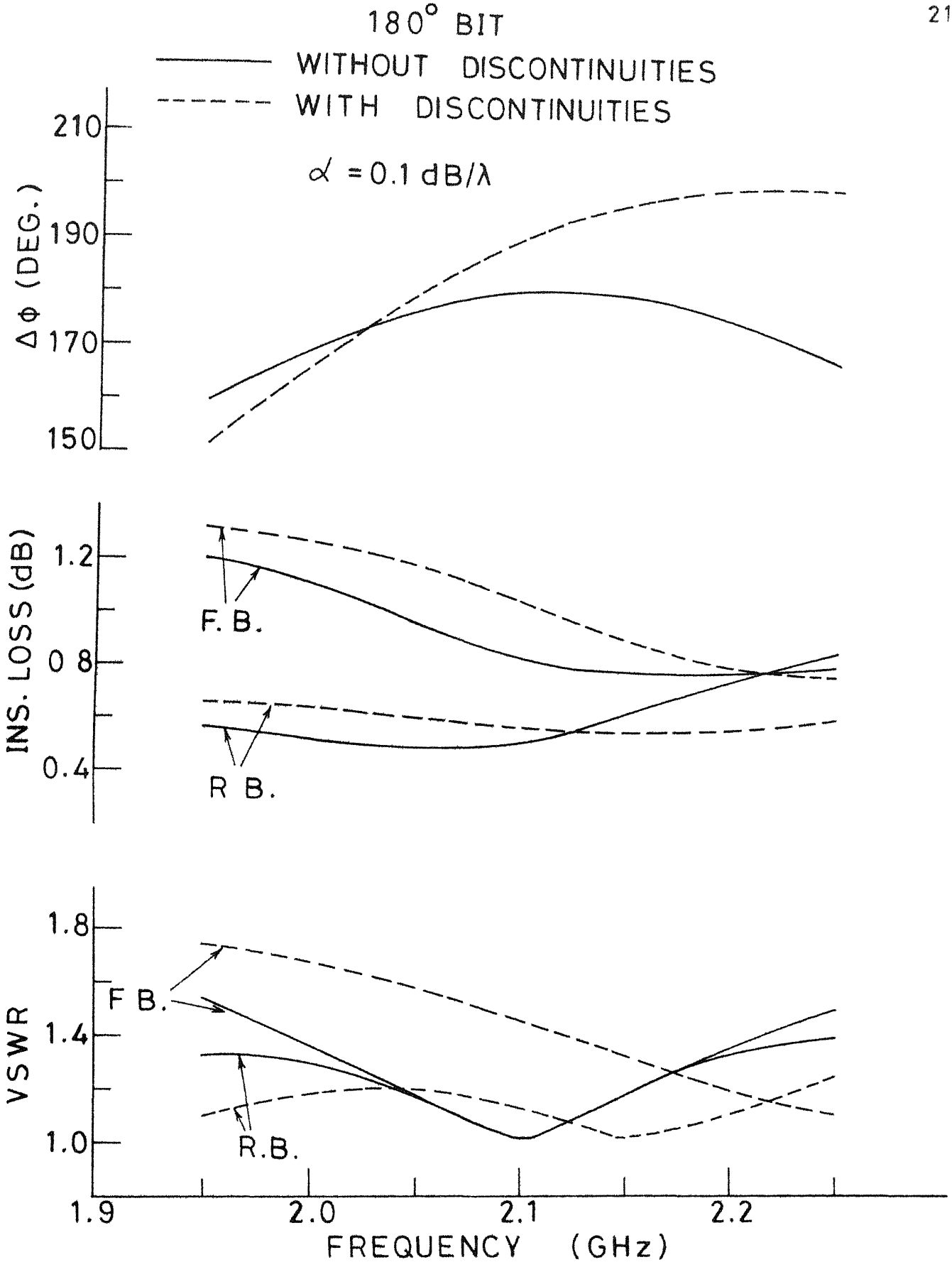


FIG. 7.5 PERFORMANCE OF 180° PHASE BIT WITH AND WITHOUT DISCONTINUITIES.

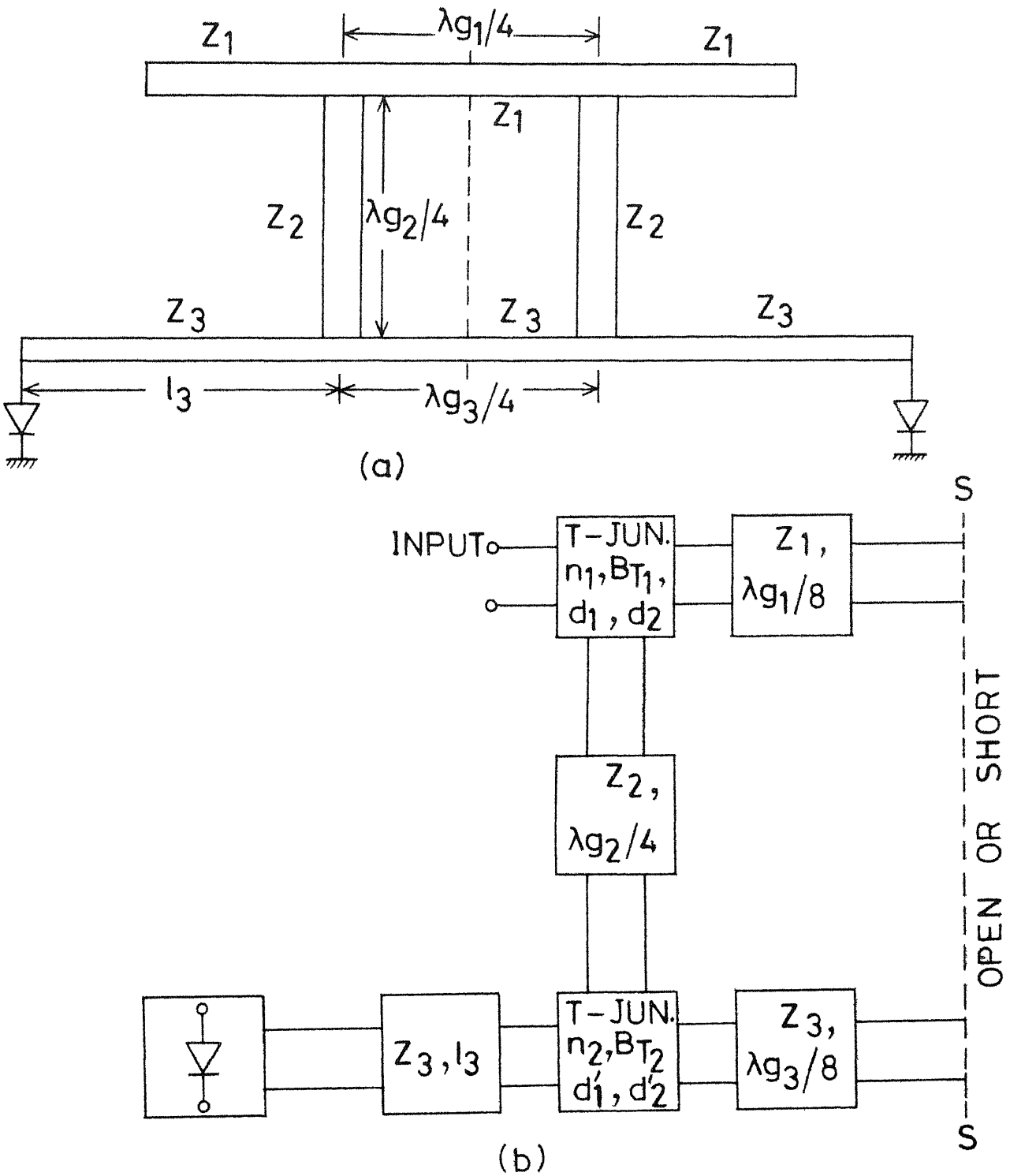


FIG. 7.6 (a) CONFIGURATION OF 90° [illegible] BIT USING TWO-BRANCH IMPEDANCE TRANSFORMING HYBRID

EQUIVALENT CIRCUIT OF 7.6(a) INCLUDING DISCONTINUITY REACTANCES

phase shift from nonideal diodes (Chapter 4). Diodes are connected to the coupled ports of this hybrid through a suitable length of transmission line.

Equivalent circuit of this phase bit including junction reactances is shown in Fig. 7.6(b). This circuit has only T-junction discontinuities. It is to be noted (Fig. 7.6(a)) that, Z_1 and Z_3 are different, λ_{g_1} and λ_{g_3} are not equal, hence the shunt branches of impedance Z_2 are not at right angles to the main branch of impedance Z_1. But in practice, λ_{g_1} and λ_{g_3} are very nearly equal and their effect on the shunt branch is negligible. In a typical case, if Z_1 = 50 ohm and Z_3 = 82.2 ohm, the ratio $\lambda_{g_1} / \lambda_{g_3}$ = 0.9926 (for substrate dielectric constant of 2.53 and height of 0.0625 inches) and the difference in two λ_g's is about 0.073 cm.

Analysis of this circuit is also carried out using even/odd mode symmetry and ABCD matrices. Equivalent circuits of PIN diodes (in two bias states) and the measured diode parameters given in Fig. 7.4 are used.

Figure 7.7 depicts the performance of the phase bit with and without discontinuities. In this case also, the VSWR and loss characteristics shift towards higher frequency. 2.1 GHz is the centre frequency when discontimuities are not considered. Differential phase shift is found to have value of approximately 86° instead of 90° at the centre frequency of 2.1 GHz.

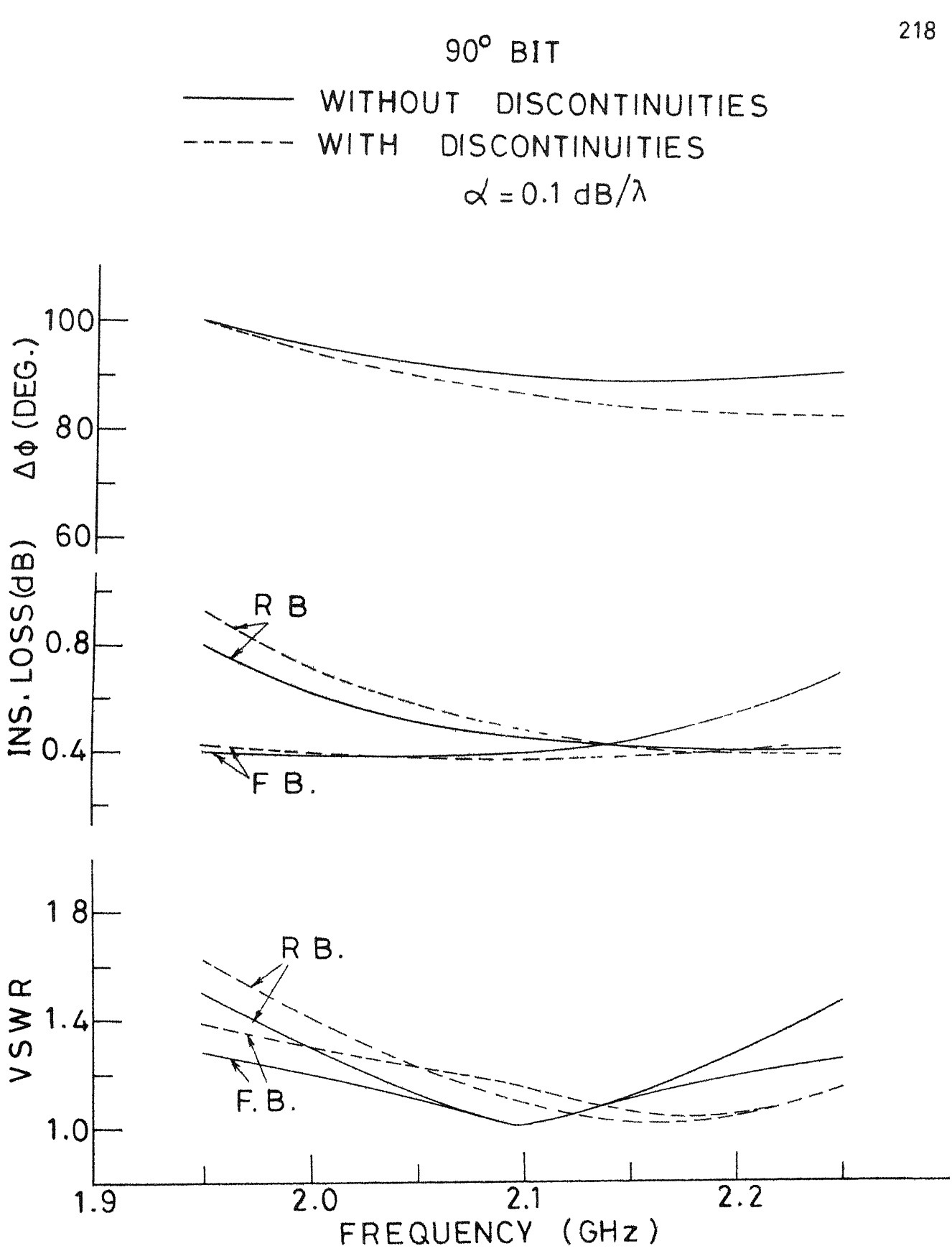


FIG. 7.7 PERFORMANCE OF 90° PHASE BIT WITH AND WITHOUT DISCONTINUITIES.

7.2 OPTIMIZATION OF HYBRIDS

The significant deterioration in the performance of the phase bit (Section 7.1) has been attributed mainly due to the junction reactances. Compensations for these discontinuity reactances of the hybrids used for 180° and 90° bits are discussed in this section. This compensation is carried out by optimization of the hybrid. A direct search method described by Hook and Jeeves [44] called pattern search has been used in the present investigation. Optimization of normal 3 dB branch guide couplers taking into account dispersion, coupling and discontinuity reactances are given in [45]. Optimization of the hybrid is desirable since it provides the initial starting value (base point) while optimizing the complete phase bit. Two hybrids considered for optimization are: (i) two-branch normal hybrid and (ii) two-branch impedance transforming hybrid.

7.2.1 Optimization By Pattern Search

Iterative modification of circuit parameters in order to achieve a given objective (i.e. to meet a set of given specifications) is termed as optimization. Methods of optimization developed for other diciplines are useful for the design of microwave circuits also. These methods can be classified in two groups [46]: Gradient methods and Direct search methods. In the gradient methods, information about derivatives of performance functions (with respect to

designable parameters) is used for arriving at the modified set of parameters at each step in moving towards the optimum solution. Direct search methods, on the other hand, do not use gradient information and the optimization is carried out by searching for the 'optimum' solution in a systematic manner. Direct search strategies are simpler to use than gradient search techniques for the problems involving less number of variables, and require less computing time in function evaluation. A direct search method of Hook and Jeeves has been used for optimization and is discussed in this section.

A typical flow diagram for optimization procedure is shown in Fig. 7.8. The performance of the circuit to be optimized is evaluated by computer-aided circuit analysis program. Numerical models for various components used in a circuit are called from the library of subroutines developed for this purpose. Circuit performance thus obtained is compared with given specifications. If the results fail to satisfy the desired specifications the designable parameters of the circuit are altered in a systematic manner. This constitutes the key step in computer-aided design. The sequence of circuit analysis, comparison with desired performance and parameter modification is performed iteratively till the specifications are met.

Hooke and Jeeves Method

The pattern search method of Hooks and Jeeves [44] makes two types of moves. The first type of move is called

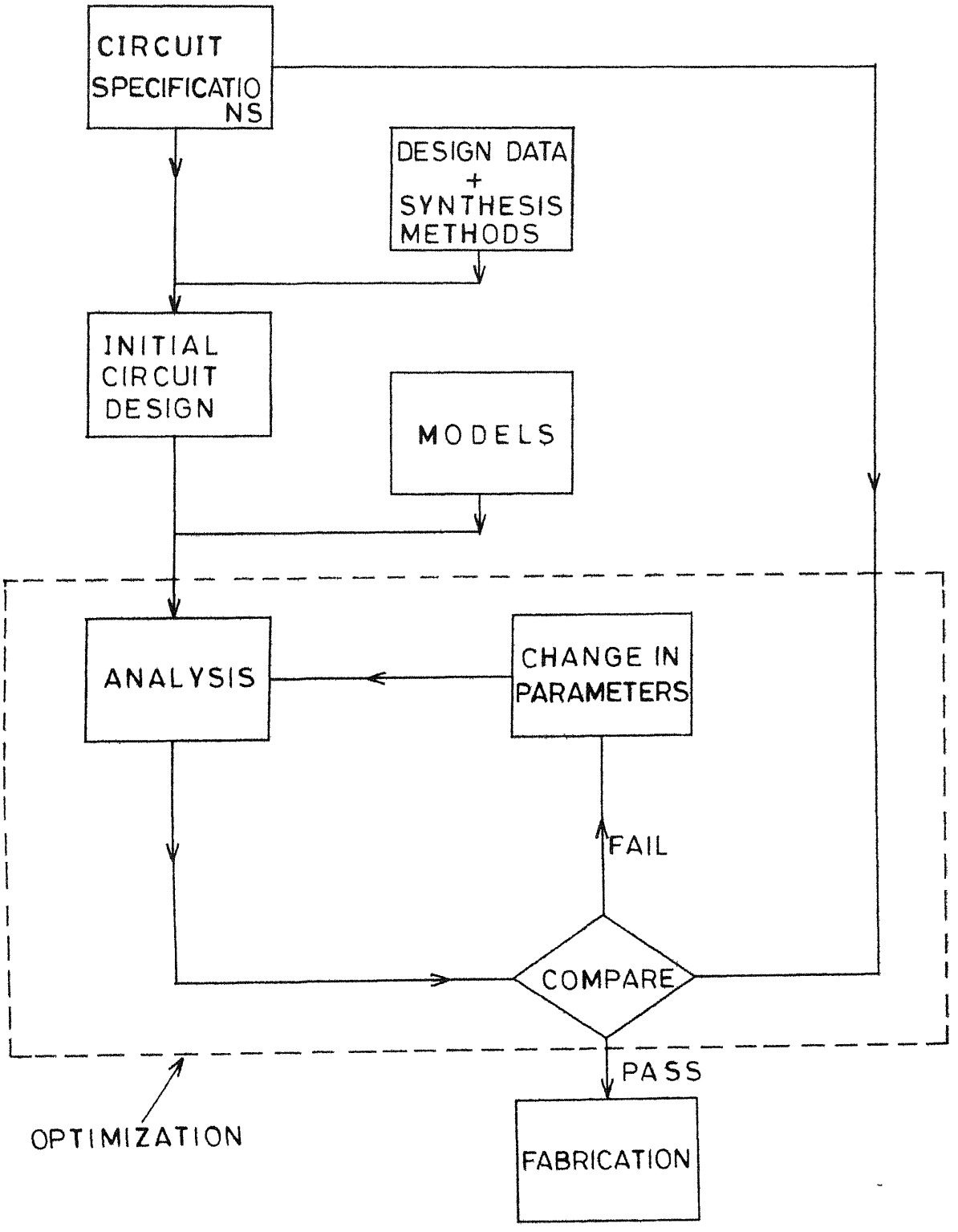


FIG. 7.3 FLOW CHART FOR OPTIMIZATION PROCEDURE

exploratory move and the other is pattern move. Exploratory moves do the local searching around the base point. Pattern direction is the probable direction for a successfull move. Each pattern move is followed by a sequence of exploratory moves which continually revise the pattern.

The strategy consists of using an exploratory search along the coordinate axes from a base point, in order to determine the direction in which minimum lies. A pattern move is then made along the direction selected by a successful exploratory move, in the hope that the previous success will be repeated. When a pattern move and subsequent exploratory moves fail, the parameter increments are reduced and the whole procedure restarted at that base point. The search terminates if the increments fall below prescribed values. An algorithm and the flow chart for this method are given in Appendix A.

7.2.2 Two-Branch Hybrid

Figure 7.9 (inset) shows a layout of the two-branch hybrid. Note that the output lines are in continuation of branches of 50 ohm impedance. This arrangement gives rise to only symmetric T-junction for which characterization is available. The equivalent circuit of the T-junction used is the one given by Hammerstad and Bekadal [39] . A method for compensating T-junction reactances in microstrip couplers is described by Vogel [47] .

The equivalent circuit of the hybrid including T-junction is similar to that shown in Fig. 7.3(b). Analysis of the hybrid is carried out by using even/odd mode symmetry and ABCD matrices.

In the present study three parameters ℓ_1, Z_2 and ℓ_2 are considered as variables(Fig. 7.9 (inset)). The impedance of the branch (main arm) Z_1 is not kept variable, otherwise the T-junction formed would become asymmetrical.

The error function chosen in this case is of the form:

$$\text{Error Function (EF)} = \frac{1}{N}\left[\sum_{f_1}^{f_f} W_1 \; |S_{11}|^2 + W_2\,(|S_{21}| - 1/\sqrt{2})^2 + W_3(|S_{31}| - 1/\sqrt{2})^2\right] \qquad (7.9)$$

where,

N is the number of frequency points, f_1 and f_f are the initial and final frequencies and W_1, W_2 and W_3 are weighting factors. S_{11}, S_{21} and S_{31} are the scattering parameters of the hybrid.

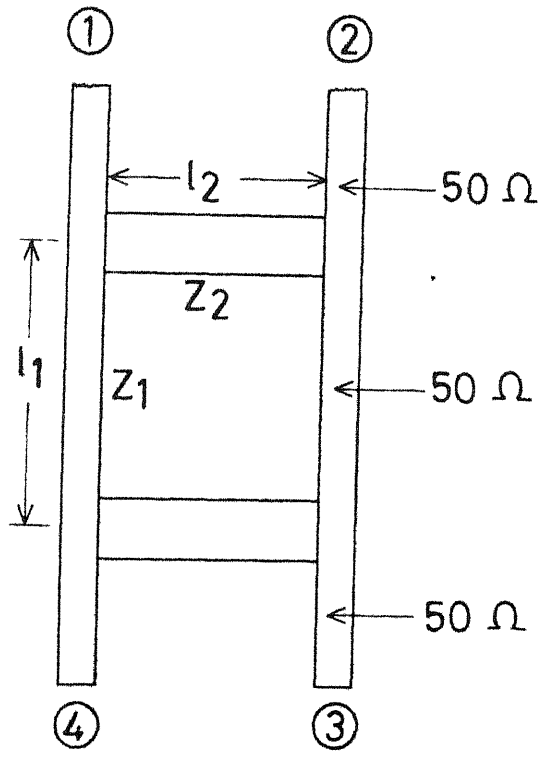
Results are presented for the hybrid on Rexolite substrate (ϵ_r = 2.53), substrate thickness h = 0.159 cm (1/16 inches). Hybrid is optimized in the frequency range of 2.0 to 2.2 GHz with the centre frequency of 2.1 GHz. Nine frequency points are chosen in this frequency range.

The weighting factors W_1, W_2 and W_3 are all assumed unity. The initial and the final parameters values are given in Table 7.1.

TABLE 7.1 Parameter values in the optimization of Two-branch hybrid.

Parameter	Initial	Final
ℓ_1	90°	92.28°
Z_2	35.35 Ω	33.4 Ω
ℓ_2	90°	96.5°

Figure 7.9 and 7.10 show the plot of hybrid performance with and without junction reactances and the optimized one. We see from these plots that the performance of the optimized circuit very well matches with the performance of the hybrid without discontinuities. It is to be noted that the VSWR and the isolation achieved from the optimized circuit (off the centre frequency) are better than those of the hybrid without T-junction reactances. These results are summarized in Table 7.2.



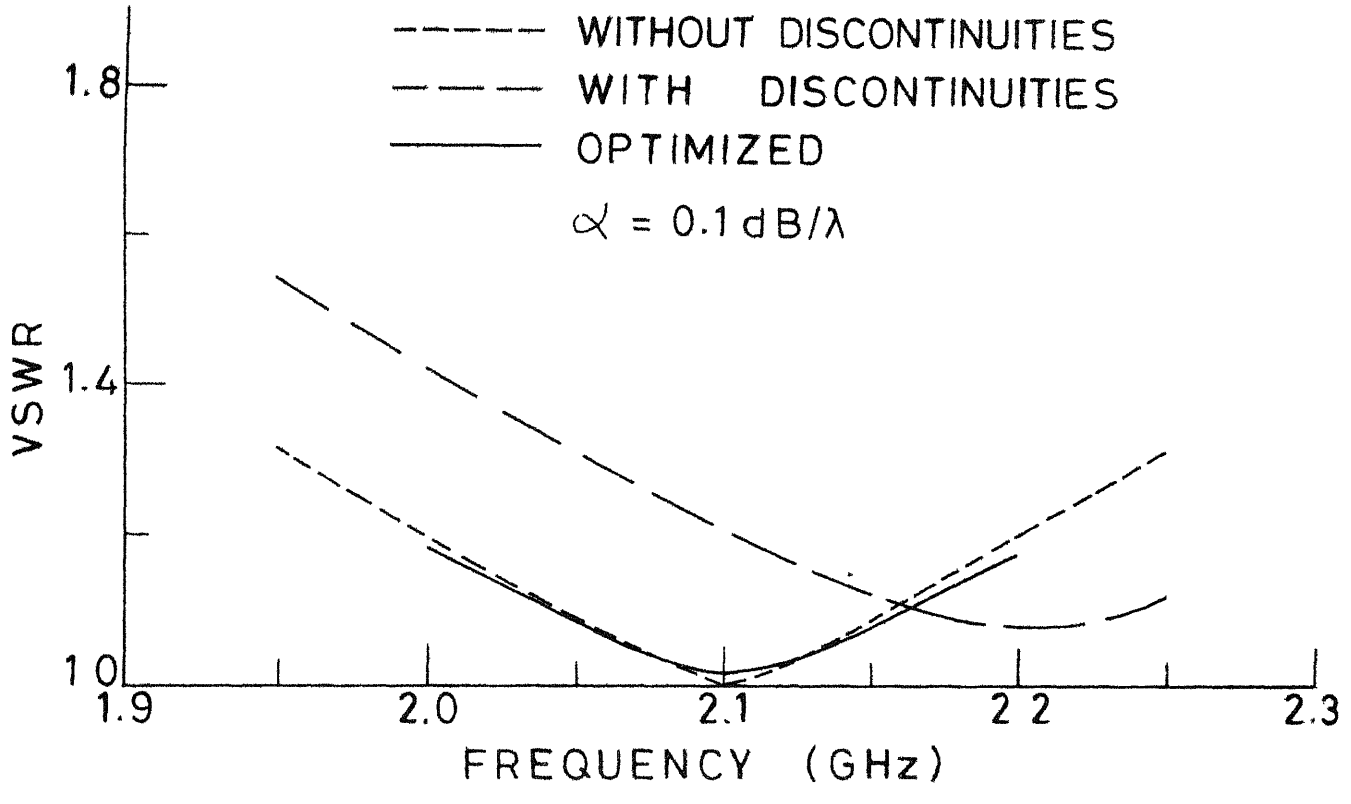


FIG. 7.9 VARIATION OF VSWR WITH FREQUENCY FOR 2.0-BRANCH HYBRID WITH AND WITHOUT DISCONTINUITIES AND OF THE OPTIMIZED CIRCUIT

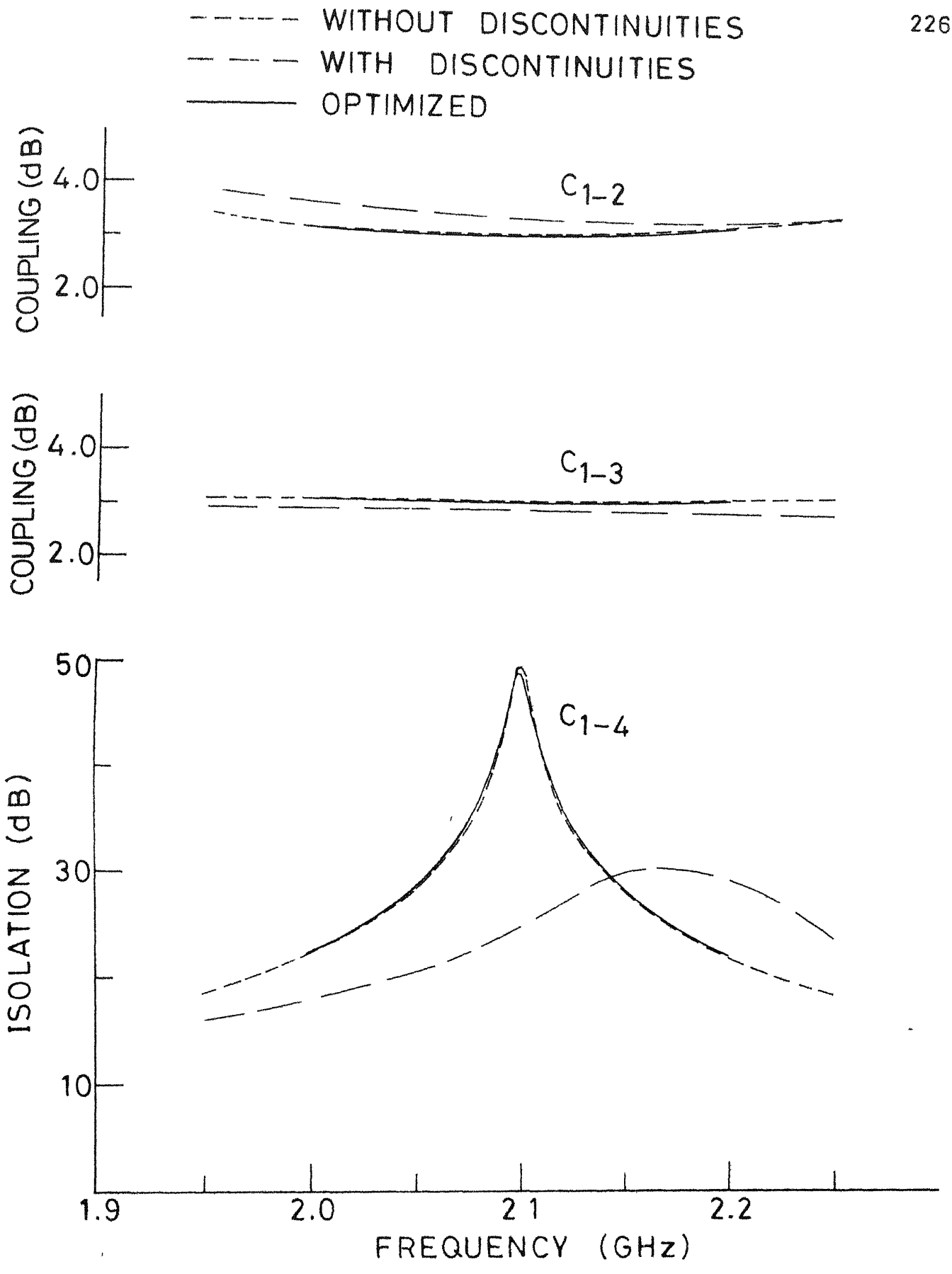


FIG. 7.10 PERFORMANCE OF TWO-BRANCH HYBRID WITH AND WITHOUT DISCONTINUITIES AND OF THE OPTIMIZED CIRCUIT.

TABLE 7.2 VSWR and Isolation for two-branch hybrids

Frequency (GHz)	VSWR			ISOLATION (dB)		
	Ideal*	With Discontinuties	Optimized	Ideal*	With Discontinuties	Optimized
2.0	1.199	1.423	1.183	21.06	15.92	21.61
2.1 (centre frequency)	1.006	1.211	1.019	50.11	20.66	48.51
2.2	1.199	1.085	1.173	21.06	25.90	22.15

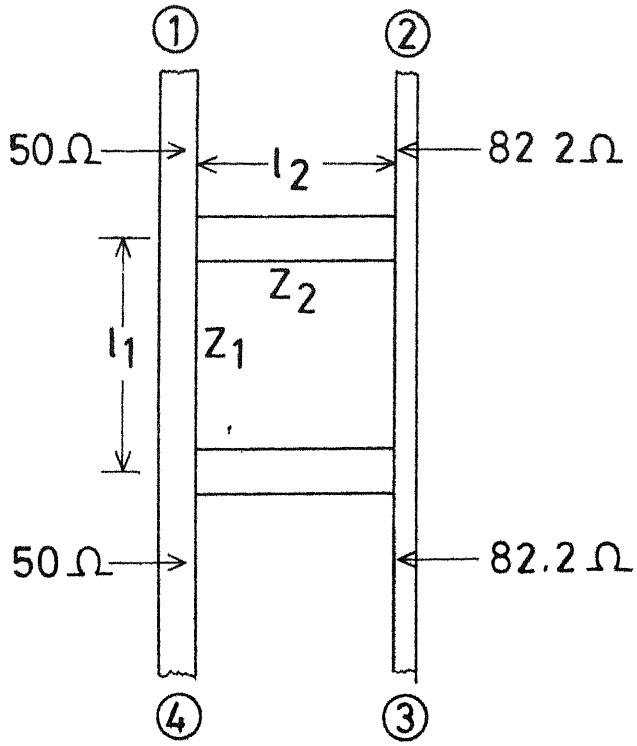
*Circuit with discontinuity reactances ignored.

7.2.3 Impedance Transforming Hybrid

Figure 7.11 (inset) shows the layout of the two-branch impedance transforming hybrid. In this case also, only symmetrical T-junctions are formed. The equivalent circuit of the hybrid including T-junction is similar to that shown in Fig. 7.6(b) but without the diodes and line length ℓ_3. Analysis is carried out by using even/odd mode symmetry and ABCD matrices.

In this case also three parameters ℓ_1, Z_2 and ℓ_2 are considered as variable (Fig. 7.11 (inset)). The error function considered in this case also is given by Eqn. (7.9).

Figures 7.11 and 7.12 show the plot of hybrid performance



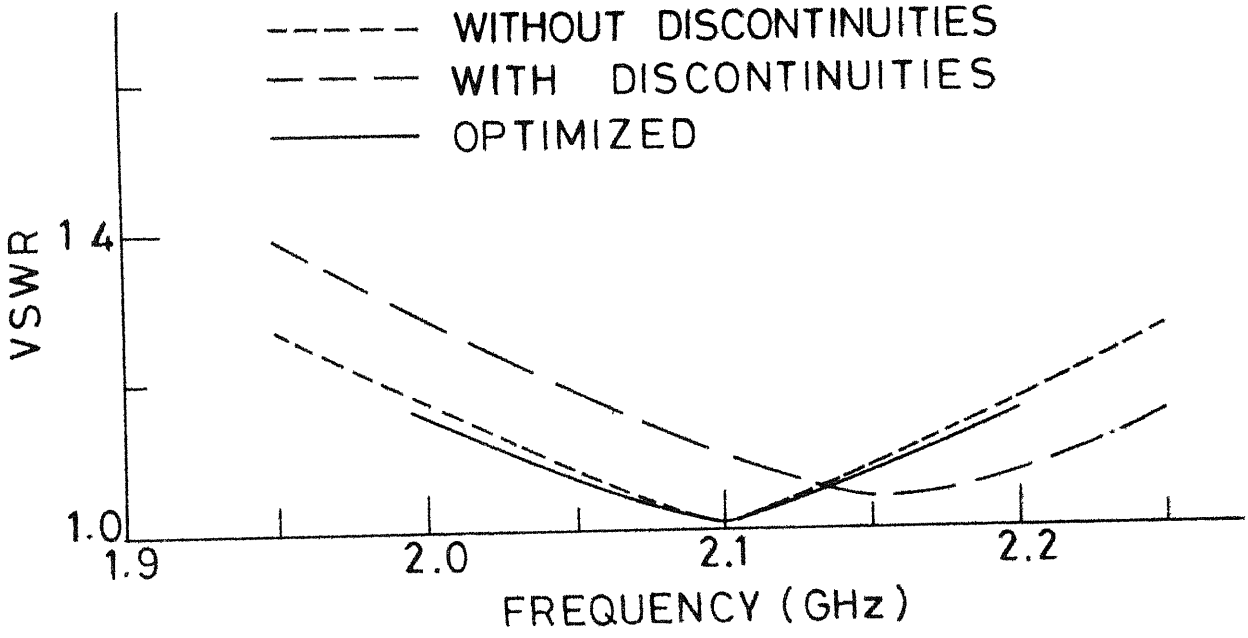


FIG. 7.11 VARIATION OF VSWR WITH FREQUENCY FOR TWO-STRANCH IMPEDANCE TRANSFORMING HYBRID WITH AND WITHOUT DISCONTINUITIES AND OF THE OPTIMIZED CIRCUIT.

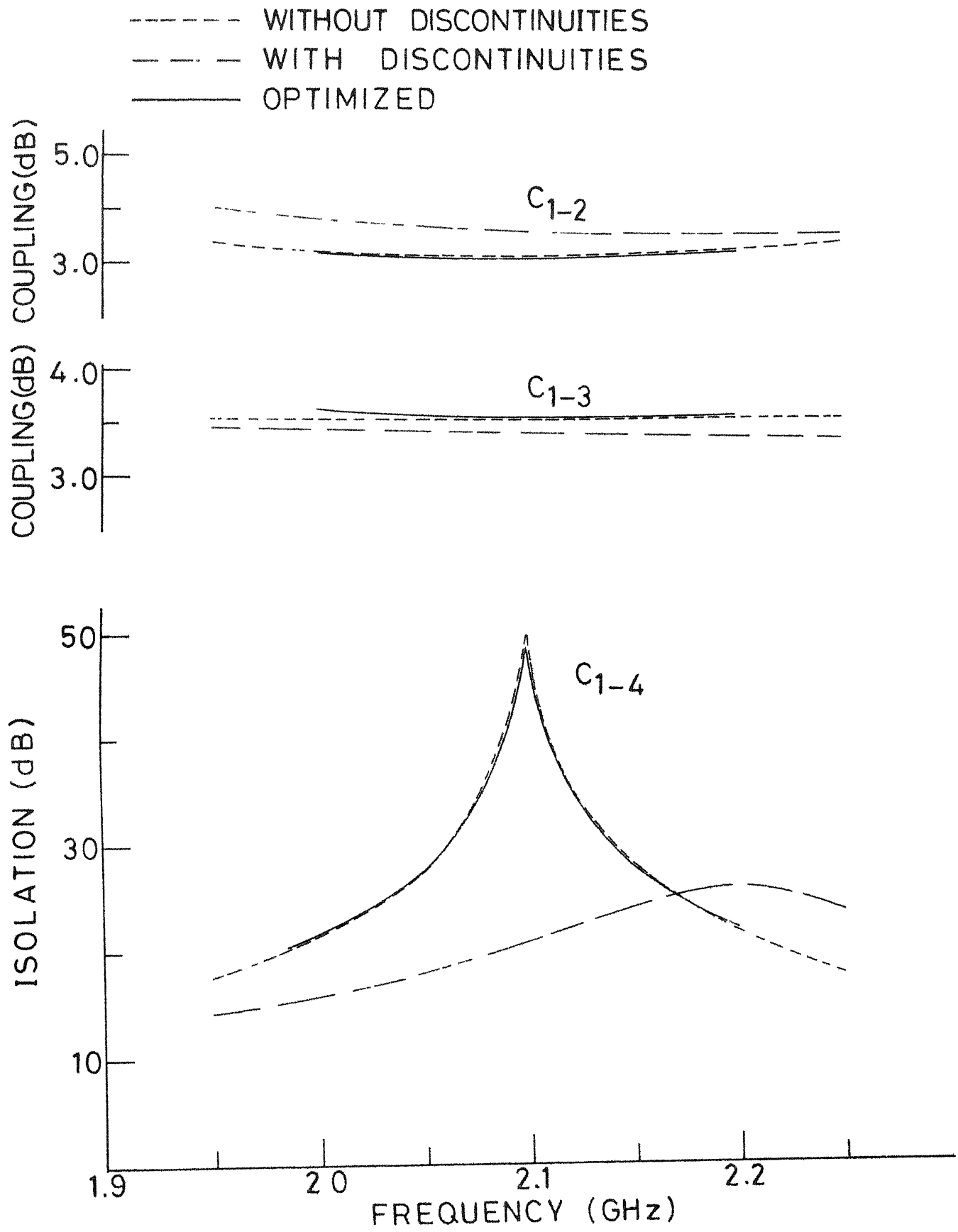


FIG. 7.1 PERFORMANCE OF TWO-BRANCH IMPEDANCE TRANSFORMING HYBRID WITH AND WITHOUT DISCONTINUITIES AND OF THE OPTIMIZED CIRCUIT.

with and without discontinuity reactances along with the optimized results. In this case also, a rexolite substrate with ε_r = 2.53 and height h= 0.159 cm is considered. The hybrid is optimized in the frequency range of 2.0 to 2.2 GHz. Plots in Figs. 7.11 and 7.12 show that the performance of the optimized hybrid is better than the performance of the ideal hybrid (i.e. without junction reactances). Performances of the hybrid before and after optimization are summarized in Table 7.3. Values for ideal hybrid without discontinuities are also indicated. The process of optimization does more than

TABLE 7.3 VSWR and Isolation for two-branch impedance transforming hybrids (50 Ω to 82.2 Ω)

Frequency (GHz)	VSWR			ISOLATION (dB)		
	Ideal	With Discon-tinuities	Optimi-zed	Ideal	With Discon-tinuities	Optimi-zed
2.0	1.172	1.288	1.166	21.89	18.03	22.16
2.1	1.006	1.110	1.007	49.51	24.78	48.02
2.2	1.172	1.082	1.155	21.89	29.42	22.68

compensating for junction reactances. Table 7.4 gives the initial and final parameter values for impedance transforming two-branch hybrid.

TABLE 7.4 Parameter values in the optimization of two-branch impedance transforming hybrid (50 Ω to 82.2 Ω)

Parameter	Initial	Final
ℓ_1	90°	80.18°
Z_2	45.33 Ω	43.76 Ω
ℓ_2	90°	94.8°

7.3 OPTIMIZATION OF PHASE SHIFTER CIRCUITS

As pointed out in Section 7.1, the effect of junction reactances on phase shifter performance is significant. 180° phase bit using two-branch hybrid and single stub type transforming network is found to have differential phase of 190°, while 90° bit using two-branch impedance transforming hybrid has differential phase of 86° at 2.1 GHz. Compensation of hybrid discontinuities by the process of optimization has been discussed in Section 7.2. When the optimized hybrid and the transforming network designed at the centre frequency are put together to make the phase shifter, the performance of the phase shifter still deviates from the desired one due to junction reactances in the transforming network. Once these junction reactances are compensated for, desired phase shift is obtained at the centre frequency. Performance of the phase shifter at frequencies away from the centre frequency, would depend upon the type of hybrid

and phase shift network used. By optimizing the parameters of the phase shift network broader bandwidth of the phase shifter can be achieved. It has been observed that instead of optimizing phase shift network alone, if both hybrid and phase shift network parameters are made variable and the total phase shifter circuit is optimized, a better optimum performance is achieved. Both 180° and 90° bits described in Section 7.1 have been optimized in this manner.

Not many previous reports on CAD of PIN diode phase shifters are available. Only one reference [48] , that has been spotted by this author, gives brief results for optimization of a 3-bit phase shifter using 180° and 90° reflection type bits which consists of two-branch hybrids and single stub type of transforming networks.

7.3.1 180° Phase Bit Using Two-Branch Impedance Transforming Hybrid and Stub Type Network

Figure 7.3(a) shows the layout of this phase bit. Optimization of the phase bit is carried out in two steps. First hybrid is optimized with respect to parameters ℓ_1, Z_2 and ℓ_2 (Fig. 7.9),and then whole phase shifter circuit is optimized with additional parameters ℓ_3, ℓ_4 , ℓ_5 and Z_5 (Fig. 7.3(a)). Optimized hybrid parameters are used as the starting point for phase shifter optimization.

The error function chosen in this case is of the form

$$EF = \frac{1}{N}\left[\sum_{f_1}^{f_f} K_1\,(\Delta\phi - \Delta\phi_o)^2 + K_2(|S_{11F}| - |S_{11o}|)^2 + K_3\,(|S_{11R}| - |S_{11o}|)^2 + K_4(|S_{11F}| - |S_{11R}|)^2 + K_5\,(|S_{41F}| - |S_{41o}|)^2 + K_6(|S_{41R}| - |S_{41o}|)^2\right] \tag{7.10}$$

where,

$|S_{11o}| = 0.0$ and $|S_{41o}| = 1.0$.

Subscripts F and R represent the forward and the reverse bias states, respectively, of the diode. $K_1, K_2, \ldots K_6$ are the weighting factors.

Results are presented for the phase bit (180° bit) using rexolite substrate ($\epsilon_r = 2.53$) of height, h = 0.159 cm. It is optimized in the frequency range of 2.05 to 2.15 GHz (approximately 5% bandwidth, which is expected from this circuit as discussed in Chapter 5). Eleven frequency points have been taken for evaluating error function given in Eqn. (7.10). The numerical value of $\Delta\phi$ is 180° and the values of other scattering parameters are less than unity. The weighting coefficient K_1 is taken as unity while all other have a value of 1000. This would try to limit phase error to about $\pm$ 3° when S parameters are within 0.1 of the nomial values. Equal emphasis is given to reflection and transmission coefficients and also to the equalization of these coefficients in two bias states. The initial and final parameter values in an

optimization run are given in Table 7.5.

TABLE 7.5 Parameter values in the optimization 180° phase bit.

Parameter	Initial	Final
ℓ_1	92.28°	90.15°
Z_2	33.4 Ω	33.4 Ω
ℓ_2	96.5°	98.25°
ℓ_3	45°	50.87°
ℓ_4	53.58°	58.01°
ℓ_5	27.42°	24.92°
Z_5	50.0 Ω	51.75 Ω

Figure 7.13 shows the plot of phase shifter performance for the two cases. The dotted curves are for the case when optimized hybrid and unoptimized phase shift network are used. The continuous curves are when both hybrid and phase shift networks are optimized. Line losses are considered negligible for these calculations. We observe that the phase variation has been reduced by optimization (Fig. 7.13). Optimized bit gives equal VSWR in the two states. Loss is not equal in the two diode states (F.B. and R.B.), but the values come closer to each other in the optimized circuit. Table 7.6 summarizes the performance of the phase bit with optimized hybrid, and with optimized phase shifter.

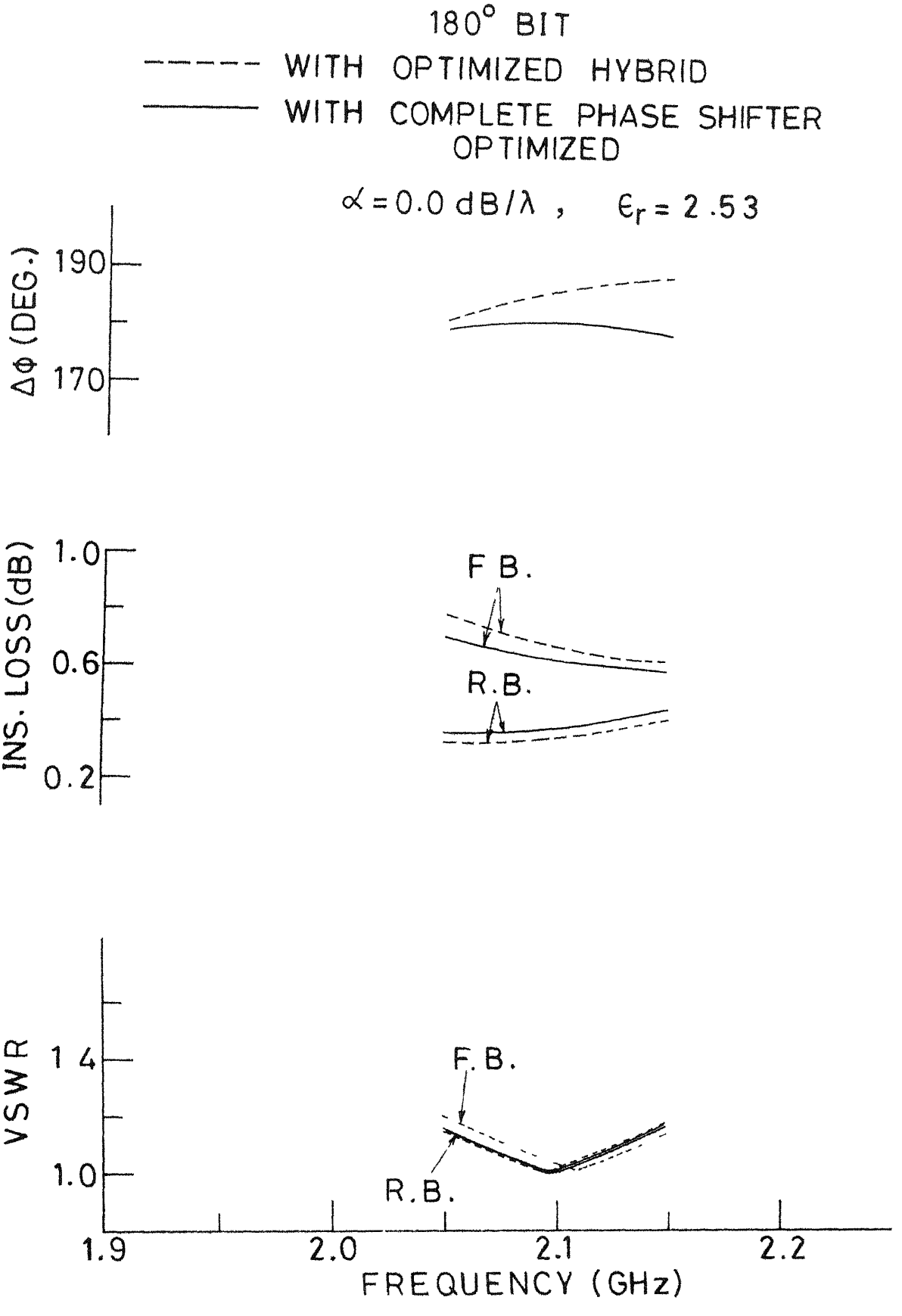


FIG. 7.13 PERFORMANCE OF 180° BIAS BIT WITH OPTIMIZED HYBRID ALONE AND WITH COMPLETE PHASE SHIFTER OPTIMIZED.

TABLE 7.6 Performance of 180° bits with only hybrid, optimized and with complete phase bit optimized.

Frequency (GHz)	VSWR				PHASE ERROR (DEG.)	
	Optimized Hybrid		Optimized phase bit		Optimized Hybrid	Optimized phase bit
	F.B.	R.B.	F.B.	R.B.		
2.05	1.207	1.148	1.163	1.165	+0.81	-0.60
2.10	1.029	1.008	1.006	1.007	+6.15	+0.72
2.15	1.145	1.172	1.160	1.158	+8.46	-1.3

7.3.2 90° Phase Bit Using Two-Branch Impedance Transforming Hybrid with Length of Line

Figure 7.6(a) shows the layout of this phase bit. As for the case of 180° bit, in this case also hybrid is optimized first and then the total phase shifter with additional parameter ℓ_3 is considered. Optimized hybrid parameters are used as the starting point for optimization of the total circuit.

The error function chosen in this case is similar to Eqn. (7.10). The weighting factor K_1 has a value of 0.5 as compared to unity for 180° bit while others are same. This bit is optimized in the frequency range of 2.03 to 2.17 GHz (approximately 7% BW, expected from this phase bit as discussed in Chapter 5). Fifteen frequency points were chosen for the evaluation of the error function. Table 7.7 gives initial and final parameter values in an optimization run.

Figure 7.14 shows the plot of phase shifter performance. The dotted curves are for the case when the optimized hybrid and unoptimized phase shift networks are used. The continuous curves are for the case when complete phase shifter is optimized. We observe that there is not much difference between the optimized and unoptimized performance. The reason being, the transforming network used in this case is a single line and

TABLE 7.7 Parameter values for 90° phase bit

Parameters	Initial	Final
ℓ_1	90.18°	93.54°
Z_2	43.76 Ω	44.22 Ω
ℓ_2	94.8°	91.87°
ℓ_3	17.0°	22.48°

does not have any other discontinuities. Table 7.8 summarizes the performance of this phase bit with optimized hybrid and with complete phase bit optimized.

7.4 EXPERIMENTS USING OPTIMIZED DESIGN

In order to verify the improvement in the circuit performance resulting from the optimization, experiments have been carried out on two phase shifter circuits. 180° and 90° phase bits using microstrip transmission lines have been

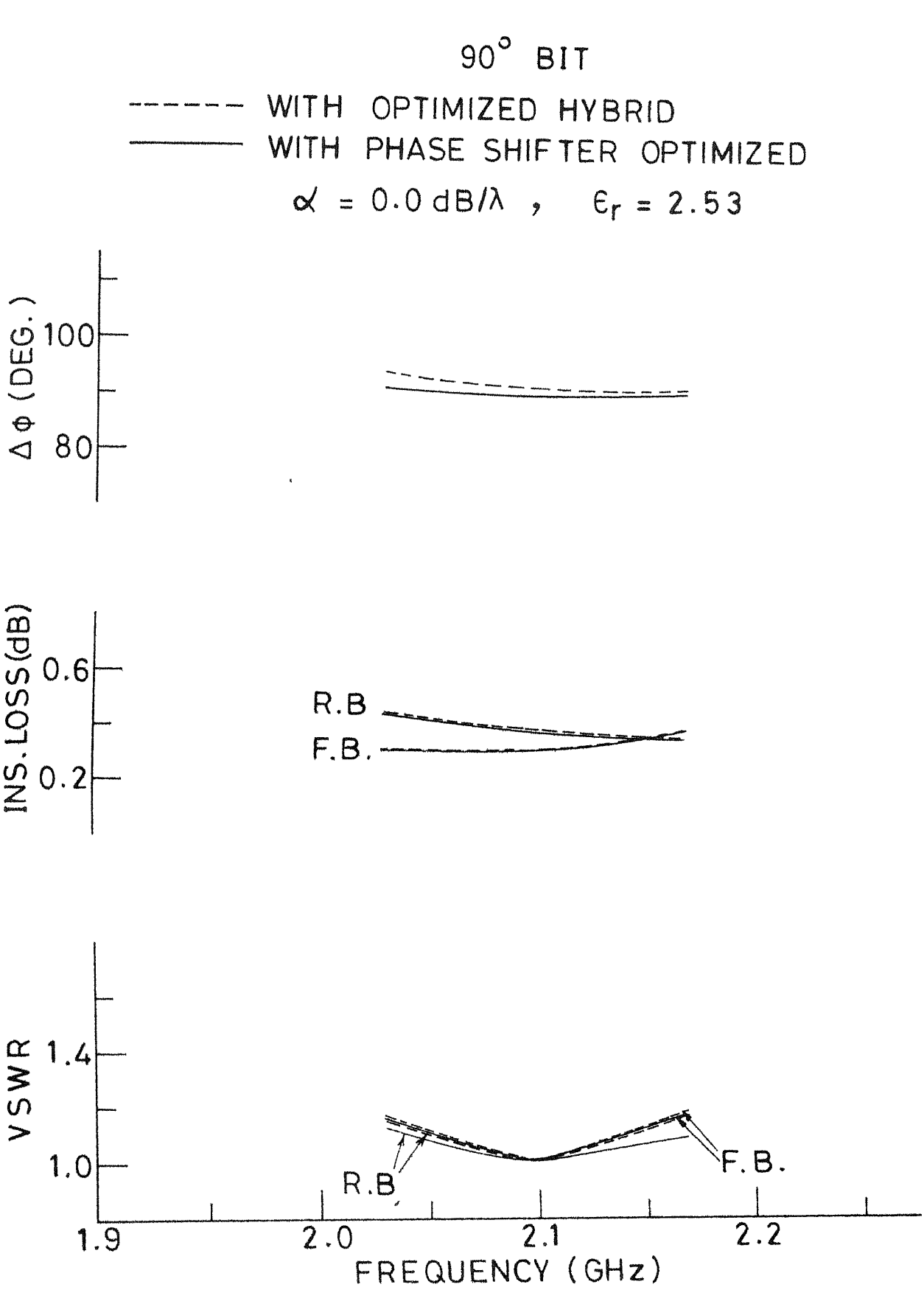


FIG. 7.14 PERFORMANCE OF 90° [illegible] BIT WITH OPTIMIZED HYBRID AND WITH [illegible] PHASE SHIFTER OPTIMIZED.

TABLE 7.8 Performance of 90° bits with only hybrid optimized and with complete phase bit optimized.

Frequency (GHz)	VSWR				PHASE ERROR (DEG.)	
	Optimized hybrid		Optimized phase bit		Optimized hybrid	Optimized phase bit
	F.B.	R.B.	F.B.	R.B.		
2.05	1.113	1.115	1.115	1.089	+2.68	0.19
2.10	1.005	1.003	1.000	1.003	+0.77	-0.76
2.15	1.117	1.083	1.127	1.070	+0.03	-0.57

fabricated on Rexolite substrate (ε_r = 2.53) of height 0.159 cm (1/16 inch). Hewlet Packard PIN diodes (HP 3041) in stripline package are used. Diodes are characterized by measuring their impedances in the forward and reverse bias states using Network analyzer (HP 8410). Diode is mounted at the end of the microstrip line and is biased through a bias network HW-30N (Microlab/FXR). Forward bias of 20 mA and reverse bias of zero volt is applied. By measuring return loss and phase, diode impedance can be calculated. Considering the equivalent circuits of the diode in the two states as shown in Fig. 7.4, diode parameters can be evaluated. These measured values for diode parameters at 2.1 GHz are given in Figure 7.4.

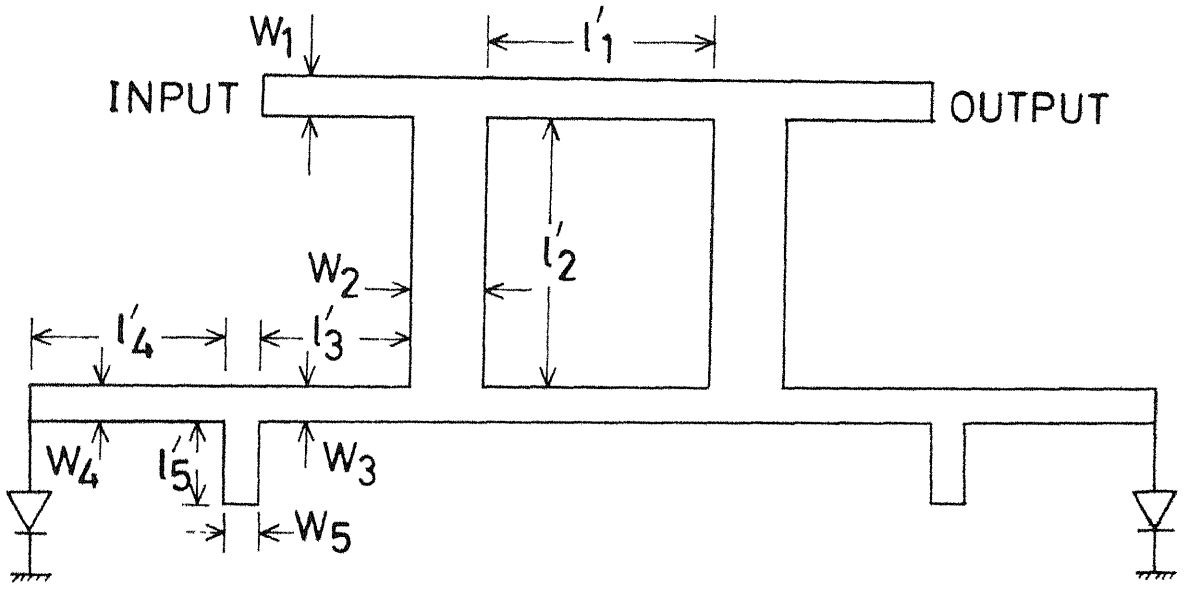
7.4.1 180° Phase Bit

The optimized results for this phase bit are shown in Figure 7.13 and the corresponding parameter values are given in Table 7.5. These results are for zero line loss (α=0.0 dB/λ). Figure 7.15 shows the layout for this phase bit along with various dimensions listed. Circuit with these dimensions was fabricated and its performance measured using the Network Analyzer (HP 8410).

Figure 7.16 shows the plot of experimental and theoretical performance of this phase bit. We observe from these plots that the experimental results are shifted towards lower frequency side. One of the possible reasons for this shift could be the tolerance in the dielectric constant of the substrate. It has been found that the theoretical and the experimental results agree well if ε_r is taken to be 2.7 instead of 2.53 (Fig. 7.17). This value is within the specified tolerance (2.53$\pm$0.2) of the dielectric constant [43]. Figure 7.18 is the photograph of this phase bit.

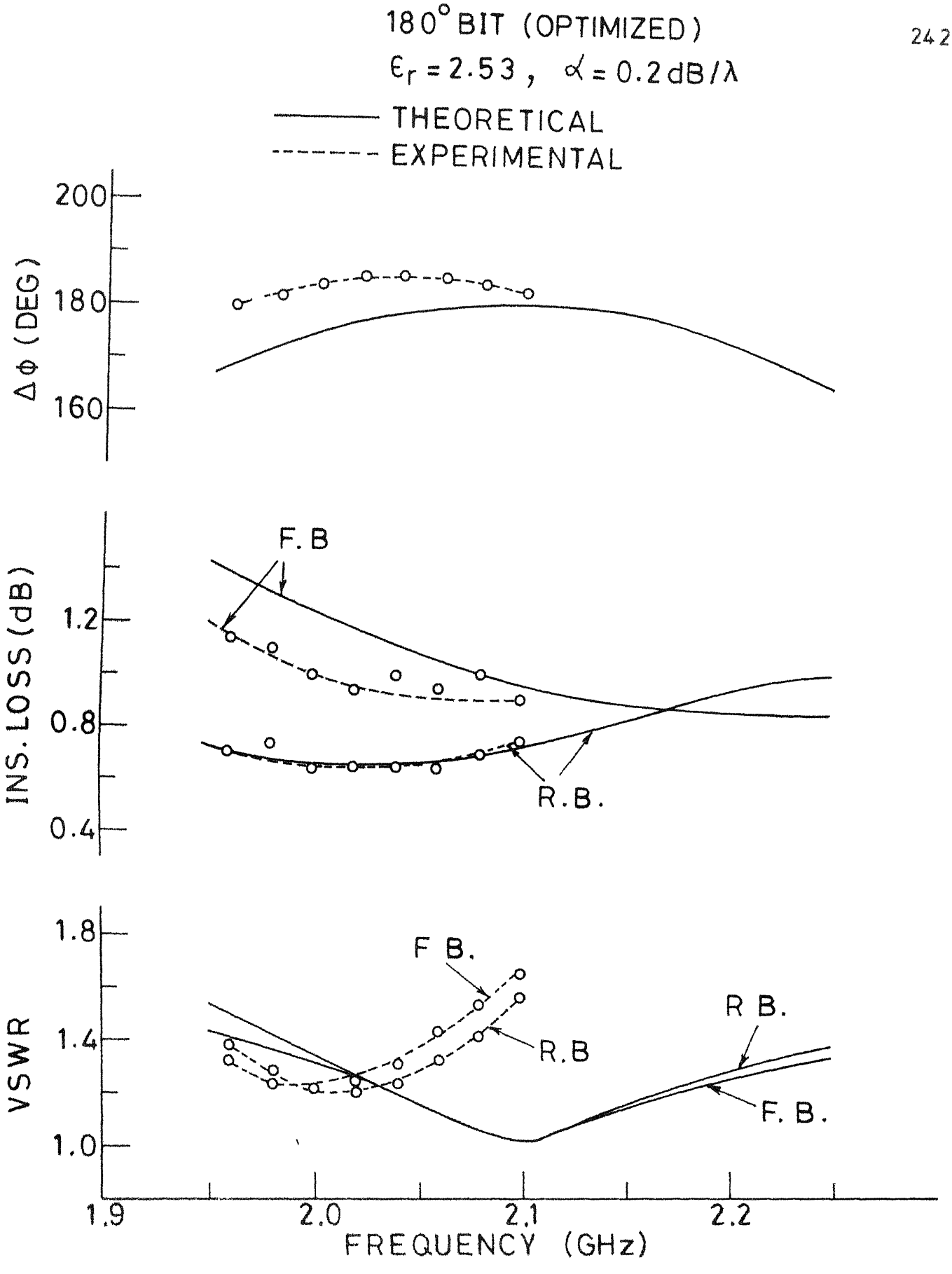
7.4.2 90° Phase Bit

Figure 7.14 shows the optimized results for this phase bit and the corresponding parameter values are given in Table 7.4. Figure 7.19 shows the layout and the



PARAMETERS	DIMENSIONS (cm)
W_1	0 445
W_2	0.790
W_3	0.445
W_4	0.445
W_5	0 422
l'_1	1.659
l'_2	2 624
l'_3	0.767
l'_4	1.356
l'_5	0.678

Fig. 7.15 LAYOUT FOR 1.8 GHz OPTIMIZED BIAS-TEE ALONG WITH VARIOUS DIMENSIONS



[illegible] THEORETICAL & EXPERIMENTAL PERFORMANCE
[illegible] BIT

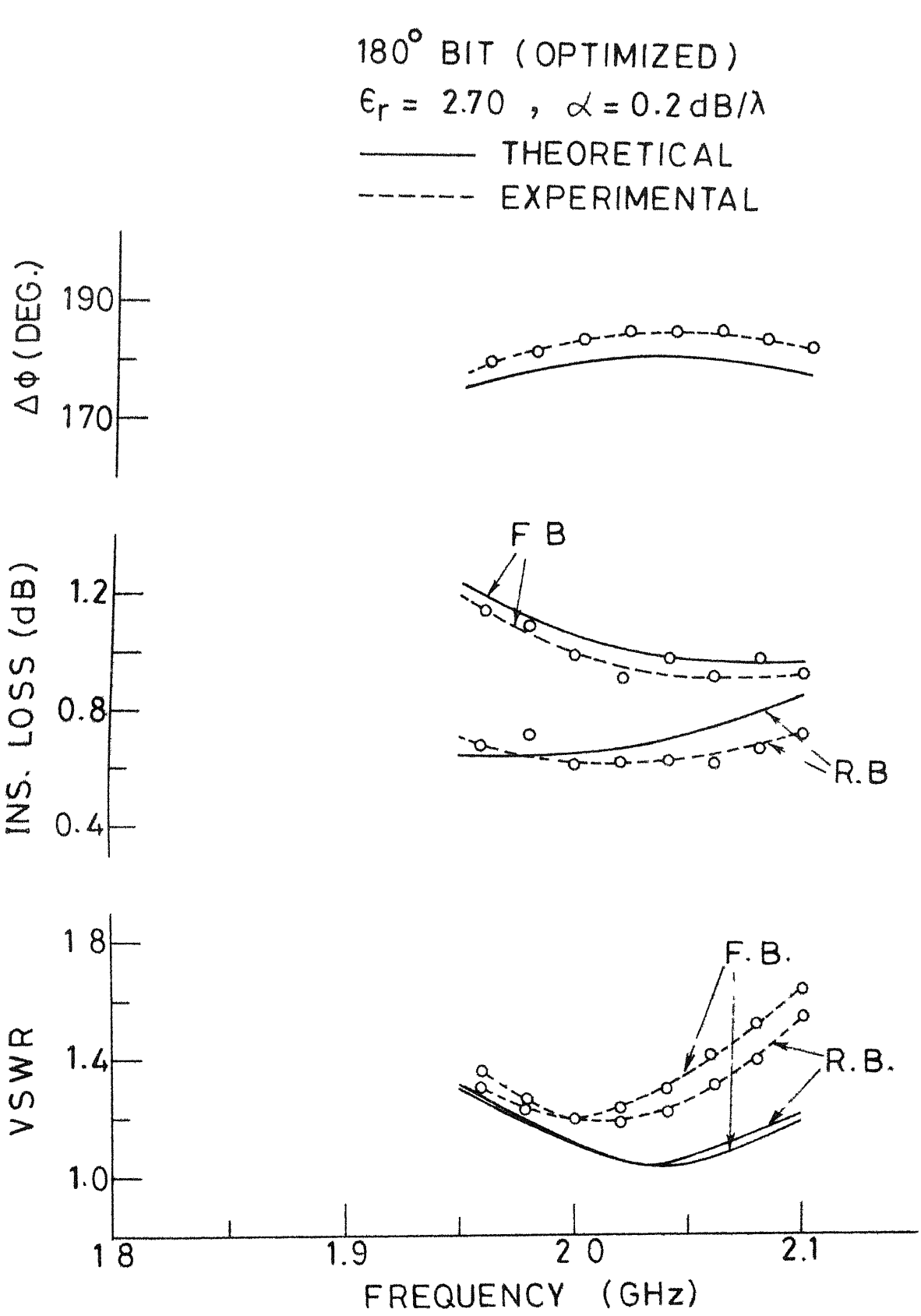
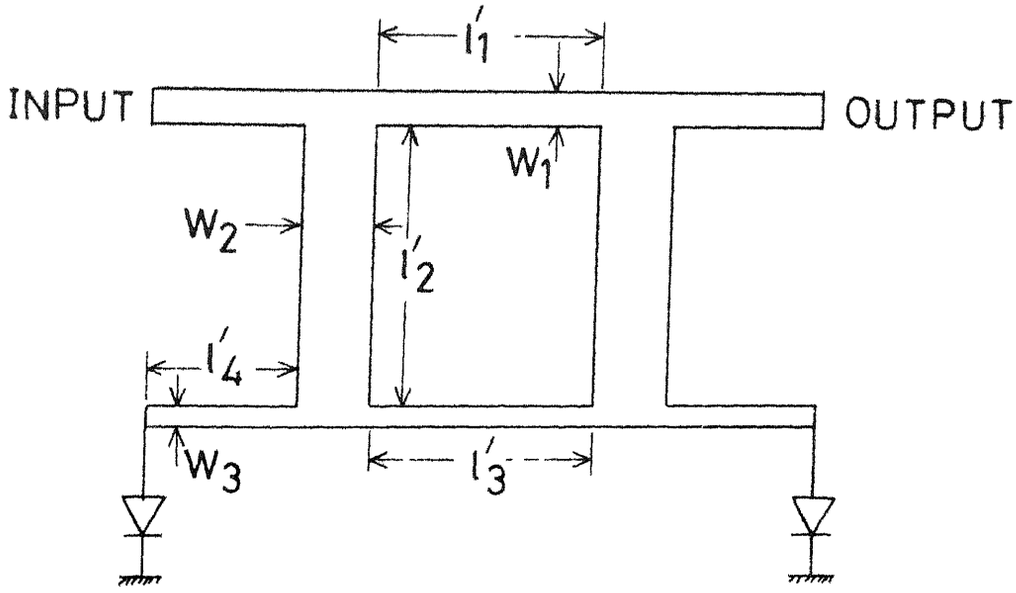


FIG. 7.17 PLOT OF EXPERIMENTAL AND THEORETICAL PERFORMANCE FOR OPTIMIZED 180° 3-BIT LIT

FIG. 7.18 PHOTOGRAPH OF OPTIMIZED 180° PHASE BIT.



PARAMETERS	DIMENSIONS (cm)
W_1	0.445
W_2	0.535
W_3	0.354
l'_1	2.008
l'_2	2.489
l'_3	2 027
l'_4	0 346

FIG. 7.19 LAYOUT FOR 90° OPTIMIZED PHASE SHIFT ALONG WITH VARIOUS DIMENSIONS.

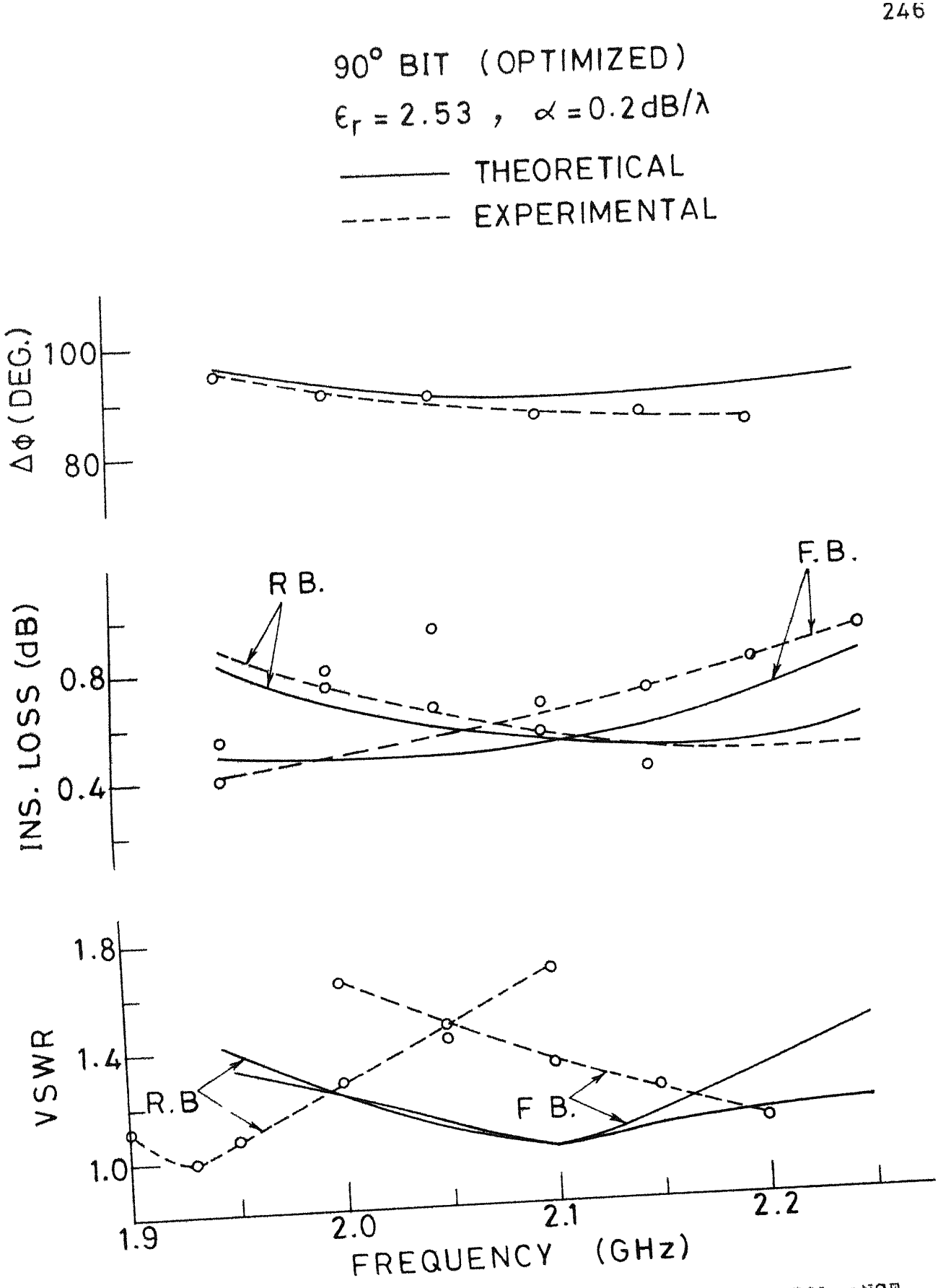


Fig. 7.20 [illegible] AND THEORETICAL PERFORMANCE [illegible]

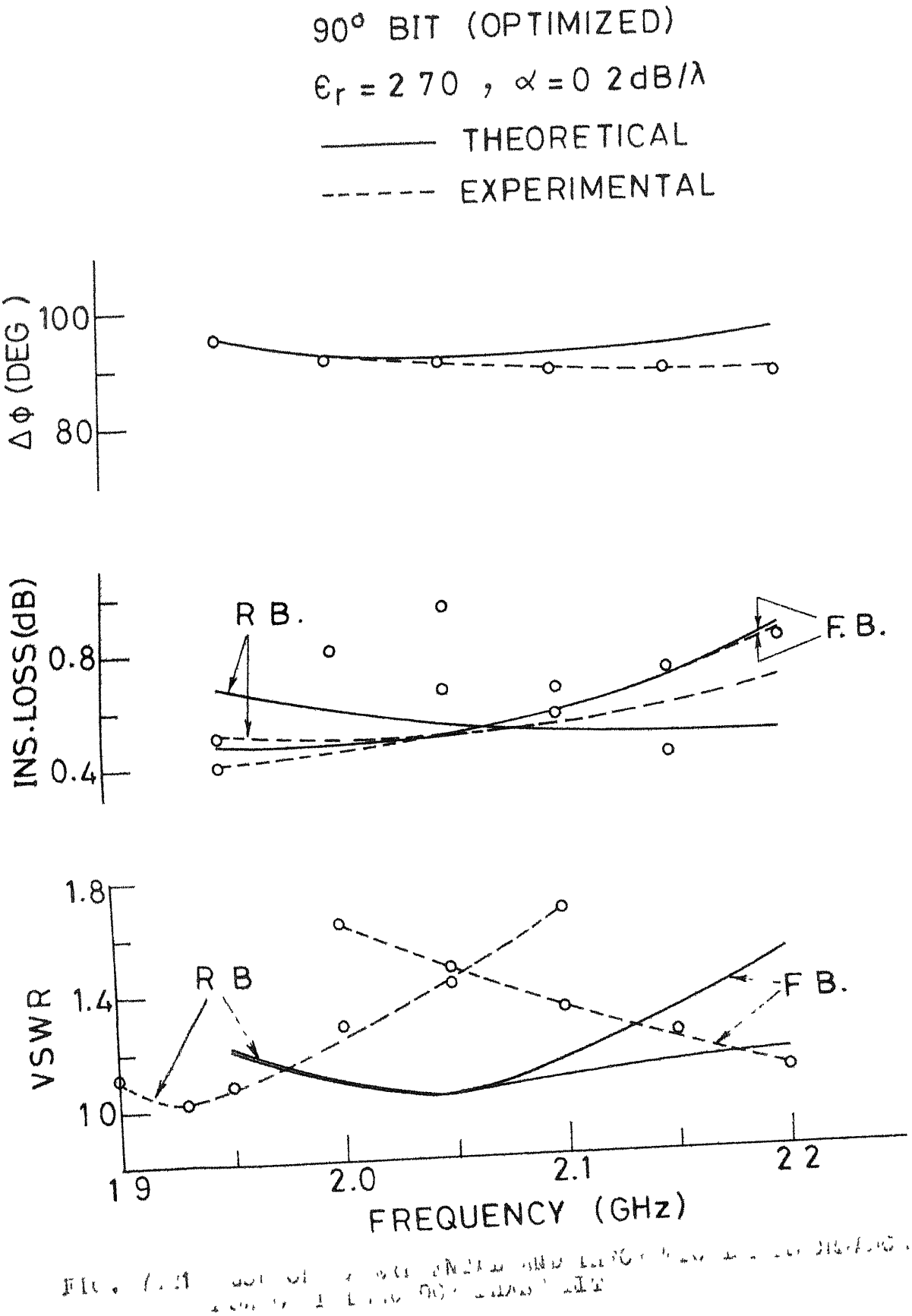

90° BIT (OPTIMIZED)
$\epsilon_r = 2.70$, $\alpha = 0.2$ dB/λ
THEORETICAL
EXPERIMENTAL
Δφ (DEG)
100
80
INS. LOSS (dB)
0.8
0.4
R B.
F. B.
VSWR
1.8
1.4
1.0
R B
F B.
1.9
2.0
2.1
2.2
FREQUENCY (GHz)

FIG. 7.22 PHOTOGRAPH OF OPTIMIZED 90° PHASE BIT.

physical dimensions for this phase bit. Performance of the fabricated circuit was measured using Network Analyzer.

Figure 7.20 shows the plot of experimental and theoretical results for $\varepsilon_r = 2.53$. In this case also the experimental results agree with the theoretical results when ε_r value is taken as 2.7 (Fig. 7.21). Both these circuits (180° and 90° bits) were fabricated from the same sheet of the substrate. Figure 7.22 is the photograph of this phase bit.

CHAPTER 8

CONCLUSION

8.1 SUMMARY OF RESULTS 251

8.2 SUGGESTIONS FOR FURTHER WORK 255

CHAPTER 8

CONCLUSION

8.1 SUMMARY OF RESULTS

Investigations reported in this thesis are related to the design and performance of reflection-type hybrid coupled PIN diode phase shifters. These phase shifter circuits consist of three main sub-circuits namely (i) the hybrid, (ii) two transforming networks connected to the two coupled ports of the hybrid and (iii) two PIN diodes connected at the far ends of the two transforming networks. The effect of each of these components on the phase shifter performance has been studied.

The effect of hybrid parameters on the performance of reflection-type phase shifters is found to be significant. The most important hybrid parameter is directivity (and hence input VSWR). It is found that a directivity of 20 dB in a 90° hybrid can cause, in the worst case, an input VSWR of the phase shifter to be 1.56, an insertion loss of 0.215 dB and a phase error as high as ± 22.8°. 1.0 dB inequality in the amplitudes of signals at the coupled port of the hybrid can increase input VSWR of the phase shifter to 1.26. Phase error (ϕ_e) of the phase shifter is independent of the amplitude coupling. Phase error of 10° in the coupled signals of the hybrid can give rise to an input VSWR of 1.42.

The study of the effect of variations in diode parameters on phase shifter performance is useful in specifying the tolerances in diode parameters for given performance characteristics. Sensitivities of differential phase shift ($\Delta\phi$) with respect to diode reactances for 180° and 90° phase bits have been evaluated for the three types of transforming networks. It is observed that the 90° phase bit is most sensitive to reverse bias reactance (X_R) of the diode. For 180° phase bit using quarter wave transforming network or impedance transforming hybrid, sensitivities with respect to X_F and X_R are equal in magnitude. As an example, for a 180° phase bit with a diode having $X_R/X_F = -60$, the sensitivity of $\Delta\phi$ with X_R is -0.08 and the corresponding value of the sensitivity of $\Delta\phi$ with X_R for 90° bit is 0.64. Hence tighter tolerances in diode capacitances are needed for a 90° bit than for a 180° bit. The effect of diode resistances on the phase shifter performance has been studied quantitatively. It is observed that the effect of diode resistances R_F and R_R on the phase shift is small as compared to that of the reactances. Hence, the design equations, derived by ignoring diode losses, may also be used for lossy diodes.

Phase shifter performance using mismatched diodes is more sensitive to variations in the phase of reflection coefficient (Γ) of the phase shift network, than those in their magnitudes. If $\pm\delta\phi$ is the phase difference between

the two reflection coefficients ($\angle\Gamma_2 \neq \angle\Gamma_3$), then the maximum phase error (ϕ_e) of the phase bit is also $\pm \delta\phi$. The effect of differences in magnitudes of Γ's does not affect the phase error of the phase bit.

Performance of phase shifters using ideal 180° and 90° switches allows one to study phase shifter circuits independent of the PIN diode characteristics and thus enables one to investigate the limitations in performance imposed by the characteristics of the hybirds. For this study three types of moderate bandwidth hybrids and two types of broad band hybrids have been considered. Results of this study point out the need of designing the transforming networks such that the impedances seen by the hybrid in the two bias states of the diode are placed symmetrically on two sides of the X = 0 axis on the Smith chart. For 180° phase bits using two-branch and rat-race hybrids, this is achieved by inserting an interconnecting line length of $\beta L = 45°$ between the switches and the hybrid ports. This results in maximum bandwidth of the phase shifter. Corresponding line length for 90° phase bit is 22.5°. Phase bits using three-branch hybrids are found to give maximum bandwidth for $\beta L = 0°$. For circuits using ideal switches, the values of bandwidths ($\phi_e \leq \pm 2.5°$ and VSWR ≤ 1.2) for 180° bit using two-branch, three-branch and rat-race hybrids are 5%, 10.5% and 10.2%, respectively.

Design of phase shifters using nonideal diodes is essentially the design of the transforming network to achieve the desired phase shift at the centre frequency, and minimum phase error over the band of frequencies. Closed form design equations are derived for the design of three types of transforming networks namely (i) single line length (to be used with impedance transforming hybrid) (ii) quarter wave transformer and (iii) a single stub.

Performances of phase shifters using three types of transforming networks with two-branch, three-branch and rat-race hybrids are evaluated. Bandwidths for various designs have been computed for two specifications of bandwidth and for wide range of diode reactances. Insertion loss for the above designs have also been calculated. It is observed that in most of the cases, wide bandwidth is obtained when X_F is large and X_R is small i.e. for 'high L-C' diodes. Circuits using two-branch impedance transforming hybrid give lowest loss as compared to other circuits considered. This is probably due to shorter line lengths required in this case. The size of this circuit is also minimum because of the same reason.

There is a significant effect of microstrip discontinuity reactances on the phase shifter performance. A 180° phase bit using two-branch hybrid and single stub type of transforming network on rexolite substrate (ε_r = 2.53 and

and h = 0.0625") gives a differential phase shift of 190° instead of 180°. Compensation of these discontinuities (mainly contributed by T-junctions) is carried out by an optimization process. First, the hybrid is compensated for its discontinuities, then the whole phase shifter circuit is optimized for discontinuities in both the transforming network and the hybrid. It is observed that the optimized phase shifter gives slightly wider bandwidth than an ideal circuit without discontinuities. Both 180° and 90° phase bits (using optimized design) have been fabricated in microstrip configuration on Rexolite substrate (ε_r = 2.53). Diodes used were characterized experimentally. The theoretical and experimental results are found to agree within the specified tolerance of the dielectric constant of the substrate.

8.2 SUGGESTIONS FOR FURTHER WORK

Studies contained in this thesis deal mainly with the digital phase shifters with moderate and constant phase bandwidth (less than 20%). Thus, the transforming networks of wide band type such as a double stub, a two-section quarter-wave transformer etc. have not been considered. Other networks of the type described in reference [49], namely, a single line length and a $\lambda/4 - \lambda/8$ transformer need be studied for bandwidth, insertion loss and size comparisons. Power handling capabilities of these types of circuits have

not been reported in literature. A comparitive study for various designs mentioned above would be desirable.

The effect of 90°-hybrid parameters on phase shifter performance have been studied in this thesis. Similar results for 180°-hybrids (such as rat-race hybrid) are not available and need be worked out.

It has been observed that impedance transforming two-branch hybrid coupled phase shifter gives wider bandwidth, low insertion loss and minimum size. Similar studies for three-branch impedance transforming hybrids and parallel-coupled impedance transforming hybrids would be worthwhile.

APPENDIX A

HOOK AND JEEVES ALGORITHM

This algorithm finds minimum of a multivariable unconstrained, nonlinear function: $F(X_1, X_2, \ldots X_N)$. This method assumes unimodal function (i.e. only one minimum in the region considered). If more than one minimum exists, several sets of starting values are recommended to get best minimum. The algorithm proceeds as follows:

(1) A base point is chosen and the objective function evaluated.

(2) Local searches (exploratory moves) are made in each direction by changing the variable X_i a distance S_i to each side and evaluating the objective function to see if a lower function value is obtained.

(3) If there is no function descdecrease the step size is reduced and the searches are made from the previous best point.

(4) If the value of the objective function has decreased a 'temporary head', $X_{1,o}^{(k+1)}$ is located using the two previous base points $X_i^{(k+1)}$ and $X_1^{(k)}$

$$X_{1,o}^{(k+1)} = X_1^{(k+1)} + \alpha[X_1^{(k+1)} - X_1^{(k)}]$$

where,

i is the variable index = 1,2,3,...N

o denotes temporary head

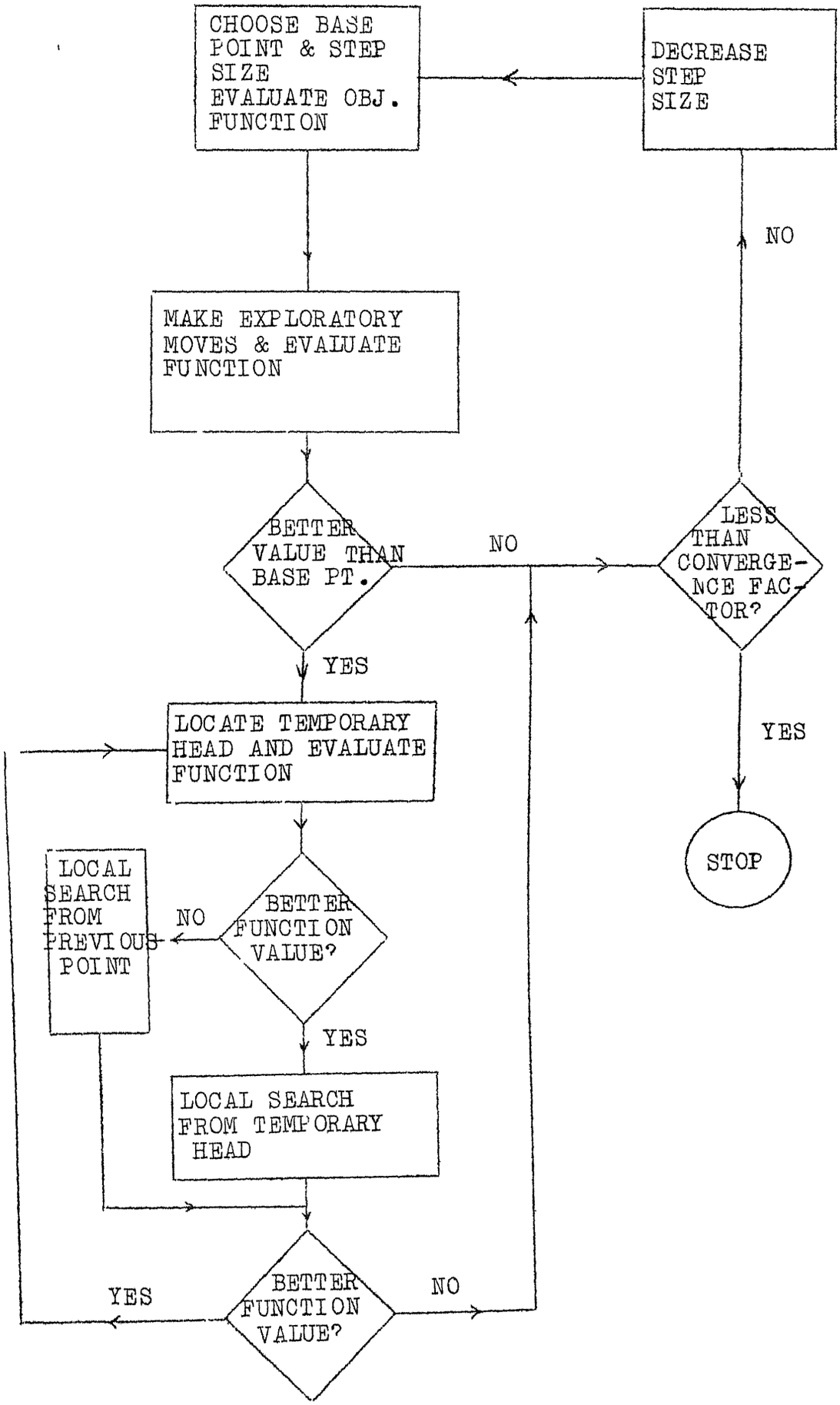
k is stage index (one stage is the end of N searches)

(5) If the temporary head results in a lower function value, a new local search is performed about the temporary head, a new head is located and the value of F checked. This continues as long as F decreases.

(6) If the temporary head does not result in a lower function value, a search is made from the previous best point.

(7) The procedure terminates when the difference between the current value and the previous stage value is less than the specified small number ε.

Flow chart given in Fig. A-1 illustrates this procedure.


CHOOSE BASE POINT & STEP SIZE EVALUATE OBJ. FUNCTION
DECREASE STEP SIZE
NO
MAKE EXPLORATORY MOVES & EVALUATE FUNCTION
BETTER VALUE THAN BASE PT.
NO
LESS THAN CONVERGE-NCE FAC-TOR?
YES
YES
LOCATE TEMPORARY HEAD AND EVALUATE FUNCTION
STOP
LOCAL SEARCH FROM PREVIOUS POINT
NO
BETTER FUNCTION VALUE?
YES
LOCAL SEARCH FROM TEMPORARY HEAD
YES
BETTER FUNCTION VALUE?
NO

REFERENCES

[1] M.I. Skolnik, 'Radar Handbook', New York: McGraw-Hill, 1970, Ch. 12.

[2] R.V. Garver, 'Microwave Diode Control Devices', Dedham: Artech House, 1975, Ch. 10.

[3] J.F. White, 'Semiconductor Control', Dedham: Artech House, 1977, Ch. 9.

[4] L. Stark, 'Microwave theory of phased array antennas - review', Proceedings of the IEEE, vol. 62, pp. 1661-1701, December, 1974.

[5] A. Uhlir, 'The potential of semiconductor diodes in high frequency communications', Proc. IRE, vol. 46, pp. 1099-1115, June 1958.

[6] E.M. Rutz and J.E. Dye, 'Frequency translation by phase modulation', 1957 IRE WESCON Conv. Rec. Pt. 1, pp. 201-207.

[7] E. Stern, 'A variable reactance diode phase shifter', IRE-PGMTT Natl. Symp., Harvard Univ., Cambridge, Mass., June 2, 1959.

[8] H.N. Dawirs and W.G. Swarner, 'A very fast voltage controlled microwave phase shifter', Microwave Journal, vol. 5, no. 1, pp. 99-107, Jan. 1962.

[9] P. Onno and A. Plitkins, 'Miniature multi-killowatt PIN diode MIC digital phase shifters', in IEEE G-MTT Int. Microwave Symp. Dig., 1971, pp. 22-23.

[10] R.V. Garver, 'Broad band diode phase shifters', IEEE Trans. Microwave Theory Tech., vol. MTT-20, pp. 314-323, May 1972.

[11] R.V. Garver, 'Broad band binary 180° diode phase modulators', IEEE Trans. Microwave Theory Tech., vol. MTT-13, pp. 32-38, Jan. 1965.

[12] R.W. Burns and L. Stark, 'PIN diodes advance high power phase shifting', Microwaves vol. 4, no. 11, pp. 38-48, Nov. 1965.

[13] J.F. White, 'Review of semiconductor microwave phase shifters', Proc. IEEE (special issue on Electronic Scanning), vol. 56, pp. 1924-1931, Nov. 1968.

[14] R.E. Fisher et.al., 'Digital-reflection-type microwave phase shifters', Microwave J., vol. 12, no. 5, pp. 63-68.

[15] R.W. Burns et.al., 'Low cost design techniques for semiconductor phase shifters', IEEE Trans. Microwave Theory Tech., vol. MTT-22, pp. 675-688, June 1974.

[16] T. Yahara et.al., 'Broad band 180° phase shift section in X-band', IEEE Trans. Microwave Theory Tech. vol. MTT-23, pp. 307-309, Mar. 1975.

[17] I.J. Bahl and K.C. Gupta, 'Design of loaded line PIN diode phase shifter circuits', IEEE Trans. Microwave Theory Tech., vol. MTT-28, pp. 219-224, March 1980.

[18] P. Wahi and K.C. Gupta, 'Effect of diode parameters on reflection type phase shifters', IEEE Trans. Microwave Theory Tech., vol. MTT-24, pp. 619-621, Sept. 1976.

[19] J. Piotr Starski, 'Optimization of the matching network for a hybrid coupler phase shifter', IEEE Trans. Microwave Theory Tech., vol. MTT-25, Aug. 1977.

[20] R.L. Camisa et al., 'Microwave integrated circuit MIS varactor phase shifter', RCA Review, vol. 36, pp. 296-315, June 1975.

[21] R. Levy, 'Directional couplers', in Advances in Microwaves, vol. 1, L. Young Ed., New York: Academic Press, 1966.

[22] R. Levy, 'Hybrid junctions-frequency characteristics as phase dividers and duplexers', Electronic and Radio Engineer, vol. 36, pp. 308-312, Aug. 1959.

[23] W.H. Leighton, Jr., and A.G. Milnes, 'Junction reactances and dimensional tolerance effects on X-band 3-dB directional couplers', IEEE Trans. Microwave Theory Tech., vol. MTT-19, pp. 818-824, Oct. 1971.

[24] R.V. Garver et al., 'Errors in S_{11} measurements due to residual SWR of the measurement equipment', IEEE Trans. Microwave Theory Tech., vol. MTT-20, pp. 61-69, Jan. 1972.

[25] J. Read and G.J. Wheeler, 'A method of analysis of symmetrical four port networks', IRE Trans. Microwave Theory Tech., vol. MTT-4, pp. 246-252, Oct. 1956.

[26] R. Levy and L.F. Lind, 'Synthesis of symmetrical branch guide couplers', IEEE Trans. Microwave Theory Tech., vol. MTT-16, pp. 80-89, Feb. 1968.

[27] E.G. Cristal and L. Young, 'Theory and tables of optimum symmetrical TEM mode coupled transmission line directional couplers',IEEE Trans. Microwave Theory Tech., vol. MTT-13, pp. 544-558, Sept. 1965.

[28] R. Shelton et al., 'Tandem couplers and phase shifters for multioctave bandwidth' MicroWaves, vol. 4, no. 4, pp. 14-19, April 1965.

[29] F.C. De Ronde, 'A new class of microstrip directional couplers', in IEEE G-MTT Int. Microwave Symp. Digest 1970, pp. 184-189.

[30] B. Shiek, 'Hybrid branch line couplers - a useful new class of directional couplers', IEEE Trans. Microwave Theory Tech., vol. MTT-22, pp. 864-869, Oct. 1974.

[31] J. Lange, 'Interdigitated stripline quadrature hybrid', IEEE Trans. Microwave Theory Tech. (1969 Symp. issue) (corresp.), vol. MTT-17, pp. 1150-1151, Dec. 1969.

[32] L.W. Chua, 'New broad-band matched hybrids for microwave integrated circuits' in Proc. European Microwave Conference, Stockholm, 1971, Sec. C4/5, pp. 1-4.

[33] S. Rehnmark, 'Theory and application of microwave couplers, phase shifter, and power dividers', Ph.D. dissertation, Chalmers Univ. of Technology, Goteborg, Sweden, April 1976.

[34] H. Howe, Jr., Stripline circuit design, Massachusetts: Artech House, 1974, Ch.5.

[35] R.B. Eking, 'On the design of impedance transforming directional couplers',IEEE Trans. Microwave Theory Tech., vol. MTT-19, April 1971

[36] L.F. Lind, 'Synthesis of assymmetrical branch guide directional coupler - impedance transformers', IEEE Trans. Microwave Theory Tech., vol. MTT-17, pp. 45-48, Jan. 1969.

[37] C.Y. Ho, 'Transform impedance with a branch line coupler', Microwaves, vol. 15, no. 5, pp. 47-52, May 1976.

[38] P. Silvester and P. Benedek, 'Equivalent capacitance of microstrip open circuits', IEEE Trans. Microwave Theory Tech., vol. MTT-20, pp. 511-516, Aug. 1972.

[39] E.O. Hammerstad and F. Bekkadal, Microstrip Handbook, ELAB report STF 44A74169, The University of Trondheim, The Norwegian Institute of Technology, 1975.

[40] B. Easter, 'The equivalent circuit of some microstrip discontinuities', IEEE Trans. Microwave Theory Tech., vol. MTT-23, pp. 655-660, Aug. 1975.

[41] P. Silvester and P. Benedek, 'Microstrip discontinuity capacitance for right angle bends, T-junctions and crossings', IEEE Trans. Microwave Theory Tech., vol. MTT-21, pp. 341-346, May 1973. (Also correction IEEE Trans. Microwave Theory Tech., vol. MTT-23, p. 456, May 1975).

[42] A.F. Thompson and A. Gopinath, 'Calculation of microstrip discontinuity inductances', IEEE Trans. Microwave Theory Tech., vol. MTT-23, pp. 648-655, Aug. 1975.

[43] K.C. Gupta et al., Microstrip lines and slotlines. Dedham, MA: Artech House, 1979, Ch.3.

[44] R. Hook and T.A. Jeeves, 'Direct search solution of numerical and statistical problems', J. ACM, vol. 8, pp. 212-229, Apr. 1961.

[45] H. Tromp and G. Hoffman, 'Coupler optimization of 3 dB microstrip hybrids taking into account dispersive coupling and junction effects' in Proc. European Microwave Conf.,1973, Paper A.12.4.

[46] J.W. Bandler, 'Optimization methods for computer aided-design', IEEE Trans. Microwave Theory Tech. MTT-17, pp. 533-552, August 1969.

[47] R.W. Vogel, 'Effect of the T-junction discontinuity on the design of microstrip directional couplers', IEEE Trans. Microwave Theory Tech., vol. MTT-21, pp. 145-146,Mar. 1973.

[48] H. Brenner, H. Kraus, 'Computer-aided design of an S-band phase shifter using PIN diodes for phased array antennas' in Proc. European Microwave Conf., 1971, Sec. B9/2, pp. 1-3.

[49] H.A. Atwater, 'Reflection coefficient transformations for phase shift circuits', IEEE Trans. Microwave Theory Tech., vol. MTT-28, pp. 563-568, June 1980.